Functional characterization of guanylate binding proteins (GBPs) in the innate and adaptive host defence against pathogens

Inaugural dissertation

for the attainment of the title of doctor
in the faculty of Mathematics and Natural Sciences
at the Heinrich Heine University Düsseldorf

presented by

Valesca Lindenberg

from Leiden (Netherlands)

Düsseldorf, June 2017

From the Institute for Medical Microbiology and Hospital Hygiene
at the Heinrich Heine University Düsseldorf

Published by permission of the
Faculty of Mathematics and Natural Sciences at
Heinrich Heine University Düsseldorf

Supervisor: Prof. Dr. Klaus Pfeffer
Co-supervisor: Prof. Dr. Lutz Schmitt

Date of oral examination: 04.08.2017

Table of Contents

Table of Contents ..... *I*

List of Figures ..... *V*

Table Directory ..... *VI*

Abbreviations ..... *VII*

Summary ..... *IX*

Zusammenfassung ..... *XI*

1 Introduction *1*

1.1 Immunity **1**

1.1.1 Innate and adaptive immune responses 1

1.1.2 Cytokines 3

1.1.3 IFNγ 4

1.2 Cell autonomous immunity **7**

1.2.1 Inducible GTPases 10

1.2.1.1 Immunity-related GTPases (IRGs) 12

1.2.1.2 Guanylate Binding Proteins (GBPs) 14

1.3 *Infection models with intracellular replicating pathogens* **20**

1.3.1 Toxoplasma (Toxoplasmosis) 20

1.3.1.1 *Toxoplasma gondii* organelles required for cellular entry 21

1.3.1.2 A parasitic life cycle through various hosts 22

1.3.1.3 Intracellular battleground, *Toxoplasma gondii* vs. it's host 24

1.3.1.4 Cellular immune defences against *Toxoplasma gondii* 29

1.3.2 Chlamydia (chlamydial infection) 31

1.3.2.1 Intracellular biphasic lifecycle of *Chlamydia trachomatis* 31

1.3.2.2 Immunity against *Chlamydia trachomatis* 35

1.3.3 *Mycobacterium* (Tuberculosis) 39

1.3.3.1 *Mycobacterium tuberculosis* elicited immune responses 41

1.3.3.2 *Mycobacterium bovis* BCG 44

1.4 Aims of the study **47**

2 Materials *48*

2.1 Expendables **48**

2.2 Chemicals, solutions and enzymes **49**

2.3 Kits and other reagents **51**

2.4 Buffers **52**

2.5 Cultures 53
2.5.1 Eukaryotic cell lines 53
2.5.2 Microorganisms 54
2.5.3 Media used for cultures 55
2.6 Antibodies 56
2.6.1 Primary and secondary antibodies 56
2.6.2 Directly labelled antibodies 56
2.7 Vectors and oligonucleotides 57
2.7.1 Plasmids 57
2.7.2 Primers for site directed mutagenesis 57
2.7.3 Primers for sequencing 58
2.7.4 Generated mutated vectors 58
2.7.5 Primers for evaluating Chlamydial progeny 59
2.8 Machines 59
2.9 Software 60
2.10 Statistical analysis 61
3 Methods 62
3.1 Molecular biological methods 62
3.1.1 Site directed mutagenesis (SDM) 62
3.1.2 Transformation of DH5α *Escheria coli* 62
3.1.3 Confirmation of successful SDM 62
3.1.4 Restriction analysis 63
3.1.5 Agarose gel electrophoresis 64
3.1.6 Analysis of *Chlamydia trachomatis* genome copies 64
3.2 Cell Biological Methods 67
3.2.1 Cultivation of eukaryotic cell lines 67
3.2.2 Lentiviral transduction to create cell lines expressing mutant mGBPs and controls 67
3.2.3 Cultivation of *Toxoplasma gondii* 68
3.2.4 Infection with *Toxoplasma gondii* 68
3.2.5 Cultivation of *Chlamydia trachomatis* 68
3.2.6 Infections with *Chlamydia trachomatis* 68
3.2.7 Analysis of *Chlamydia trachomatis* progeny 69
3.2.8 Cultivation of mycobacteria 69
3.2.9 Macrophage mycobacterial kill assay 70
3.2.10 Immunofluorescencent staining of fixed cells 70
3.2.11 Live cell imaging 71
3.2.12 FACS analysis 71
3.3 Animal experiments 72
3.3.1 Mice 72

3.3.2 Preparation of murine organs for FACS analysis ... 72
3.3.3 Isolation of murine bone marrow ... 73
3.3.4 Differentiation of bone marrow ... 73

4 Results ... 74

4.1 Protein sequences of interferon inducible GTPases ... 74
4.1.1 Splice variants ... 74
4.1.2 Putative C-terminal motif in mGBPs ... 77

4.2 Recruitment of mutated mGBPs to intracellular *Toxoplasma gondii* ... 81
4.2.1 mGBP1 ... 82
4.2.2 mGBP2 ... 84
4.2.3 mGBP3 ... 86
4.2.4 mGBP5 ... 88
4.2.5 mGBP6 ... 90
4.2.6 mGBP7 ... 92
4.2.7 mGBP8 ... 93
4.2.8 mGBP9 ... 94
4.2.9 mGBP10 ... 95
4.2.10 mCherry and GFP controls ... 96
4.2.11 Exploring mGBP6 in depth ... 97

4.3 Accumulation of mGBPs onto chlamydial inclusions ... 99
4.3.1 Extensive qualitative analysis mGBP recruitment towards chlamydia inclusions ... 100
4.3.2 Quantitative analysis of mGBP colocalization with pathogen containing compartments ... 103
4.3.3 Live cell imaging of mGBP recruitment to chlamydial inclusions ... 108
4.3.3.1 mGBP2 ... 109
4.3.3.2 mGBP9 ... 113
4.3.4 Inhibition with 4-BPB does not affect inclusion formation ... 115
4.3.5 Exploring mGBPs biological effect against Chlamydia ... 116

4.4 Characterization the mGBP5 deficient mouse line ... 118
4.4.1 Phagocytosis capacity of macrophages ... 118
4.4.2 Immune cell populations in organs of mGBP5$^{-/-}$ mice ... 119
4.4.3 mGBP5 deficient macrophage killing of mycobacteria ... 121

5 Discussion ... 124

5.1 Homology analysis of IFN-Inducible GTPases ... 124

5.2 Exploring functional motifs required for the antimicrobial action of mGBPs ... 125

5.3 Function of mGBPs in antimicrobial defence ... 129
5.3.1 Several mGBPs localize at chlamydia inclusions ... 129
5.3.2 mGBPs enclose chlamydia inclusions in living cells ... 129
5.3.3 Measures to optimize quantification of mGBP colocalization at PCVs ... 132
5.3.4 Elucidating the mGBP anti-microbial action at the pathogen containing compartment ... 133

5.3.5 The role of mGBP5 in host immunity 138

5.4 Future perspectives 141

5.4.1 Defining the function & prerequisites of mGBP9 recruitment during chlamydia infection ..141

5.4.2 A potential role for mGBP5 in mycobacterial infection 142

5.4.3 Roles for mGBPs in other infections 143

Literature 145

Publications 176

Appendices 176

Thanks to 185

Eidesstattliche Erklärung 187

List of Figures

Figure 1: Scanning electron microscopy observation of a macrophage and particle **6**

Figure 2: phylogenetic tree of conserved G domains of expressed GTPases. **11**

Figure 3: Genomic organisation of mGBPs..... **15**

Figure 4: IFN-inducible transcription factor-binding sites within GTPases. **16**

Figure 5: Structure and oligomerization of hGBP1. ..... **17**

Figure 6: *Toxoplasma gondii* morphology **21**

Figure 7: Lifecycle of *Toxoplasma gondii*. **23**

Figure 8: *Toxoplasma gondii* host cell entry & modulation **27**

Figure 9: Lifecycle of *Chlamydia trachomatis* serovar L2 ..... **32**

Figure 10: Cell autonomous immunity against *Chlamydia trachomatis* **37**

Figure 11: Overview of cellular immunity against *Chlamydia* **38**

Figure 12: Lifecycle of *Mycobacteria*. **40**

Figure 13: Significant induction of hGBP2 and hGBP5 during mycobacterial infection.. **45**

Figure 14: Phylogenetic tree of IFN-induced GTPases **76**

Figure 15: Alignment of C-terminal sequences of mGBPs **78**

Figure 16: Recruitment of mGBP1-Q545E and -Q545A to intracellular *T. gondii* **83**

Figure 17: Recruitment of mGBP2-E545Q and-C586S to intracellular *T. gondii* **85**

Figure 18: Recruitment of mGBP3-E540Q to intracellular *T. gondii* **87**

Figure 19: Recruitment of mGBP5-Q542E to intracellular *T. gondii* **89**

Figure 20: Recruitment of mGBP6-D542K and -D542N, to intracellular *T. gondii* **90**

Figure 21: Recruitment of mGBP7-E546Q to intracellular *T. gondii* **92**

Figure 22: Recruitment of mGBP8-N460D to intracellular *T. gondii* **93**

Figure 23: Recruitment of mGBP9-D542N to intracellular *T. gondii* **94**

Figure 24: Recruitment of mGBP10-N542D to intracellular *T. gondii*. **95**

Figure 25: No recruitment of mCherry and GFP to intracellular *T. gondii* **96**

Figure 26: mGBP6 WT, mGBP6-D542K and mGBP6-D542N MFI histograms **97**

Figure 27: mGBP6 structural model **98**

Figure 28: Intensity loss of chlamydial pGFP::SW2 signal after mGBP recruitment. ... **100**

Figure 29: Colocalization of mGBPs with *C. trachomatis* inclusions. **102**

Figure 30: Qualitative analysis of mGBP colocalization with Chlamydial Inclusions and Toxoplasma parasitophorous vacuoles. **104**

Figure 31: MFI histograms of cell lines expressing mGBPs. **106**

Figure 32: Two recruitments of mCh::mGBP2 towards *C. trachomatis* **109**

Figure 33: Accumulation of mCh::mGBP2 onto *C. trachomatis* in a living cell 1..... **110**

Figure 34: Accumulation of mCh::mGBP2 onto C. trachomatis in a living cell 2..... **111**

Figure 35: Accumulation of mCh::mGBP9 onto C. trachomatis in a living cell **114**

Figure 36: Inhibitor 4-BPB does not influence formation of chlamydial inclusions..... **115**

Figure 37: Chlamydial replication in mGBP2$^{-/-}$, mGBP5$^{-/-}$ or mGBP7$^{-/-}$mEFs. **117**

Figure 38: Bone marrow derived macrophages (BMDM) ability to phagocytose **119**

Figure 39: FACS staining and quantification of mGBP5$^{-/-}$immune cell populations **120**

Figure 40: mGBP5$^{-/-}$ BMDM kill assay of *M. bovis* BCG / *M. tuberculosis* H37Rv..... **122**

Figure 41: Structural model of mGBP2, mGBP6, mGBP7 and mGBP10.

Table Directory

Table 1: Predicted distinct motifs and domains in murine and human GBP's. **79**

Table 2: Inserts in pWPXL (EF1α) plasmids. **80**

Abbreviations

Abbreviation	Meaning
å	ångström
aa	amino acid
ATG16L1 complex	comprising ATG16L1, ATG5 and ATG12
BAD	Bcl-2-Antagonist of Cell Death
BAG	E3 Ubiquitin Ligase
Ca^{2+}	calcium
cFLIP	cellular FLICE-inhibitory protein
cIAP2	cellular inhibitor of apoptosis 2
CREB	cAMP response element-binding protein
CRISPR	clustered regularly interspersed short palindromic repeat
CXC, CC, CX3C	chemokine motifs:
Cy	cyanin fluorescent dye
DMSO	dimethylsulphoxide
DNA	deoxyribonucleic acid
dNTP	deoxy nucleoside triphosphate
EDTA	ethylenediaminetetraacetic acid
EGR2	Early growth response protein 2
etc.	etcetera
FACS	fluorescence activated cell sorting
FITC	fluorescein isothiocyanate (fluorescent dye)
GRA	*Toxoplasma gondii* dense granule protein(s)
GTP / GDP / GMP	Guanosin tri/di/mono phosphate
h	hours
H_2O	water
IRF	Interferon regulatory factor
ISG/GAS	Interferon stimulated gene / Interferon-Gamma Activated Sequence
kb	kilobasepairs
iso	isoform
kDa	kiloDalton
MAPK-ERK signaling pathway	Ras/Raf induced Mitogen-activated protein kinase kinase signaling through Extracellular-signal Regulated Kinases
MCL1	anti-apoptotic Bcl-2 family member myeloid cell leukemia 1
mRNA	messenger RNA
mTOR	mechanistic target of rapamycin
MYD88	Host TLR adaptor protein myeloid differentiation primary response gene 88
NADP/NADPH	nicotinamide adenine dinucleotide phosphate
NO	nitric oxide

ORF	open reading frame
PerCP	Peridinin chlorophyll protein (fluorescent dye)
pi	post infection
PI3KC3 complex	phosphoinositide 3-kinase catalytic subunit type III (comprising beclin 1, vacuolar protein sorting 34 (VPS34), VPS15 and ATG14L)
PKC	Proteinkinase C
RNA	ribonucleic acid
RON	*Toxoplasma gondii* rhoptry neck protein(s)
ROP	*Toxoplasma gondii* rhoptry protein(s)
rpm	rounds per minute
RT	room temperature
SAG1	surface antigen 1 of *Toxoplasma gondii*
SDS	sodium dodecyl sulfate
SPF	**Specific pathogen free**
TRAF	TNF receptor associated factor
U	units
ULK1 complex	ULK1, FIP200, ATG13 and ATG101
UV	ultraviolet
WT	wild type

Summary

Interferon gamma (IFNγ) is a potent cytokine which orchestrates host immunity against intracellular pathogens. Upon stimulation with IFNγ a wide range of genes is induced, amongst which the guanylate binding proteins (GBPs) are abundant. GBPs are a family of large GTPases which can localize at specialized compartments within the mammalian cell. Previously, it was shown that GBPs contribute to the control of *Toxoplasma (T.) gondii* infection in mice. Some murine (m) GBPs were described to localize and to subsequently disrupt toxoplasma's parasitophorous vacuole (PV).

Localization of mGBP2 towards the PV was shown to be dependent on a C-terminal CaaX-box motif that allows membrane anchoring. However, this motif is shared only by murine and human GBP1, GBP2 and GBP5. This raises the question how other mGBPs lacking this motif recruit to the PV. In this study, additional novel motifs required for the recruitment to the *T. gondii* PV were investigated. It was found that a single aspartic acid in the C-terminal part of mGBP6, D542, is important for mGBP6 localization towards the PV. This residue could be part of the predicted Fes/CIP4 homology Bin-Amphiphysin-Rvs167 (F-BAR) motif, which is shared by mGBP6, mGBP7, and mGBP10. However, the dependency on single nucleotide mutation of D542 to a neutrally charged asparagine (N) for recruitment to the PV is unique to mGBP6. The localization towards the parasite was not diminished after corresponding mutations of other mGBPs.

Previously, mice deficient for mGBP1 and mGBP2 were shown to be susceptible to infection with intracellular pathogens, specifically *T. gondii*. To examine further members of the mGBP family, an mGBP5 deficient mouse line was investigated. However, mGBP5 deficient mice were not susceptible to toxoplasma infection. Therefore, in this study, the mGBP5-deficient mouse was investigated in more depth. Here, it is described that immune cell populations do not vary between mGBP5$^{-/-}$ and wild type mice. Also, the phagocytosis capacity of bone marrow derived macrophages was unchanged. Additionally, macrophages of both genotypes invariably killed *Mycobacterium bovis* BCG or *Mycobacterium tuberculosis* H37Rv bacteria after IFNγ stimulation.

To further characterize the function of mGBPs, an additional *in vitro* infection model was established. *Chlamydia trachomatis* is a sexually transmittable intracellular bacterium against which cell autonomous immunity plays a role. Nevertheless, the different mechanisms contributing to anti-chlamydial defence remain vastly elusive. In this study, a panel of fibroblast cell lines constitutively expressing mGBPs N-terminally fused to

mCherry or GFP were established and subjected to chlamydial infection. These experiments reveal that the majority of mGBPs can colocalize with intracellular chlamydia inclusions. Colocalization at the chlamydial inclusion membrane was shown for mGBP1, mGBP2, mGBP3, mGBP6, mGBP7, mGBP9, and mGBP10, whereas mGBP5 and mGBP8 were virtually absent. Quantification revealed that mGBP9 accumulates as often onto chlamydial inclusions (13%), as the most frequently colocalizing mGBP1 (13%) and mGBP2 (17%). By comparing quantifications of mGBP colocalization between chlamydia and toxoplasma infections, a specific pattern in recruitment of mGBPs appears. Whereas chlamydia inclusions most often attract mGBP1, mGBP2 and mGBP9, the toxoplasma PVs are recruited at a high rate by mGBP1, mGBP2 and mGBP6. This pattern suggests that mGBP6 plays a major role in toxoplasma infection, whereas mGBP9 is an important factor in cell autonomous immunity against chlamydial infection. Furthermore, live cell imaging and time lapse microscopy of mGBP2 and mGBP9 in chlamydia infected cells revealed that the accumulation at the inclusion membrane is authentic, fast and transient. These results, for the first time, show the dynamics of mGBP recruitment in chlamydial infection.

In summary, this work demonstrated that the majority of mGBPs have functions both in toxoplasma and chlamydial infections, however pathogen specific patterns of recruitment to the pathogen containing compartment exist. This study draws attention to the immunological role of mGBPs encoded on murine chromosome 5, e.g. mGBP6 and mGBP9, which have up till now not been assigned a role in pathogen defence.

Zusammenfassung

Interferon gamma (IFNγ) ist ein wichtiges Zytokin, das die Wirtsreaktion gegen intrazelluläre Pathogene reguliert. Durch Stimulation von Zellen mit IFNγ wird eine grpße Zahl von Genen induziert, unter denen die Guanylat-bindenden Proteine (GBPs) hoch exprimiert werden. GBPs sind eine Familie von großen GTPasen, die sich in spezialisierten Kompartimente innerhalb von Zellen lokalisieren können. Bisher wurde gezeigt, dass GBPs zur Kontrolle der *Toxoplasma (T.) gondii*-Infektion bei Mäusen beitragen. Es konnte gezeigt werden, dass einige murine (m) GBPs um die parasitophore Vakuole (PV) von Toxoplasma lokalisieren und diese schließlich zerstören können.

Die Lokalisierung von mGBP2 an der PV ist abhängig von einem C-terminalen CaaX-Box-Motiv, welches eine Verankerung in die Membran ermöglicht. Dieses Motiv ist jedoch nur in murinen und humanen GBP1, GBP2 und GBP5 vorhanden. Dies wirft die Frage auf, wie andere mGBPs ohne dieses Motiv zur PV rekrutieren. In dieser Studie wurden weitere, bislang unerforschte Motive für die Rekrutierung zur *T. gondii* PV untersucht. Es wurde festgestellt, dass eine einzige Asparaginsäure im C-terminalen Teil von mGBP6, D542, für die Lokalisation von mGBP6 an der PV wichtig ist. Diese Aminosäure könnte Teil eines vorhergesagten Fes/CIP4 homology Bin-Amphiphysin-Rvs167 (F-BAR)-Motivs sein, das potentiell in mGBP6, mGBP7, und mGBP10 zu finden ist. Allerdings ist die Abhängigkeit der Lokalisation des Proteins von der Punktmutation von D542 zu einem neutral geladenen Asparagin (N) einzigartig für mGBP6. Eine Verminderung der Lokalisierung zum Parasiten konnte nicht beobachtet werden nachdem andere mGBPs in vergleichbarer Weise an den korrespondierenden Positionen mutiert wurden.

Bisher wurde gezeigt, dass Mäuse, die für mGBP1 und mGBP2 defizient sind, anfällig für Infektionen mit intrazellulären Pathogenen sind, insbesondere für *T. gondii*. Um ein weiteres Mitglied der mGBP Familie zu untersuchen, wurde eine mGBP5-defiziente Mauslinie analysiert. Diese Mauslinie wies jedoch keine veränderte Suzeptibilität gegenüber Toxoplasma-Infektion auf. Daher wurde in dieser Studie die mGBP5-defiziente Mauslinie weiter charakterisiert.

Es konnte gezeigt werden, dass die Populationen von Immunzellen zwischen mGBP5$^{-/-}$ und Wildtyp-Mäusen in ihren Frequenzen unverändert sind. Die Phagozytose-Kapazität von aus dem Knochenmark differenzierten Makrophagen war ebenfalls unverändert.

Weiterhin konnten Makrophagen beider Genotypen nach IFNγ Stimulation gleichermaßen *Mycobacterium bovis* BCG oder *Mycobacterium tuberculosis* H37Rv abtöten.

Um die Funktion von mGBPs weiter zu charakterisieren, wurde ein zusätzliches *in vitro* Infektionsmodell etabliert. *Chlamydia trachomatis* ist ein sexuell übertragbares intrazelluläres Bakterium, gegen das die zellautonome Immunität eine Rolle spielt. Bisher sind die Mechanismen, die zur Abwehr von Chlamydien beitragen, großteils unklar. In dieser Studie wurden Fibroblasten-Zelllinien, die mGBPs N-terminal mit mCherry oder mit GFP fusioniert exprimieren, einer Chlamydien-Infektion unterworfen. Diese Experimente zeigen, dass die Mehrheit der mGBPs mit intrazellularen Chlamydien-Einschlüssen kolokalisieren kann. Die Kolokalisierung an der Chlamydien-Einschlussmembran zeigte sich für mGBP1, mGBP2, mGBP3, mGBP6, mGBP7, mGBP9 und mGBP10, während für mGBP5 und mGBP8 kaum eine Kolokalisation beobachtet wurde. Die Quantifizierung ergab, dass mGBP9 mit ähnlicher Häufigkeit (13%) wie mGBP1 (13%) und mGBP2 (17%) an Chlamydien-Einschlüsse akkumuliert. Durch Vergleich von Quantifizierungen der mGBP-Kolokalisation zwischen Chlamydien- und Toxoplasma-Infektionen wurde ein spezifisches Muster bei der Rekrutierung von mGBPs aufgezeigt. Während zu Chlamydien-Einschlüssen mGBP1, mGBP2 und mGBP9 häufig akkumuliert, wird zur Toxoplasma PV mGBP1, mGBP2 und mGBP6 rekrutiert. Diese Muster implizieren, dass mGBP6 eine wichtige Rolle bei Infektionen mit *T. gondii* spielt, während mGBP9 eher einen wichtigen Faktor bei der zellautonomen Immunität gegen Chlamydia darstellt. Darüber hinaus zeigen Lebendzellmikroskopie von mGBP2 und mGBP9 in Chlamydien-infizierten Zellen, dass die Akkumulation an der Einschlussmembran authentisch, schnell und transient ist. Diese Ergebnisse zeigen zum ersten Mal die Dynamik der mGBP-Rekrutierung bei der Chlamydialeninfektion.

Zusammenfassend belegt diese Arbeit, dass die Mehrheit der mGBPs sowohl bei Toxoplasma- als auch bei Chlamydien-Infektionen eine Rolle spielen, es jedoch Pathogen-spezifische Muster gibt. Diese Studie lenkt insbesondere die Aufmerksamkeit auf die immunologische Rolle von mGBPs, die auf dem murinen Chromosom 5 codiert sind, z.B. mGBP6 und mGBP9, die bislang in Hinblick auf deren Rolle bei der Abwehr von Pathogenen noch nicht untersucht wurden.

1 Introduction

1.1 Immunity

The vast majority of organisms on the earth are microbes, most of which coexist as commensals or symbionts, but few of which can invade and be potentially harmful to multicellular organisms (metazoa) such as mammals. This subset is called ‘pathogens’ (Madigan et al., 2012). Pathogens can be viruses, bacteria, fungi or eukaryotic parasites, all of which have short replication cycles, leading to a fast growth and adaptation through genetic recombination, thus providing an advantage over mammals (Daugherty and Malik, 2012). In addition, around 1400 phylogenetically distinct and continuously evolving microorganisms can infect a single host (MacMicking, 2012). In response, mammals have developed a plethora of defence mechanisms to protect against pathogens, these concerted actions are termed ‘Immunity’ (Murphy et al., 2012). The foremost of which is prevention of invasion through spatial separation of ‘outside’ versus ‘inside’, formed by the skin and well-connected epithelial cell layers covered in mucus (Murphy et al., 2012). These surfaces are rendered hostile to pathogens by pre-colonization with commensal microorganisms and the presence of anti-pathogenic compounds, such as lysozyme, mucins, defensins, cathelicidins, histatins, etc. (Murphy et al., 2012). If pathogens succeed in penetrating these barriers and reach the blood and bodily fluids, they encounter the complement system. The complement system is an elaborate panel of soluble proteins, capable of binding pathogen surface molecules such as mannose, and inducing a proteolytic cascade cleaving zymogens thus causing excessive deposition of complement onto the pathogen to directly lyse it or mark it as dangerous, a process called opsonisation (Murphy et al., 2012). Additional redundant defence mechanisms are induced and have been subdivided in innate and adaptive immune responses. The innate immune system is present at birth and is characterized by a fast response to a wide range of pathogens (Murphy et al., 2012). In contrast the adaptive, or acquired, immune response is characterized by a high specificity but requires a longer time for initial activation (Murphy et al., 2012).

1.1.1 Innate and adaptive immune responses

After pathogen penetration of barrier tissues, the pathogen encounters immune cells expressing highly specialized pattern recognition receptors (PRRs) which bind pathogen-associated molecular patterns (PAMPs, such as lipopolysaccharide (LPS) or lipoteichoic acid (LTA)) or specific host cell components that are released during damage or death. Several families of PRRs exist, i.e. Toll-like receptors (TLRs), RIG-I-like receptors

(RLRs), C-type lectin receptors (CLRs), NOD-like receptors (NLRs), and cytosolic sensors for DNA (e.g. AIM2, STING, ZBP1) all of which, upon ligand binding, lead to complex signalling cascades, thus inducing immune responses (Beutler et al., 2006). The fastest inducible immune response is non-specific and involves degranulation of myeloid-derived neutrophils, eosinophils, basophils and mast cells and lymphoid-derived NK cells releasing antimicrobial substances in the vicinity of the pathogen (Murphy et al., 2012). In addition to pathogen destruction these cells also release molecules for autocrine and paracrine signalling, such as cytokines (see 1.1.2) and chemokines (e.g. CXC, CC and CX3C class ligands), which accumulate at the site of infection to signal inflammation and diffuse through the tissues creating a gradient to alarm neighbouring cells and attract additional immune cells (Rivera et al., 2016). If a pathogen directly invades a tissue, circumventing the bloodstream, this function is executed and tailored by tissue-resident innate lymphoid cells (ILCs) whose prototypic function is cytokine production (Fuchs, 2016). In parallel, recruited macrophages and dendritic cells ingest pathogens, destroy them, or produce additional signalling molecules which can activate the adaptive immune system. Therefore these phagocytes are also called professional antigen-presenting cells (APCs) (Mantegazza et al., 2013; Murphy et al., 2012).

Within macrophages and dendritic cells the phagocytosed pathogen is compartmentalized in the phagosome which fuses with acidic lysosomes to destroy its content, or an intracellular pathogen is detected and destroyed in a compartment called the ‘immunoproteasome’, in both cases producing short amino acid fragments called peptides or antigens. These are loaded onto major-histocompatibility complexes (MHC) type 1 and type 2 for presentation or cross presentation on the cell surface (Mantegazza et al., 2013). APCs then migrate into lymphatic organs where the MHC-bound peptide is presented together with co-stimulatory and soluble signals to naïve B and T cells (Murphy et al., 2012). Like a subset of dendritic and NK cells, also B and T cells develop from a common lymphoid progenitor, however B and T cells undergo somatic recombination giving rise to a large variety of unique surface receptors which subsequently undergo continuous positive and negative selections involving different migratory routes leading to selection and education resulting in a pool of mature naïve cells in the periphery (Murphy et al., 2012). When these unique T cell receptor(s) can bind the peptide presented in MHC-II on an activated APC, this activates these cells ultimately resulting in antigen-specific clones to proliferate, creating a pool of adaptive immune cells capable of recognizing the infecting pathogen or pathogen antigens displayed in the context of MHC-I on infected cells (Murphy et al., 2012).

Highly specific T cells develop diverging functions by differentiating, based on the additional signals presented by the APC, into CD4 expressing helper (T_H1, T_H2, T_H17, T_{FH}), regulatory or CD8-expressing regulatory or cytotoxic T cells which then migrate to the inflamed site to alter the microenvironment or directly kill infected cells (those expressing the antigen in MHC type 1 on the surface), respectively (Murphy et al., 2012). B cells mature into plasma cells capable of producing specific antibodies (also called immunoglobulins, Ig) which bind to the surface of the pathogen resulting in neutralization, opsonisation or complement activation (Murphy et al., 2012). Limited numbers of these antigen-specific cells can differentiate into resting cells which constitute a memory allowing rapid reactivation of the pathogen specific responses, like those observed after vaccination, which cell populations are called memory T cells (Macallan et al., 2017) or memory B cells (Goodnow et al., 2010; Pupovac and Good-Jacobson, 2017). These concerted immune actions are highly effective in clearing infections.

After induced immune responses cleared the infection, the inflammation needs to be reduced to prevent unnecessary tissue damage, a task accomplished by negative feedback loops in signalling cascades (Cui et al., 2014; Hu et al., 2008) and by regulatory T cells by promoting an immunosuppressive environment. (Stephen-Victor et al., 2017). Recently, *in vivo* observations showed anti-inflammatory action of regulatory T cells co-clustering with a dendritic cell and an effector T cell within secondary lymphoid tissues (Liu et al., 2015b). However, the evolutionary advantage microorganisms hold over mammals allows for constant immune evasion strategy development to limit detection, reduce inflammation and/or induce tolerance (Finlay and McFadden, 2006). Some pathogens evade systemic immune responses by infecting and ‘hiding’ within a host cell, which poses additional constraints on pathogen survival (further described in 1.2) (Pareja and Colombo, 2013).

Many immune responses described above, as well as the interplay between innate and adaptive immunity are only partly understood (Howard, 2007). An advantage of pathogen-mediated interference of host immune responses is that this provides a tool which disrupts the steady state of the immune systems, thus allowing a deeper exploration of immunity.

1.1.2 Cytokines

Cytokines, for example those proteins secreted by immune cells upon PRR stimulation, are proteins which can bind dedicated receptors on neighbouring cells thereby affecting

their behaviour (Murphy et al., 2012). Cytokines are a structurally diverse group of proteins including interleukins (IL), hematopoietins, the TNF family and interferons (IFNs) (Murphy et al., 2012). There are three types of IFNs, namely types I (IFN α, β, δ, ε, ζ, κ, ν, τ, ω), II (IFNγ) and III (IL28A, IL28B and IL29, dubbed IFN-like proteins) (Pestka, 2007; Pestka et al., 1987). These interferons bind to their dedicated receptors which are IFNAR1 / IFNAR2, IFNGR1 / IFNGR2 or IL28R1 / IL10R2, respectively (Krause and Pestka, 2007). After cytokine binding, the receptors dimerize thus allowing pre-associated signalling molecules to phosphorylate each other, e.g. IFNGR1 with Jak1 dimerizes with IFNGR2 with Jak2 allowing the Jaks to transactivate and induce the intensively studied STAT signalling cascades, which activate transcription factors allowing tailored rapid transcriptional responses (Krause and Pestka, 2007; Majoros et al., 2017). These IFN-induced responses have been shown to play roles in immune responses against viruses, bacteria and parasites but can also act as regulators of cell proliferation, differentiation, survival and death and activate specialized immune functions (Hertzog et al., 2003). These diversified functions stem from the ability of IFNs to induce thousands of immunity related genes, also called interferon stimulated genes (ISGs), which combined are called 'the interferome', which complexity is compiled in the interferome v2.0 database to allow bioinformatics research approaches (Hertzog et al., 2011; Rusinova et al., 2013; Samarajiwa et al., 2009). For immunity to the intracellular pathogens under study in this thesis, IFNγ is the most important cytokine (see 1.3) (Shtrichman and Samuel, 2001).

1.1.3 IFNγ

Upon infection and inflammation, APC derived cytokines, predominantly IL12 and IL18, initiate local IFNγ production in NK cells, subsequently attract T_H1 and cytotoxic T cells which bind antigen thus crosslinking their T cell receptors and produce increasing amounts of IFNγ locally (Boehm et al., 1997). In addition, other cell types, such as various APCs (Hume, 2008), T_H17, T_H2 and T_{FH} (Bonelli et al., 2014) and specific ILC subsets (Lim et al., 2017) have also been shown to produce IFNγ under certain conditions at the site of infection. The biologically active form of IFNγ is a noncovalently bound 34-kDa homodimer, which is being sensed by the IFNγ receptor (IFNGR) complex, consisting of two 90-kDa α-chains IFNGR1 that bind the IFNγ homodimer with high affinity and two 314 aa β-chains called IFNGR2 that are required to induce signalling via Jak1/Jak2 (Ealick et al., 1991; Fountoulakis et al., 1992; Greenlund et al., 1993; Muller et al., 1993; Neubauer et al., 1998; Rodig et al., 1998; Watling et al., 1993). Jaks phosphorylate STAT1, which forms a homodimer (also known as IFNγ activation factor), or a trimeric complex made up of STAT1, STAT2 and IRF9, called ISGF3, that

enter the nucleus and binds gamma interferon-activated sites (GAS) and interferon-stimulated response elements (ISREs) to initiate a wave of transcription, including additional transcriptions factors of the IRF family (initially IRF1) for subsequent transcription within 15-30 minutes (Krause and Pestka, 2007; Schroder et al., 2004). The extend of these transcriptional events are also regulated by chromatin remodelling, primarily of the IFNγ gene locus itself (Schoenborn and Wilson, 2007). The numerous transcribed genes result in induction of proteins playing a role in a multitude of innate and adaptive immune responses listed below, and are also interconnected with other cytokine signalling pathways, e.g. TNFα (Boehm et al., 1997; Hu et al., 2008; Hu and Ivashkiv, 2009; Johnson and Ahmed, 2006; Martens and Howard, 2006; Schoenborn and Wilson, 2007; Schroder et al., 2006; Shtrichman and Samuel, 2001):

- producing additional chemokines to induce immune cell extravasation from the blood into inflamed tissues,
- induction of protease subunits of the immunoproteasome to increase peptide formation and up regulation of cell-surface MHC type 1 to improve immune surveillance by cytotoxic T cells since antigen is readily presented,
- up regulation of MHC type 2 in APCs to improve antigen-specific activation of CD4-positive T cells,
- Enforcing T_H1 type polarisation by creating a continued loop of IFNγ and IL12 production, at the cost of T_H2 differentiation,
- B cell isotype switching from IgM to IgG2a,
- induction of the phox complex to produce reactive oxygen species (ROS, respiratory burst) within the cell,
- induction of nitric oxide synthase (NOS) to produce reactive nitrogen intermediates (RNI)
- activation of intracellular microbial effectors such as resistance-associated macrophage protein 1 (NRAMP1), cathepsins, RNA-dependent protein kinase (PKR), oligoadenylatesynthase (OAS) and adenosine deaminase (dsRAD) and inducing and activating immunity related GTPases and guanylate binding proteins (see 1.2),
- initiate intracellular metabolic competition by tryptophan depletion via induction of IDO, and sequestering cations like magnesium and iron,
- priming macrophages for more rapid and heightened TLR responses, for example to LPS by increasing signalling components TLR4, Myd88 and IRAK,
- inhibiting cell growth and,

- Inducing cellular uptake (processes like pinocytosis, receptor-mediated uptake, autophagy, xenophagy and phagocytosis, for an example of the latter see Fig.1), antigen processing and influencing cell survival, which can lead to either beneficial or detrimental outcome, depending on the infecting microorganism and will therefore be discussed in the next paragraph

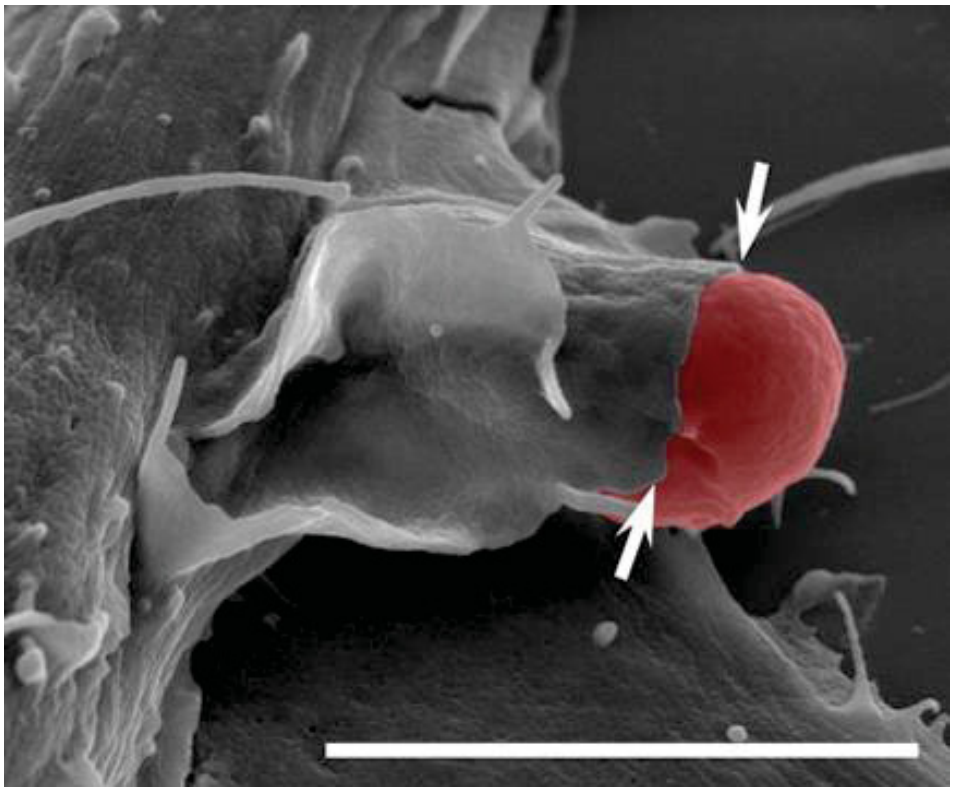

Figure 1: Scanning electron microscopy observation of an immortalized macrophage taking up an antibody-opsonized particle, 10 minutes after particle was added, bar : 5 µm modified from (Egami et al., 2011).

After clearance of invading pathogens a balance has to be struck to limit collateral damage to the host which involves the down regulation of IFNγ signalling (Hu and Ivashkiv, 2009): After stimulation the IFNGR complex is internalised via the endosomal pathway and can be dephosphorylated and recycled onto the surface or degraded (Farrar and Schreiber, 1993). Further negative regulation is obtained by suppressor of cytokine signalling (SOCS) proteins, USP18 and protein inhibitors of activated STAT (PIAS) which are induced by cytokines and reduce signalling on several levels (Darnell, 1997; Schneider et al., 2014; Yasukawa et al., 2000)

The elaborate effects of IFNγ described above, function both systemically on various cell types of innate and adaptive immunity, and autocrine on the cell itself to alter its activation status (Blanco et al., 2008). The immune responses which occur within one cell after interferon stimulation will be discussed in the next paragraph.

1.2 Cell autonomous immunity

Cell autonomous immunity is the ability of one single cell to defend itself against microorganisms, spanning both the sensory apparatus and the effector mechanisms directly responsible for microbial killing (Beutler et al., 2006; MacMicking, 2012). This ability was first recognized in fibroblasts by Isaacs and Lindenmann sixty years ago (Isaacs and Lindenmann, 1957). At this point, it is imperative to appreciate the complex organisation within cells, where various membranes divide the extracellular environment from the cytoplasm, the various specialized organelles from the cytosol and divide organelles in compartments with vastly different features, e.g. osmotic and pH values (Alberts et al., 2014). The sensory apparatus are PRRs in the plasma membrane capable or recognizing microorganisms, their cytoplasmic signal transduction pathways and the stimulating role of IFNγ, have been discussed above (1.1.1). In addition IFNγ stimulates other, pre-positioned mechanisms such as phagocytosis (Levine, 2005). If a microorganism interacts with PRRs, APCs are stimulated to ingest this particle by engulfing it with specialized patches in the plasma membrane (phagocytic cup) and subsequently enclosing it forming a bilayered vesicle thus compartmentalizing the pathogen and restricting its movement (Randow et al., 2013). This is called the phagosomal compartment, which traffics through the cytosol and fuses with endosomes and lysosomes in a process called phagosome maturation (Fairn and Grinstein, 2012; Pauwels et al., 2017). Fusion of these organelles, e.g. endosomes and lysosomes, results in acidification of the phagosome thus chemically denaturing proteins to destruct the ingested particle (Yates et al., 2005). This trafficking process has to be regulated within the midst of other cellular processes, such as metabolism (part of which is the electron transport chain taking place on the mitochondrial membrane) and protein synthesis, which originates in the nucleus but advances through the adjoining endoplasmic reticulum (ER) modifying proteins and further into the Golgi apparatus which allows transport to the plasmamembrane (Alberts et al., 2014). In this crowded cytoplasm, previously mentioned ROS and RNI are directed to phagosome and released to further enhance degradation of the particle (Olekhnovitch and Bousso, 2015; Rybicka et al., 2012). Destruction of the pathogen proteins in the phagosome releases short peptides fragments which are loaded onto recycled MHC-II molecules to subsequently activate adaptive immune cells, thus placing the phagosome as a signalling platform in the interface between innate and adaptive immunity (Kagan and Iwasaki, 2012; Mantegazza et al., 2013). Because of this central function, many pathogens have evolved strategies to manipulate phagosome maturation, trafficking and fusion to adapt

this cellular compartment to their own needs, thus creating a replicative niche (Colonne et al., 2016).

In response, host cells rely heavily on the interferome to execute additional cell autonomous defences via the ISGs (Moretti and Blander, 2017). As mentioned in 1.1.2, the plethora of ISGs is only understood in part, examples of known ISGs will be summarized in the following. It was discovered that the most abundantly expressed ISGs are interferon inducible GTPases (Martens and Howard, 2006), which will be discussed in the next paragraph. Also ISG15 is induced, an ubiquitin-like protein which can be covalently attached to target proteins by ISGylation to support host defence (Bogunovic et al., 2013; Zhao et al., 2013). Similar to ISG15, the diverse family of TRIM proteins also exhibit ubiquitin ligase activity (Ozato et al., 2008). An alternative defence strategy is the induction of tetherins and IFITM family of proteins which alter cellular membrane properties, thus influencing fusion/scission events and subsequently phagosome maturation, but potentially also impeding pathogen manipulations (Diamond and Farzan, 2013; Mahauad-Fernandez and Okeoma, 2016). Comparable membrane alterations can be reached by influencing sterol and oxysterols biosynthesis, e.g. by induction of Cholesterol-25-hydroxylase (Fessler, 2016). Also hampering the pathogens growth by depleting the cellular pool of nutritional factors such as tryptophan, by inducing IDO (MacKenzie et al., 2007), or sequestering intracellular cations with help of NRAMP1 (MacMicking, 2012). A recent discovery is the relevance of cell metabolism, and in particular mitochondria, in impeding microorganisms within the cell (Mills et al., 2017; Van den Bossche et al., 2017). On top of these integrated and closely controlled mechanisms, many ISGs are proteins delivered into the phagosome which have direct anti-microbial effects. One of the first and best characterized is PKR (Pindel and Sadler, 2011) (listed in 1.1.3, 6th bullet).

If these defences fail, host cells utilize a natural cellular process called autophagy, in order to eradicate pathogens which escaped classical phagosomal degradation (Deretic, 2016; Deretic et al., 2013; Shintani and Klionsky, 2004). Autophagy (depending on the detailed circumstances also called: macroautophagy, microautophagy, chaperone-mediated autophagy, endocytosis or xenophagy) is a process in which a vacuole forms *de novo* to sequester excess or defective organelles, which subsequently fuse with the lysosome for degradation in order to recycle cytoplasm or as a part of programmed cell death (Yin et al., 2016). Autophagosomes are initiated at a pathogen containing vacuole (PCV) by concerted action of the ULK1- and PI3KC3 complex thus forming a membrane compartment enclosing the PCV which is subsequently coated with

phosphatidylethanolamine (PE) and microtubule-associated protein 1 light chain 3 (LC3) by the ATG16L1 complex, and thus being marked for fusion to an autolysosome (Cadwell, 2016). Nevertheless, some pathogens evolved methods to interfere with autophagocytosis, e.g. *Listeria monocytogenes* expresses a virulence factor which hijacks the host major vault protein, thus preventing their ubiquitination and escape from autophagic recognition (Dortet et al., 2011). Crosstalk exists between autophagy and immune signaling, allowing for other host cell actions, e.g. regulation of type 1 interferons, PRR signaling and cell death programs, if autophagy fails (Desai et al., 2015).

If the pathogen is not cleared, as a last resort, the infected cell can initiate different modes of cell death, including pyroptosis (Fink and Cookson, 2005) and necroptosis, which are 'loud' programs for death programs which release many DAMPs into the environment (Kearney and Martin, 2017) or apoptosis, a 'silent' form resulting in an anti-inflammatory milieu thus supporting tissue reconstruction (Kawamoto et al., 2016). Several proteins are shared among phagocytosis, autophagy and cell death signaling, most prominently of which the ATGs, which recently have been found to also play autophagy-independent roles in immune signalling (Paulus and Xavier, 2015). Also, during these processes additional DAMPs and PAMPs are released which trigger intracellular PRRs, e.g. endosomal TLRs and cytosolic receptors such as NLRs to kick-start additional signalling cascades (Deretic, 2012; Dostert et al., 2008; Meylan et al., 2006). Recently a subset of NLRs (NLRP1, NLRP3, NRLP12, NLRC4) and AIM2 have been discovered to activate inflammasomes, platforms for cell death signalling which enforce cellular defence against pathogens (Broz and Dixit, 2016; Chen and Schroder, 2013; Coll et al., 2016). Inflammasomes are multiprotein-structures, which were first discovered by Jurg Tschopp in 2002, and have become a major focus of immunological research (de Vasconcelos et al., 2016; Martinon et al., 2002). In short, NLR or AIM2 receptors oligomerize and recruit additional inflammasome components (e.g. ASC) to function as signalling complexes steering cell death programmes (de Vasconcelos et al., 2016). Inflammasome induction of caspases 8, 9, and 10 induces apoptosis, whereas ASC cleavage of procaspase-1 ultimately leads to caspase 11, IL1β and IL18 production, activation of gasdermins, subsequent pyroptosis, or even necroptosis (if part of the inflammasome components are absent) (Man and Kanneganti, 2016). Cell death terminates cell autonomous immunity, but the cell death programme executed influences the factors released, thus priming the surrounding cells to take adequate immune modulatory and anti-, or inflammatory actions (Gregory and Pound, 2011).

From the first PRR activation, the interferome is elegantly fine-tuned by lncRNAs, miRNAs, alternative splicing, altered translation, post-translational modification, relocalization, and secretion, which aside from transcription also allows prompt responses stemming from pre-existing RNA and proteins (Schneider et al., 2014). This exquisite orchestration resulting in a cell autonomous immune response occurs not only in APCs, as exemplified here, but in essentially all other cell types including fibroblasts and endothelial skin cells (Pauwels et al., 2017).

1.2.1 Inducible GTPases

Among the most abundantly expressed proteins after IFNγ stimulation are the inducible GTPases (Martens and Howard, 2006). All GTPases are proteins, which through conserved domains, can adopt different shapes and therewith functions (Bourne, 1995). GTPases undergo these conformational changes upon hydrolysis of GTP, spontaneously or with the help of guanine-nucleotide exchange factors (GEFs) that exchange GDP with GTP (Bourne et al., 1991) or after even further hydrolysis from GDP to GMP (Cheng et al., 1991). This process can be accelerated by GTPase-activating proteins (GAPs), which assist the conversion of GTP to GDP to rapidly down regulate the activity in small GTPases, e.g. K-Ras and Rac1 (Murphy et al., 2012). Small and large GTPases have been found to function in protein biosynthesis (initiation and elongation factors), intracellular signalling, vesicular transport, endocytosis and cell cycle differentiation (Bourne et al., 1990).

The interferon inducible GTPases consist of four protein families, i.e. very large inducible GTPases (VLIG or GVIN), the Myxovirus resistance proteins (Mx), immunity-related GTPases (IRGs) and guanylate binding proteins (GBPs) (Hunn et al., 2011; MacMicking, 2004). The IRG subfamily has been found to contribute tremendously to resistance against diverse pathogens (MacMicking, 2005) and have been found consistently throughout host-evolution, from cephalochordates till mammals (Bekpen et al., 2005; Li et al., 2009). These GTPases share a conserved bidomain architecture (Daumke and Praefcke, 2016). The globular N-terminal G-domain is responsible for spontaneous GTPase activity. The C-terminal domain contains several α-helices which allow assembly in tetramers. Tetramerization causes inhibition of GTPase activity until protein-lipid interactions allow conformational changes resulting in spontaneous hydrolysis (Daumke and Praefcke, 2016; Praefcke and McMahon, 2004).

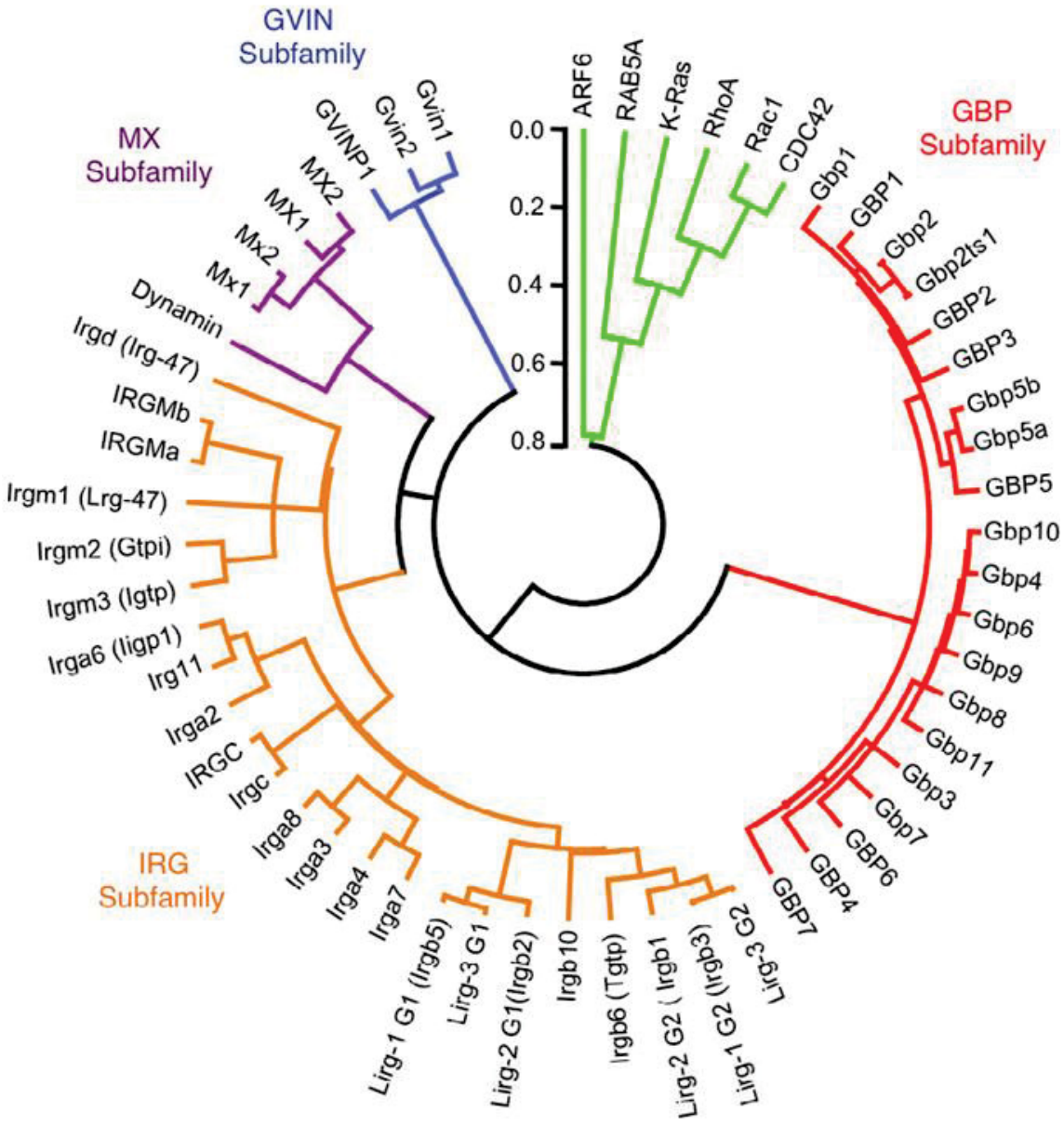

Figure 2: phylogenetic tree of conserved G domains of expressed GTPases in human (capital letters) and mouse (only leading capital letter), modified from (Kim et al., 2011) Figure S1A.

The largest inducible GTPases are 200-285 kDa in size and called GVIN (or VLIG) for which there are two genes in mice, but appears to be a pseudogene in humans, since it contains duplicated GTPase domains which lack canonical nucleotide-contact sites usually required for GTP-binding (Klamp et al., 2003).

Mx proteins are 72-82 kDa in size, represented by two copies in both mice and humans, are elicited solely by type I and III interferons and very efficiently block several steps in the viral replication cycle thus functionally restricting itself to a diverse range of viruses (Haller et al., 2015).

Surprisingly, based on transcript number it was discovered that of the inducible GTPase families, the IRGs and GBPs dominate the interferon response (Boehm et al., 1998) for which they will be discussed in greater depth in the following.

1.2.1.1 Immunity-related GTPases (IRGs)

The *IRG* family consists of 21 murine genes (plus pseudo genes Irga5 and Irgb7) on chromosomes 7, 11 and 18 that are strongly inducible by IFNγ through the classical GAS and ISRE elements in promoters. In humans 1 full length gene on chromosome 19 (*Irgc*) and 1 truncated gene (*Irgm*) on chromosome 5, in both cases organized as tandem gene clusters which translate into proteins of 21-47 kDa in size are described (Bekpen et al., 2005). Additionally, IRG-homologs were found and named IRGQ, for their similarity to IRG proteins but stressing their lack of GTP binding and hydrolysis (Bekpen et al., 2005). Among these transcripts splice events occur, which give rise to additional IRG proteins, the most prominently example of which is *Irgm*, that gives rise to several isoforms (Kim et al., 2012a). These numerous splice events might be explained by the finding that human IRGM experienced diverse evolutionary pressures over time, most obvious of which are a disruption through retrotransposition in conjunction with a retrovirus insertion altering its expression (Bekpen et al., 2010), thus becoming a pseudogene (Bekpen et al., 2005; Bekpen et al., 2009). In addition, tissue specific expression was observed for IRGA6 in the liver (Zeng et al., 2009) and IRGC IFNγ-independent expression exclusively in the testis which implies functions outside of immunity (Bekpen et al., 2005) as opposed to the 21 functional murine IRG genes.

Exploration of the murine protein family was pioneered by Taylor and his research group, investigating IRGM3 (Taylor et al., 1996), which was found to locate to the ER independent of GTP binding (Taylor et al., 1997) dependent on myristolation, for which sites are predicted in approximately half of the IRG proteins (Martens et al., 2004). Other research groups subsequently found IRGM1/LRG-47 to associate with the Golgi membrane, but upon phagocytosis to relocalize onto the plasma membrane and ensuing phagocytic vacuole (Martens et al., 2004) and in an nucleotide-binding dependent likely transient way onto endosomal and lysosomal compartments (Zhao et al., 2010). These typical localizations were soon found to confer resistance to pathogens, since IRGM1 and IRGM3 deficient mice were susceptible to mycobacterium and toxoplasma infection (MacMicking et al., 2003; Taylor et al., 2000). Since then, extensive work on different members of this protein family revealed a role for IRGs in haematopoiesis and infections with *Toxoplasma gondii, Mycobacterium tuberculosis*, *Chlamydia trachomatis* and murine cytomegalovirus (Coers et al., 2011; Howard et al., 2011; Singh et al., 2006;

Taylor et al., 2007), the eukaryotic of which will be described in more detail in the dedicated sections (1.3).

It became clear that this protein family is functionally divergent, and can be divided into 2 groups based on the catalytic properties of their G-domain. The largely conserved G1-domain contains a GX4GKS-motif (GKS) which is responsible for nucleotide binding, during evolution a methionine substitution resulted in a noncanonical sequence, GX4GMS-motif (GMS), which gave rise to the IRGM subfamily (Boehm et al., 1998). Upon dimerization with IRGM proteins the GMS sequence stabilizes GDP in GKS containing IRGs, thus keeping them in an inactive state and down regulating IRG activity (Hunn et al., 2008) resembling the function GAPs exert on small GTPases (Gasper et al., 2009). When GKS containing IRGs are not repressed by IRGM proteins, they spontaneously oligomerize in a nucleotide dependent way and thus are activated. They then can accumulate onto PCVs of phylogenetically diverse pathogens, as exemplified by IRGA6, IRGB6 and IRGB10 in *Chlamydia* infection (Bernstein-Hanley et al., 2006; Coers et al., 2008; Miyairi et al., 2007), which will be discussed in greater depth in paragraph 1.3.2. In addition, IRGA6 has been found to bind and preserve a microtubule-binding protein named HOOK3. HOOK3 was discovered in *Salmonella* infection, during which the pathogen secretes SpiC to bind and disable HOOK3 to prevent fusion of its phagosomal vacuole with lysosomes (Kaiser et al., 2004; Shotland et al., 2003).IRGA6 stabilizing HOOK3 is therefore an example of the pathogen vs. host ‘arms race’. IRGM1 was found to act collectively with IRGM3 in regulating GKS containing IRG expression and localization. Therefore mice deficient for both were very susceptible to infections (Henry et al., 2009). It was proposed that absence of IRGM1-3 proteins might directly cause the mislocalization of GKS containing IRGs, e.g. IRGA6 and IRGB6 (Coers, 2013; Hunn and Howard, 2010). Indeed, in absence of both IRGM1 and IRGM3, another inducible GTPase, namely of mGBP2, accumulated onto intracellular compartments also positive for p62 (previously called SQSTM1) and LC3, thus likely initiating the induction of autophagy (Traver et al., 2011). By using both chlamydia and toxoplasma infections it was discovered that IRGM1 and IRGM3 always localize on ‘self’-membranes where they guard the organelle by continuously inhibiting GKS activity, however on non self pathogen-modified membranes the GKS containing IRGs immediately converge (Coers, 2013; Haldar et al., 2013). In addition to the ‘self’ and ‘non-self’ paradigm, additional IRG regulation is conceivable through binding of specific lipids (phosphatidylinositide (PIP)2 and PIP3) (Tiwari et al., 2009), but also murine IRGM1 and human IRGM binding to cardiolipin, a membrane constituent of many bacteria (Matsumoto et al., 2006), and the potential to recognize membrane curvature (Kim et al., 2012a).

GKS IRG action results in recruitment of an E3 ubiquitin ligase, in this case TRAF6, subsequent ubiquitination, p62 recruitment and coating of LC-3 and potential additional effectors on the non-guarded membrane which can lead to lysis of the PCV (Haldar et al., 2015). Pathogens have adapted to this recent host resistance mechanism thus displaying an exquisite evolutionary interplay which will be addressed later. Important to note now, is that the loss of IRGM1-3 does not only disrupt PCV recognition, but also other events such as direct pathogen recognition through cytosolic LPS (dos Santos, J.V., Broz, P, personal communication, March 22, 2017) (Johnston et al., 2016; Meunier and Broz, 2016; Pilla et al., 2014) or lysosomal damage (Maric-Biresev et al., 2016).

1.2.1.2 Guanylate Binding Proteins (GBPs)

The GBPs were amongst the first described inducible GTPases (Gupta et al., 1979; Knight and Korant, 1979). This family comprises of 7 functional GTPases and one pseudogene (Figure 2) in humans (Cheng et al., 1983; Degrandi et al., 2007; Haudek-Prinz et al., 2012; Indraccolo et al., 2007; Lubeseder-Martellato et al., 2002; Nguyen et al., 2002; Schwemmle and Staeheli, 1994; Slany et al., 2016; Staeheli et al., 1983) clustered on chromosome 1 (Olszewski et al., 2006). In mice, 11 genes and 2 pseudogenes (Figure 2) have been described located in 2 clusters on chromosome 3, mGBP1, mGBP2, mGBP3, mGBP5 and mGBP7, and on chromosome 5, mGBP4, mGBP6, mGBP8, mGBP9, mGBP10 and mGBP11, the last of which likely arose due to a gene cluster duplication event (Boehm et al., 1998; Cheng et al., 1991; Degrandi et al., 2007; Han et al., 1998; Konermann et al., 2007; Kresse et al., 2008; Vestal et al., 1998; Wynn et al., 1991) (see Figure 3). Representatives of the GBPs are conserved throughout vertebrate evolution, including the bird lineage, as opposed to IRGs (Asundi et al., 1994; Kaspers, 1996; Li et al., 2009; Robertsen et al., 2006; Schwemmle et al., 1996; Shenoy et al., 2012; Vestal et al., 1996).

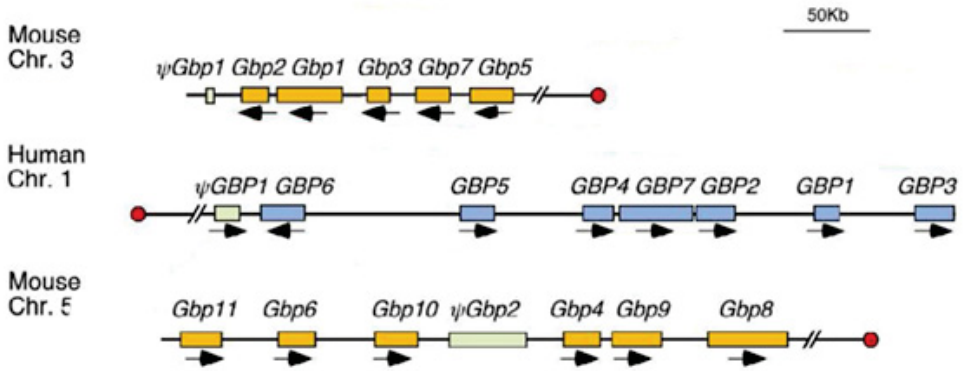

Figure 3: Genomic organisation of mGBPs in human (capital letters) and mouse (leading capital letter only), modified from (Kim et al., 2011)-Figure S1B.

Gene induction occurs in many cell types, e.g. endothelial and relevant peripheral immune cells such as monocytes (Degrandi et al., 2007; Haudek-Prinz et al., 2012; Indraccolo et al., 2007; Slany et al., 2016) during infections (e.g. *Salmonella* and *Toxoplasma*) and after stimulation with IFNγ, IFNβ and for some family members (e.g. mGBP1, mGBP2 and mGBP6/10) also after stimulation with IL1β, TLR4 agonist LPS or TLR9 agonist CpG oligodeoxynucleotide (Degrandi et al., 2007). However, previously observed induction by TNFα could not be confirmed (Nguyen et al., 2002). The amount of induction varied depending on the stimulant (combination) and potential basal expression, as observed for mGBP3 and mGBP5 in spleen and liver (Degrandi et al., 2007). Differences in induction lead back to differences in transcription factor-binding moieties in promoters of the respective GBPs, such as having either a GAS element, an ISRE element or both and in individual cases also a NF-κB binding site (Shenoy et al., 2007).

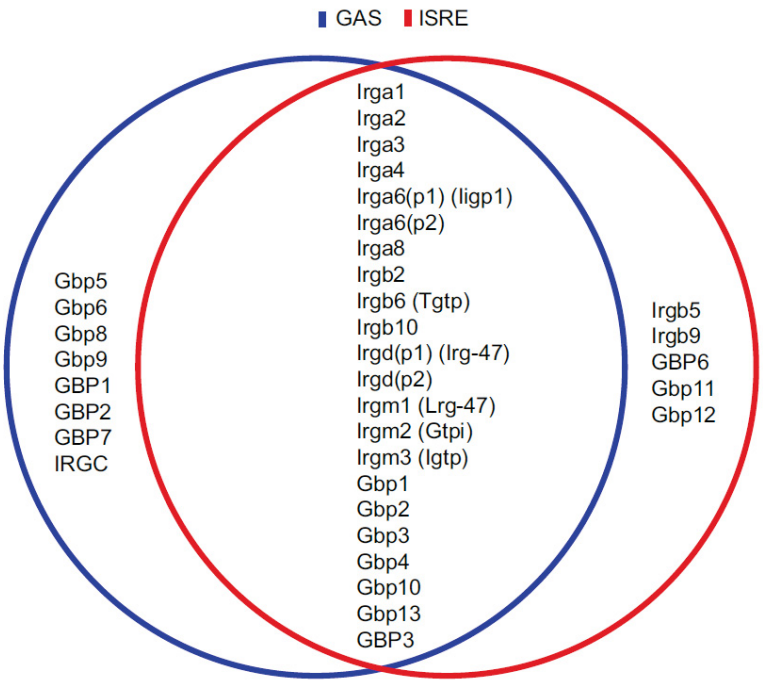

Figure 4: IFN-inducible transcription factor-binding sites within GTPases of the IRG and GBP families in human (capital letters) and mouse (leading capital letter only) summarized schematically, GAS : gamma interferon-activated sites and ISRE : interferon-stimulated response element, modified from (Shenoy et al., 2007) Figure 4.

In the case of mGBP7, several additional transcription factor-binding sites for activating protein-1 (AP-1) were described (Beuter-Gunia, 2008). The difference in binding sites among GBP promoters allow differential expression (Kim et al., 2012a).

Several splice variants of GBPs were identified, such as hGBP-3ΔC, with a largely modified C-terminal α-helical domain showing prominent antiviral activity by repressing the activity of the viral polymerase complex within epithelial cells requiring GTP-binding, but not hydrolysis (Nordmann et al., 2012), two variants of mGBP4, one with a premature stop codon after 312 bp and the other resulting in a transcript with a disrupted G2 domain named mGBP4.1 for which this is considered a pseudogene (Degrandi et al., 2007; Konermann et al., 2007). MGBP-5 lacks the second GTP binding motif and differs at the C-terminus (Nguyen et al., 2002) and hGBP5 is spliced into three variants, e.g. hGBP5a, -5b,and -5ta, leading to two different proteins (hGBP-5a/b, GBP-5ta) of which GBP-5ta is C-terminally truncated by 97aa and has therefore lost its isoprenylation site and is predominantly present in tumor tissues (Fellenberg et al., 2004; Wehner and Herrmann, 2010).

Upon IFNγ stimulation, together with the IRGs, the immune response is dominated by GBP transcripts, which give rise to 64 - 73kDa proteins (Degrandi et al., 2007; Martens

and Howard, 2006). The first protein structure described was that of hGBP1 using X-ray crystallography (Prakash et al., 2000). Taken as a role model of all GBPs, hGBP1 was further described to consist of a globular N-terminal GTPase domain, with a conserved GKS motif containing G1, G2 and a G3 domain G3 but with substitution in the G4 domain which results in lower affinity for GTP-binding, and several C-terminal amphipathic helices (Kunzelmann et al., 2006; Praefcke et al., 2004; Schwemmle and Staeheli, 1994). hGBP1 has the ability to hydrolyse GTP, via GDP to GMP and through this action initiate dimerization via the GTPase domain, and subsequently tetramerization via C-terminal α-helices (Ghosh et al., 2006; Kunzelmann et al., 2006; Praefcke et al., 2004; Syguda et al., 2012a; Syguda et al., 2012b; Vestal, 2005; Vopel et al., 2014; Vopel et al., 2009; Vopel et al., 2010; Wehner et al., 2012) in a temperature dependent way (Rani et al., 2012). Similar features are also observed in hGBP2 (Abdullah et al., 2010; Neun et al., 1996) mGBP2 (Kravets et al., 2012) and mGBP5 (Nguyen et al., 2002).

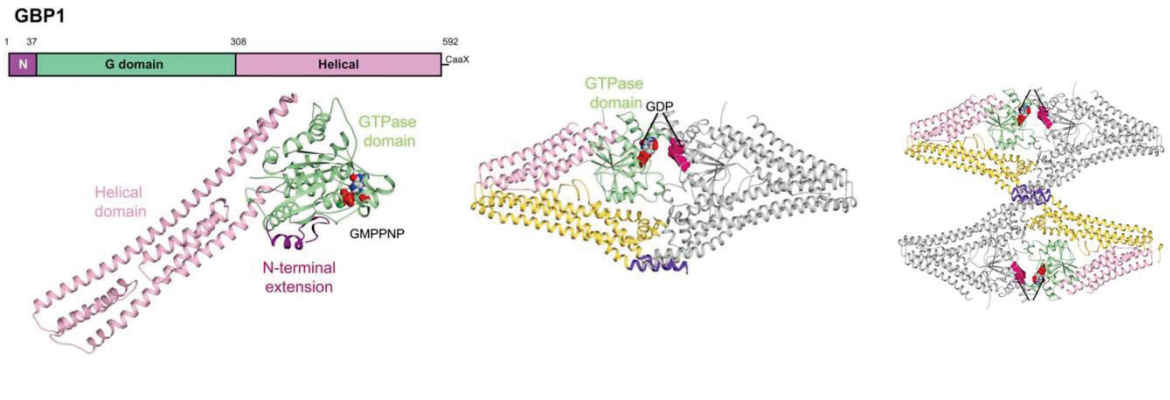

Figure 5: Structure and oligomerization of hGBP1. Top left) linearized depiction of bidomain structure, Bottom left) structure of hGBP1 monomer, Middle) Dimerization over GTPase domains, Right) Suggested tetramerization over N-terminal extension, modified from (Daumke and Praefcke, 2016) Figure 1 & 3.

Multimerization of mGBPs can occur with itself (homomerization), but also with other GBPs (heteromerization) either in the cytoplasm or, in the murine situation, onto PCVs thus forming supramolecular complexes and rupturing the vacuolar membrane (Broz, 2016; Kravets et al., 2016). The same study showed that in uninfected cells mGBPs show a punctuate cytosolic distribution called vesicle-like structures (VLS). Within VLS mGBP2 is often preassembled in homodimers, less often as heterodimers with mGBP1 and seldom as heterodimers with mGBP3. These structures are distinctly different from other VLS which contain mGBP6 (Kravets et al., 2016) or mGBP7 (Reich, A., Kravets, E., personal communication, march 15, 2015) and are pre-assembled in uninfected cells. However, upon infection VLS dwindle in numbers, as previously explained by redistribution of mGBP2 molecules from the cytoplasm to the PV in time lapse videos of

mEFs reconstituted with GFP::mGBP2. The mGBP1, mGBP2, mGBP3 or mGBP6 are compartmentalized in distinct VLS, whereas mGBP5 resides in the cytosol, but all studied mGBPs colocalize at PCVs (Kravets et al., 2016). In vitro, mGBPs were shown to accumulate onto PCVs, disrupt or permeabilize the PCV membrane and to target the plasma membrane of toxoplasma parasites (Finethy and Coers, 2016; Kravets et al., 2016)

An additional feature in hGBP1, hGBP2, hGBP5, mGBP1, mGBP2, and mGBP5 is the C-terminal CaaX-box, which allows isoprenylation (farnesylation or geranylgeranylation) and subsequent membrane anchoring (Nantais et al., 1996; Stickney and Buss, 2000; Tripal et al., 2007). The VLS observed in uninfected cells show no colocalization with a variety of organelle markers, but through isoprenylation can relocalize to other compartments within the cell, e.g. at Golgi membranes (Balasubramanian et al., 2011; Britzen-Laurent et al., 2010; Degrandi et al., 2007; Gorbacheva et al., 2002; Modiano et al., 2005; Vestal et al., 2000). Disruption of GTP binding by mutation of S52N in mGBP1 and mGBP7 (Kim et al., 2011) or K51A in mGBP2 abrogates the formation of VLS (Kravets et al., 2012), whereas mGBP2 S52N does not (Balasubramanian et al., 2011). Localization is important since loss of this ability reduces resistance to intracellular pathogens dramatically (Beuter-Gunia, 2008; Carter et al., 2005; Degrandi et al., 2013; Kim et al., 2011; Klümpers, 2013; Kravets et al., 2016; Kravets et al., 2012; Lindenberg et al., submitted; Meunier et al., 2014; Meunier et al., 2015; Tietzel et al., 2009; Virreira Winter et al., 2011; Zhao et al., 2009a; Zhao et al., 2009b), details which will be discussed in context with pathogens in 1.3.

Besides the GTPase domain and CaaX-box, no further functional domains have been described in GBPs. However, a mutational analysis stemming from a comparison between mGBP6 and mGBP10 for PCV membrane association, pointed to the potential of a domain in the C-terminal α-helix prior to the N-terminal extension (Klümpers, 2013), which has been examined closely in this thesis.

Originally, it was thought that GBP-mediated lysis of the PCV, as occurs with *Salmonella typhimurium* containing vacuoles (Meunier et al., 2014), and subsequent pathogen lysis, as described with *Francisella novicida* (Meunier et al., 2015), releases PAMPs into the cytosol for inflammasome receptors to respond to. However, localization-independent action of GBPs was found to activate the AIM2 inflammasome (Johnston et al., 2016; Man et al., 2015; Meunier et al., 2015) and Casp11-NLRP3 inflammasome through IRGB10 (Man et al., 2016b) which leads to pyroptotic cell death (Kim et al., 2016a) or

even through non-lytic functions (Pilla et al., 2014). Specifically mGBP5 is associated with NLRP3 assembly after infection (Shenoy et al., 2012). Concerted action between AIM2 and NLRP3 inflammasomes is conceivable as it has been previously described in fungal infections (Karki et al., 2015)

If mice are deficient for a cluster of GBPs on chromosome 3, as well as for mGBP1 or mGBP2 individually, they are more susceptible to *T. gondii* infection (Degrandi et al., 2013; Selleck et al., 2013; Yamamoto et al., 2012). However, in similar infections differences occurred between mice lacking the cluster versus single mGBPs, which may indicate disrupted regulatory interactions among family members (Britzen-Laurent et al., 2010; Virreira Winter et al., 2011) or nonspecific intergenic effects being associated with the 173kb deletion in Gbpchr3 mice (Yamamoto et al., 2012). In part, these differences can be explained by remaining flanking regions from the original 129-derived embryonic stem cell after backcrossing onto a C57BL/6 background, which drive expression of GBPs differently than C57BL/6 loci (Pilla-Moffett et al., 2016). Chromosomal deletions of each mGbp locus without 'foreign' flanking regions will thus be needed to correctly ascribe the effects in PCV lysis, pathogen lysis and or assembly of immune signalling platforms that are observed after GBP cluster deletion, to individual mGBP members (Kim et al., 2012a).

Beside immune functions, also other, less well described roles for GBPs have been found in cytoskeleton modification (Forster et al., 2014; Ostler et al., 2014), inhibition of cell proliferation and vascularization (Gorbacheva et al., 2002; Guenzi et al., 2001; Guenzi et al., 2003; Messmer-Blust et al., 2010), and in binding pro-survival kinase PIM1 to allow cancer cells to become increasingly resistant (Persico et al., 2015; Tipton et al., 2016).

This thesis will focus on the role of mGBPs in immune responses against *Toxoplasma gondii, Chlamydia trachomatis and Mycobacterium bovis* and *tuberculosis* infections. These pathogens will be introduced in the next chapter.

1.3 *Infection models with intracellular replicating pathogens*

Worldwide, infections with intracellular pathogens are among the top ten leading causes of mortality (WHO, 2017- www.who.int/mediacentre/factsheets). For pathogens, hiding within a host cell provides protection from humoral and cellular immunity. Which is topped off, by the added advantage of circumventing cytosolic immunity when hiding in a modified intracellular vacuole (Di Russo Case and Samuel, 2016). Despite intensive research efforts, host resistance mechanisms to these microorganisms are poorly understood. However, inducible GTPases have been found to play a profound role in resistance against intracellular pathogens (Degrandi et al., 2013; Hunn et al., 2011; Kim et al., 2012a; Kravets et al., 2016; Meunier and Broz, 2016; Pilla-Moffett et al., 2016; Spekker et al., 2013). However, the functions of these GTPases on phagosomal maturation, initiation of autophagy (Cardoso et al., 2010; Deretic, 2016; Paulus and Xavier, 2015), rupture of PCVs and subsequently pathogens themselves (Kravets et al., 2016), sensing of cytosolic PAMPs (Pilla et al., 2014) and crosstalk to inflammasomes and cell death are only partly understood. Therefore, this thesis will examine the role on one family of these GTPases, GBPs in intracellular infections with *Toxoplasma gondii, Chlamydia trachomatis* and Mycobacteria, which will be introduced below.

1.3.1 Toxoplasma (Toxoplasmosis)

Toxoplasma (T.) gondii belongs to the phylum Apicomplexa and is an enteric coccidian, an intracellular protozoan parasite that infects around 30 % of the human population, mostly persistently without symptoms, although in immunocompromised people an infection can be fatal (Antczak et al., 2016). In the Western world, three clonal variants of *T. gondii* are described: type I, II or III strains which are characterised by their different virulence in animal models (Howe and Sibley, 1995; Sibley et al., 2009). In fact, *T. gondii* can infect almost all nucleated cells of warm-blooded mammals, and has spread worldwide, thus giving rise to a largely diverse spectrum of strains (Pappas et al., 2009; Reid et al., 2012; Saraf et al., 2017). For this reason, virulence of *T. gondii* and host susceptibility vary greatly, and is examined in this thesis using a common model for experimental study: the intermediately virulent type II strain ME49 (Szabo and Finney, 2017).

1.3.1.1 *Toxoplasma gondii* organelles required for cellular entry

Single-celled *T. gondii* are obligate intracellular organisms which, at one apex, accommodate a complex of organelles that help to penetrate host cells (Madigan et al., 2012). This apical complex is made up of micronemes and bulbous rhoptries which contain specialised secretory proteins (Seeber and Steinfelder, 2016), (See Figure 6). Additionally, *T. gondii* contains dense granules as a third secretory organelle and two devolved endosymbionts, namely mitochondria and the apicoplast, a vestigial plastid homologous to the chloroplasts (McFadden and Yeh, 2017; Seeber and Steinfelder, 2016). Research has unveiled some features of the many proteins secreted by these specialized organelles, however their functions remain largely unknown (Behnke et al., 2016; Mercier and Cesbron-Delauw, 2015).

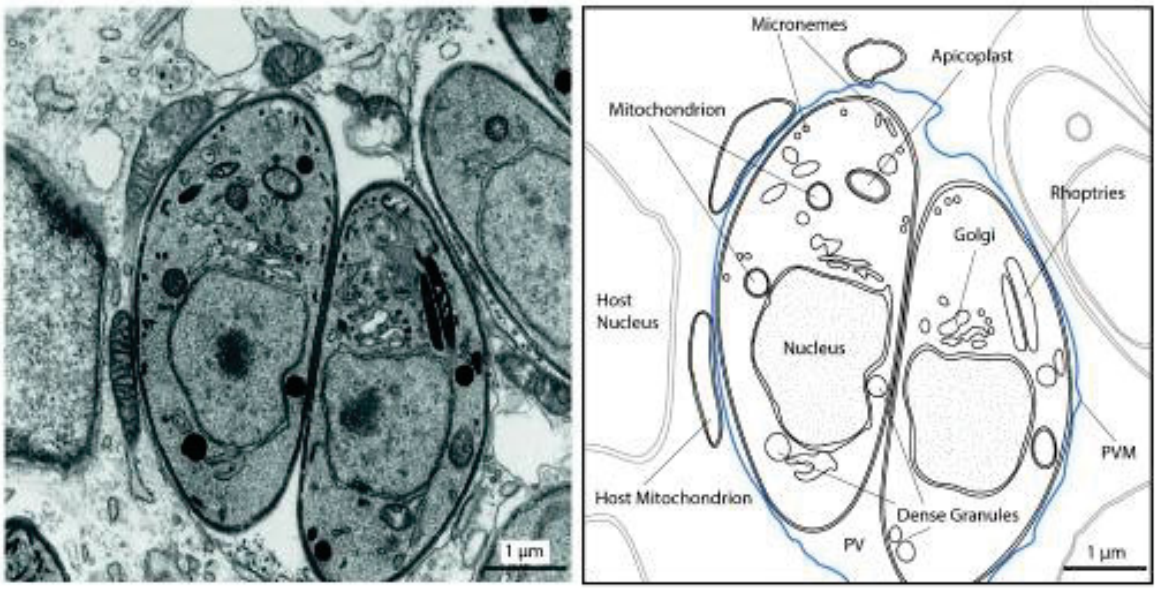

Figure 6: *Toxoplasma gondii* morphology Left) as seen through transmission electron microscopy and Right) schematic representation, PVM : parasitophorous vacuole membrane, bar : 1 µm, modified from (Seeber and Steinfelder, 2016) Figure 1.

Upon cell contact, *T. gondii* receptor proteins like apical membrane antigen 1 (AMA1), engage glycoconjugates on the hosts plasma membrane to facilitate attachment, allowing the micronemes to release proteins which facilitate cell entry (Carruthers and Tomley, 2008). Next, rhoptries secrete neck proteins (RONs, predominantly RON2/4/6 which form a trans membrane complex interacting with AMA1) which provide anchorage and the establishment of a moving junction (Shen and Sibley, 2012), and inject ROP effector proteins such as ROP18 into the host cell cytosol (Bradley and Sibley, 2007). Through this moving junction the parasite glides into the host cell, thus invaginating the host plasma membrane, to form its vacuole (Shen and Sibley, 2012). Initially, this gliding motion was thought to rely on an actin-myosin motor complex located beneath the

parasites plasma membrane (Heintzelman, 2015; Shen and Sibley, 2012), however, later studies showed this motor complex is not essential (Egarter et al., 2014). Rather, the motor complex promotes surface attachment thus increasing the efficiency of invasion (Whitelaw et al., 2017) which however depends on toxoplasma's actin (Drewry and Sibley, 2015) and calmodulin-like proteins (Long et al., 2017). During this invagination, the host plasmamembrane is 'filtered' to exclude membrane molecules, for example IRGM and trans membrane molecules required for endosome-lysosome recruitment (Mordue et al., 1999). The importance of injected ROPs has been shown by absence of invasion when using a small molecule inhibitor to block their secretion (Ravindran et al., 2009). Subsequently, dense granule proteins (GRAs) are secreted to shape the newly formed parasitophorous vacuole (PV) and its membrane (PVM) to shelter the parasite (Nam, 2009). All in all, invasion is a rapid process completed in about 30 seconds, fundamentally different from phagocytosis since it is driven by *T. gondii* and can occur in essentially all nucleated cells (Tardieux and Baum, 2016).

1.3.1.2 A parasitic life cycle through various hosts

The well-tuned cell invasion mechanism described above works on many but not all cells, in many but not all species. Although toxoplasma can infect a wide range of hosts, courageous pioneering work by J. Frenkel, J.P. Dubey and Nancy Miller in the late 1900s testing many hard-to-handle species revealed that only felines shed oocysts (Dubey, 2009). Since then it has been learned that initially, ingested *T. gondii* undergo clonal replication by endodyogeny, followed by repeated endopolygeny in epithelial cells of the small intestine (Tenter et al., 2000). Subsequently, *T. gondii* reproduces sexually via gamogenythus forming oocysts in gut epithelial cells of cats (Dubey et al., 1970; Elmore et al., 2010). Lysis of these cells releases unsporulated oocysts into the gut which are then shed with the faeces into the environment (Tenter et al., 2000). The oocysts are spore-like particles, resistant to dehydration, mechanical forces, disinfectants, etc., which can contaminate water and food and survive various environmental conditions. After a trigger the oocysts undergo sporulation resulting in eight highly infectious sporozoites with an abundance of micronemes, rhoptries, and granules (Dubey et al., 1998).

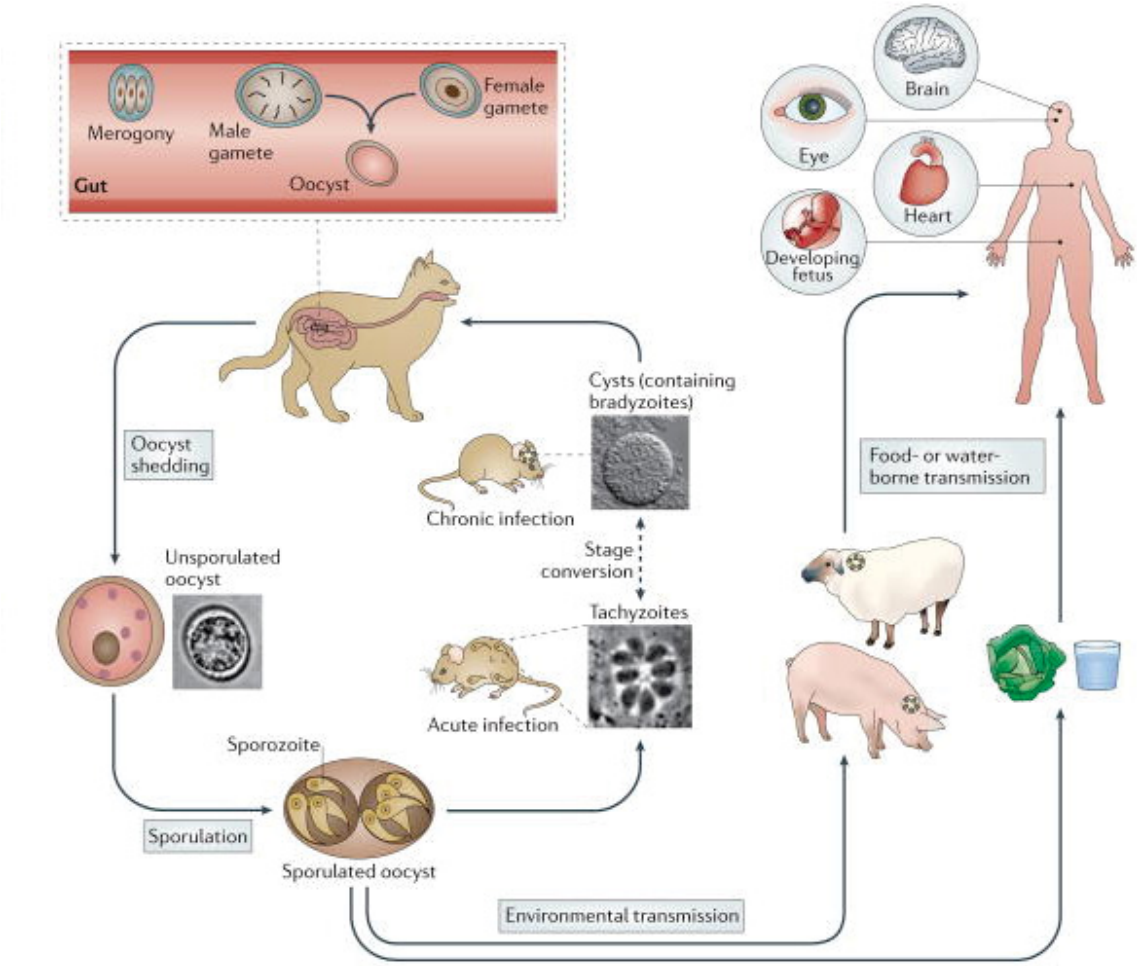

Figure 7: Lifecycle of *Toxoplasma gondii*. Modified from (Hunter and Sibley, 2012).

These oocysts are then ingested by an intermediate host, naturally mice, and during digestion the oocyst wall is destroyed, releasing the sporozoites (Tenter et al., 2000). Subsequently, sporozoites undergo stage conversion to the fast-growing tachyzoite, replicating and disseminating throughout the whole host, thus causing acute disease which is however quickly controlled by a healthy immune system (Lyons et al., 2002). When host immune responses against the tachyzoites arise, they convert into latent encysted bradyzoites (White et al., 2014), thus forming cysts throughout the organism, predominantly in long lived cells such as the skeletal muscle and central nervous system tissues (Weiss and Kim, 2000). Bradyzoites were thought to be a semi-dormant, metabolically inactive stage of *T. gondii*, but this was recently challenged by evidence for cyclical, episodic bradyzoite growth within tissue cysts, *in vivo*. (Watts et al., 2015). This encysted stage endures, until occasionally bradyzoites re-emerge from and convert back into rapidly growing tachyzoites thus constituting persistent, chronic infection (Lyons et al., 2002). During this chronic phase, *T. gondii* manipulates the epigenetic landscape of cells in the host brain to rewire the neurological circuit thus transforming the response induced by cat odour from sensations of fear into those of sexual attraction (Flegr and

Markos, 2014). When an infected mouse is predated by a cat, the parasitic life cycle is completed (Hunter and Sibley, 2012).

T. gondii oocysts can infect humans as accidental, intermediate hosts by horizontal transmission, e.g. contaminated water and food or contact with infected mammals (Derouin et al., 2008; Jones and Dubey, 2012; Tenter et al., 2000). The acute disease called toxoplasmosis is usually asymptomatic but can cause mild symptoms (e.g. fever, muscle weakness and enlarged lymph nodes), ocular disease or even encephalitis and death (Saadatnia and Golkar, 2012), which symptoms are observed recurrently in outbreaks of toxoplasmosis (Meireles et al., 2015). An additional danger exists towards immunocompromised individuals, e.g. transplant recipients or AIDS patients (Derouin et al., 2008; Montoya and Liesenfeld, 2004). Also pregnant women should prevent infection since tachyzoites can cross the placenta into the foetus, which has no effective immune system allowing a rampant acute infection causing severe neurological damage and can lead to stillbirth (McLeod et al., 2012). For these groups, the risk is being counteracted by health education, cooking/freezing food, diagnostics and reducing exposure risk by vaccinating cats and food animal populations (Opsteegh et al., 2015).

1.3.1.3 Intracellular battleground*, Toxoplasma gondii* vs. it's host

Once having gained entry into the cell through moving junction formation and injection of evacuoles composed of microneme proteins, ROPs and GRAs (described 1.3.1.1) like beads-on-a-string into the host cytosol, those proteins associate with the PVM (Hakansson et al., 2001; Ravindran and Boothroyd, 2008). *T. gondii* further optimizes its PVM to allow the diffusion of nutrients, like tryptophan, cholesterol and iron, therefore the dense granule proteins GRA17 and GRA24 are inserted into the PVM to form a pore (Gold et al., 2015). An additional transporter in the PVM is formed from Myc regulation 1 (MYR1) in order to export parasitic proteins into the host cytosol (Franco et al., 2016; Zhou et al., 2016). To facilitate protein transport, *T. gondii* forms membranous nanotubules called an intravacuolar network (Plattner and Soldati-Favre, 2008). At the same time, host intermediate filaments and microtubules are reorganized to optimally position the PV within the cytosol: in close proximity to the host microtubule organizing centre (MTOC), mitochondria and the endoplasmatic reticulum for efficient nutrient shuttling, which at least partly depends on trans PVM protein GRA7 (Laliberte and Carruthers, 2008). Most prominent is the endoplasmatic reticulum, which covers more than half of the PV surface, and is drawn in by *T. gondii* factors GRA3, GRA1 and ROP2 (Nunes-Hasler and Demaurex, 2017). In this way *T. gondii* establishes a replicative niche

which is nutrient rich and being cloaked from adaptive and cytosolic immune responses (Lim et al., 2012).

The host cell can detect *T. gondii* prior to cell invasion via TLR2 and TLR4 sensing of glycosylphosphatidylinositol, and intracellular by endosomal TLR7 and TLR9 detecting *T. gondii* RNA and genomic DNA, however, this elicits only mild cytokine responses (Beutler et al., 2006; Gazzinelli and Denkers, 2006). Instead, dependent on ER-protein UNC93B1, murine TLR11 and TLR12 recognize an unconventional actin-binding protein called profilin, that is passively released from parasites during host cell invasion (Andrade et al., 2013; Koblansky et al., 2013; Pifer et al., 2011; Plattner et al., 2008; Yarovinsky et al., 2005). Any single deletion of these TLRs did not abrogate the cytokine release, but deficiency of its shared adaptor protein MYD88 disrupted cytokine responses and made mice severely susceptible to *T. gondii* infection (Dupont et al., 2012; Scanga et al., 2002). The subsequent IFNγ-driven immune response effectively restricts *T. gondii* growth by limiting essential amino acids tryptophan and arginine by induction of IDO and inducible (i)NOS, respectively, as well as production of microbicidal ROS, RNI and other IFNγ induced proteins (Yarovinsky, 2014,Takacs, 2012 #107). Among the induced genes, the GTPases play a preeminent role in defence against this parasite (MacMicking, 2012).

On the PVM, either the absence of ‘self-’ IRGM1-3 proteins (Coers, 2013) or the prior LC3 conjugation by autophagy proteins, notably ATG7, ATG3, and the ATG12-ATG5-ATG16L1 (Choi et al., 2016,Zhao, 2008 #6441; Choi et al., 2014; Haldar et al., 2014; Ohshima et al., 2014) attracts ‘executor’ GKS IRGs, predominantly IRGA6 and IRGB6, which after IFNγ stimulation activate, multimerize and are deposited onto the PVM (Martens and Howard, 2006; Papic et al., 2008; Pawlowski et al., 2011; Pilla-Moffett et al., 2016). In concert, mGBP1, mGBP2, mGBP3, mGBP5, mGBP6, mGBP7 and mGBP9 are recruited to the PVM, where they are involved rupture of the PV and exposed parasite, the mechanisms of which is described above (Paragraph 1.2.1.2). Opposed to increased infection in absence of mGBP2, an improved mGBP2 action by knocking out a newly identified interacting protein Rab GDP dissociation inhibitor α (RabGDIα) increased recruitment of mGBP2 and IRGA6 towards the PVM and subdued infection (Ohshima et al., 2015). These joint GTPase actions result in ubiquitination, PVM stripping to expose *T. gondii* PAMPs to the cytosol triggering a profusion of immune mechanisms like intracellular PRRs and inflammasomes, ultimately initiating autophagy (Haldar et al., 2015; Ling et al., 2006).

The parasite evolved mechanisms to disturb different steps in the above described *T. gondii* directed cell autonomous immunity. Foremost, ROP16 targets specifically STAT3 and STAT6 and phosphorylates them, resulting in prolonged activation, to induce a less inflammatory milieu benefitting the PV (Saeij et al., 2006; Saeij et al., 2007). Also, anchored on trans-PVM GRA7, the ROP5/ROP18/ROP17 complex can bind IRGA6 to hold it in an inactive conformation to prevent assembly, similar to IRGM proteins, or ROP17 and GRA7 can phosphorylate the IRGs to accelerate their assembly and turnover (Alaganan et al., 2014; Etheridge et al., 2014; Fleckenstein et al., 2012; Hakimi et al., 2017; Hermanns et al., 2016; Reese et al., 2014; Steinfeldt et al., 2010). Comparisons between different *T. gondii* strains revealed effectors which can prevent mGBPs recruitment, e.g. ROP5, ROP16, ROP18, ROP54 and GRA15 (Kim et al., 2016b; Rosowski et al., 2011; Selleck et al., 2013; Virreira Winter et al., 2011; Zhao et al., 2009a). In addition, ROP18 has also been found to target activating transcription factor 6 β (ATF6β) to down regulate antigen presentation, which will be discussed in the next paragraph (Yamamoto et al., 2011). These microbial effectors that directly counteract cell autonomous immune responses are augmented by effectors which subvert host transcription, to alter processes like metabolism and immune signalling in order to render the cell more permissive (Blader and Koshy, 2014; Bougdour et al., 2014).

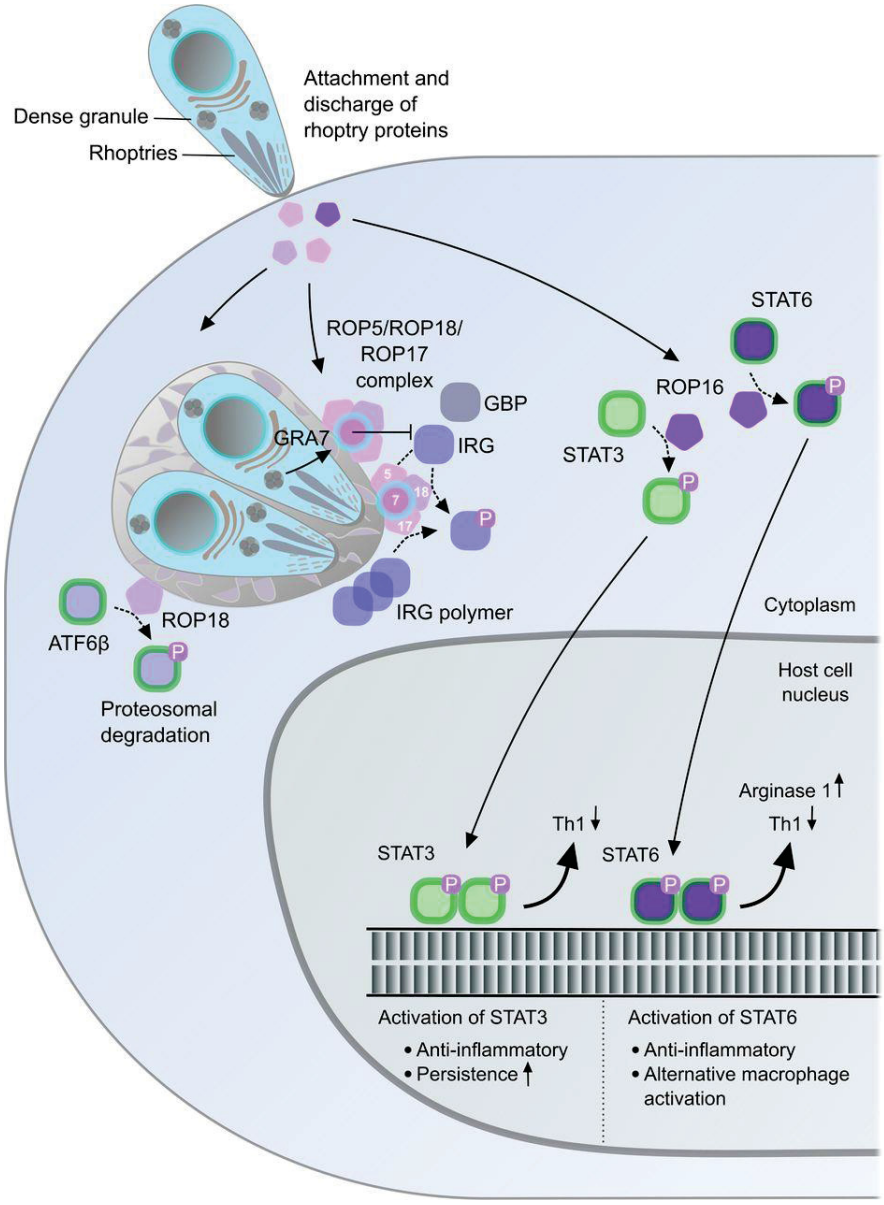

Figure 8: *Toxoplasma gondii* host cell entry and modulation. Modified from (Hakimi et al., 2017) Figure 1.

After having hijacked the cellular machinery, the close proximity to the endoplasmatic reticulum allows GRA6 to activate the calcium-dependent transcription factor NFAT (Ma et al., 2014; Nunes-Hasler and Demaurex, 2017), rendering cells unresponsive to PAMPs like LPS (Gazzinelli and Denkers, 2006).

GRA16 translocates into the host nucleus where its interactions stabilize p53 and therewith the expression of host genes involved in metabolism and cell cycle progression (Bougdour et al., 2013). Similarly, GRA24 and TgIST travel into the nucleus, forming hyper stable complexes with host proteins to alter transcription factor activities, e.g. of c-Fos, EGR1 and STAT1, and chromatin configuration in order to alternatively regulate cytokine production (Braun et al., 2013; Gay et al., 2016; Hakimi et al., 2017; Olias et al.,

2016). In addition, the host protein reservoir is also negatively regulated by ROP16 inducing micro-RNAs, e.g. *miR-17*, *miR-106b*, miR-155 and miR-146a, which target immune relevant mRNAs prior to translation (Cannella et al., 2014; Zeiner et al., 2010). Also, unidentified effectors derived from *T. gondii* have been implicated in altering hypoxia-inducible factor (HIF), EGR2, c-Myc, mTOR, ribosomal protein S6 and CREB-phosphorylation, the latter independent of GRA24 (Hakimi et al., 2017) which may in part explain the blocking of apoptosis in *T. gondii* infected cells (Nash et al., 1998).

Initially the PV is non-fusogenic thus preventing phagosomal maturation, but is rendered recognizable by ubiquitination accomplished as described above, allowing the cell to overcome *T. gondii* manipulations by inducing autophagy (Subauste, 2009). A different pathway leading to autophagy induction in *T. gondii* infection is CD40 (a member of the tumor necrosis factor receptor superfamily) signalling, dependent on the autophagy machinery but not IRGs or mGBPs (Late de Late et al., 2017). Via autophagy the fusion with lysosomes can be achieved and the parasitic cargo destructed, for antigen presentation on the cell surface allowing activation of nascent cells (Cadwell, 2016). The parasite tries to subvert autophagy by activating epidermal growth factor receptor (EGFR) AKT signalling, to prevent targeting of LC3 to the PV and thus avoiding autophagic clearance (Muniz-Feliciano et al., 2013). A recent finding suggests that host cells retaliate, by initiating a noncanonical autophagy pathway depending on core autophagy proteins involved in LC3 conjugation, which results in multiple host layers engulfing the PV (Selleck et al., 2015).

If all these host resistance mechanisms cannot protect the cell, it may eventually switch to a ‘loud’ cell death programme, e.g. necroptosis, which releases many DAMPs into the host tissue alarming and attracting additional immune cells to take over parasite clearance (Zhao et al., 2009b). However, a balance must be struck between parasite clearance and tissue protection, since excessive inflammation can cause more severe tissue damage than the infection (Dupont et al., 2012).

Evolutionary pressure exerted on the IRG family, resulted in many copy numbers and genetic polymorphisms of the coding sequences within closely related species, part of which diversity is lost in inbred C57BL/6 mice (Reese, 2013). In a mouse strain derived from wild type mice, a polymorphic tandem protein IRGB2-B1 was shown to increase *T. gondii* PV recruitment of IRGA6, likely by binding ROP5 pseudokinase at the vacuole, thereby blocking the GRA7/ROP5/ROP18/ROP17 complex from inactivating IRGA6 (Lilue et al., 2013). Similarly, evolutionary pressure resulting from *T. gondii* infection has

been proposed to have driven the emergence of TLR11 and TLR12 in mice (Gazzinelli et al., 2014). Another view, is the deliberate, release of immunostimulatory profillin by *T. gondii* to enable immunity to improve the mouse life span thus, increasing the chance of being predated by a cat, thus completing the parasitic life cycle (Sher et al., 2017). In humans, the IRG and TLR11 genes have devolved, whereas TLR12 is not present at all. Nonetheless, *T. gondii* infection is effectively controlled, constituting a puzzle how immunity to this pathogen is build up in humans (Muller and Howard, 2016).

1.3.1.4 Cellular immune defences against *Toxoplasma gondii*

The success of the intracellular battle against *T. gondii* determines whether parasitic antigens are processed and (cross-)presented on the surface of the infected cell (Luder et al., 2001; Pepper et al., 2008). In the case of death, the specific death-programme activated determines the inflammation induced in the tissue and thus the activation of additional immune cells to fight the parasite (Zhao et al., 2009b). DAMPs released by 'loud' cell death programmes attract, among others, dendritic cells and monocytes. On these phagocytes the surface TLR11/TLR12 can recognize profillin, a soluble PAMP released from *T. gondii,* thus activating the APC (Andrade et al., 2013; Dunay et al., 2008; Egan et al., 2009; Yarovinsky et al., 2005). Dendritic cells and macrophages can be infected by *T. gondii,* upon which they produce little IL12, but surrounding 'untouched' phagocytic cells and neutrophils are the main source of this cytokine (Bliss et al., 2000; Christian et al., 2014; Pepper et al., 2008). Early IL12 from unaffected APCs stimulates and activates NK cells, and later T cells, to produce IFNγ in order to establish an inflammatory milieu required for effective T_h1 response (Gazzinelli et al., 2014). The importance of this process is evidenced by decreased survival of mice deficient for IFNγ or its receptor (Deckert-Schluter et al., 1996; Suzuki et al., 1988). Additional neutrophils are recruited to the inflamed tissue, which release anti-microbial peptides and can produce a „neutrophil-extracellular-trap" (NET), a web made out of their chromatin connected with granular and selected cytoplasmic proteins (Abi Abdallah and Denkers, 2012), this process is called NETosis (Vorobjeva and Pinegin, 2014).

To influence the inflammatory milieu, the *T. gondii* effector GRA15 with its specific polymorphisms determines macrophage polarisation into either classically (type II *T. gondii*) or alternatively activated macrophages (type I/III *T. gondii*), through inducing nuclear translocation of NF-κB (Rosowski et al., 2011).

Additionally, *T. gondii* manipulates dendritic cells, the cells which bridge the innate and adaptive immune responses by priming B- and T-cells in the spleen and lymph nodes

(Dupont et al., 2012). The small numbers of infected dendritic cells have been shown to employ their migratory capacity to promote parasite dissemination after manipulation by intracellular *T. gondii* (Kanatani et al., 2015; Lambert et al., 2006). In addition, ROP18 has been found to target the transcription factor ATF6β which downregulates antigen presentation by DCs to T cells (Yamamoto et al., 2011). Confusingly, *T. gondii* also boosts antigen presentation on DCs by subversion of p62 (Lee et al., 2015) and improving the presentation capacity (Pepper et al., 2008). DC priming induces T_h cells to produce cytokines and cytotoxic T cells to migrate to the inflamed site in order to destroy infected cells. Notably, the DC-activated production of IFNγ by T_h1 cells has recently been questioned (Yarovinsky, 2014).The exact composition of cytokines in the inflamed tissue has major effects on cytotoxic T cell expansion and the killing of infected cells by releasing amongst others perforin, granzymes, granulysin (Grover et al., 2014). Similarly, B cells are influenced by T_h cells to differentiate into *T. gondii* antigen-specific plasma cells and secrete antibodies which opsonize parasites effectively forcing the tachyzoites to retreat into cysts, thus proceeding from acute to chronic toxoplasma infection (Johnson and Sayles, 2002; Kobayashi and Suzuki, 1987).

To tip the balance in this sequence of events leading to T_h1 primed inflammation, the previously described *T. gondii* effector ROP16 alters STAT3 and STAT6 signalling, to induce transcription of T_h2 polarizing responses. This induced T_h2 polarized response is less effective against parasitic infections (Denkers et al., 2012). In this way *T. gondii* creates a dynamic interplay, in which the parasite modulates host immune responses.

Recently, a novel field of investigation showed how these *T. gondii* manipulations are thwarted by an additional signalling pathway, which can complement intracellular nucleic acid sensing by TLR7 and TLR9 to lead to a very strong inflammatory response (Krishnamurthy et al., 2017). Inflammasome sensors NOD-like receptors NLRP1 and NLRP3 (also called NALP) have been found to recognize *T. gondii* (Ewald et al., 2014; Gorfu et al., 2014). Polymorphisms in NLRP1/3 genes are linked to susceptibility to *T. gondii*. Other pathogens have been shown to subvert the inflammasome signalling process, but the exact signalling and whether *T. gondii* evolved virulence factors which manipulate this process remains to be discovered (Garib et al., 2016; Shin and Brodsky, 2015; Zamboni and Lima-Junior, 2015).

1.3.2 Chlamydia (chlamydial infection)

Historically, chlamydia was thought to be a virus due to lack of detectable peptidoglycan and their persistence in harsh environments. Chlamydia have been unveiled as Gram-negative, obligate intracellular spherical shaped bacteria (Moulder, 1966). The genus *Chlamydia* consists of several species and many strains which have evolved to suit their diverse hosts. For example, *Chlamydia (C.) muridarum* is adapted to survive in mice and *C. trachomatis* in humans (Stephens et al., 2009). The human pathogen *C. trachomatis* has been extensively typed and about 19 distinct, geographically distributed, biovars were found, e.g. serovars A, B/Ba, C, D/Da, E, F, G/Ga, H, I/Ia, J, K, L1, L2/L2a and L3 (Rawre et al., 2017). Due to the amount of chlamydial species in both domestic animals and cattle, and a surprisingly large capacity for horizontal gene transfer (Nunes et al., 2013), there is a large zoonotic potential (Rohde et al., 2010) threatening both the meat industry and human health (Wheelhouse and Longbottom, 2012). The currently existing *C. trachomatis* biovars usually cause asymptomatic infections (Detels et al., 2011). Nevertheless, serovars A, B and C can infect the eye which leads to severe inflammation and scarring. Increased scarring leads to curvature of the eyelid, so that the eyelashes rub against the cornea causing blindness, this disease is called trachoma (Mohammadpour et al., 2016). Serovars D-K cause urogenital infections and serovars L1-L3 cause lymphogranuloma venereum (LGV). These infections induce scarring, which leads to ectopic, aborted pregnancy or even sterility in women. Particularly the genital infections increase in prevalence (Harris et al., 2012; O'Connell and Ferone, 2016). The Centers for Disease Control estimates 4 million new cases in the United States annually (Diebel and Williams, 1995). Chlamydial infections are the leading cause of sexually transmitted bacterial diseases globally (WHO 2012).

1.3.2.1 Intracellular biphasic lifecycle of *Chlamydia trachomatis*

The persistence of infectious chlamydia particles under harsh conditions has been attributed to the elementary body (EB), which is only about ~0.2 µm large due to hyper condensation of its chromatin reached through interactions with histone-like proteins (Grieshaber et al., 2004). In addition, evolutionary pressure reduced the genome of obligate intracellular *C. trachomatis* to 1.04 x 10^6 nucleotides coding for only 895 ORFs (open reading frames) (Clarke, 2011; Collingro et al., 2011). The EB particle is infectious but metabolically inactive. The EB can develop into the metabolically active, non-infectious reticulate body (RB), which is ~1 µm in size (Madigan et al., 2012).

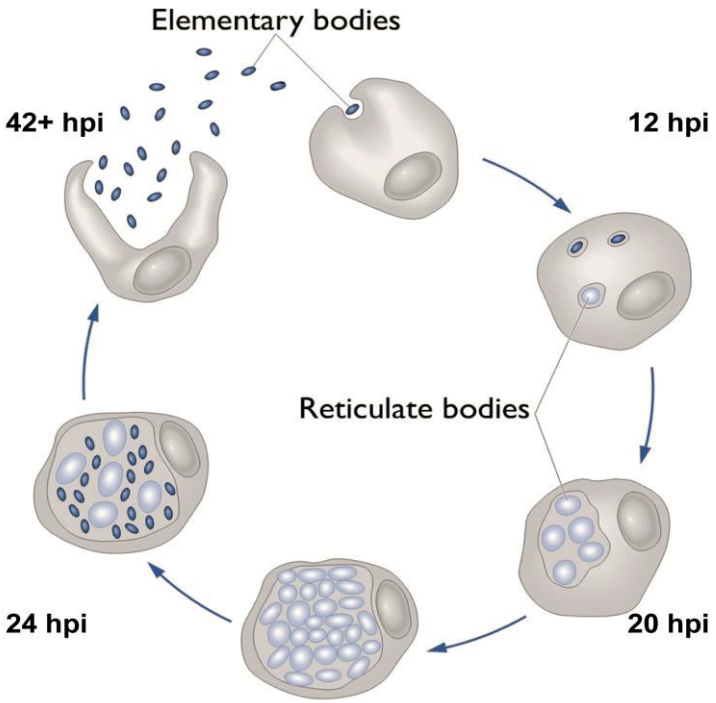

Figure 9: Lifecycle of *Chlamydia trachomatis* serovar L2. Modified from www.ppdictionary.com

When an EB encounters a host cell, electrostatic interactions decelerate the particle allowing protruding adhesion molecules, e.g. CTAD1 and the Pmp protein family, to bind host cell receptors thus facilitating membrane contact (Abdelrahman and Belland, 2005; Mehlitz and Rudel, 2013; Molleken et al., 2013; Molleken et al., 2010; Stallmann and Hegemann, 2016), particularly at cholesterol-rich lipid micro domains in the plasma membrane referred to as 'lipid rafts' (Jutras et al., 2003). The EB triggers greatly diverse host plasma membrane extrusions and is eventually taken up by endocytosis (Nans et al., 2015). Chlamydia possesses a type 3 secretion system, allowing it to form a needle like structure for injecting effectors into the host cell cytosol (Dumoux et al., 2015). These effectors modulate the host cytoskeleton, like translocated actin recruiting phosphoprotein (TARP) which becomes phosphorylated (Jewett et al., 2008; Mehlitz et al., 2008) to remodel actin at the site of entry (Dunn and Valdivia, 2010) and recruit, amongst others, RhoA, dynamin-2 (Hybiske and Stephens, 2007a), and Rac1 to facilitate host cell entry through 'trigger and zipper mechanisms' (Lane et al., 2008). Internalised and surrounded by a host-derived membrane the EBs immediately start weakening their cell wall by reducing disulphide bridges between cysteine-rich membrane proteins in the outer membrane complex, consisting of the major outer membrane protein (MOMP, 60 %), outer membrane complex protein A and B (OmcA & OmcB). At the same time EBs decondensate their DNA by disrupting attachment with histon-like proteins, to allow early gene expression. These genes code for effectors which are secreted to the bacterial

surface via a type V secretion system (T5SS) (Elwell et al., 2016), and into the inclusion lumen via a Type II secretion system (T2SS) (Cianciotto and White, 2017). In these first hours after cell entry, early expressed genes produce proteins that allow dramatic modification of the vacuole membrane (Abdelrahman and Belland, 2005). These modifications render the chlamydial vacuole resistant to fusion with endosomes and lysosomes, thus diverging from the phagosome maturation pathway (Rockey et al., 2002). Additionally, Type III secretion system (T3SS) needles are inserted into the PCV membrane, to continually secrete additional effectors into the host cytoplasm, throughout development of metabolically active RBs (Ferrell and Fields, 2016). Meanwhile, TARP binds PI3K to produce phosphoinositol triphosphate (PIP3) to resemble an exocytic compartment which is not recognized by lysosomal fusion machinery, thus preventing fusion with lysosomes (Betts et al., 2009). During this process, the PCV travels along microtubules to the MTOC in a dynein-dependent way to position itself in the vicinity of the Golgi apparatus (Grieshaber et al., 2003).

After 8 hours the replicative phase ensues and is marked by mid-cycle gene expression. The RBs are anchored to the membrane of the chlamydia vacuole which is now called ‘inclusion’, where they undergo fast growth by binary fission. This fast growth requires large amounts of nutrients (Miyairi et al., 2006). To obtain these, chlamydia use nucleotide and amino acid transport proteins and also a family of integral inclusion membrane (Inc) proteins are used to recruit host proteins and subvert cellular vesicular transport. Among these recruited proteins are Rab GTPases and SNAREs (Damiani et al., 2014; Dumoux and Hayward, 2016; Valdivia, 2008) which regulate trafficking of multivesicular bodies and lipid droplets (Cocchiaro et al., 2008; Elwell and Engel, 2012; Saka and Valdivia, 2010). In addition, chlamydia induce Golgi fragmentation by cleaving golgin-84, in order to generate Golgi mini-stacks surrounding the bacterial inclusion for sphingolipid and cholesterol acquisition (Heuer et al., 2009; Robertson et al., 2009). Also, IncE, which co-opts sorting nexin (SNX) protein 5/6 (Mirrashidi et al., 2015), and IncD interact with the ceramide transfer protein CERT, to subvert retrograde trafficking and provide additional nutrients (Personnic et al., 2016). These host derived and *de novo* synthesized nutrients result in a glycogen-rich vacuole which promotes optimal intracellular growth of RBs (Gehre et al., 2016). The rapid and substantial expansion of the inclusion, is dependent on RB protein synthesis, but not on RB replication, which can be inhibited using KSK120 (Engstrom et al., 2015)

Under stressful conditions, such as antibiotics, IFNγ presence or nutrient scarcity, the RBs transit into a quiescent state in which transcription, less translation and no division

occurs (Mpiga and Ravaoarinoro, 2006). This results in large RBs, named aberrant bodies, which are nonetheless viable since the persisting state can be quickly reversed when stress factors dissolve (Schoborg, 2011). To stabilize the inclusion during these phases, chlamydia co-opts RHO-GTPases, EGFR signalling and at least two bacterial effectors to modulate actin, and microtubules to form a protective superstructure (Elwell et al., 2016). An interesting observation is the *C. trachomatis* SNARE domain protein IncA, which promotes homotypic fusion of inclusions when several EBs infect a single cell (Delevoye et al., 2008). Homotypic fusion also occurs among inclusions of different chlamydial species. Purposefully infecting cells with two distinct species thus allows the study of chlamydial proteins in the context of their own inclusion, as well as in mixed inclusions which yields additional information on protein function (Haldar et al., 2016).

Approximately 24 h after infection, by unknown triggers, an asynchronical redifferentiation into EBs occurs through expression of 'late' genes which produce the histon-like particles required for DNA supercoiling (Wilson et al., 2009; Wyrick, 2000), and membrane complex proteins, OmcA and OmcB, which allow tight and stable packaging of the EB (Belland et al., 2003). During late expression a virulence factor called CPAF is abundantly expressed. The function of CPAF has been debated and currently three hypothesis exist which suggest that 1) CPAF cleaves OmcB thus increasing infectivity, or CPAF is released into the extracellular space by an unknown mechanisms where it 2) 'primes' neighbouring cells for infection, or 3) cleaves host immunity effectors, e.g. mucin, IgA or antimicrobial peptides to allow EBs to infect nascent cells (Conrad et al., 2013). At 40-48 h post infection the EBs are released, usually through host cell lysis. In addition to lysis, also actin- and myosin-dependent extrusion of the inclusion was observed *in vitro* and *in vivo*, which leaves the host cell intact (Hybiske and Stephens, 2015; Hybiske and Stephens, 2007b).

Proteomics of isolated inclusions (Aeberhard et al., 2015) and comparative genomic approaches revealed around 30 genes associated with increased pathogen fitness, which might reveal additional host-modulating factors (Borges and Gomes, 2015). Genetic alteration of such targets has only recently become possible with the establishment of the first stable transformation system for chlamydia. This transformation system is based on redesign of a chlamydial endogenous plasmid (Wang et al., 2011). Since then, reverse genetic approaches using the plasmid-based transformation system have yielded single nucleotide variant libraries of chlamydia, while further opportunities by encoding CRISPR/Cas9 on the plasmid exist, allowing new insights into chlamydial biology (Bastidas and Valdivia, 2016).

1.3.2.2 Immunity against *Chlamydia trachomatis*

Due to its modified LPS-ortholog *C. trachomatis* fails to induce robust TLR4 responses (Nguyen et al., 2011) characteristic of many gram-negative bacteria (Kawai and Akira, 2010). Instead, chlamydia's macrophage inhibitory protein (MIP) and heat shock protein (HSP60) (Da Costa et al., 2004) can be recognized at the inclusion membrane by TLR2 (Kakutani et al., 2012; O'Connell et al., 2006). Upon recognition, TLR2, TLR1 and/or CD14 signal via MYD88 resulting in NF-κB mediated transcription (Wang et al., 2017). However, TLR2-mediated recognition depends on the endogenous plasmid carried by chlamydia (O'Connell et al., 2011; O'Connell et al., 2007). In addition, chlamydia's atypical peptidoglycan can be recognized by cytosolic NLRs (Abdul-Sater et al., 2010a). Also, a role has been identified for the dsRNA sensor TLR-3, solely in epithelial and possibly in dendritic cells (Derbigny et al., 2012). Furthermore, chlamydial DNA can be recognized by NLRP3 which stimulates apoptosis-associated speck-like protein containing a carboxy terminal CARD motif (ASC) (Abdul-Sater et al., 2009), via the sensor cyclic GMP-AMP (cGAMP) synthase (cGAS) which activates stimulator of interferon genes (STING), or via absent in melanoma 2 (AIM2) (Finethy et al., 2015), all of which result in cytokine production (Zhang et al., 2014; Zuck et al., 2015). Signalling triggered through these pathways, and indirectly through the caspase 11 containing inflammasome, activates caspase 1 cleavage and subsequently the NLRP3 inflammasome to specifically produce IL1β and IL18 (Abdul-Sater et al., 2010b; Lu et al., 2000; Man et al., 2017). To hamper this signalling cascade chlamydia expresses effectors, such as ChlaDUB1 (also known as CT868 or CDU1) which suppresses NF-κB signalling (Le Negrate et al., 2008). Combined TLR, NLR and inflammasome signalling nevertheless accumulate IFNβ, IL1β and IL18 in the tissue. Furthermore, IFNγ is secreted by NK cells which combine to initiate various cell autonomous immune programmes (Elwell et al., 2016; Finethy and Coers, 2016) (see above).

As previously described, IFNγ stimulated induction of IDO and iNOS plays a role in chlamydial infection, although with species specificity. Human immunity to *C. trachomatis* relies heavily on the induction of IDO. As opposed to mice, which largely rely on the inducible GTPase IRG-system which is absent in humans (described 1.2.1.1). This difference is likely due to alternate adaptation through host-pathogen interactions.

In humans, IDO depletes intracellular tryptophan pools to starve the *C. trachomatis* inclusion of an essential nutrient thus restricting growth (Nelson et al., 2005; Roshick et al., 2006). Chlamydia reacts on this stressful condition by transforming into its persistent, metabolically less active state. In this state, aberrant bodies survive by up regulation of a partial *trp* operon, thus enabling consummation of exogenous indole present in the genital environment (Caldwell et al., 2003; MacKenzie et al., 2007; Wyrick, 2010) which is likely originating from other microbiota (Ziklo et al., 2016). Conversely, the mouse adapted pathogen *C. muridarum* did not evolve a *trp* operon, and consequently cannot generate tryptophan *de novo* like the human pathogen *C. trachomatis.* These adaptations illustrate the adaptation of chlamydia to their respective hosts (Abdelsamed et al., 2013). In mice, however, the *C. trachomatis* LGV strains have adapted to survive in macrophages. Within this specialized cell type the determining host immune response is induction of iNOS. Inducible NOS results in nitric oxide synthesis, that together with ROS form RNI which directly damage chlamydia (Bogdan, 2015; Rajaram and Nelson, 2015).

Since Chlamydia quickly departs the phagosome maturation pathway, as described above, host cells can only intercept the inclusion by inducing autophagy (Boyle and Randow, 2013), towards which mechanistic understanding tremendously progressed in the past years. Aided by comparable observations between *C. trachomatis* and *T. gondii* it was found that also here guarding IRGM prevents host organelles from being targeted by GKS-containing IRGA6, IRGB6, IRGB10, mGBP1 and mGBP2 onto PCVs, in a ATG3, ATG5 and ATG8 dependent manner (Coers et al., 2008; Haldar et al., 2014; Haldar et al., 2013). In addition, this process co-dependently draws in adaptor p62, and E3 ligases TRAF6 and TRIM21 which ubiquitinate the PCV in a poly-K48- and K63-linked manner (Haldar et al., 2015). The ubiquitination eventually results in autophagosome formation, thus constituting a parallel in cell autonomous immune responses to apicomplexan *T. gondii* and bacterium *C. trachomatis*.

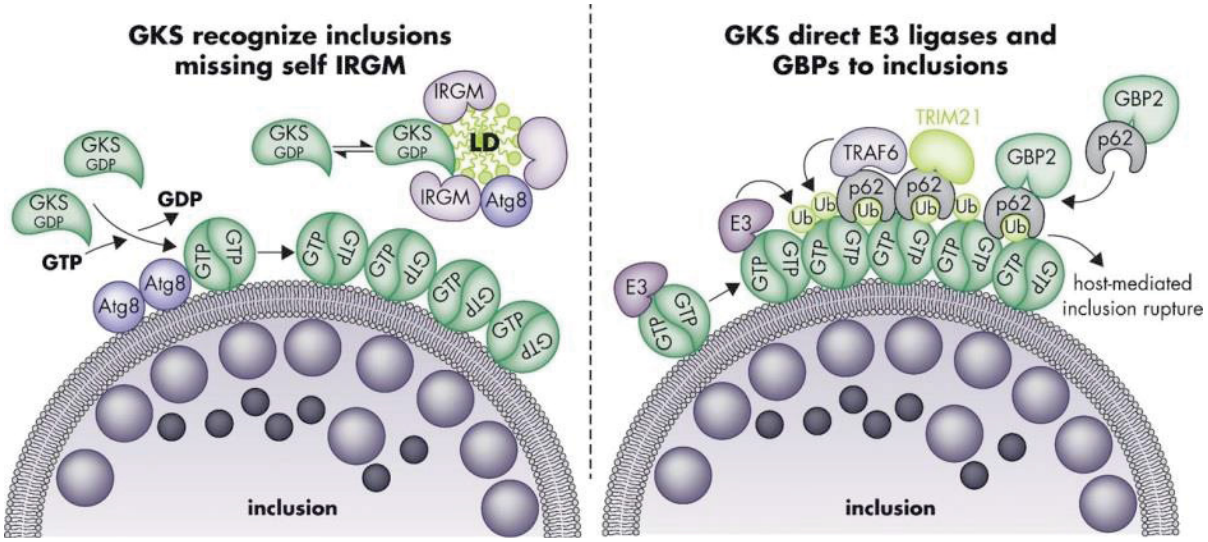

Figure 10: Cell autonomous immunity against *Chlamydia trachomatis*. Modified from (Finethy and Coers, 2016) Figure 2

Targeting of the PCV appears an interdependent process amongst these proteins. Nevertheless, different research groups put up an argument that the leading protein family be either ATGs (Bestebroer et al., 2013), IRGs (Coers and Haldar, 2015) or GBPs (Kravets et al., 2016; Lindenberg et al., submitted). However, consensus exists that these concerted actions induce PCV lysis, to expose pathogens form their protective niche into the host's cytosol (Haldar et al., 2015; Kravets et al., 2016). Direct GBP-mediated lysis of chlamydia or chlamydial inclusions has not yet been shown, however IRGs and GBPs are involved in potentiating the IFNγ-induced anti-chlamydial effects through a p62 and LC3 dependent regulation of autophagy (Al-Zeer et al., 2009; Al-Zeer et al., 2013; Johnston et al., 2016; Tietzel et al., 2009).

While examining inclusion ubiquitination, an additional role for ChlaDUB1 and the newly identified ChlaDUB2 were discovered, which are the first known bacterial effectors that possess deubiquitinating activity and may potentially interfere with host-ubiquitination of PCVs (Bastidas et al., 2013; Claessen et al., 2013). One additional function of these proteins is deubiquitination, and thus stabilization, of apoptosis regulator (MCL-1) at the chlamydial inclusion (Fischer et al., 2017). Another multipurpose chlamydial effector, CPAF, is implicated in impeding inflammasome signalling (Verma et al., 2016). Inflammasome mediated immunity of the host, with the aid of GBPs, has been implicated to induce cell death via pyroptosis, thus attracting cellular immunity to the site of the dying cell (Man et al., 2015; Meunier et al., 2014; Meunier et al., 2015; Pilla et al., 2014).

Cell death is circumvented by chlamydia modification of host transcriptional responses, through CT737 histone methyltransferase, and additional poorly described effectors like CT694 effectors (Cocchiaro and Valdivia, 2009) which influence protein stability. Chlamydia infected cells were observed to have increased activation of MEK-ERK signalling, PI3K survival pathways and induction of p53 degradation, sequestering agonists of cell death, e.g. PKC and BAD, and blocking cFLIP to resist apoptotic signals. Up regulation of anti-apoptotic proteins such as MCL1 described above, as well as cIAP2 and BAG have also been described (Bohme and Rudel, 2009). These concerted effects influence cell autonomous, but also cellular immunity through altered secretion of IL10, thus counterbalancing the inflammatory milieu constituted by IFNβ, IL1β and IL18 (Hakimi et al., 2014). Among the uncharacterized genes in the chlamydial genome, additional virulence factors that modulate the above described host cell signalling are expected (Cocchiaro and Valdivia, 2009), particularly factors aiming to resist cell death (Sharma and Rudel, 2009).

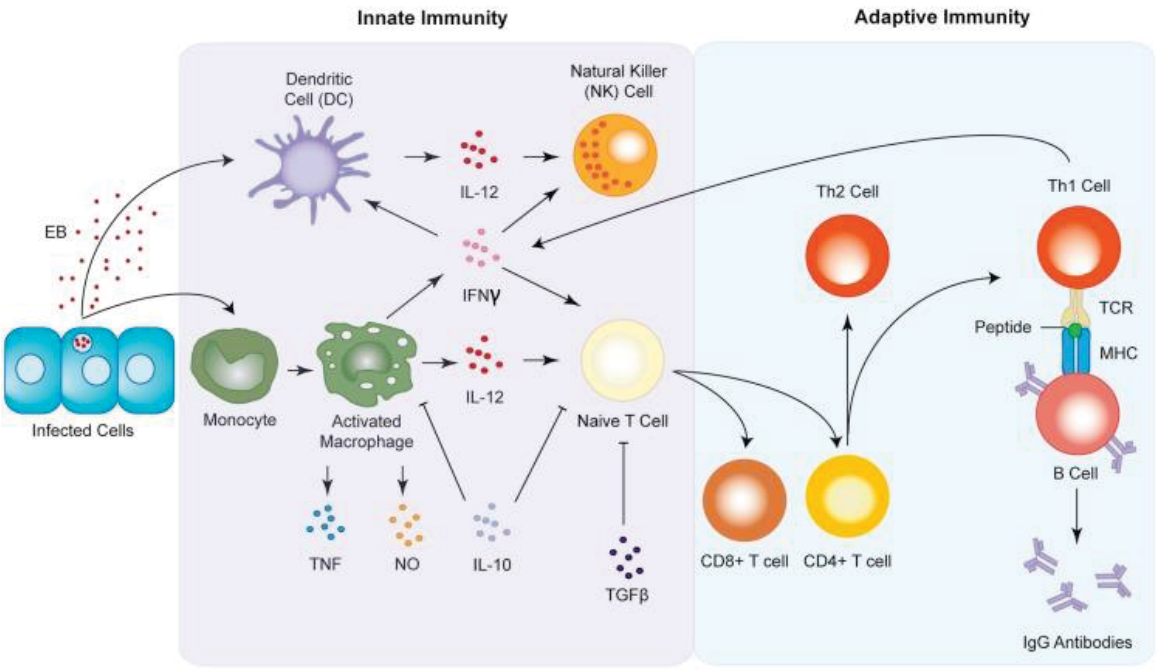

Figure 11: Overview of cellular immunity against *Chlamydia*. Modified from (Redgrove and McLaughlin, 2014)

When chlamydia infected epithelial cells lyse, they release many PAMPs and DAMPs into the environment thus attracting macrophages, NK cells and dendritic cells. Alternatively, chlamydia can escape epithelial cells though extrusion of the complete inclusion, leaving the epithelium intact. These extrusions were observed to be taken up by dendritic cells, which led to prolonged bacterial survival, improved dissemination and

dampened immune responses (Hybiske and Stephens, 2015; Sherrid and Hybiske, 2017). Similarly, macrophages can serve as vehicles for the dissemination of bacteria from the primary infection site (urogenital or respiratory tract) to distant sites in the body (Herweg and Rudel, 2016). Residing in a phagocyte most likely benefits the pathogen by circumvention of complement activation, antibodies and host defence peptides, while disseminating over large distances (Di Francesco et al., 2013; Hammerschlag, 2002; Kumar and Valdivia, 2009). However, the consequences of this process for the host remain elusive and require further investigation. B cells actively participate in chlamydial infection, but fail to provide protective immunity (Li and McSorley, 2015). Although cytotoxic T cells are adept at lysing infected epithelial cells, they do not confer lasting immunity. It is believed that an excess of cytokines like IL12 during infection, contributes to poor memory $CD8^+$ T cell development (Johnson and Brunham, 2016). Although all these adaptive immune cells participate, the main players, solely responsible for clearing chlamydia infection, are T_h1 cells (Coers et al., 2011; Johnson and Brunham, 2016).

1.3.3 *Mycobacterium* (Tuberculosis)

Tuberculosis is one of the major causes of death. Currently one third of the global human population is asymptomatically, latently infected, risking a chance of developing active disease later on. Multidrug-resistant (MDR) and extensively drug-resistant (XDR) *Mycobacterial (M.) tuberculosis* strains spread, causing disease particularly of immune compromised individuals, e.g. in organ recipients or in patients with acquired immune deficiency syndrome (AIDS) (Russell et al., 2010) (WHO, 2017, http://www.who.int/mediacentre/factsheets/fs104/). The causative agent was discovered by Robert Koch employing his postulates (published in 1884) (Madigan et al., 2012). *M. tuberculosis* is a gram-positive rod-shaped bacterium, belonging to the phylum Actinobacteria, with a small genome, e.g. 4.41 x 10^6 bp containing 3924 ORFs. Mycobacteria possess unique lipids, called mycolic acids, which are covalently bound to peptidoglycan in the cell wall composing a hydrophobic capsule which hinders antibiotic access and influences the immune system (Jankute et al., 2017; Madigan et al., 2012).

Transmission of mycobacterial infection was described (Russell et al., 2010), in short occurring as follows:

> Infection occurs through an actively infected person exhaling, thus releasing mycobacteria-containing aerosols which remain airborne for several hours, allowing them to be inhaled by a healthy individual. Within the airway, the bacterium lands in on arbitrary mucosal site, is opsonized, phagocytosed by

alveolar macrophages in which it resides in a non-fusogenic phagosomal vacuole. A local inflammatory response is established, the primary site of infection. The inflamed lung tissue attracts macrophages, monocytes and neutrophils, which in turn become infected and differentiate. For example, macrophages can differentiate into foamy macrophages, which are characteristic of this infection. Meanwhile the adaptive immune response is triggered, and lymphocytes migrate to the infected site to surround the lump of infected and uninfected cells which develop into an organized, stratified structure; the granuloma, the hallmark of mycobacterial infection.

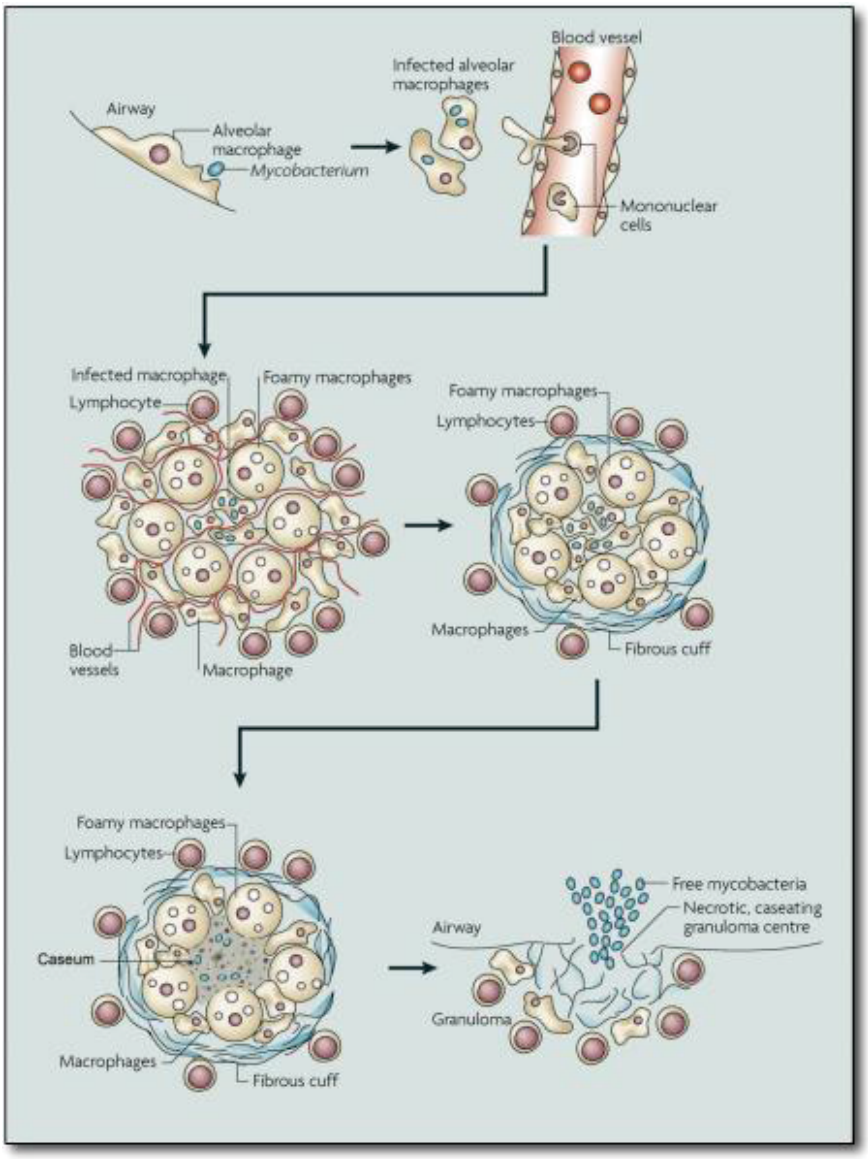

Figure 12: Lifecycle of *Mycobacteria* after transmission via aerosols (Russell et al., 2010) Figure 1.

Within the macrophage-rich centre necroptosis of infected cells results in a space termed ‘caseum’, which is enclosed in a fibrous cuff. Occasional rupture of such

caseating granulomas releases an overwhelming number of infectious bacteria, PAMPs and DAMPs into the lung which cause the characteristic symptoms of active tuberculosis, e.g. coughing, hemoptysis, thus allowing transmission.

Genomic studies have shown substantial genetic variability among isolates of *M. tuberculosis* from around the world, which reflects either accumulated genetic drift associated with patterns of human migration. Similarly, comparative studies between strains could uncover lineage-specific virulence factors (Pai et al., 2016). Laboratory models involving mice yielded many insights into mycobacterial infection biology, however not all facets of the disease, most importantly granuloma morphology and latency development, occur comparably to humans (Modlin and Bloom, 2013; Orme and Ordway, 2016). Comparable pathology of mycobacterial disease can be reached through infecting non-human primates, however the associated larger effort, risk, costs and ethical considerations do not favour large scale studies in these primates (Scanga and Flynn, 2014).

1.3.3.1 Mycobacterium tuberculosis elicited immune responses

In vivo infections showed that IFNγ and TNFα are necessary for initial protection through cell autonomous immunity and cytokine-activated macrophages, while cytotoxic T cells play a role later in infection (Bloom and Modlin, 2016). How these findings on the organism-level translate back into molecular, intracellular and cellular host-pathogen interactions is poorly understood, and is the focus of on-going research. The state of the art finds on which consensus exists displays an intricate host-pathogen relationship which is summarized briefly below.

Within the alveolar macrophage *M. tuberculosis*, manipulates phagosome formation through mannosylated-lipoarabinomannan (ManLAM) and phosphatidylinositol mannoside (PIM) in its hydrophobic capsule. In addition, *M. tuberculosis* effectively excludes V-ATPase and modulates the RABs associated with its vacuolar membrane and, thus resembling early endosomes and continuously protecting itself form fusion to lysosomes (Di Russo Case and Samuel, 2016; Rohde et al., 2007). Focussing on the infected macrophage, *M. tuberculosis* PAMPs cause prolonged stimulation of TLR1, TLR2, TLR4, and TLR9 through MYD88- and MAPK-dependent-signaling, purinergic (P2X7) receptors, NOD1, NOD2, CLRs Dectin-1,DC-SIGN, Mincle, NLRP3-ASC and Pentraxin 3 (PTX3, also known as TSG-14, a soluble PRR which binds complement component C1q). Although all these parallel immunostimulatory pathways are activated, the macrophage cannot kill the *M. tuberculosis* (Juarez et al., 2012; Juarez et al., 2014;

Mortaz et al., 2015; Villasenor et al., 2017). Nevertheless, external activation of the macrophage through cytokines such as IFNγ and TNFα induces the most effective intracellular defence against mycobacteria: RNI (Bloom and Modlin, 2016). This cytokine-signalling induces NOS, leading to production of NO gas, additional induction of NADPH oxidase creates ROS, both of which react at the site of the mycobacterial pathogen containing phagosomal vacuole (PCV) resulting in direct killing (MacMicking, 2014). Interestingly, IFNγ induced mGBP7 delivers NADPH-subunits onto the PCV for local ROS production (Kim et al., 2011). *M. tuberculosis* can limit but not prevent damage from ROS and RNI through effectors like alkyl hydroperoxide reductase subunit C (AhpC) or methionine sulfoxide reductase (MsrA), breaking down ROS and RNI (Peddireddy et al., 2017). In addition, recognition of the *M. tuberculosis* containing altered phagosome can be improved by repositioning of RAB10 (Cardoso et al., 2010) or IRGM-binding on the compartment interacting with SNAREs and SNAPSIN for ATG14L-mediated lysosomal fusion (Kim et al., 2012b; Tiwari et al., 2009). However, the intracellular ROS and RNI burst, and lysosomal fusion, require macrophage activation through other cells, such as pro-inflammatory cytokines producing T_H1 cells, in order to overcome the mycobacterial manipulation (Bloom and Modlin, 2016). Besides T_H1 cells also cytotoxic T cells, NKT cells and NK cells can contribute to IFNγ production (Travar et al., 2016). If phagosome maturation is rescued, the potency of lysosomal content is critical. This was demonstrated by mGBP1, which interacts with p62 to transport additional substrates for microbicidal peptide generation, since mice deficient for mGBP1 are more susceptible to infection (Alonso et al., 2007; Kim et al., 2011). To gain an added advantage, the cell engages nutritional competition for cations and essential amino acids with the PCV, which the therein residing mycobacteria counteract by their own cation-transporters (Awuh and Flo, 2017). Strikingly, *M. tuberculosis* has also been proposed to completely alter cell metabolism (Shi et al., 2016) and cell cycle signalling via the Wnt-pathway, to facilitate its survival and persistence in the host (Villasenor et al., 2017).

If these cell autonomous responses fail, cells initiate autophagy via elaborate signalling cascades (Sumpter and Levine, 2010) to target the PCV for degradation by auto-lysosomes, called xenophagy (Sumpter and Levine, 2010) thus combatting the infection, at the same time improving antigen presentation and sparing the tissue destructive inflammation (Deretic, 2016; Deretic et al., 2009; Gutierrez et al., 2004). In these processes a particular role for inducible GTPases was observed (Man et al., 2017; Meunier and Broz, 2016). *M. tuberculosis* phagosomes were found to recruit murine IRGM1 and human IRGM in their respective cells, which induced lipid modifications,

fusion with lysosomes, and induction of autophagy and eventual killing of mycobacteria (MacMicking et al., 2003; Martens et al., 2004; Singh et al., 2006; Singh et al., 2010; Tiwari et al., 2009), although this localization for murine IRGM1 is contested (Springer et al., 2013). Autophagy was also enhanced through proteins described in other infection models to interact with IRG-GBP dependent vacuole recognition, like ubiquitin peptides (Alonso et al., 2007), p62 (Ponpuak et al., 2010), E3 ligases Parkin and LRSAM1 (Finethy and Coers, 2016) and LC-3 (Liang et al., 2017). Whether a role for IRG and GBP mediated disruption of the mycobacterial phagosome exists remains to be investigated. In addition, *M. tuberculosis* infection was shown to activate the AIM2-inflammasome, but can simultaneously be suppressed by the bacteria, dependent on a mycobacterial genetic region called RD1 (Briken et al., 2013; Kurenuma et al., 2009). Furthermore, the autophagy-process itself is manipulated by mycobacteria to reduce MHC-II presentation to prevent attraction of T_H1 cells (Goldberg et al., 2014). Next, the host cell induces cell death programmes, which *M. tuberculosis* manipulates by inhibition of apoptosis during early stages of infection while inducing necroptosis during late stages (Briken, 2013). Necroptosis is induced via effectors NuoG and secA2, increasing levels of host lipoxin A4 (LXA4) and inhibiting prostaglandin E2 (PGE2), to cause inflammation and attract more macrophages to hijack. Host cells can control the infection by switching back to apoptotic cell death during early phases of infection (Amaral et al., 2016; Behar et al., 2010; O'Garra et al., 2013). If this switch is successful, *M. tuberculosis* which is sequestered within the apoptotic macrophage is further compartmentalized via engulfment by uninfected macrophages through a process called efferocytosis, thus delivering apoptotic debris into the lysosomal compartment, and killing mycobacteria (Martin et al., 2012). Additionally mycobacteria induce altered transcription through several mechanisms, leading to altered metabolism, immune signalling and cell death, of which the details will have to be explored in the future (Briken, 2013; Ehrt et al., 2001).

Besides down regulating MHC-II, *M. tuberculosis* also delays priming of adaptive immune responses by meddling with APC signalling. In addition, *M. tuberculosis* secretes immunological “decoys” which have a high affinity for MHC class I and II molecules. These peptides out-compete other, potentially more important epitopes for control of mycobacterium, thus leading to the formation of impotent effector and memory T cells (Goldberg et al., 2014)

In humans, mycobacterial killing is additionally orchestrated by vitamin D-dependent activation of macrophages. Both innate signalling via TLR2-MYD88, and acquired immune activation via IFNγ-STAT1, induces the vitamin D receptor. Activation of the

vitamin D receptor leads to expression of cathelicidin and β-defensin 2 (DEFB4), which exert antimicrobial activities (Bloom and Modlin, 2016).

All these simultaneous pathogen- and host-initiated events, constitute a delicate balance which can result in either mycobacterial killing, persistence or replication (Kumar and Rao, 2011). Meanwhile, in the inflamed site, lymphocytes are recruited which promote the formation of the granuloma. The granuloma has an ambivalent role, either aiding the host immune system or rather providing a platform enabling mycobacterial persistence to allow reactivation if the immune system is weakened later on (Pai et al., 2016; Peddireddy et al., 2017). Since inflammation promotes mycobacterial persistence, the role of neutrophils (Warren et al., 2017) and Th17 cells (Lyadova and Panteleev, 2015), type 1 IFNs and IL17 (Mourik et al., 2017) in host defence are contested.

1.3.3.2 Mycobacterium bovis BCG

M. bovis bacillus CalmetteGuerin (BCG) is a strain of *M. bovis* selected after repeated passages by Albert Calmette and Camille Guerin at the beginning of the 20th century. BCG is used to date as a live vaccine against *M. tuberculosis* (Murphy et al., 2012). BCG is the only approved vaccine against tuberculosis, and improves containment of *M. tuberculosis* after acute infection, however it is only partly effective against pulmonary disease in adults (Russell et al., 2010). The prolonged culturing of BCG led to the loss of DNA sequences termed ’regions of difference’ (RD, as compared to *M. tuberculosis* complex a total of 14 different regions were identified) which encode amongst others, the type VII secretion system ESX1, which mediates the delivery of bacterial virulence factors into the host cell (Kozak et al., 2011; Pai et al., 2016).

The immune responses to BCG are largely similar to *M. tuberculosis* albeit loss of effectors with the RDs tip the balance toward host-cell clearance of the bacteria, as evidenced by a more prominent role of DCs and a faster adaptive immune response (Moliva et al., 2017). In detail, the loss of the RD1 locus in the case of inflammasome activation (Kurenuma et al., 2009) allows the association of mGBP1, mGBP7 and mGBP10 with BCG-containing endosome-like phagosomes (Kim et al., 2011). However, further studies need to be performed to clarify the role of mGBPs in defence against *M. tuberculosis* strains of varying virulence.

Current research efforts are mainly focussed on the development of an improved vaccine, by overexpression of strong antigens and adjuvants in the BCG background, in order to reach complete protection from disease (Kaufmann, 2013). These studies

perform transcriptome analysis during infections with marginally different strains of BCG. Differential gene induction after infection with minimally adjusted pathogens yields information on the underlying immune mechanisms. For example, infection with a strain of BCG deficient for the urease subunit alpha (ureC), to prevent interference with phagosomal pH acidification, and expressing the immunogenic membrane-perforating listeriolysin O (Hly; encoded by the gene *hly* of *Listeria monocytogenes*) (Grode et al., 2005) was observed to induce hGBP2 and hGBP5 (Figure 13) which was not significant after infection with the parental BCG strain (Saiga et al., 2015).

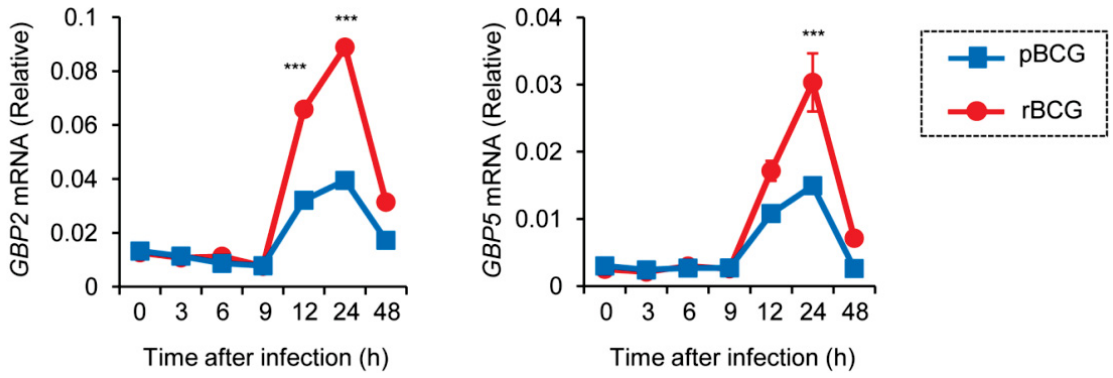

Figure 13: Significant induction of hGBP2 and hGBP5 in THP-1 macrophages during the hours after infection (MOI:5) with parental BCG (pBCG) or recombinant BCG ΔureC::hly (rBCG). Data are shown as the relative mRNA levels normalized by the corresponding GAPDH level. ***, P < 0.005. Modified from (Saiga et al., 2015) Supplementary figure 3.

Additional evidence for a role of GBPs in human tuberculosis is the robust up regulation of hGBP5, which was therefore classified as part of an unique set of biomarkers to discriminate patients with tuberculosis from those with similar clinical symptoms caused by other etiological agents (Laux da Costa et al., 2015; Satproedprai et al., 2015). Many efforts go into the search for such biomarkers for both latent and active mycobacterial disease (Berry et al., 2010; Doherty et al., 2009) and more inducible GTPases might be found to be correlated with tuberculosis.

In mice, repeated BCG treatment of the mouse bladder induces GTPases, e.g. IRGB6, mGBP1, mGBP2, mGBP5, and several HLA antigens (Saban et al., 2007). After vaccination with recombinant BCG-strains, mGBP2, mGBP3 and mGBP5 were up regulated (Gengenbacher et al., 2016). MGBP5 was also found in a systems biology approach to discover membranous protein alterations in BCG-activated murine macrophages (Lun et al., 2009). Additionally, small interfering RNA knockdown of mGBP1, mGBP5, mGBP7, or mGBP6/10 showed improved BCG growth, mGBP1,

mGBP7, and mGBP10 colocalized with the BCG PCV and are proposed to aid ATG-, p62-dependent ubiquitination and LC3 association at the PCV (Kim et al., 2011). Unpublished results of our laboratory and collaboration partners implied presence of mGBP5 on the phagocytic cup during BCG endocytosis and the subsequently developing mycobacterial phagosome. This opens an avenue for investigation of the previously established mGBP5 deficient mouse line after BCG compared to *M. tuberculosis* infection.

1.4 Aims of the study

MGBPs are cell autonomous immune effectors that can defend the host against intracellular pathogens. An anti-parasitic role was described for several mGBPs in *T. gondii* infection (Degrandi et al., 2013; Kravets et al., 2016; Selleck et al., 2013; Yamamoto et al., 2012).

These mGBPs translocate to the toxoplasma PV after infection. It was shown that mGBP2 is involved in rupturing the vacuolar membrane (Degrandi et al., 2013; Kravets et al., 2016). This action is dependent on the CaaX-motif of mGBP2, which is also present in mGBP1, and mGBP5. Previous work in the laboratory described a residue involved in targeting of mGBP6 to the PV (Klümpers, 2013). In this thesis, this residue is evaluated in all mGBPs, to gain a better understanding of the requirements for mGBP targeting of the PV. Therefore, plasmids expressing mGBPs N-terminally fused to mCherry or GFP should be subjected to side-directed mutagenesis in order to obtain the proposed mutations. Subsequently, fibroblasts should be lentivirally transduced to constitutively express each of the original and mutated constructs. This panel of cell lines should be used to compare localization of mutated and wild type mGBP proteins at the toxoplasma PV.

Additionally, the previously generated mGBP5-deficient mouse line should be used to investigate immunological defects occurring in the innate immune responses, particularly focussing on mycobacterial infection.

Also, the role of mGBPs in intracellular infections with *Chlamydia trachomatis* should be addressed. The fibroblast cell lines, constitutively expressing fluorescent protein-tagged mGBP proteins, described above, should be used to extensively analyse which mGBPs play a role in chlamydial infection. From this panel, candidates should be selected for further investigation using live cell imaging, Fluorescence-activated cell sorting (FACS) analysis and bacterial growth quantification assays. For all these experiments, in-house protocols had to be established in this thesis.

A detailed comparison of mGBP action against the apicomplexan pathogen *T. gondii* or against the bacterial pathogen *C. trachomatis* should be performed to investigate similarities and/or differences in mGBP family action against these different pathogens.

2 Materials

2.1 Expendables

Object		Order #	Manufacturer
12 well plate (sterile)		353043	Falcon, BD Biosciences, Heidelberg
24 well plate (sterile)		353047	Falcon, BD Biosciences, Heidelberg
48 well plate (sterile)		353078	Falcon, BD Biosciences, Heidelberg
6 well plate (sterile)		353046	Falcon, BD Biosciences, Heidelberg
96 well plate flatbottom		353072	Falcon, BD Biosciences, Heidelberg
96 well plate flatbottom plates		3596	Costar, Corning, NY, USA
96 well plate U- bottom plates		353077	Falcon, BD Biosciences, Heidelberg
Autoclaveable bag for table waste		861197	Sarsted, Nümbrecht
Cell scrapers		CC7600-0250	Starlab International, Hamburg
		541070	Greiner Bio One, Frickenhausen
Cell strainer	40 µm	352340	BD Biosciences, Heidelberg
	100 µm	352360	
Cryotube 1,8 ml starred bottom, INT		340711	Nunc, Thermo, Braunschweig
Dispenser tips (sterile)	1,25 ml	S4786-0125	Starlab International, Hamburg
	2,50 ml	S4788-0250	
	12,50 ml	S4792-1250	
Eppendorf Tube	2 ml	0030 120.094	Eppendorf, Hamburg
	0,5 ml	0030 121.023	
Eppendorf Tube, 1.5 ml		72.706.	Sarstedt, Nümbrecht
FACS tubes (sterile)		352052	BD Biosciences, Heidelberg
Falcon 15 ml(sterile)		60.540.014	Sarstedt, Nümbrecht
Falcon 50 ml (sterile)		62.547.254	Sarstedt, Nümbrecht
Flask T162 with filter		3151	Costar, Corning, NY, USA
Flask T25 with filter		3056	Costar, Corning, NY, USA
Flask T75 with filter		430641	Costar, Corning, NY, USA
Microscope Coverslips high precision		0117530	Paul Marienfeld, Lauda-Königshofen
Microscope slide cut edges frosted		K123	Engelbrecht, Edermünde
Micro-Touch Nitra-Tex Gloves S		700112	Ansell, Brussels, Belgium
Parafilm M		PM996	American National Can, Chicago, USA
Petr idish 10 cm coated (sterile)		353003	Falcon, Corning, NY, USA
Petr idish 10 cm uncoated (sterile)		633181	Greiner Bio One, Frickenhausen
Pipet tips (sterile)	10 µl	S1120-3810	Starlab International, Hamburg
	20 µl	S1120-1810	
	200 µl	S1120-8810	
	1000 µl	S1126-7810	
Pipet tips refill	10 µl	S1110-3700	Starlab International, Hamburg
	200 µl	S1111 1806	
	1000 µl	S1112-1720	
Pipets (sterile)	5 ml	4487	Costar, Corning, NY, USA
	10 ml	4488	

25 ml	4489	
Plate Sealers	3095	Costar, Corning, NY, USA
Slides CellOmeter	SD100	Nexelcom,Lawrence, Massachusetts,USA
Spade (Drichalsky, one-way)	I612-1561	VWR Darmstadt
Sterilfilter 0,2 µM PN#514-0061	83.1826.001	Sarsted, Nümbrecht
Syringes Omnifix 20 ml and Injection needles sterican 12 (sterile)	4657624 4617207V	Braun, Melsungen
Tubes for sonification (sterile)	4034501	Sarstedt, Nümbrecht

2.2 Chemicals, solutions and enzymes

Chemical/solution	Order #	Manufacturer
4',6-diamidino-2-phenylindole (DAPI)	D3571	Thermo Scientific, Braunschweig
4-Bromophenacyl Bromide (4-BPB)	D38308	Sigma-Aldrich, Taufkirchen
Acetic acid	1.00063.2500	Merck, Darmstadt
Acetone	1.00013.2500	Merck, Darmstadt
Agarose	00005208364	Biozym, Hamburg
Bovine Serum Albumin Fraction V (BSA)	10735094001	Sigma-Aldrich, Taufkirchen
Cell Dissociation Solution (non-enzymatic)	C5789	Sigma-Aldrich, Taufkirchen
Chloroform	3313.2	Roth, Karlsruhe
Cycloheximide (1 mg in 10 ml PBS)	C4859	Sigma-Aldrich, Taufkirchen
D+Glucose (waterfree)	A3666	Pan Reac Applichem, München
Diemethylsulfoxid Hybri-Max(DMSO)	D2650	Sigma-Aldrich, Taufkirchen
Dimethylsulfoxide (DMSO)	D2650	Sigma-Aldrich, Taufkirchen
distilled water (sterile)	10977-035	Thermo Scientific, Braunschweig
EDTA	ED-500G	Sigma-Aldrich, Taufkirchen
Erythrocyte lysis buffer	12972.00500	Morphisto, Frankfurt am Main
Ethanol absolute	1.00983.2511	Merck, Darmstadt
Ethidiumbromide solution (1 %)	1.11608.0030	Thermo Scientific, Braunschweig
FACS Clean solution	340345	BD Biosciences, Heidelberg
FACS Flow solution	342003	BD Biosciences, Heidelberg
FACS Rinse solution	340346	BD Biosciences, Heidelberg
Fetal Bovine Serum (FBS) FBS VLE	2602-p2720 DE14-801F	PAN Biotech, Aidenbach Lonza, Vervies, Belgium
FluoromountG	0100-01	Southern Biotechnology Associates
Glycerine	24386.298	VWR, Darmstadt
Glycerine (water free)	1.04093.1000	Merck, Darmstadt
Goat normal serum	X0907	DakoCytomation, Hamburg
HCL	1.00316.1000	Merck, Darmstadt
Hoechst 33258, pentahydrate (bis-benzimide)	H3569	Molecular probes/Life technologies, Eugene, oregon, USA
Immersion oil W	2010	Zeiss, Jena

Immersion oil	518F	
Isopropanol	20842.330	Merck, Darmstadt
jetPRIME reagents buffer	114-15 712-60	Polyplus, Illkirch-Graffenstaden, France
KCl	1.04936.1000	Merck, Darmstadt
KH_2PO_4	104873	Merck, Darmstadt
L929-Supernatants containing M-CSF	-	Prepared from laboratory owned L-cells by Karin Buchholz
LB medium (Luria/Miller)	X968.2	Roth, Karlsruhe
L-glutamine	G7513	Sigma-Aldrich, Taufkirchen
Loading Dye Solution orange(6x)	R0631	Fermentas, St. Leon Roth
MassRuler DNA-Ladder Mix	SM 0403	Fermentas, St. Leon Roth
Medium Dulbeccos Modified Eagle (DMEM)	41966-029	Thermo Scientific, Braunschweig
Medium FluoroBrite DMEM	A1896701	Thermo Scientific, Braunschweig
Medium IMDM	BE 12 722F	Lonza, Belgien
Medium Middlebrook - 7H10 - Agar	262710	BD Diagnostics, New Jersey, USA
Medium Middlebrook - 7H9 - Agar	271310	BD Diagnostics, New Jersey, USA
Medium Roswell Park Memorial Institute 1640 Medium L-Glutamin (RPMI VLE)	FG1415	Merck, Darmstadt
MEM vitamins, non-essential amino acids	11140035	Thermo Scientific, Braunschweig
Methanol	20864.320	VWR Darmstadt
$Mg^{2+}Cl$	8.14733.0500	Merck, Darmstadt
Na_2HPO_4	106586	Merck, Darmstadt
NaCl	6404	Merck, Darmstadt
NaCl AnalaR NORMAPUR® ACS,	27810.295	27810.295
NaOH	1.069489.500	Merck, Darmstadt
Oligo-(dT)-Primer	18418-012	Thermo Scientific, Braunschweig
Para-formaldehyde (PFA)	1.04005.100	Merck, Darmstadt
PBS chemical powder	L-182-10	Biochrom, Berlin
PBS powder	L182-10	Merck, Darmstadt
PCR Nucleotide-Mix (dNTPs)	R0193	Fermentas, St.Leon-Roth
Percoll	P1644	Sigma-Aldrich, Taufkirchen
Polybrene	TR 1003-G	Merck, Darmstadt
Proteinase K (10mg/ml)	03115828001	Roche, Mannheim
qPCR MasterMix-No ROX	RT-QP2X-3+NR	Eurogentec, Liege, Belgien
Restriction buffer CutSmart	B7204S	New England BioLabs Frankfurt a. M.
Restriction buffer SUREcut	11417991001	Roche, Mannheim
RNase Zap	9780.9782	Ambion, Darmstad
Rotiphenol /Cl/I	0038.2	Roth, Karlsruhe
Saponin	159665	Merck, Darmstadt
SDS (20% (w/v))	20.763	Honeywell Fluka, Bucharest, Romania

sterile Phosphate-Buffered Saline Dulbeccos (PBS)	14190-094	Thermo Scientific, Braunschweig
Sucrose	107651	Merck, Darmstadt
TRIS-HCl	15506017	Thermo Scientific, Braunschweig
Triton X-100	17-1315-0	Plus One, Uppsala, Sweden
TRIzol	15596-026	Thermo Scientific, Braunschweig
Trypan Blue	T 8154	Sigma-Aldrich, Taufkirchen
Tyloxapol	T8761-50G	Sigma-Aldrich, Taufkirchen
Yeast extract Bacto	212750	BD Biosciences, Heidelberg
β-Mercaptoethanol (β-ME)	31350-010	Thermo Scientific, Braunschweig

Enzyme	Order #	Manufacturer
Collagenase type VIII	C2139	Sigma-Aldrich, Taufkirchen
DNAse I	4716728001	Sigma-Aldrich, Taufkirchen
Proteinase K (10mg/ml)	03115828001	Roche, Mannheim
Restriction enzymes detailed in 3.1.4	-	New England BioLabs Frankfurt a. M. Roche, Mannheim Fermentas, St. Leon Roth
Trypsin/EDTA 0.05% 0,25%	P10-0231SP	PAN Biotech, Aidenbach Thermo Scientific, Braunschweig

2.3 Kits and other reagents

Name	Order #	Manufacturer
FluoSpheres carboxylate modified microspheres 2.0 µm red fluorescent (580/605)	F8826	Molecular Probes, Eugen, Oregon, USA
DNA T4 Ligase	10 481 220 001	Roche, Sigma-Aldrich, Taufkirchen
Zyppy Plasmid miniprep kit	D4036, 4037, 4019, 4020	Zymo Research Coperation, Irving USA
Zymoclean Gel DNA Recovery Kit	D4002	Zymo Research Coperation, Irving, USA
DNA Polymerase, High Fidelity	03300234001	Roche, Mannheim
NucleoBond Xtra Maxiprep Kit Including RNase A	740414.100	Macherey-Nagel, Düren
Cytometer Setup and Tracking Beads	641319	BD Biosciences, Heidelberg
Quik-Change XL Site Directed Mutagenesis	200521-5	Stratagene, California, USA
Interferon gamma (IFNγ)	485-ml	R&D Systems, Wiesbaden-Nordenstadt
Ampicilline (100 mg/mL in ddH_2O)	1083524200	Sigma-Aldrich, Taufkirchen
Gentamycin	G1397	Sigma Aldrich, Taufkirchen

2.4 Buffers

Buffer	Concentration	Composites
5x DNA loading buffer	15 % (v/v)	Ficoll Type 400
	0.05 % (w/v)	Bromphenolblau
	0.05 % (w/v)	Xylencyanol
ADC		Millipore H_2O
	0.05 % (w/v)	BSA
	0.02 % (w/v)	D+Glucose (waterfree)
	0.0085 % (w/v)	NaCl AnalaR NORMAPUR
	mixed for several hours	0,2 µm filtered
Blocking buffer	Goat serum 1:10 diluted in permeabilisation buffer	
Collagenase VIII	100 mg/ml	in PBS
DNAse I	3000 Units/ml	in PBS
dNTP Mix	1 mM	dATP
	1 mM	dGTP
	1 mM	dTTP
	1 mM	dCTP
Gastrographine solution	30 % (v/v) gastrographine solution in PBS	
FACS STOP buffer	1x	PBS
	10 mM	EDTA
FACS-Buffer		PBS
	2 % (v/v)	FBS
	2 mM	EDTA
Organ-digestion buffer	6 % (v/v)	Collagenase VIII solution
	1 % (v/v)	DNAse I solution
	93 % (v/v)	PBS
PBS-T	0.5% (v/v) Tyloxapol in PBS	
Permeabilisation buffer	0.02 % (w/v) saponin in PBS	
PFA fixation buffer		PBS
(pH=7.4)	4 %	Paraformaldehyde
	2 mM	$MgCl_2$
	1.25 mM	EDTA
SDS containing digestion		ddH_2O
buffer	100 mM	TRIS-HCl, pH 8,5
	5 mM	EDTA
	0.2 % (v/v)	SDS
	200 mM	NaCl
SPG Buffer		ddH_2O
	220 mM	Sucrose
	3.8 mM	KH_2PO_4
	10,8 mM	Na_2HPO_4
	4.9 mM	L-glutamine
Storage of DNA in TE-Buffer	10mM	Tris-HCL pH 8,0
	1mM	EDTA

TAE (Elektrophoresepuffer) pH 8,0	2 M 1 M 0,1 M mM	Tris/HCL Acetic acid (glacial) EDTA
Tissue digestion buffer	93 % (v/v) 6 % (v/v) 1 % (v/v)	PBS Collagenase type VIII 100 mg/ml DNase I 3000 Units/ml

2.5 Cultures

2.5.1 Eukaryotic cell lines

Cell line	Characteristics	Source
293FT	fast-growing, highly transfectable clonal isolate derived from human embryonal kidney cells, SV40 transformed #P/N 51-0035	Thermo Scientific, Braunschweig
HEp2	Epithelial cervix carcinoma cell line, human origin ECACC#86030501, ATCC#CCL-23	Hegemann Laboratory
HFF	human foreskin fibroblasts ATCC#SCRC-1041	ATCC, Wesel
HS27	human foreskin fibroblasts ATCC#CRL-1634	ATCC, Wesel
NIH/3T3	Derived from murine embryonal fibroblasts, also known as ECACC#93061524, ATCC#CRL1658	ECACC operated by Public Health England
Primary WT, mGBP2$^{-/-}$, mGBP5$^{-/-}$ and mGBP7$^{-/-}$ embryonic fibtroblasts	Embryonal fibroblasten isolated day 14.5 from C57BL/6 embryos	Prepared by dr. Beuter-Gunia (Beuter-Gunia, 2008)

2.5.2 Microorganisms

Bacterial species	Strain/Genotype	Source
Chlamydia muridarum	NIGG 2, mouse pneumonitis (also known as MoPn) ATCC #123-VR	ATCC, Wesel
Chlamydia trachomatis	L2/434/Bu (LGV) ATCC #VR-902B	Hegemann Laboratory
Chlamydia trachomatis	L2 (LGV) transformed with pGFP::SW2	(Wang et al., 2011) via Rudel Laboratory
Escherichia coli	DH5α /supE44, ΔlacU169, (Φ80lacZΔM15), hsdR17,recA1, endA1, gyrA96, thi-1, relA1	Thermo Scientific, Braunschweig (Life tech 18258-012)
Mycobacterium bovis	BCG, Dhanish isolate, Wild type	Kalscheuer research group
Mycobacterium tuberculosis	H37Rv, Wild type	Kalscheuer research group

Apicomplexan	Strain/Genotype	Source
Toxoplasma gondii	ME49, Type 2 strain, wild type	ATCC, Wesel (Parmley et al., 1994)

2.5.3 Media used for cultures

Medium used for	Concentration	Components
C. trachomatis culture		DMEM
	10% (v/v)	FBS, inactivated 30 min 56°C
	1% (v/v)	MEM vitamins, non-essential aa
	1.2 mg/ml	Cycloheximid
E. coli culture	25 g	LB medium (Luria/Miller)
(heated 121.5°C / 2 bar / 20	Ad 1 l	ddH_2O
min, LB-Medium)	Evt. 13.5 g	Agar, when preparing plates
	Evt. 100 µg/ml	Ampicillin, when selecting bacteria
HS27/HFF cells & *T. gondii*		IMDM
culture	10 % (v/v)	FCS
	0,05 mM	β-ME
Human cell culture		DMEM
	10 % (v/v)	FBS, inactivated 30 min 56°C
Murine cell culture		DMEM
	10 % (v/v)	FBS, inactivated 30 min 56°C
	0.001 % (v/v)	β-ME
Freezing/storage of cell lines	40 % (v/v)	medium dedicated for cells
	50 % (v/v)	FBS, inactivated 30 min 56°C
	10 % (v/v)	DMSO
Imaging of live cells		Phenol free DMEM
	10 % (v/v)	FBS, inactivated 30 min 56°C
	0.001 % (v/v)	β-ME
improved imaging of live cells		FluoroBrite
	10 % (v/v)	FBS, inactivated 30 min 56°C
	0.05 mM	β-ME
maturing murine bone		RPMI VLE
marrow cells into BMDMs	15 % (v/v)	L-Sup (sterile filtered 0.2 µM)
	10 % (v/v)	FBS VLE (Lonza)
mycobacterial liquid culture		Middlebrook-7H9-medium (4,7 g + 900 ml dest H_2O. 0.2 µm filtered)
	10% (v/v)	ADC
	0,5% (v/v)	Glycerin (0.2 µm filtered)
	0,05% (v/v)	Tyloxapol (0.2 µm filtered)
murine BMDM culture (up to		RPMI VLE
5 days post differentiation)	10 % (v/v)	FBS VLE (Lonza)
mycobacterial plate culture		Middlebrook-7H10-medium (19 g + 900 ml dest H_2O. 0.2 µm filtered) heated 121°C / 2 bar / 20 min and cooled to 50°C
	10% (v/v)	ADC
	0.5% (v/v)	Glycerin (0.2 µm filtered)

2.6 Antibodies

2.6.1 Primary and secondary antibodies

Antibody	Manufacturer
Anti-*Toxoplasma gondii* [TP3] (SAG1) **# ab8313**	Abcam, Cambridge, UK
Goat anti-mouse IgG (H+L) /Alexa-633 **#A21050**	Thermo Scientific, Braunschweig
Goat anti-mouse IgG IgM (H+L) /Cy3 **#115-165-044**	Jackson ImmunoResearch
Goat anti-rabbit IgG (H+L) /Alexa 633 **#A21070**	Thermo Scientific, Braunschweig
monoclonal mouse IgG2a anti-Chlamydia trachomatis Major Outermembrane Membrane Protein (MOMP) BIOD166 **#20881**	Abcam, Cambridge, UK
polyclonal rabbit anti-CT868 Chlamydial inclusion membrane protein also known as ChlaDUB1, Cdu1, Ctad8. Immunized with CT868 Δ1-60 AS.	Peptide synthesis and rabbit immunization by Eurogentec, Liege, Belgium for Hegemann research group; (Fischer et al., 2017; Lindenberg et al., submitted; Stallmann, 2015)
polyclonal rabbit anti-mGBP2 (EVNGKPVTSDEYLEHC)	peptide synthesis and rabbit immunization by Eurogentec, Liege, Belgium for Pfeffer research group; (Degrandi et al., 2007)

2.6.2 Directly labelled antibodies

Antigen	Clone	Fluorochrome	Order #	Manufacturer
αCD16/CD32 (FC block)	93	unconjugated	14.0161.85	Thermo Scientific, Braunschweig
CD3ϵ	145-2C11	FITC	553062	BD Biosciences, Heidelberg
CD4	RM4-5	PerCP	553052	BD Biosciences, Heidelberg
CD8α	53-6.7	Pe-Cy7	552877	BD Biosciences, Heidelberg
NK1.1	PK136	PE	553165	BD Biosciences, Heidelberg
B220	Ra3-6B2	APC	553092	BD Biosciences, Heidelberg
F4/80	BM8	FITC	11.4801.82	Thermo Scientific, Braunschweig
CD11b	M1/70	APC-Cy7	557657	BD Biosciences, Heidelberg
CD11c	HL3	PE-Cy7	558079	BD Biosciences, Heidelberg
Gr1 (Ly6G & Ly6C)	RB6-8C5	PE	553128	BD Biosciences, Heidelberg
monoclonal anti-chlamydial	Unknown, Pathfinder®	FITC	30701	Bio-Rad, Redmond, WA, USA

2.7 Vectors and oligonucleotides

2.7.1 Plasmids

Plasmid	Characteristics	Source / Previously published
pWPXL	EF1-Promoter, Amp^R	D. Trono Laboratory, Lausanne, Switzerland
pWPXL/GFP	w/o-STOP	(Kravets et al., 2012)
pWPXL/mCh	w/o-STOP EF1-Promoter, Amp^R	(Klümpers, 2013) (Kravets et al., 2016)
pWPXL/mCh::mGBP1	EF1-Promoter, Amp^R	(Kravets et al., 2016)
pWPXL/GFP::mGBP2	EF1-Promoter, Amp^R	(Klümpers, 2013) (Kravets et al., 2012)
pWPXL/GFP::mGBP2 C586S	EF1-Promoter, Amp^R	(Degrandi et al., 2013)
pWPXL/mCh::mGBP2	2 silent mutations, EF1-Promoter, AmpR	(Kravets et al., 2016)
pWPXL/mCh::mGBP3	EF1-Promoter, Amp^R	(Kravets et al., 2016)
pWPXL/mCh::mGBP5	EF1-Promoter, Amp^R	(Kravets et al., 2016)
pWPXL/mCh::mGBP6	EF1-Promoter, Amp^R	(Kravets et al., 2016)
pWPXL/mCh::mGBP7	EF1-Promoter, Amp^R	Cloned by Kravets, E.
pWPXL/mCh::mGBP8	EF1-Promoter, Amp^R	Cloned by Buchholz, K.
pWPXL/mCh::mGBP9	EF1-Promoter, Amp^R	Cloned by Buchholz, K.
pWPXL/GFP::mGBP10	EF1-Promoter, Amp^R	(Klümpers, 2013)
pLP/VSVG	Vector encoding envelope VSV-G glycoprotein for lentivirus production, CMV Promotor, Amp^R	Invitrogen
psPAX2	Packaging vector encoding Gag, Pol and Env for lentivirus production, CMV Promotor, Amp^R	D. Trono Laboratory, Lausanne, Switzerland (Yang et al., 2012)

2.7.2 Primers for site directed mutagenesis

All oligonucleotides described below were synthesized by Metabion International AG and delivered as HPLC highly purified desalted stocks and routinely resuspended at a final concentration of 100 pmol/µl.

Primers (SDM)	Top (sequence 5' to 3`)	Bottom (sequence 5' to 3`)
mGBP1-Q545A	GAAGTTTAAGGGATATGATTCTTGCTTGC TCTGCCATTAACTCTTTCCG	CGGAAAGAGTTAATGGCAGAGCAA GCAAGAATCATATCCCTTAAACTTC
mGBP1-Q545E	AGTTTAAGGGATATGATTCTTTCTTGCTCT GCCATTAACTCTTTC	GAAAGAGTTAATGGCAGAGCAAGA AAGAATCATATCCCTTAAACT
mGBP2-E545Q	AGTTTAGCAGCTATGATGTTTTGCTGTTCT GCTAATAACTGTTTC	GAAACAGTTATTAGCAGAACAGCAA AACATCATAGCTGCTAAACT
mGBP3-E540Q	CTCCAGCATCTTCTGCTGCTCCCTCAGCA	TGCTGAGGGAGCAGCAGAAGATGC TGGAG
mGBP5-Q542E	TCAGGATCCACTCTTGCTCTTGTGCAACTC	GGCAAGAGTTGCACAAGAGCAAGA

	TTGCC	GTGGATCCTGA
mGBP6-D542N	GCAGGACATCAAAGACCATAATATGATGC TGAAGAAGCT	AGCTTCTTCAGCATCATATTATGGTC TTTGATGTCCTGC
mGBP6-N542K	TAGCTTCTTCAGCATCATCTTATGGTCTTT GATGTCCTGC	GCAGGACATCAAAGACCATAAGATG ATGCTGAAGAAGCTA
mGBP7-E546Q	CCAGCTTCACCTGTTGCTCTCTCAGGATGT TCTTCC	GGAAGAACATCCTGAGAGAGCAAC AGGTGAAGCTGG
mGBP8-N460D	TCCACCATCATGTCATGGTCTTTGATGAGC TGCTCT	AGAGCAGCTCATCAAAGACCATGAC ATGATGGTGGA
mGBP9-D542N	GCTTCTCCAGCATCATATTATGGTCTTTGA TGTCCTG	CAGGACATCAAAGACCATAATATGA TGCTGGAGAAGC
mGBP10N542D	CTTCAGCATCATGTCATGGTCTTTGATGA GCTGCTCTCT	GAAGTCGTAGTACAGTACCAGAAAC TACTCGACGAGAGA

2.7.3 Primers for sequencing

All oligonucleotides described below were synthesized by Metabion International AG and delivered as purified desalted stocks and routinely resuspended at a final concentration of 100 pmol/µl.

Primer	Forward (sequence 5'-3')	Reverse (sequence 5'-3')
pWPXL (WPRE)	-	GAATACCAGTCAATCTTTCAC
mCherry	ACCATCGTGGAACAGTACG	-
mGBP1-middle	GGGCCCAGCTGGAAGCCAAA	TTTGGCTTCCAGCTGGGCCC
mGBP2-middle	GCCGCGACTGTGCATCAGGA	TCCTGATGCACAGTCGCGGC
mGBP3-middle	CCCTGGCCCAGCGTGAGAAC	GTTCTCACGCTGGGCCAGGG
mGBP5-middle	GCGGATGCTTCTGCAGCCCT	AGGGCTGCAGAAGCATCCGC
mGBP6-middle	AGCGCTCACTGCTGGGGAGA	TCTCCCCAGCAGTGAGCGCT
mGBP7-middle	AGGCTCCCCACAGACACGCT	AGCGTGTCTGTGGGGAGCCT
mGBP8-middle	AGCCCTCACTGCTGGGCAGA	TCTGCCCAGCAGTGAGGGCT
mGBP9-middle	TAGAGCCCTCACTGCTGGGG	CCCCAGCAGTGAGGGCTCTA
mGBP10-middle	GCCCAGCGACTGAGGCTTCC	GGAAGCCTCAGTCGCTGGGC

2.7.4 Generated mutated vectors

Plasmids	Characteristics
pWPXL/mCh::mGBP1-Q545A	EF1-Promoter, Amp^R
pWPXL/mCh::mGBP1-Q545E	EF1-Promoter, Amp^R
pWPXL/mCh::mGBP2-E545Q	EF1-Promoter, Amp^R
pWPXL/mCh::mGBP3-E540Q	EF1-Promoter, Amp^R
pWPXL/mCh::mGBP5-Q542E	EF1-Promoter, Amp^R
pWPXL/mCh::mGBP6-D542K	EF1-Promoter, Amp^R
pWPXL/mCh::mGBP6-D542N	EF1-Promoter, Amp^R
pWPXL/mCh::mGBP7-E546Q	EF1-Promoter, Amp^R
pWPXL/mCh::mGBP8-N460D	EF1-Promoter, Amp^R
pWPXL/mCh::mGBP9-D542N	EF1-Promoter, Amp^R
pWPXL/GFP::mGBP10-N542D	EF1-Promoter, Amp^R

2.7.5 Primers for evaluating Chlamydial progeny

All oligonucleotides described below were synthesized by Metabion International AG and delivered as purified desalted stocks and routinely resuspended at a final concentration of 100 pmol/µl.

Oligo name	Forward (sequence 5'-3')
CT-Fw omp1	GGT TTC GGC GGA GAT CCT
CT-Rev2 omp1	AGT AAC CCA TAC GCA TGC TGA T
Ct-Probe omp1 FAM	6-Fam-CTT GCA CCA CTT GGT GTG ACG C-BHQ-1
mIFNβ FW	CAG GCA ACC TTT AAG CAT CAG
mIFNβ REV	CCT TTG ACC TTT CAA ATG CAG
mIFNβ probe	Roche UPL 95, 04692128001 (#122740)

2.8 Machines

Machine	Manufacturer
Balance ABT 120 5 DH	Kern, Buchholz
Balance Chyo JL-180	Welabo, Düsseldorf
Balance EMB 2200-0	Kern, Buchholz
Balance Precisa 600	Oehmen Labortechnik, Essen
Biological safety cabinet	Kendro, Langenselbold
Cell Density Meter Ultraspec 10	Amersham Bioscience,
Cell shaker 3015	GFL, Burgwedel
Centrifuge Biofuge A	Thermo Fisher Scientific, Bonn
Centrifuge Heraeus Biofuge Primo R	Thermo Fisher Scientific, Bonn
Centrifuge Megafuge 1.0R	Thermo Fisher Scientific, Bonn
Centrifuge Rotana 46 RC	Thermo Fisher Scientific, Bonn
Centrifuge tabletop: Biofuge fresco	Thermo Fisher Scientific, Bonn
Centrifuges tabletop 5415D, 5415, 5417R	Eppendorf, Hamburg
Electrophoresis chamber	Hoefer, Amsterdam
FACS Aria III	BD Bioscience, Heidelberg
FACS Canto II	BD Bioscience, Heidelberg
Freezer -80°C Ultra Low	Sanyo, San Diego, USA
Gel analysis system *BioDocAnalyze*	Biometra, Göttingen
Gel analysis system	Bio-Rad, München
Heated mixer MR3001 K	Heidolph, Schwabach
Heatlock/ Thermoblock Thermomix	Eppendorf, Hamburg
Hood	WRT-Laborbau, Stadtlohn
Incubator BBD6220	Thermo Fisher Scientific, Bonn
Incubator HEPA Class 100 (Hegemann Lab)	Thermo Electron Corp, Waltham, MA, USA
Laminar flow, HLB 2472 GS	Thermo Fisher Scientific, Bonn
Microscope Axioskop 50 + (Hegemann Lab)	Zeiss, Jena
Microscope Axiovert 11	Zeiss, Jena
Microscope Axiovert 200 (Hegemann Lab)	Zeiss, Jena
Microscope Binoc Axiovert 25C (Hegemann)	Zeiss, Jena

Microscope confocal LSM780	Zeiss, Jena
Microscope TE2000	Nikon, Minato, Japan
Millipore Elix advantage 3	Millipore, Schwabach
Mixer for bacterial cultures, Ecotron	Infors HT, Schweiz
Multistep-Dispenser Handystep	Brand, Wertheim
NanoDrop 1000	Peqlab, Erlangen
Neubauer Counting chamber	LO-Laboroptik, Friedrichsdorf
pH-Meter MP225	Mettler-Toledo, Giessen
Photometer: TECAN Sunrise	Tecan, Männedorf, CH
Pipet multichannel	Thermo Fisher Scientific, Bonn
Pipet-Boy, accu-jet	Brand, Wertheim
Power source PS 500 XT	HIS, San Francisco, USA
Power source, Power Pack P25	Biometra, Göttingen
qRT-PCR CFX96 machine	Bio-Rad, München
qRT-PCR iCycler iQ5	Bio-Rad, München
Sonification devices Labsonic U and TG 1503	Bandelin
Surgical toolset	Fine Science Tools, Heidelberg
Thermocycler T1, T3 & T-gradient	Biometra, Göttingen
Thermomixer	Eppendorf, Hamburg
Ultra-Turrax T25	IKA, Staufen
Vortex VVR	VWR, Darmstadt
Water bath	Köttermann Labortechnik
WNB22	Memmert, Schwabach

2.9 Software

Software
Microsoft Office 2010
Graphpad Prism 5
NCBI-tools
Adobe Acrobat XI Pro
Adobe Illustrator
Adobe Photoshop CS1
GelDoc
Geneious 5.5.6
Facs Diva (BD Biosciences)
Flowjo software vs. 8 & 10 (Tree Star, Ashland, USA)
Bio-Rad iQ5 2.0 Standard Edition Optical Systems Software
Bio-Rad CFX Manager 3.1 & 2.1
Zen 2010, 2011 and 2012 software (grey, blue, 2.1 SP3)
Imaris Bitplane
EndNote X7.0.1

2.10 Statistical analysis

Results are represented as means +SD or +SEM as indicated. The unpaired two-tailed Student's t-test was used to test for statistical significance, * indicates $p < 0.05$, ** indicates $p < 0.01$ and *** indicates $p < 0.001$, which were considered significant.

3 Methods

3.1 Molecular biological methods

3.1.1 Site directed mutagenesis (SDM)

To analyse potential motifs in mGBP proteins' C-terminus, base pair triplets were selected, in which one base was mutated in order to translate into an amino acid with different side chain properties. To obtain such mutations the QuikChange® XL Site-Directed Mutagenesis Kit was utilized. Using the 'QuikChange primer Design tools' in Stratagenes homepage several primers were designed (2.7.2), synthesized, highly purified by Metabion. These primers were used to introduce site-directed mutations described (Results table 2) in lentiviral expression vectors available in the research group (2.7.1). Polymerase chain reactions (PCRs) were performed according to the manufacturer's instructions. After amplification the PCR-product was digested with the restriction enzyme *DpnI* for 1 h at 37°C, allowing fragmentation of non-mutated methylated vectors. Subsequently, 3 µl of the digested PCR mixture was used to transform competent DH5α *Escheria (E.) coli* (3.1.2).

3.1.2 Transformation of DH5α *Escheria coli*

E. coli DH5α was rendered competent by $CaCl_2$ treatment, aliquoted and frozen for future use. For this study, aliquots containing 100 µl of these bacteria were thawed on ice after which a 100 ng of the PCR mixture described above was gently added. After 20 min of incubation on ice a heat shock of 42°C for 1 min was administered either by insertion in a water bath or heat block, to allow plasmid uptake into the bacteria. Subsequently the bacteria were shortly cooled on ice, 500 µl LB-Medium was added and incubated for 1 h at 37°C while swivelling. From these cultures 100 µl were plated on solid LB medium containing ampicillin to exert selection pressure on those bacteria which gained antibiotic resistance from acquiring a pWPXL plasmid. Plates were incubated at 37°C under aerobic conditions overnight. Subsequently, single colonies were picked to create monocultures in liquid medium containing ampicillin, of which the pWPXL plasmid was then further inspected.

3.1.3 Confirmation of successful SDM

By utilizing the modified alkaline- lysis method (Birnboim and Doly, 1979) low amounts of plasmids were extracted from different *E. coli* clones using the Zyppy Plasmid miniprep kit, or higher yields were obtained with the NucleoBond Xtra Maxiprep Kit. Both were used according to manufacturer's instructions. The plasmids extracted from different

clones were all subjected to restriction analysis (described below 3.1.4), and gel electrophoresis (described below 3.1.5). Bands with a length matching insertion of an mGBP clone in the pWPXL vector were carved from the agarose gel under UV-Light (λ=230 nm) and extracted using a Zymoclean Gel DNA Recovery Kit according to the manufacturer's instructions. These purified plasmids were sent for sequencing to Beckman Coulter Genomics (Germany). The site which was intended for SDM was investigated with 4-fold coverage by 4 different primers (2.7.3). The sequences were aligned in Geneious software (Biomatters Ltd., Auckland, New Zealand) and in the compiled sequence the targeted base pair was evaluated. Those *E. coli* clones containing successfully mutated plasmids were expanded and high concentrations of the expression plasmids isolated for the creation of lentiviral particles.

3.1.4 Restriction analysis

Prior to analytical agarose gel electrophoresis, plasmid DNA was linearized and/or digested by restriction enzymes. Restriction was performed according to the enzyme manufacturer's instructions.

Component	amount
DNA	x µL
Buffer (10x)	3 µL
Enzyme	2–5 Units / µg DNA (max 10% total volume)
ddH_2O	ad 30 µL

In this study, solely type 2 endonucleases with defined, palindromic dsDNA cleavage sites were used for restriction (see table below).

Restriction enzyme	Recognizes and digests		Manufacturer
BamHI	5'-G*GATCC-3'	ER0055	Thermo Scientific, Braunschweig
EcoRI	5'-GAA*TTC-3'	ER0273 1184053	Fermentas, St. Leon Roth Roche, Manheim
Nde1	5'-CA*TATG-3'	R0111S 13643821	New England BioLabs, Frankfurt a. M. Roche, Manheim
Cla1	5'-AT*CGAT-3'	10404217001	Thermo Scientific, Braunschweig
Spe1	5'-A*CTAGTAT-3'	11008951001	Thermo Scientific, Braunschweig
Sal1	5'-G*TCGAC-3'	R0138S	New England BioLabs, Frankfurt a. M.

After restriction the product was cooled to 4 °C and an agarose gel prepared.

3.1.5 Agarose gel electrophoresis

Agarose gel (1 % (w/v)) was prepared by melting agarose in 1x TAE buffer using a microwave. The solution was cooled down and subsequently ethidium bromide was added to a final concentration of 0.5 µg/ml. The mixture was poured out in a mould and the gel allowed to polymerize for at least 45 min. Each DNA sample was mixed with 1/5 volume of 6 x loading buffer. The solidified gel was placed in an electrophoresis chamber filled with TAE buffer, samples were loaded and the electrophoresis started by applying 100-120 V. The DNA was visualized on a Gel analysis system.

3.1.6 Analysis of *Chlamydia trachomatis* genome copies

To assess growth of chlamydia in mGBP knock out cells, a strategy to identify genome equivalents after one cycle of infection was developed. At 42 hpi, chlamydia were harvested from primary fibroblasts by lysis, repeatedly rinsed with PBS, supernatants aspirated and the pellet frozen at -20°C as described. Since at 42 hpi inclusions contain both fragile RBs and many resistant, spore-like EBs, an experimental strategy capable of accessing the genomic DNA in EBs was required. Several different DNA isolation techniques such as SDS buffers, Proteinase K digestion, and the CTAB-lysozyme method (Larsen et al., 2007) combined with no, 1 x 40 s or 3 x 10 s sonication were compared for their maximum DNA yield of the same sample. The following protocol displayed the highest DNA yield as visualized by agarose gel electrophoresis: pellets containing chlamydia were thawed at RT and subsequently strenuously resuspended in 900 µL SDS containing digestion buffer. The solution was transferred to tubes which do not release plastic particles upon vibrations and sonicated three times for 10 s, more than 90 s apart. To the mixture 45 µl proteinase K (10 mg/ml) was added and incubated overnight at 55°C while shaking at 800 rpm. Afterwards proteinase K was inactivated by heating to 98°C for 10 min. Subsequently 900 µl Rotiphenol was added, vortexed vigorously and left to settle for 5 min at RT. Phase separation was obtained by centrifugation for 15 min at 13,000 rpm. The upper phase was carefully transferred (without touching the protein layer between the phases) and 0.7 times its volume of isopropanol was added. Tubes were inverted to mix both solutions, incubated at RT for 5 min and centrifuged for 10 min at 13,000 rpm. The supernatants were aspirated and the pellet washed in ice cold 75% ethanol in ddH_2O. Centrifugation for 8 min at 13,000 rpm pelleted the DNA, supernatant was aspirated and ethanol allowed to evaporate under the hood. Afterwards the DNA was immediately dissolved in TE-buffer and 10 minute incubation at 56°C after which the DNA was cooled down to 4°C and the DNA concentration was determined.

In order to analyse chlamydial genome equivalents in the collected DNA, all real time quantitative (q)PCR strategies published previously (Schaeffer and Henrich, 2008) were compared for their sensitivity. As a result, the single-copy-gene *C. trachomatis omp 1* as detected with reverse primer 2 was selected (see 2.7.5) to be the most sensitive and specific analysis of the Hegemann laboratory LGV strain. A plasmid containing the targeted sequence was amplified and diluted into a standard. Due to known number of *omp 1* genes in the standard, their exponential amplification allows more and more probes to adhere to their specific sequence and be cleaved by polymerases to release a fluorescent signal to be measured as an exponential curve in which we can set a threshold resulting in a value (CT) which can be compared to samples thus measuring the genome equivalents of chlamydia.

It is conceivable that also murine genomes are present within the collected DNA. In addition, varying ratios between murine and chlamydial genomes within the total DNA might reduce the sensitivity of this experiment. In order to estimate and normalize the contribution of murine DNA to the total DNA tested, a murine single-copy-gene, namely IFNβ, was also measured for each sample. In addition, every sample was run in triplicate.

Sample DNA was diluted 1:5 times and 2.5 µl were pipetted into each well of a 96-well plate containing 22.5 µl of the responding the mastermixes were prepared as follows:

Components per 96-well	Ct *Omp 1*	mIFNβ
distilled water	8.9 µl	9.8 µl
qRT-PCR MasterMix -No ROX	12.5 µl	12.5 µl
Forward primer	0.075µl	0.3 µl
Reverse primer	0.075 µl	0.3 µl
Probe	0.05 µl	0.5 µl

For every primer pair there was a DNA free well as a negative control included in the qRT-PCR reaction. The qRT-PCR reactions performed in an iQ5 cycler or CFX cycler under following conditions:

qRT-PCR programme
1. Start 50°C for 10 min
2. DNA denaturation at 95°C for 10 min
3. DNA denaturation at 95°C for 20 s
4. Hybridisation and elongation of at 60°C for 1 min
Steps 3 - 4 were periodically repeated for around 30 cycles
5. Hold at 4 °C

Of all repeated experiments, the percentage of genomes after passage in wild type fibroblasts was set to 100 % and mGBP knock out fibroblasts were depicted accordingly.

3.2 Cell Biological Methods

All cultures came into contact exclusively with sterile solutions and plastics and were handled wearing one-way nitril gloves in Laminar AIR Flow cabinets (Thermo Fisher Scientific, Bonn).

3.2.1 Cultivation of eukaryotic cell lines

Cell lines were cultured in dedicated medium (2.5.3) in tissue-culture-treated flasks, petridishes or well plates seeded at a confluence of 10-30% and allowed to grow for 2-3 days into 80-100% confluence and passaged when necessary. Therefore, adherent cells were rinsed with PBS, incubated with Trypsin/EDTA for 3-5 min at 37°C, resuspended in medium to mitigate enzyme activity, followed by centrifugation for 5 min at 1,200 rpm, aspiration of the supernatants and resuspension of the cell pellet in fresh medium. Single cell solutions were diluted and incubated with trypan blue to exclude dead cells during counting. Subsequently, cells were seeded into new tissue culture flasks for subculture. Primary bone marrow derived macrophages were cultured in untreated petridishes and passaged by cooling cells on ice and subsequent scraping from the dishes in order to create single-cell suspensions for dilutions. All cell lines and primary cells were cultured at 37 °C and 10 % CO_2 in a humidified incubator.

After expansion 2 x 10^6 cells were preserved in 1 ml freezing medium containing 10% DMSO in cryotubes by freezing for 30 min at -20°C followed by overnight incubation in -80°C and definite storage in liquid nitrogen.

3.2.2 Lentiviral transduction to create cell lines expressing mutant mGBPs and controls

In order to express the mutated genes in a cell line a lentiviral transduction approach was used. One of the previously listed pWPXL-expression vectors (2.7.1, 2.7.4) together with pLP/VSVG and psPAX2 plasmids was transfected into 293FT cells thus bringing all components together for a single round of lentivirus production, in a cell line capable of producing high titers. Transfection with JetPRIME was performed according to manufacturer's instructions in a 6-well format. After approximately 48 h incubation, syncytia, expression of fluorescence-tags and cell death indicative of virus production could be observed and were the cue for virus collection. The complete supernatant was centrifuged for 10 min at 2,000 rpm to reduce cell debris and either used immediately or shock-frozen in liquid nitrogen prior to storage at -80 °C.

NIH/3T3 fibroblasts were cultured to confluence in 24 well plates. The collected virus was thawed and mixed with 5 µg/ml polybrene. The medium was replaced by the virus-mixture and cells were allowed to regain temperature by 30 m incubation. The plate was centrifuged at 1,200 rpm at about 32°C and subsequently incubated for 5-6 h until the medium was refreshed to improve infection rates. Cells were cultivated further until constitutive expression was evaluated and fluorescence expression set as a selection criterion for fluorescent activated cell sorting (FACS) as described under (3.2.12). Sorted NIH/3T3 fibroblasts were expanded and frozen for storage until use.

3.2.3 Cultivation of *Toxoplasma gondii*

Apicomplexan *T. gondii* strain ME49 was maintained by serial passage. A total of 1 x 10^6 tachyozoites was used to infect a confluent monolayer of HFF cells (as host cells) in T25 tissue-culture-treated culture flasks containing IMDM-medium containing 10 % FCS and 0,05 mM β-mercaptoethanol. After parasite multiplication in the host cells, the tachyozoites were harvested from culture supernatant by centrifugation at 50 x g (600 rpm) to discard host cell debris and ultimately collection by centrifugation at 600 x g (1800 rpm) for 15 min at RT. Parasites were resuspended in medium, counted, and immediately used for infections of NIH/3T3 cell lines constitutively expressing mGBPs.

3.2.4 Infection with *Toxoplasma gondii*

After the steps described above, *T. gondii* tachyzoites were taken up in DMEM VLE medium for culturing murine cells, counted and immediately used. Cells were pre-stimulated overnight with 100 Units/ml IFNγ and infected with tachyzoites at a nominal multiplicity of infection (MOI) of 50 for 2 h at 37 °C and 10 % CO_2. Afterwards, cells were rinsed with PBS and prepared for immune fluorescence analysis.

3.2.5 Cultivation of *Chlamydia trachomatis*

C. trachomatis L2/434/Bu and *C. trachomatis* L2/434/Bu transformed with green fluorescent protein on an essential plasmid (pGFP)::SW2 (Wang et al., 2011) were propagated in HEp-2 cells cultured in DMEM medium supplemented with 10% foetal bovine serum (FBS), MEM vitamins and non-essential amino acids. Chlamydial elementary bodies (EBs) were purified using a 30% gastrographine solution and stored in SPG buffer and stored at -80°C.

3.2.6 Infections with *Chlamydia trachomatis*

Prior to infection, the SPG buffer containing chlamydial EBs was thawed and sonicated (3 x 10 s) to reduce clumping. Infections with *C. trachomatis* were performed with

NIH/3T3 or primary murine embryonic fibroblasts (mEFs) constitutively expressing mGBPs fused to GFP or mCherry seeded on coverslips (Ø 13 mm) or tissue-culture-treated 6-well plates at a nominal multiplicity of infection (MOI) of 3 for progeny or fixed cell analysis or an MOI of 30 for live cell analysis. In progeny or fixed cell experiments the infection was optimized by centrifugation (1 h, 2,920 rpm, 30°C). Subsequently, the cells were incubated for 3 h at 37 °C and 6% CO_2 in a humidified incubator. At 3 hpi, cells were stimulated by addition of fresh media containing IFNγ (final concentration of 100 Units/ml) and were incubated further. At indicated time points cells were either rinsed with PBS and fixed with 4% PFA for immunofluorescence analysis or used to determine progeny.

3.2.7 Analysis of *Chlamydia trachomatis* progeny

After one chlamydial infection cycle in primary mEFs as described above, at 42 hpi chlamydial particles were harvested by osmotic lysis to analyse the progeny as previously described (Nguyen and Valdivia, 2012). In short, cells were lysed by incubation with ddH_2O for 10 min and strenuous pipetting up and down. Immediately afterwards, culture medium was added in equal ratios, the mixture centrifuged (5 min, 1000 rpm, 4°C) to discard cellular debris and the supernatants centrifuged (20 min, 15000 rpm, 4°C) to collect chlamydial particles. The pellet containing chlamydia was washed with PBS, pelleted and a dilution series was made. The remaining chlamydial suspension was pelleted, supernatants aspirated and frozen at -20 °C for DNA isolation by a protocol developed in this study (described 3.1.6). Dilutions of chlamydial mixture were given in triplicate onto a confluent layer of HEp-2 cells in a 96-well plate and infection was optimized by centrifugation (1 h, 2,920 rpm, 30°C). Afterwards, cells were incubated for 24 h in medium containing cyclohexamide and incubated at 37 °C / 10% CO_2, allowing optimal development of infectious particles into inclusions. At 24 hpi, all wells were rinsed with PBS, fixed with ice cold methanol for 5 min, rinsed twice over and stained with the Pathfinder® Chlamydia Culture Confirmation System, according to the manufacturer's instructions. Each complete 96-well with separable GFP-stained inclusions was counted under a fluorescent microscope to determine inclusion forming units (IFU).

3.2.8 Cultivation of mycobacteria

All protocols dealing with mycobacteria, such as cultivation in submerged liquid and solid cultures, were performed as previously described (Larsen et al., 2007). In short, from glycerol stocks in -80°C storage mycobacteria BCG and H37Rv were seeded in liquid Middlebrook-7H9-medium, enriched with 10% (v/v) ADC, 0.5% (v/v) Glycerine and

0.05% (v/v) Tyloxapol. The culture was incubated at 37°C and continuous swivelling for 6-14 days until optical density (OD) values indicated that the bacteria grew exponentially, at which point they were used for infection studies or sub culturing.

3.2.9 Macrophage mycobacterial kill assay

Bone marrow derived macrophages (BMDMs) were made as described (3.3.3) were stimulated with 100 Units/ml IFNγ overnight or left untreated. Subsequently, 2 x 10^5 BMDMs were seeded per well in a 24-well plate in triplicates per condition: without or with stimulation, without or with infection of BCG or H37Rv. Mycobacteria in the exponential growth phase were prepared as described above (3.2.8) were washed twice in PBS-T and centrifuged down (10 min, 4,000 rpm) and were sonicated (3 x 10 s) to reduce clumping and OD_{600} was measured to establish the bacterial concentration (OD_{600} = 1 ≈ 3x10^8 cells). BMDMs were infected at an MOI of 3 for 3 h. At 3 hpi gentamicin was added to reach a final concentration of 10 µg/ml, which kills all extracellular mycobacteria, but allowing those bacteria taken up by the macrophages to survive. Four days later the macrophages were lysed by 0.05% SDS for 5-20 min, homogenized by pipetting up and down and sonicated (3 x 10 s) after which they were plated either directly or after a dilution series in PBS-T. Plates were incubated in a humidified incubator for 10-20 days until colonies were visible and could be counted to determine colony forming units (CFUs).

3.2.10 Immunofluorescencent staining of fixed cells

Cells were washed for 5 min in PBS on a slow shaker (rinsed) and fixed with 4% paraformaldehyde (PFA) for 10 min and rinsed repeatedly. Chlamydia and Toxoplasma infected samples were permeabilized with pure methanol for 5 min and washed or 0.02% saponin/PBS for 15 min, respectively. Blocking was performed with 2% goat serum in PBS or 0.002% saponin/PBS, respectively. Subsequently cells were stained for ~60 min with a primary antibody against *T. gondii* Sag1 (Abcam) at 1:700, or *C. trachomatis* Momp (BIOD166) at 1:100, rabbit polyclonal antibody against CT868 (Fischer et al., 2017; Lindenberg et al., submitted; Stallmann, 2015) at 1:25, followed by rinsing and for ~45 min with Alexa Fluor 488- or Cy3-conjugated secondary antibodies at 1:200, both in a 1:10 dilution of the blocking-solution. Host cell and pathogen DNA were stained with 4',6-diamidino-2-phenylindole (DAPI) at 1: 2,500 in PBS, respectively. Stained cells were rinsed twice and mounted on microscope slides with FluoromountG and allowed to settle overnight. All cells were imaged using a confocal LSM780 microscope (cLSM). Image analysis was performed using ZEN (Zeiss) and Imaris (Bitplane) software. Recruitment of proteins towards pathogens was quantified in three independent experiments, in each

of which approximately 100 intracellular pathogen-compartments were analysed for mGBP colocalization. Differential interference contrast (DIC) was used to identify and exclude extracellular *T. gondii* tachyzoites.

3.2.11 Live cell imaging

In addition to the description above, for live cell analysis the cells and GFP-expressing chlamydia were cultured and imaged on imaging dishes CG in Phenol-free or FluoroBrite cell culture media. If indicated, nucleic and pathogen DNA was stained with Hoechst-3569 (5 µg/ml). The cells were incubated at 37°C with 8% CO_2 and humidity saturated air while recording confocal LSM images every 10 min. At 3 hpi recordings were halted and cells were stimulated with IFNγ, after which the incubation conditions were allowed to re-establish and the recording ensued which allowed observation of the infected cells overnight.

3.2.12 FACS analysis

Cells were subjected to a treatment such as extracellular antibody staining, incubation with fluorescent beads or lentiviral transduction as described elsewhere (3.2.10, 2.3, 3.3.2). Afterwards cells were centrifuged, the pellets were then resuspended in 100 µl of FACS buffer containing DAPI (diluted 1:200) to discriminate living from dead cells. Cells stained with antibodies or fed beads were analysed on FACS Canto II.

Transduced cell lines constitutively expressing mCherry of GFP proteins were evaluated and sorted by median fluorescence intensity by Dr. Daniel Degrandi on the FACS Aria II cell sorter. Both FACS machines were managed using Diva software and data was interpreted using Flow Jo software.

3.3 Animal experiments

All mouse experiments were performed according to German law (Tierschutzgesetzes § 8) and were approved by the `Landesamt für Natur, Umwelt und Verbraucherschutz NRW der Bezirksregierung Düsseldorf‘ number O44/03 (organ and tissue isolation) & 8.87-51.05.30.13.039 (isolation of murine embryonic fibroblasts).

3.3.1 Mice

All mice used for this study were of the C57BL/6 strain, housed under SPF conditions as defined by the ‘Zentrale Einrichtung für Tierforschung und wissenschaftliche Tierschutzaufgaben HHU Düsseldorf’ (ZETT) on site, in plastic cages designed for genetically modified organisms (GMOs) and they were subjected to a circadian rhythm of 12 light-h and 12 h darkness. Mice were fed by standard feed and drinking water *ad libitum*.

3.3.2 Preparation of murine organs for FACS analysis

After cervical dislocation different tissues like spleen, liver, lung, lymph nodes or bone marrow were harvested. Harvested organs intended for FACS analysis were transferred into 6-well plates containing tissue digestion buffer (containing DNase and collagenase VIII) where they were carefully disrupted using tweezers and incubated at 37 °C for 30 min. Afterwards, the enzymatic reactions were stopped by adding 3-5 ml of Stop buffer. Cell suspensions were resuspended by pipetting up and down repeatedly after which they were transferred into a 50 ml tube over a 40 or 100 µm cell strainer and centrifuged at 1,200 rpm for 5 min at 4 °C. For spleens, cell pellets contained many erythrocytes which were lysed by adding 3 ml of erythrocyte lysis buffer to each sample for 3 min at RT. Lysis was stopped by addition of 10 ml of FACS buffer and samples were centrifuged at 1,200 rpm for 5 min at 4°C. Supernatant was discarded and the cell pellet was resuspended in 10 ml FACS buffer. For the liver and lungs cell pellets were resuspended in medium and, underlayed with 30% and 70% Percoll and centrifuged at 2,130 rpm for 25 min at RT with no brake. Cell debris in the very top layer was aspirated and immune cells from the middle layer were carefully collected using a 1 ml pipette and transferred into a new 50 ml tube. Collected immune cells were washed with 50 ml PBS, centrifuged at 1,800 rpm for 15 min at 4 °C, supernatant was discarded and the washing step repeated. Afterwards, cells of all organs were resuspended in FACS buffer, counted, aliquoted into FACS tubes. Cell suspensions were centrifuged (5 min, 1,200 rpm, 4°C) and supernatant was aspirated. 25 µl of blocking solution (FACS buffer containing 1:100 antibody dilution of αCD16/CD32) was added to each sample to block

unspecific binding sites, mixed and incubated for 10 min at 4 °C. Subsequently. 25 µl of primary antibody cocktail against membrane proteins distinctive of immune cell populations, (diluted 1:100) was added to the samples, mixed and incubated for another 10 min at 4 °C. Subsequently, samples were washed by adding 2-3 ml FACS buffer and centrifugation (5 min, 1,200 rpm, 4°C). Supernatant was discarded and 50 µl of secondary antibody cocktail (diluted 1:50) was added to the samples, mixed and incubated for 10 min at 4°C. Afterwards, cells were washed with 2-3 ml of FACS buffer, centrifuged (5 min, 1,200 rpm, 4°C) and further prepared as described above (3.2.12).

3.3.3 Isolation of murine bone marrow

Mice of an age of 8-14 weeks were sacrificed, hind legs removed and femurs and tibias were dissected. Bones were disinfected in 70% EtOH followed by a washing step in cold PBS. Subsequently, bones were opened on both sides and bone marrow was flushed out with RPMI using a 20 ml syringe with a 23 G needle. After carefully mixing by pipetting the dissociated bone marrow cells were transferred into a 50 ml tube and centrifuged for 5 min at 1,200 rpm at 4°C. Supernatant was aspirated and the cell pellet was resuspended in fresh medium. Afterwards cells were seeded in petridishes containing media and responding growth factors and differentiated into myeloid cells.

3.3.4 Differentiation of bone marrow

To differentiate bone marrow cells into bone marrow derived macrophages (BMDMs) 1.5-2x10^6 bone marrow cells were seeded into a petridish containing 10 ml RPMI media with L-cell supernatants which contain high levels of M-CSF. Medium was supplemented with additional 5 ml after 3 days and after 6 days cells were fully differentiated. Fully differentiated cells were either left untreated, stimulated with 100 Units/ml IFNγ and / or infected with pathogens.

4 Results

4.1 Protein sequences of interferon inducible GTPases

The anti-microbial role of distinct interferon (IFN) induced GTPases, proteins with the ability do hydrolyse Guanosine-5'-triphosphate (GTP), has been unequivocally shown in several model systems of infection (Broz, 2016; MacMicking, 2004; Meunier and Broz, 2016; Pilla-Moffett et al., 2016). Before exploring functional properties within this group of GTPases, an overview on the parology and homology between the known members of human and murine interferon inducible GTPases and their isoforms was generated. The complete amino acid (aa) sequences of all conventionally expressed isoforms were compared, as opposed to Figure 2 in the introduction (Kim et al., 2012a), which compared solely conserved G-domains, enabling deeper exploration of the similarities and diversities within the different IFN-inducible GTPase families.

4.1.1 Splice variants

The number or genes coding for interferon inducible GTPases gives rise to a still bigger number of proteins, due to alternative splicing. To investigate the homologies of currently known splice variants in both mice and humans their protein sequences were compared using Aliview version 1.18 for Muscle iterative alignment (Larsson, 2014). As an out-group a small GTPase was included for both species to improve branch length estimation. Due to increased size GVINs were misalignment and therefore discarded in both mice and human datasets. Additionally murine Irgb2b1 cross splice variant aligned well with for C-terminal part, due to its additional length the N-terminal end could not be aligned well and was therefore trimmed. Trees were created using MEGA version 7 with neighbour joining statistical method and poisson substitution model and were visualised using Phylo version 1.0 (http://phylo.io/).

As input for the alignment current protein sequences were imported from the NCBI Protein database and altered or inserted as described in publications (Bekpen et al., 2005; Degrandi et al., 2007; Kim et al., 2012a), (see attachment for sequences). It was decided that 1) predicted but unconfirmed and unpublished splice variants, and 2) variations which only occur under specific circumstances were excluded from the study. For accurate calculation of branch lengths non-inducible small GTPase Ras-related C3 botulinum toxin substrate 1 (in humans RAC1/ in mice Rac1) which protein is ~21 kDa in size was included as an ‘out group’. As labels during phylogenetic analysis the same

nomenclature as in previously published analysis was used (Bekpen et al., 2005; Kim et al., 2012a).

Both in myxovirus resistance proteins (mouse Mx/ and human MX) and guanylate binding proteins (Gbp/GBPs) families cluster together. Also the immunity-related GTPases (Irg/IRG) family clusters together in both species except for murine Irgq and human IRGC. Outstanding at a first glance, is the greatly reduced number of interferon inducible GTPases in humans compared to mice due to pseudogenisation (Bekpen et al., 2005; Kim et al., 2012a; Martens and Howard, 2006)..

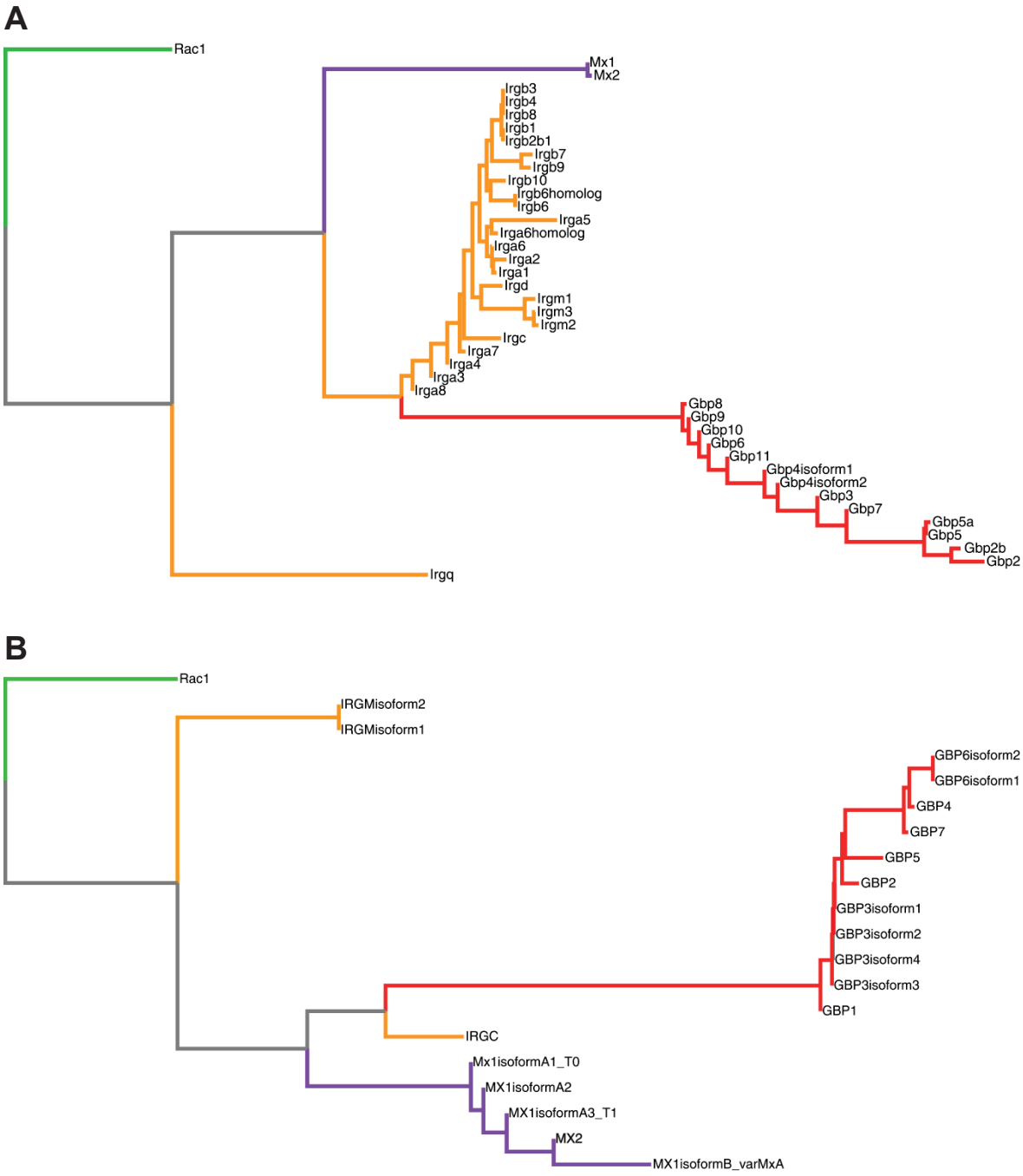

Figure 14: GBPs and splice variants of IFN-induced GTPases in A) murine (nomenclature as in introduction Figure 2 and 3: only leading capital letter, mGBP1/Gbp1 is stored in Genbank as Gbp2b) and B) human (capital letters) described by a phylogenetic tree

Due to alternative splicing several MX isoforms occur in humans, but not in mice. To additional forms are 4 variations of MX1 with divergent sequences.

Immunity Related Genes (IRGs) cluster together in both species, as expected based on their conserved G-domains containing a GKS motif, additionally those IRGs carrying a non-canonical motif, the inhibitory GMS motif (Daumke and Praefcke, 2016), also cluster

together. An exception to this rule is murine Irgq which was previously defined as an IRG-homolog (Bekpen et al., 2005). Another exception is human IRGM which is phylogenetically distinct form IRGC, due to the previously described genetic alterations caused by transposons and retrovirus modification (Bekpen et al., 2009; Bekpen et al., 2010).

In total there are 7 guanylate binding protein genes in humans (GBPs) and the 11 in mice (Gbps) which cluster together and thus share high homology to one another (Figure 14A). Murine Gbps on chromosome 3 and chromosome 5 which arose due to a gene duplication event also cluster together. CaaX-box containing mGBP1 labelled as Gbp2b (was reclassified as Gbp1, accession number NP_034389.2), mGBP2 and mGBP5 also cluster together. However, in the human GBP cluster GBP1 is divided from GBP2 and GBP5 by the four GBP3 isoforms, meaning that all isoforms of GBP3 has more similarities to GBP1, even though it lacks the CaaX domain.

Distinction between human and murine GTPases will from here onwards be made by a one-letter prefix, c.q. GBP2 will be called hGBP2, and Gbp2 will be mGBP2 in the remainder of this thesis.

4.1.2 Putative C-terminal motif in mGBPs

A subset of GBPs contains C-terminal amino acid motifs which have been shown to be essential for their function. For example, hGBP1, hGBP2, hGBP5, mGBP1, mGBP2, and mGBP5 possess a C-terminal CaaX-box which allows farnesylation or geranyl/geranylation and, as shown for mGBP2, is required for recruitment to intracellular pathogens (Degrandi et al., 2013; Kravets et al., 2016). However, other mGBPs amongst which mGBP6, do not contain such a motif, but can still recruit independently towards pathogens (Degrandi et al., 2007; Kravets et al., 2016). Previous studies in our laboratory revealed a putative motif in the C-terminal part of mGBP6 that can influence its localization. When mutated from a negatively charged aspartic acid (D) to neutrally charged asparagine (N) at positions 537 or 542, the recruitment ability of mGBP6 towards the parasitophorous vacuole (PV) of toxoplasma was diminished, most strongly for D542N (Klümpers, 2013). In addition, it was discussed that mGBPs which are known to recruit towards toxoplasma (mGBP2, mGBP3, mGBP6, mGBP7 and mGBP9; for mGBP1 is the only exception) all contain negatively charged D or glutamic acid (E) at the respective location to D542 of mGBP6 in a ClustalW alignment (Degrandi et al., 2007). Whereas mGBPs which were not found to recruit (mGBP5, mGBP8 and mGBP10), contain a neutrally charged N or glutamine (Q) at this amino acid position.

Therefore it was hypothesized that the properties of this amino acid could be a requisite of recruitment towards *T. gondii* in all mGBPs. To visualise the amino acid in question the open reading frames (ORFs) of mGBPs were aligned using Clustel omega (http://www.ebi.ac.uk/Tools/msa/clustalo/) and visualised using jalview's percentage identity view (http://www.jalview.org/).

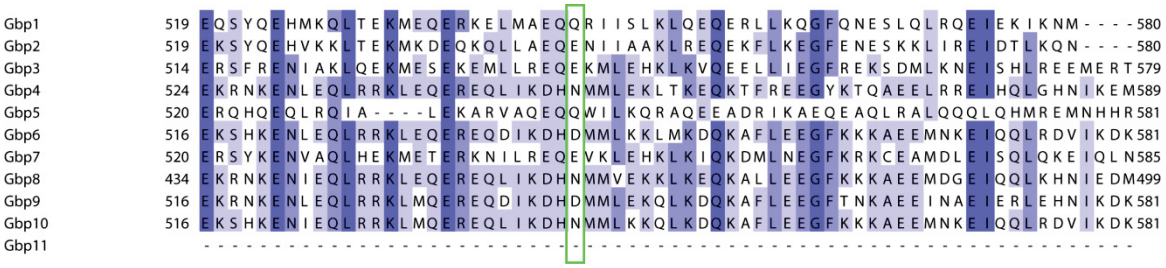

Figure 15: Alignment of C-terminal sequences of mGBPs. The amino acid position designated for mutation is highlighted in green.

To test this hypothesis, a search for C-terminally contained motifs in all GBPs was conducted using algorithms incorporated in the NCBI database (https://www.ncbi.nlm.nih.gov/cdd). Several conserved domains were found (See Table 1) amongst which the GBP-family N-terminal and C-terminal domains were conserved between all GBPs. However, different predictions were made at, or near, the predicted amino acid sequence including: Domains of Unknown Function (DUF), HAUS4, TATA, Yeast Nucleolar protein (Nop) 12, Class 2a HDAC-like and F-Bar domains. Particularly interesting is the prediction of the F-BAR domain which is named after the Fes/CIP4 homology Bin-Amphiphysin-Rvs167 domains are implicated in targeting towards lipid bilayers, moulding those membranes and have been found to modulate the function of Rho GTPases (Aspenstrom, 2014). It is unknown how the mGBPs target the bilayered pathogenic compartment within the cell if they do not have a CaaX-box, or do not multimerize with those that have one (Kravets et al., 2016). A bar-domain present in the C-terminus of mGBPs might explain the independent recruitment of for example mGBP6 towards *T. gondii* PVs (Kravets et al., 2016).

GBP	Predicted motif around relevant amino acid
hGBP1	F-BAR_FCHO 436-559
hGBP2	Glutamine-rich N-terminal helical domain 476-556
hGBP3	F-BAR_FCHO 434-539
hGBP4	-
hGBP5	CBP4 super family 425-524
hGBP6	-
hGBP7	DUF342 super family 522-608
mGBP1	Glutamine-rich N-terminal helical domain 477-556
mGBP2	-
mGBP3	TMF_TATA_bd super family 466-576
mGBP5	DUF2514 super family 487-558
mGBP6	F-BAR_PSTPIP 405-543 and HAUS4 super family 509-584
mGBP7	HAUS4 super family 509-584 F-BAR_PSTPIP 405-543
mGBP8	DUF342 super family 401-501
mGBP9	Nop25 super family 503-584
mGBP10	iSH2_PI3K_IA_R super family 509-593 F-BAR_PACSIN2 354-435

Table 1: Predicted distinct motifs and domains in murine and human GBP's C-terminus, '–' indicates no predicted motifs.

In order to test this hypothesis experimentally, all previously indicated mutations (Figure 15) were made by side directed mutagenesis of expression plasmids containing the wild type mGBP ORFs fused N-terminally to a fluorescent protein, either mCherry or GFP (for an overview of references see Table 2). By using lentiviral transduction, sequences coding for these mutant proteins were introduced into the genome of NIH/3T3 fibroblasts allowing constitutive expression of wild type or mutated mGBPs. Thus, twenty-four NIH/3T3 fibroblast cell lines were created and sorted for fluorescent protein expression. The localization of all wild type mGBPs in uninfected NIH/3T3 cells did not differ significantly from previously published results, except for mGBP5 (Degrandi et al., 2007), which is described below (Paragraph 4.2.4). Also, the generated mutants did not show any peculiar differences in localization to the corresponding wild type proteins (data not shown) except for mGBP10 (Paragraph 4.2.9).

Fusion protein	Codon	Published
mCh::mGBP1	CAA	(Kravets et al., 2016)
mCh::mGBP1-Q545A	GCA	this thesis
mCh::mGBP1-Q545E	GAA	this thesis
GFP::mGBP2	GAA	(Klümpers, 2013) (Kravets et al., 2012)
GFP::mGBP2 C586S	GAA	(Degrandi et al., 2013; Kravets et al., 2016)(Degrandi et al., 2013; Kravets et al., 2016)(Degrandi et al., 2013; Kravets et al., 2016)
mCh::mGBP2	GAA	(Kravets et al., 2016)
mCh::mGBP2-E545Q	CAA	this thesis
mCh::mGBP3	GAG	(Kravets et al., 2016)
mCh::mGBP3-E540Q	CAG	this thesis
mCh::mGBP5	CAG	(Kravets et al., 2016)
mCh::mGBP5-Q542E	GAG	this thesis
mCh::mGBP6	GAT	(Kravets et al., 2016)
mCh::mGBP6-D542K	AAG	this thesis
mCh::mGBP6-D542N	AAT	(Klümpers, 2013)
mCh::mGBP7	GAG	this thesis, Lindenberg et al., submitted
mCh::mGBP7-E546Q	CAG	this thesis
mCh::mGBP8	AAC	this thesis, Lindenberg et al., submitted
mCh::mGBP8-N460D	GAC	this thesis
mCh::mGBP9	GAT	this thesis, Lindenberg et al., submitted
mCh::mGBP9-D542N	AAT	this thesis
GFP::mGBP10	AAC	(Klümpers, 2013)
GFP::mGBP10-N542D	GAC	this thesis
GFP	-	(Kravets et al., 2012)
mCh	-	(Klümpers, 2013) (Kravets et al., 2016)

Table 2: Inserts in pWPXL (EF1α) plasmids used for retroviral transduction of NIH/3T3 fibroblasts, mCh : mCherry, GFP : green fluorescent protein.

4.2 Recruitment of mutated mGBPs to intracellular *Toxoplasma gondii*

To investigate whether the proposed amino acid described above is relevant for recruitment towards intracellular pathogens an experimental strategy was used which utilized the generated NIH/3T3 fibroblast cell lines (listed in Table 2). Previously, it was shown for mGBP2 that GTPase activity as well as IFNγ stimulation are required for optimal recruitment to *T. gondii* PVs, the peak of which is reached around 2 hours post infection (Kravets et al., 2012; Virreira Winter et al., 2011). To ensure optimal circumstances for recruitment, the transduced NIH/3T3 sub-confluent cells were stimulated overnight with 100 Units/ml IFNγ. Subsequent infection with *T. gondii* type 2 strain ME49 tachyzoites (hereafter referred to as *T. gondii)* was done for 2 hours at an MOI of 50. Afterwards, the cells were fixed and stained for *T. gondii* membrane marker 'surface antigen 1' (SAG1) and for DNA by using DAPI. Around 200 of the cells were then analysed by confocal laser scanning microscopy (cLSM) and assessed for the amount of intracellular *T. gondii,* and the percentage of PV colocalization with the mGBP in question. Diligent examination of differential interference contrast (DIC) allows recognition of extracellular *T. gondii*, in order to exclude them from the quantification. Recruitment was determined as a colocalization of fluorescent protein-tagged mGBP together with labelling of *T. gondii* with SAG1-antibody, around a DNA stain outside of the mammalian nucleus. This experimental strategy has resulted in mGBP recruitment rates varying from 38% to 77% (Degrandi et al., 2007; Degrandi et al., 2013; Klümpers, 2013; Kravets et al., 2016; Kravets et al., 2012; Virreira Winter et al., 2011) depending on the mGBP, cell type and experimental replicate. Therefore recruitment rates of mutant mGBPs were normalised to the number of colocalization events of the corresponding wild type mGBP, which was set to 100%.

4.2.1 mGBP1

After comparing the C-terminal sequences of mGBPs (Figure 15) it was proposed that those mGBPs which can recruit towards PVs have a negatively charged amino acid at the location analogous to mGBP6 D542N. For mGBP1 this position is the 545th amino acid, which is occupied by Q which has a polar and uncharged side chain. Nonetheless, mGBP1 can recruit towards *T. gondii*. Two hypotheses were developed. First, the polarity of the amino acid at this position might be relevant, for which we mutated Q to Alanine (A) which has a small, hydrophobic side chain thus preventing interactions with other (parts of the) protein(s) and thus being analogue to a 'null'-mutation. Second, since mGBP2 interacts directly with mGBP1 in VLS it might be the case that mGBP2 influences transport of mGBP1 to the PV (Kravets et al., 2016; Virreira Winter et al., 2011) and a mutant mGBP1 with a negatively charged amino acid, mGBP1-Q545E might influence interaction with mGBP2 and thus affect recruitment to the PV.

Previous studies showed that upon infection with *T. gondii*, mGBP1 can recruit around approximately half of the PVs in an IFNγ dependent manner (Degrandi et al., 2007; Virreira Winter et al., 2011). This study observed recruitment percentages around 30% in NIH/3T3 fibroblasts (Figure 30B). The appearance of mGBP1 accumulation around *T. gondii* PVs observed in this cell line was identical to previously published morphologies (Degrandi et al., 2007; Kravets et al., 2016; Virreira Winter et al., 2011). In Figure 16, representative images of mGBP1 positive PVs are shown. In the bottom panel a continuous, tight recruitment of mCherry-tagged mGBP1 (hereafter called mCh::mGBP1) around the parasite can be discerned, which is spatially separated from the plasma membrane of *T. gondii*, indicating recruitment onto the PV membrane. Interestingly, mCh::mGBP1-Q545E and mCh::mGBP1-Q545A recruited comparably to the wild type protein. In the top panel of Figure 16, a 'looser' and partial recruitment can be seen, akin to previously published images (Degrandi et al., 2007)-Figure 7a top panel and (Kravets et al., 2016)-Figure 5 second panel and Figure 9b. Judging from morphology of mCh::mGBP1-Q545A in the depicted recruitment event, accumulation at the PV membrane, disruption of the PVM and recruitment to the plasma membrane of *T. gondii* can be observed similar to previously described recruitment events of mGBP2 (Kravets et al., 2016). Thus, both wild type and mutated proteins appear to execute their functions, including the disruption of the PV membrane.

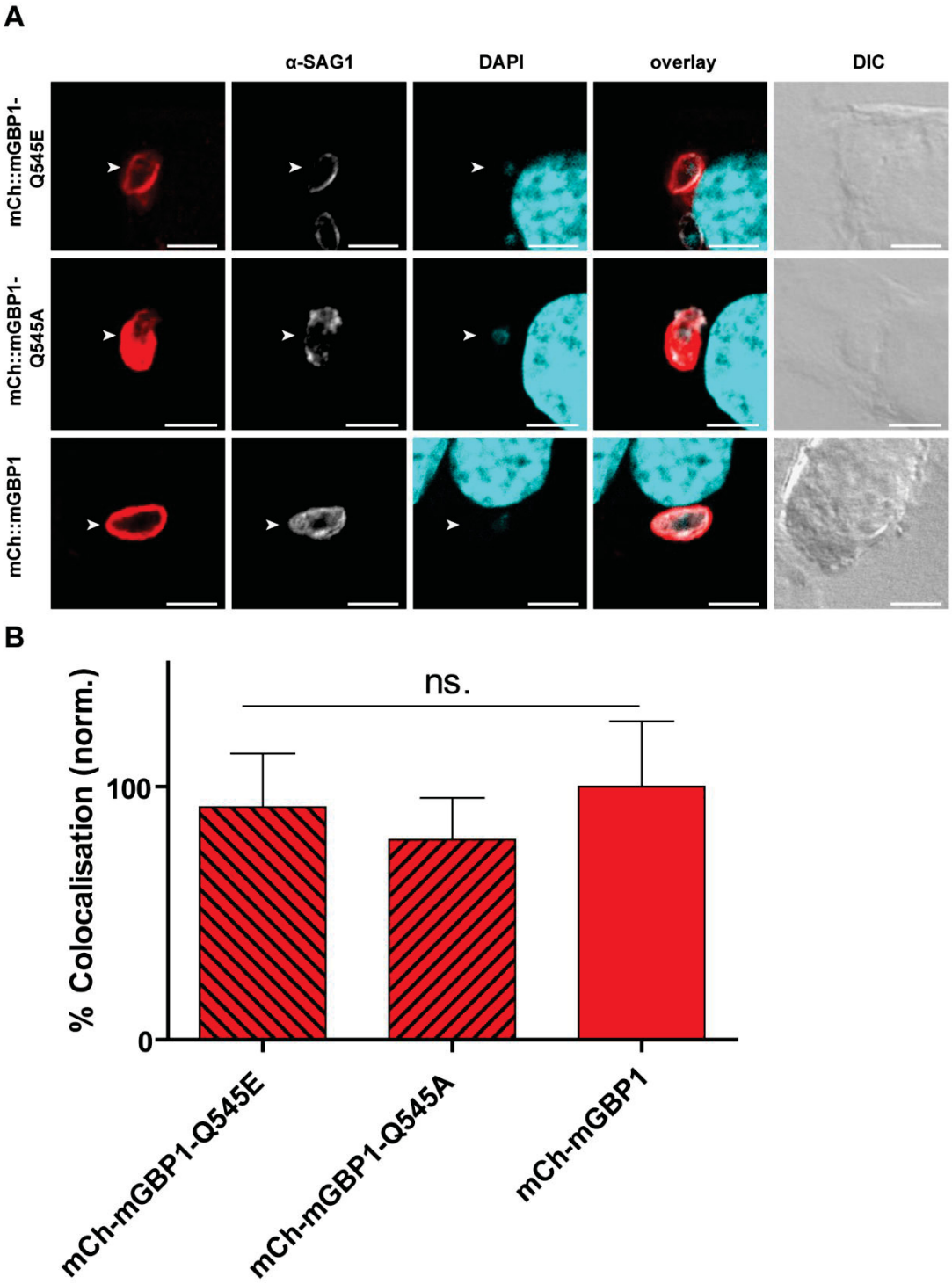

Figure 16: Recruitment of mGBP1-Q545E and mGBP1-Q545A to intracellular *T. gondii* 2 hpi. A) Representative cLSM pictures. α-SAG1 : *T. gondii* Surface antigen 1, DIC : differential interference contrast, bar : 5 µm. B) Normalized percentage of recruitment to intracellular *T. gondii*, n = 3, wild type mGBP : 100%, +SEM.

Quantification of the number of PVs colocalized with mGBP1 wild type or mutant proteins revealed no significant differences. Taken together, recruitment of mGBP1 towards *T. gondii* is not influenced by mutation of Q545 to E or amino acid A since recruitment is unaffected and PV membrane rupture occur.

4.2.2 mGBP2

Previously, it was shown that mGBP2 can recruit towards *T. gondii* PVs in murine embryonic fibroblasts (mEFs) to ~55% (Degrandi et al., 2007), ~50% (Kravets et al., 2012) or ~45% of cases (Degrandi et al., 2013). In this study, both mCherry::mGBP2 and GFP::mGBP2 recruitment was quantified, both of which recruited to 40% of PVs in NIH/3T3 fibroblasts. Thereby making mGBP2 the most frequent recruiter to the *T. gondii* PV in NIH/3T3 fibroblasts (Figure 30B).

Morphology of mGBP2 accumulation around the PV membrane is depicted in Figure 17A middle panels. The accumulation displays different intensities between various PVs within the same cell, thus being indicative of the extend of recruitment towards a particular PV, as described previously (Degrandi et al., 2007; Kravets et al., 2016; Virreira Winter et al., 2011). Both mCherry and GFP fusions recruited in in the same way and with the same percentages, thus indicating that these fluorophores do not impede mGBP function. The negatively charged amino acid predicted to play a role in mGBP2 recruitment towards *T. gondii* is ‘E’ at position 548. Mutation to an uncharged aa is hypothesized to reduce the recruitment frequency. Nevertheless, the mutated mGBP2 recruited with the same appearance Figure 17A top panel and frequency Figure 17B as the wild type protein.

When the isoprenylation site of mGBP2, a CaaX-box starting at position C586, is disrupted by mutating cysteine (C) to serine (S), the protein is found ubiquitously in the cytosol instead of in VLS and recruitment to *T. gondii* is abrogated (Degrandi et al., 2007; Kravets et al., 2016). In addition no VLS are formed and the mutated protein is found ubiquitously in the cytosol. This study confirmed this finding in NIH/3T3 fibroblasts, since virtually no recruitment was observed for mGBP2-C586S (Figure 17, bottom panel).

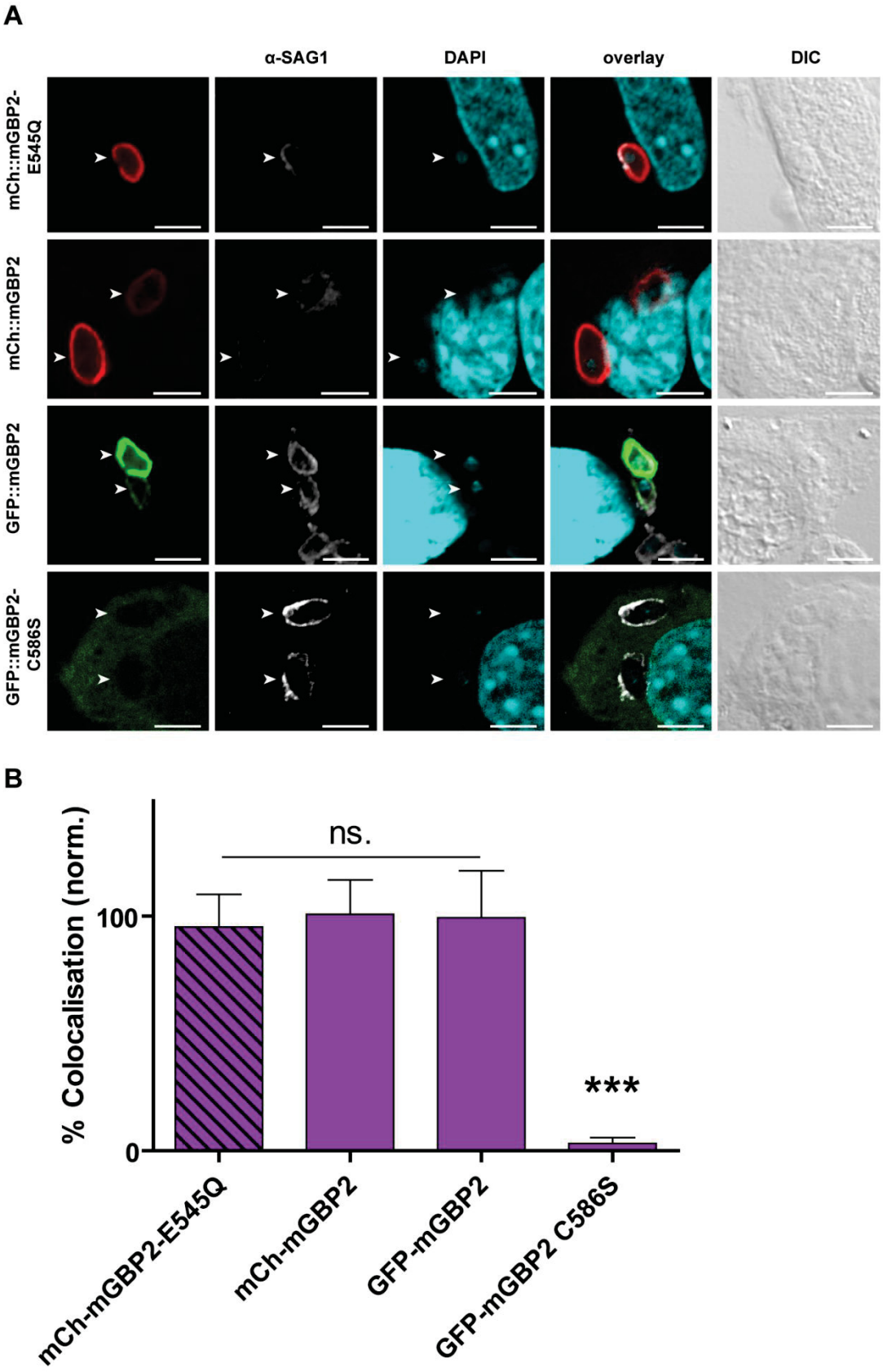

Figure 17: Recruitment of mGBP2-E545Q and mGBP2-C586S to intracellular *T. gondii* 2 hpi. A) representative cLSM pictures. α-SAG1 : *T. gondii* Surface antigen 1, DIC : differential interference contrast, bar : 5 µm. B) Normalized percentage of recruitment to intracellular *T. gondii,* n:3, wild type mGBP : 100%, +SEM.

4.2.3 mGBP3

In mGBP3 the amino acid proposed to be important for colocalization with the PV is the negatively charged E540 which was mutated to uncharged Q. Enlarged images of colocalized PVs show that both the original and mutated protein can locate to the *T. gondii* PV and have no statistical difference in the frequency of colocalization (Figure 18). A closer examination of the image of mGBP3-E540Q below the arrow shows the border of a partial mGBP3 colocalization coinciding with an uncommon ‘nick’ in parasite shape as depicted by α-SAG1 staining. This morphology can be either explained by PV membrane rupture or active escape of the parasite from its intracellular compartment, both of which suggest a function similar to mGBP2, which interacts with mGBP3 (Kravets et al., 2016) and for which an anti-parasitic function has been shown (Degrandi et al., 2013).

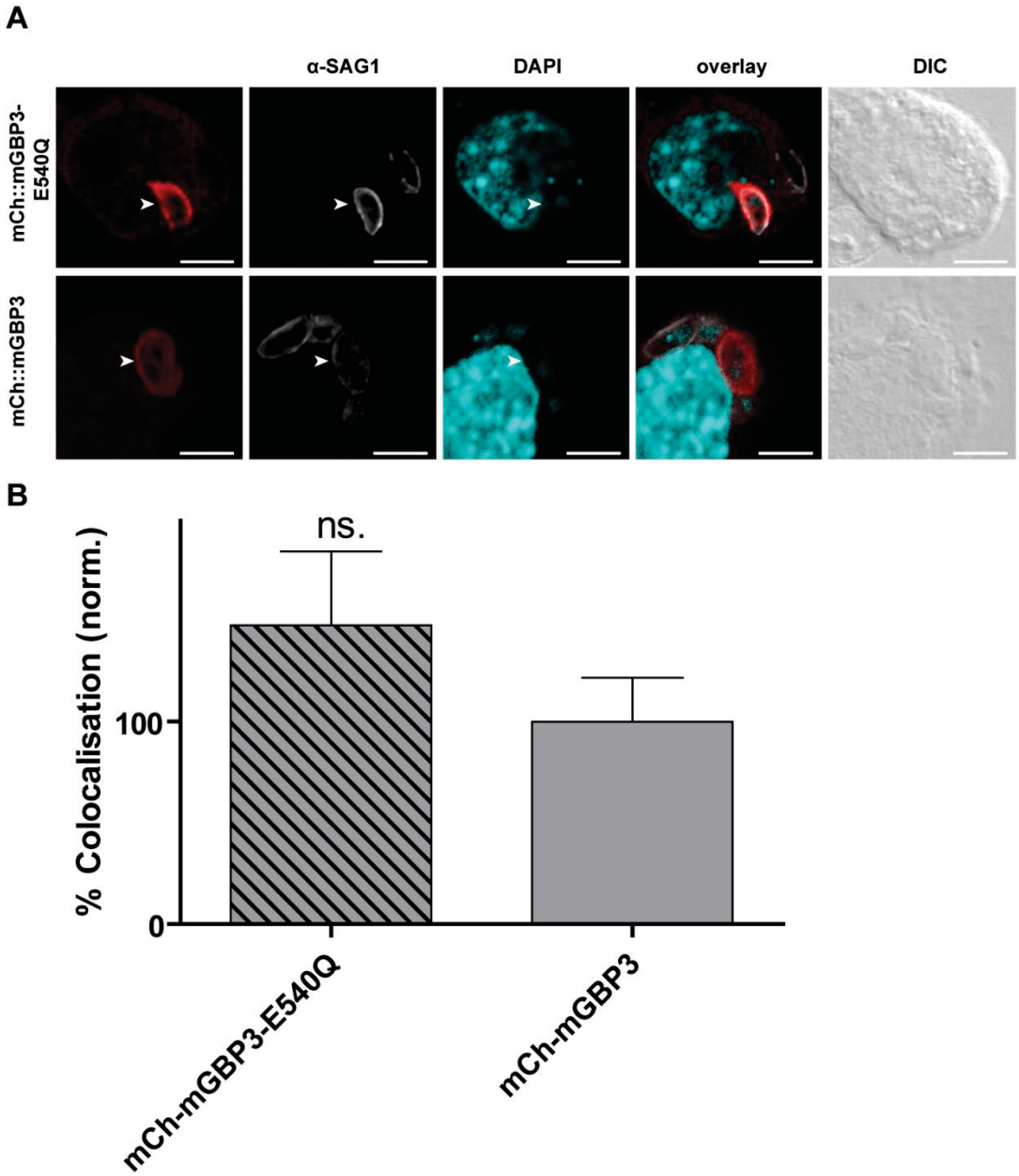

Figure 18: Recruitment of mGBP3-E540Q to intracellular *T. gondii* 2 hpi. A) representative cLSM pictures. α-SAG1 : *T. gondii* Surface antigen 1, DIC : differential interference contrast, bar : 5 µm. B) Normalized percentage of recruitment to intracellular *T. gondii*, n = 3, wild type mGBP : 100%, +SEM.

4.2.4 mGBP5

Originally mGBP5 was found to localize in VLS in the cytosol of uninfected cells using polyclonal antibodies (Degrandi et al., 2007). Opposing results were obtained using overexpression (Virreira Winter et al., 2011) and high resolution approaches measuring fluorescence parameters during live cell imaging which found mGBP5 in the cytosol, and not interacting with either mGBP1, mGBP2 and mGBP3 multimers or mGBP6 in VLS in co-transduced mEFs (Kravets et al., 2016). This study observed mCh::mGBP5 in a cytosolic distribution in uninfected cells. Upon infection mGBP5 relocated onto the PV membrane with low frequencies (Figure 19). The fluorescence intensity was markedly lower than of mCh::mGBP2, a difference also observed previously (Kravets et al., 2016-Fig5 row 5; Virreira Winter et al., 2011). Mutation from uncharged to a negatively charged amino acid (Q542E) did not influence distribution or recruitment frequency.

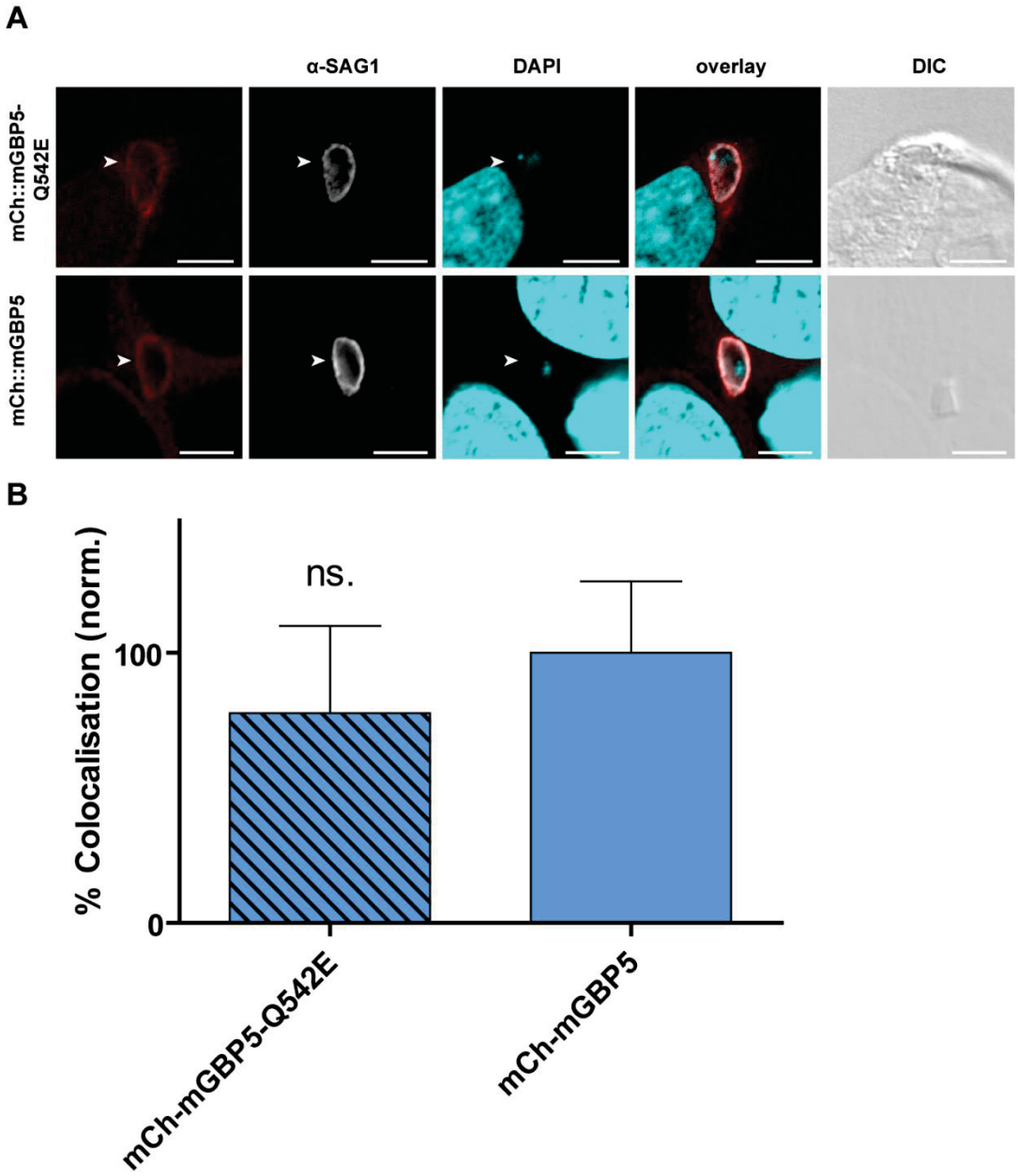

Figure 19: Recruitment of mGBP5-Q542E to intracellular *T. gondii* 2 hpi. A) representative cLSM pictures. α-SAG1 : *T. gondii* Surface antigen 1, DIC : differential interference contrast, bar : 5 µm. B) Normalized percentage of recruitment to intracellular *T. gondii*, n = 3, wild type mGBP : 100%, +SEM.

4.2.5 mGBP6

In uninfected cells mGBP6 localizes in VLS (Degrandi et al., 2007) which, strikingly, do not contain mGBP1, mGBP2 or mGBP3 which are collectively stored in disparate VLS (Kravets et al., 2016). Thus, arguing for a functionally different role for mGBP6.

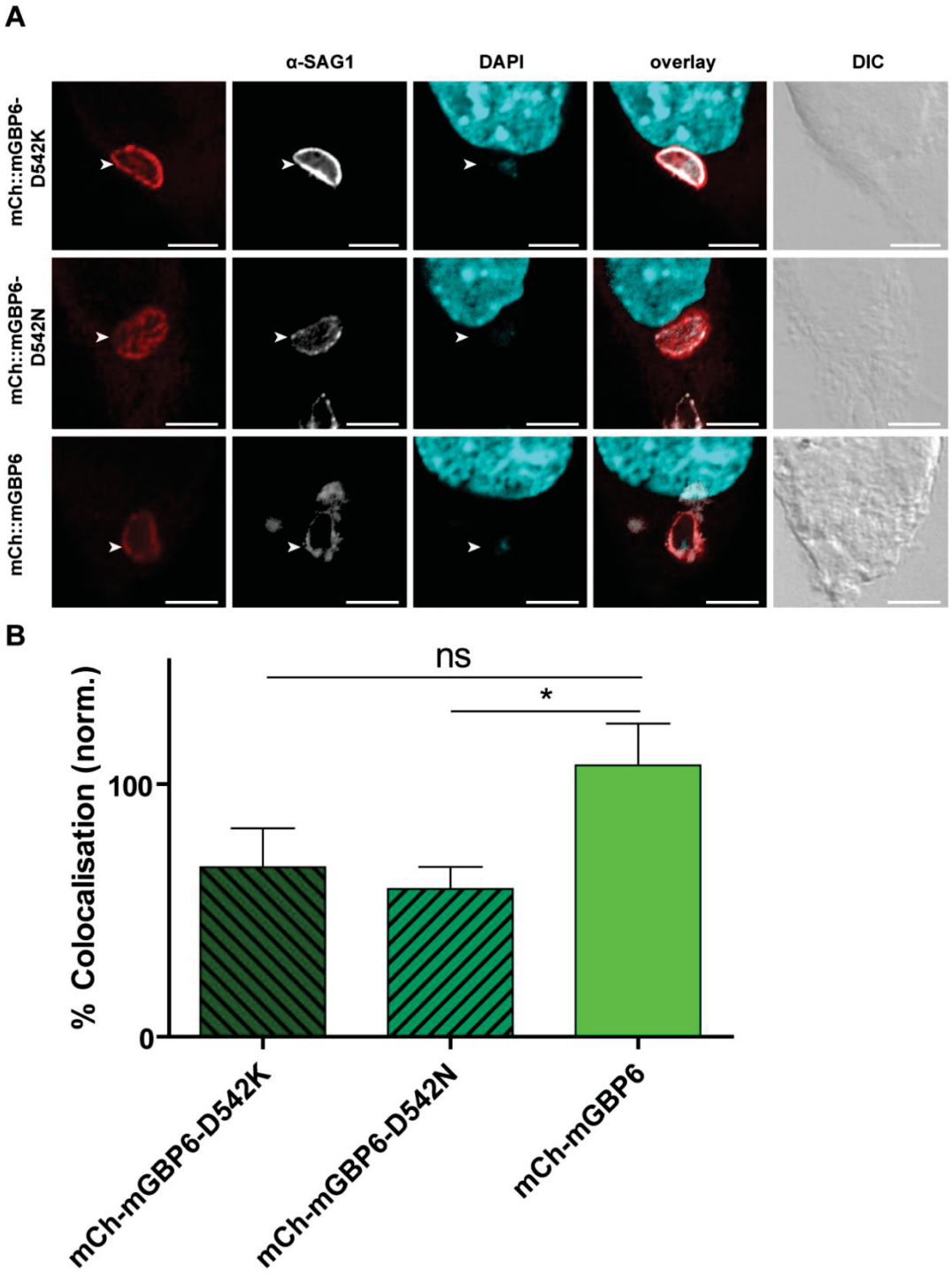

Figure 20: Recruitment of mGBP6-D542K and mGBP6-D542N, to intracellular *T. gondii* 2 hpi. A) representative cLSM pictures. α-SAG1 : *T. gondii* Surface antigen 1, DIC : differential interference contrast, bar : 5 µm. B) Normalized percentage of recruitment to intracellular *T. gondii*, n:6, wild type mGBP : 100%, +SEM.

Upon infection, all GBPs described up till now relocate to the PV membrane in both transfected (Degrandi et al., 2007) and transduced mEFs and RAW 264.7 macrophages (Kravets et al., 2016).

This study found mGBP6 recruiting on average to 25% of *T. gondii*. Therewith mGBP6 is, alongside mGBP1 and mGBP2, one of the highest recruiters to *T. gondii*. The colocalization events with mGBP6 resemble those seen for mGBP1, mGBP2 and mGBP3 in morphology. Compared to the original mGBP6 protein, the mutation to an uncharged amino acid (D542N) displayed a significant difference with the uncharged amino acid substitution (D542N) recruiting less often to the *T. gondii* PV (Figure 20). The mutation inversing the charge (D542K) colocalized less often than wild tape protein in each individual experiment; however the difference was not statistically significant. The possibility exists that different fluorescence intensities reflect different protein amounts among cell lines influence the quantification of the mCherry signal around PVs. For further elaboration on this consideration please see Paragraph 4.2.11.

4.2.6 mGBP7

Previously, mGBP7 was shown to form VLS in uninfected cells and IFNγ-dependent recruitment to PVs in several cell types infected with *T. gondii* (Beuter-Gunia, 2008; Degrandi et al., 2007). In this study, mGBP7 accumulation around the PV was equal to morphologies previously described. Mutating the amino acid under investigation from negatively charged to an uncharged amino acid (E546Q) did not hamper recruitment to the PV, as frequencies were comparable (Figure 21).

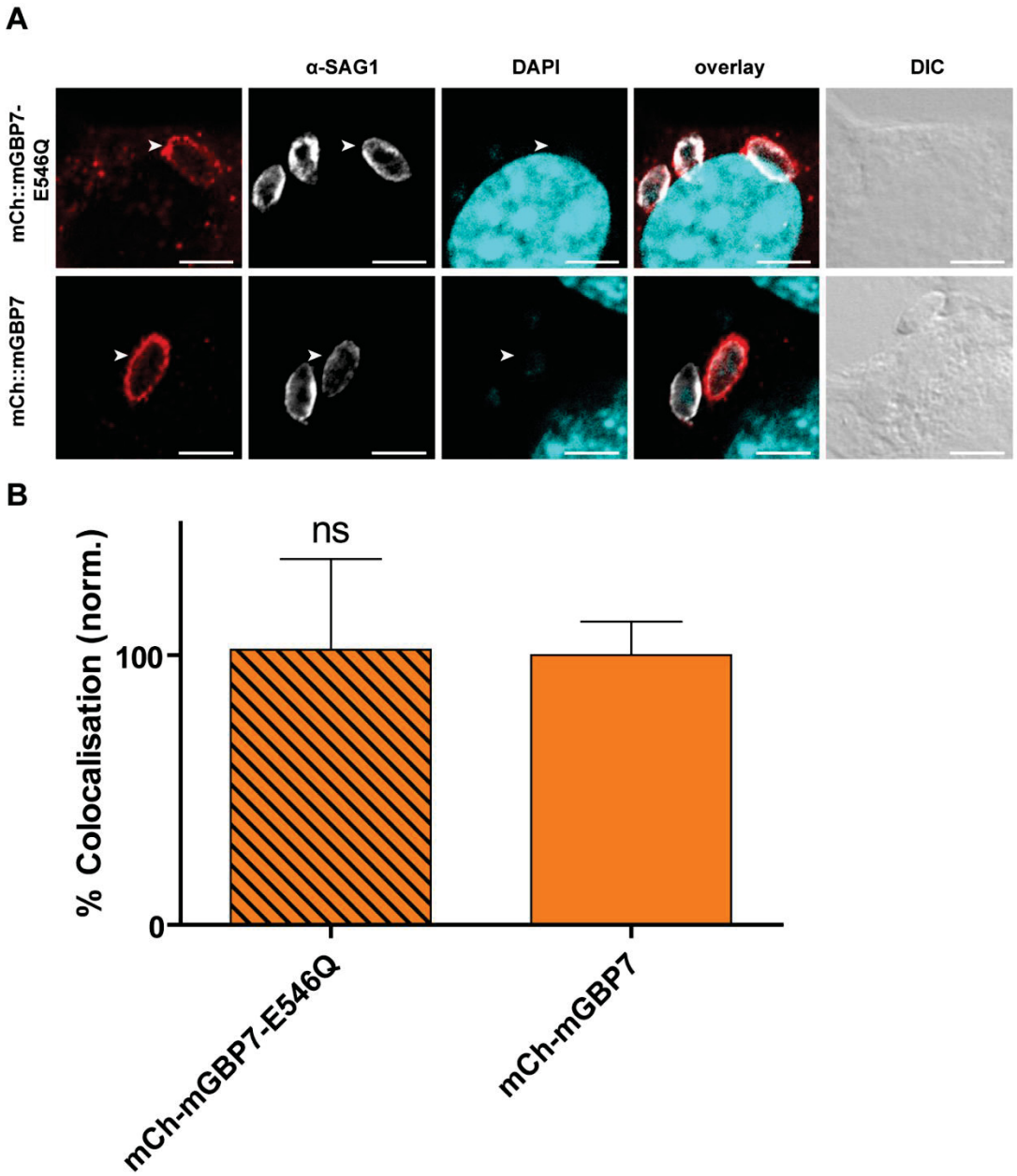

Figure 21: Recruitment of mGBP7-E546Q to intracellular *T. gondii* 2 hpi. A) Representative cLSM pictures. α-SAG1 : *T. gondii* Surface antigen 1, DIC : differential interference contrast, bar : 5 µm. B) Normalized percentage of recruitment to intracellular *T. gondii*, n = 3, wild type mGBP : 100%, +SEM.

4.2.7 mGBP8

No prior examinations of mGBP8 with regard to PV recruitment have been published. Constitutive expression of mCherry-tagged mGBP8 in NIH/3T3 fibroblasts showed a cytosolic localization of the protein. Upon infection mGBP8 remains in the cytoplasm and is excluded from intact PVs, showing virtually no recruitment. In limited cases a slight increase in mCherry intensity at the site of an intracellular parasite could not be excluded from quantification culminating in an average percentage of 3,14%, which might be explained by parasite-induced distortion of the cytoplasm and subsequent uneven distribution of cytoplasmic mCherry. Mutation from an uncharged to a negatively charged amino acid (N460D) does not affect the cytoplasmic distribution (Figure 22).

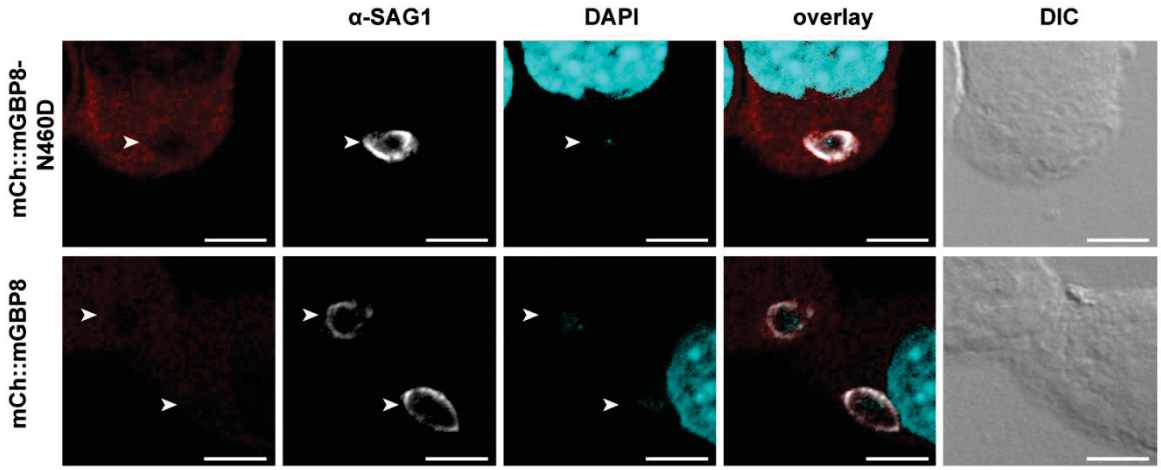

Figure 22: No recruitment of mGBP8-N460D to intracellular *T. gondii* 2 hpi. A) Representative cLSM pictures. α-SAG1 : *T. gondii* Surface antigen 1, DIC : differential interference contrast, n = 3, bar : 5 µm.

4.2.8 mGBP9

Transfection of mEFs has previously described mGBP9 to be organized in VLS and to recruit towards *T. gondii* (Degrandi et al., 2007). The NIH/3T3 fibroblast cell line display VLS, but also a disseminated mGBP9 distribution visible only when cells reduced adherence to the cover slip and/or were infected. Upon infection relocation to the PV occurred both with the original and uncharged instead of negatively charged mutant D542N to comparable extend, around 18%. In Figure 23A top row, below the arrow a 'rough' shape in the mGBP9 accumulation can be observed, adjacent to a 'nick` in the parasite, as outlined by α-SAG1, on the lower side of which it does not display any mGBP9 accumulation. This morphology reminds of disrupted *T. gondii* PVs.

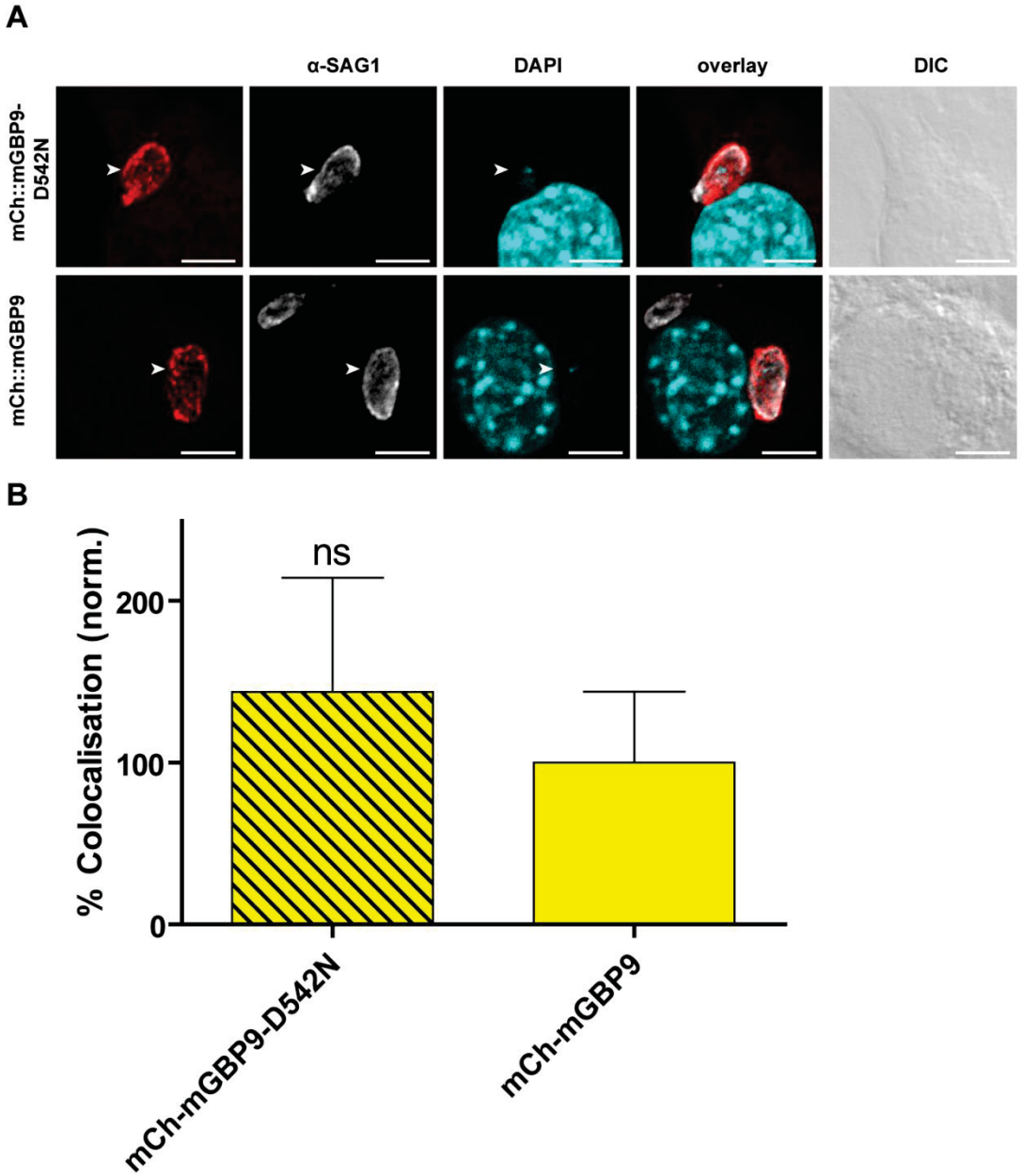

Figure 23: Recruitment of mGBP9-D542N to intracellular *T. gondii* 2 hpi. A) Representative cLSM pictures. α-SAG1 : *T. gondii* Surface antigen 1, DIC : differential interference contrast, bar : 5 µm. B) Normalized percentage of recruitment to intracellular *T. gondii*, n = 3, wild type mGBP : 100%, +SEM.

4.2.9 mGBP10

Previously, GBP10 was described to localize in VLS, which had a less sharp morphology, and never to recruit to *T. gondii* (Klümpers, 2013)-Figure 21. The recently transduced cell line displayed cytosolic aggregates making it difficult to recognize VLS. Nevertheless, upon infection with *T. gondii* irrefutable accumulation of mGBP10 to the PV was observed in many cells to approximately 12% of PVs within these experiments, see representative images Figure 24. The N542D mutation of mGBP10 showed no difference in recruitment morphology and frequencies.

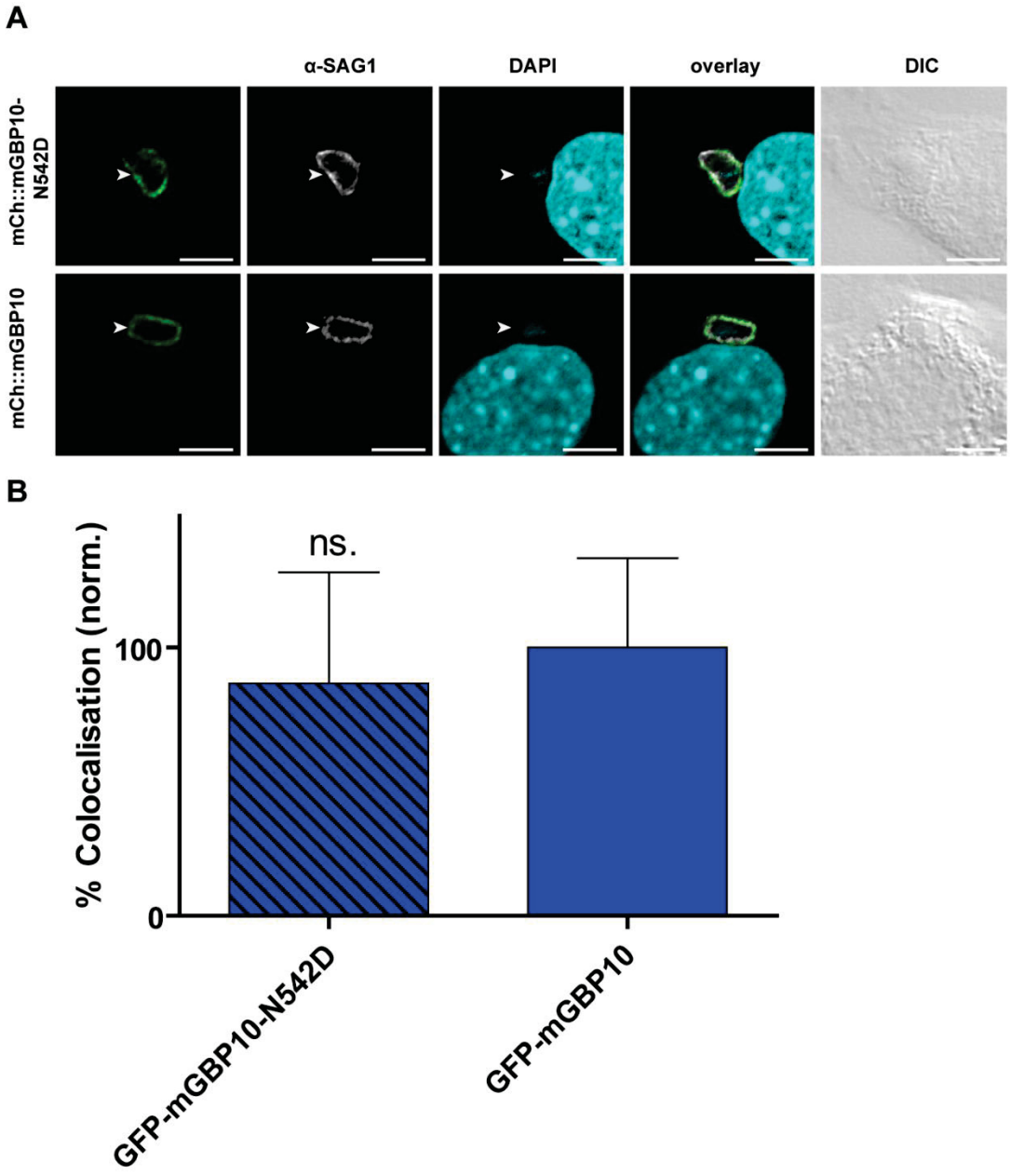

Figure 24: Recruitment of mGBP10-N542D to intracellular *T. gondii* 2 hpi. A) Representative cLSM pictures. α-SAG1 : *T. gondii* Surface antigen 1, DIC : differential interference contrast, bar : 5 µm. B) Normalized percentage of recruitment to intracellular *T. gondii*, n = 3, wild type mGBP : 100%, +SEM.

4.2.10 mCherry and GFP controls

To ensure that ‘recruitment’ does not occur independently of GBPs, the control vectors containing only mCherry or GFP constitutively expressed by the EF1α promoter were also transduced in NIH/3T3 fibroblasts. Both fluorescent proteins displayed a ubiquitous distribution in the cytoplasm and nucleus. Upon infection with *T. gondii* an exclusion of the cytosolic fluorescent proteins from the PV can be observed Figure 25. It has been described that mGBPs after IFNγ stimulation can rupture PV membranes allowing cytosolic mCherry to diffuse into the disrupted PV (Kravets et al., 2016). Indeed, in a limited number of cases homogeneous mCherry or GFP signal partly overlapped with α-SAG1 staining and was included as a count for ‘colocalization’, although these numbers were negligibly small and accounted to the action of endogenous mGBPs.

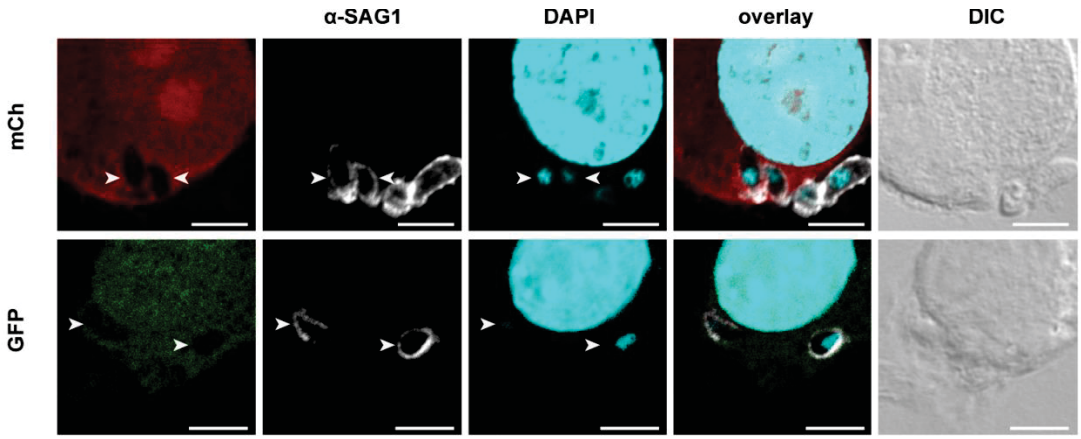

Figure 25: No recruitment of mCherry and GFP to intracellular *T. gondii* 2 hpi. Representative cLSM pictures. α-SAG1 : *T. gondii* Surface antigen 1, DIC : differential interference contrast, bar : 5 µm.

4.2.11 Exploring mGBP6 in depth

In confirmation of previous results (Klümpers, 2013), the substitution to a neutrally instead of negatively charged amino acid at position 542 (D542N) in displayed mGBP6 significantly reduced recruitment to *T. gondii* PVs (Figure 20). It was hypothesized that inversing the charge of this residue to positive could lead to an increased reduction in recruitment frequency. Surprisingly however, the mutant D542K displayed an attenuated effect on recruitment reduction as compared to the D542N mutant. In an effort to explain these observations, these cell lines were investigated in greater depth.

Accumulations of mCherry, such as recruitments to the PV, can only be recognized in microscopic analysis when a threshold amount of fluorescent particles emits enough light to be detectable. The median fluorescence intensity (MFI) of the transduced cell lines was measured by flow cytometry to assess if all cell lines possess the same amount of fluorescent protein-fused mGBP. For each investigated mGBP6 protein (wild type and mutants) the median mCherry intensity was lower than for other mCherry fused cell lines possibly causing an underestimation of mGBP6 recruitment events. In addition, mGBP6-D542N had a significantly lower MFI than mGBP6-D542K, which had a significantly lower MFI than mGBP6 (Figure 26). Therefore, the significant difference between mGBP6 and mGBP6-D542N (Figure 20) could be explained by different amounts of expression of the fusion proteins.

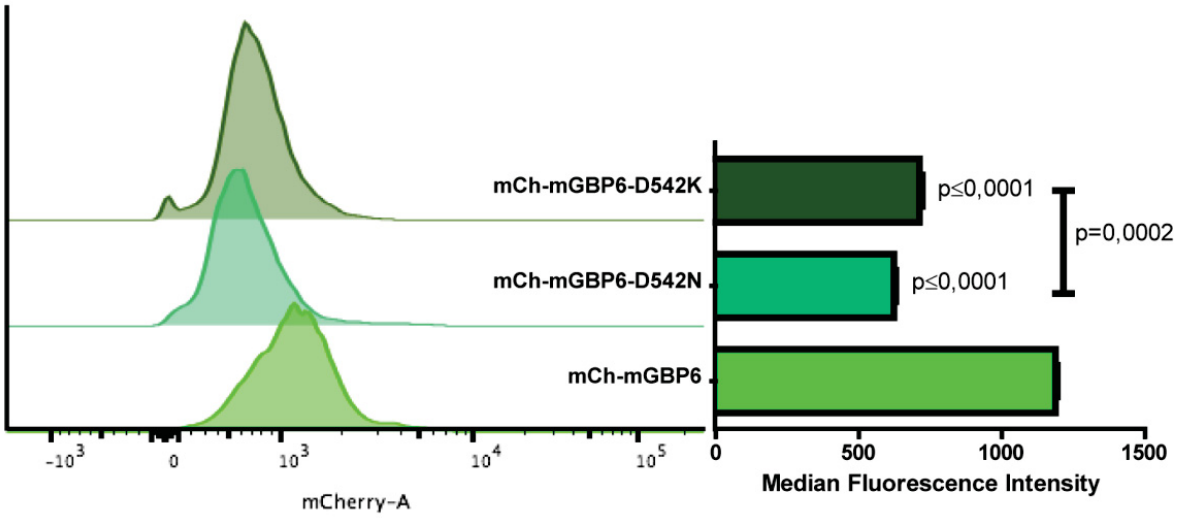

Figure 26: mGBP6 WT, mGBP6-D542K and mGBP6-D542N histograms and MFI

As an alternative approach, a protein model of mGBP6 was made in cooperation with the research group of Prof. Dr. Schmitt to determine the likelihood that the amino acid chain's charge at position 542 has an influence on protein conformation. The amino acid

side chain is depicted in colour in the otherwise green depiction of a structural model of mGBP6 (Figure 27). The amino acid in question is directed outward of the mGBP6 protein. In addition, the model divulges that the amino acid laying on α-chain 12 cannot influence α-chain 13, since the closest potentially interacting amino acid side chain is positioned at more than 2 å distance.

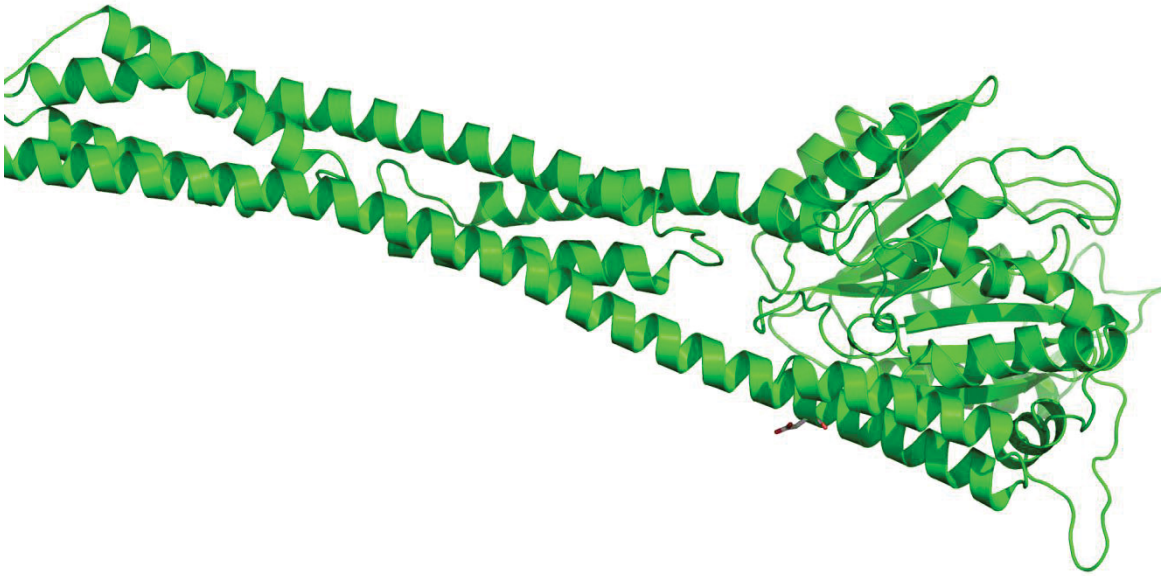

Figure 27: mGBP6 structural model, the side chain of aa 542 is depicted in its predicted orientation

4.3 Accumulation of mGBPs onto chlamydial inclusions

In the research field, a major need exist to better understand pathogen and functional specificities of GBPs (Pilla-Moffett et al., 2016). In the framework of this study, a new collaboration was initiated to investigate mGBPs within an additional infection model: *Chlamydia trachomatis (C. trachomatis)*. It *was* previously shown that mGBP1 and mGBP2 can recruit to the *C. trachomatis* containing vacuole, called an 'inclusion' (Finethy et al., 2015; Haldar et al., 2014). Based on homologies between mGBP sequences (Degrandi et al., 2007) and the ability of mGBPs to form multimers (Kravets et al., 2016), it was hypothesized that additional mGBPs might be involved in anti-bacterial resistance to *C. trachomatis*. To explore the specificity of accumulations onto these inclusions, the cell lines constitutively expressing fluorescent protein-fused mGBPs described above were infected with *C. trachomatis* and probed for colocalization.

A *C. trachomatis* inclusion contains up to hundreds of bacteria loosely packed inside its membrane (Elwell et al., 2016), as opposed to the smaller PVs which are tightly arranged around a single *T. gondii* parasite previously depicted in this study. Due to chlamydia's biphasic lifecycle, both the ~200 nm elementary bodies (EB) as well as the ~1 µM large reticulate bodies (RB) can be found inside an inclusion, depending on the time post infection (Elwell et al., 2016). In early visualization efforts, the bacteria themselves were stained with a commercially available antibody for major outer membrane protein (MOMP). Observing individual EBs proved difficult, due to their size which is close to the resolution limit of a light microscope. Therefore the term 'inclusions' is used solely to describe inclusions containing the larger metabolically active RBs. Similar limitations were observed when analysing live cells infected with *C. trachomatis* transformed with pGFP::SW2 (Wang et al., 2011). Incidentally during this study, it was observed that inclusions on which mGBPs accumulate lose their GFP-expression or antibody-signal, as compared to inclusions where no mGBPs are detected. An example encountered 20 hpi in living cells constitutively expressing mGBP2 can be recognized in figure 28 or in fixed cells where mGBP7 accumulates onto one of two inclusions in the depicted field, while no chlamydial antibody signal is detectable but bacterial DNA is still visible (Figure 29 - row 6).

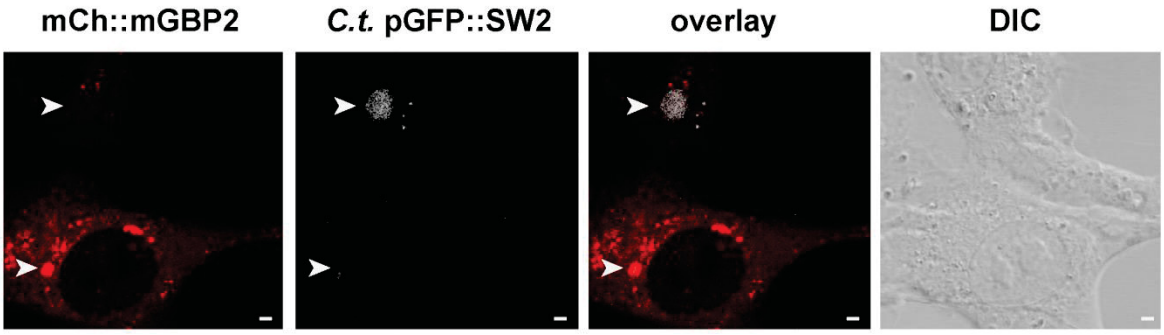

Figure 28: Intensity loss of chlamydial pGFP::SW2 signal (*C.t.*) after recruitment by mCh::mGBP2 in live NIH/3T3 fibroblasts 3,5 hpi, DIC : differential interference contrast, bar : 2 µm.

4.3.1 Extensive qualitative analysis mGBP recruitment towards chlamydia inclusions

To extensively analyse mGBPs in *C. trachomatis* infection, NIH/3T3 fibroblasts which constitutively express individual fluorescent protein-fused mGBPs were infected with *C. trachomatis* at an MOI of 3. Three hours post infection the infected cells were stimulated with IFNγ and fixed at 14 hours post infection (hpi) and subsequently stained. In order to discriminate the host-pathogen interface, the novel inclusion membrane marker CT868 (also known as ChlaDUB1, Cdu1 and CTAD-8) (Borges et al., 2015; Claessen et al., 2013; Fischer et al., 2017; Le Negrate et al., 2008; Lindenberg et al., submitted; Misaghi et al., 2006; Stallmann, 2015) was stained and colocalization with fluorescent protein-tagged mGBPs was assessed. Via cLSM analysis it could be shown that besides mGBP1 and mGBP2, also mGBP3, mGBP6, mGBP7, mGBP9 and mGBP10 are found at the inclusion-membrane (Figure 29A). Among accumulation events, a distinct morphology was observed for mGBP7, which was characterized by intense and tight accumulation onto the inclusion membrane (Figure 29A – row 6). In the case of mGBP5, a more diffuse and slightly spatially distant morphology around the inclusion was observed which does not qualify as a colocalization comparable to other mGBPs (Figure 29A- row 4). For mGBP8, essentially no colocalization could be found (Figure 29A – row 7). Interestingly, when mGBPs co-localize at an inclusion, α-CT868 stained to a lesser extend compared to inclusions without colocalization. To compensate for this loss of chlamydial signal all inclusions were also assessed for the presence of bacterial DNA defined by DAPI staining in the cytoplasm of infected cells. Taken together, the mGBPs with an ability to localize towards chlamydia can be extended from mGBP1 and mGBP2, to the additional family members mGBP3, mGBP6, mGBP7, mGBP9 and mGBP10.

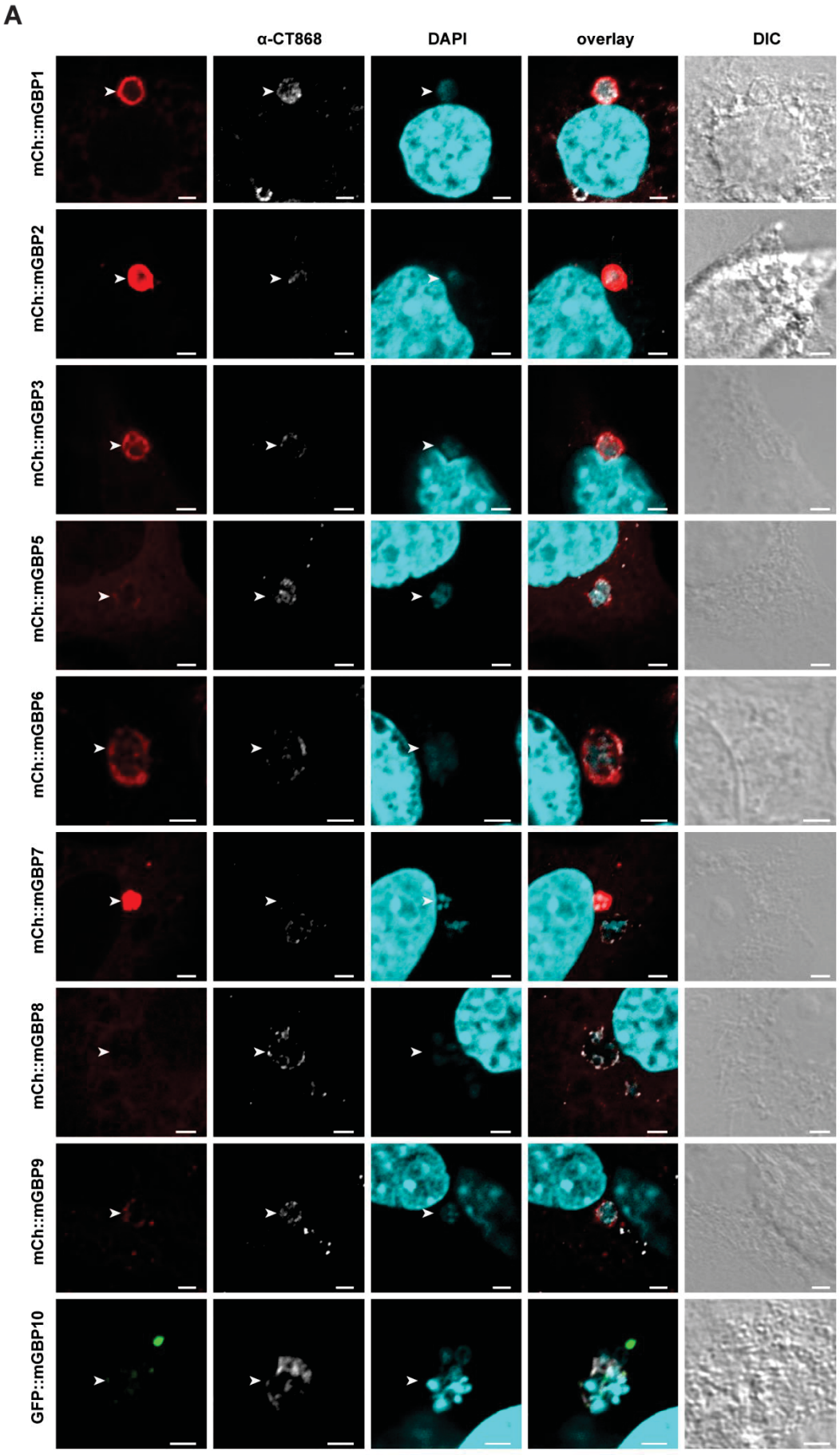
A
α-CT868
DAPI
overlay
DIC
mCh::mGBP1
mCh::mGBP2
mCh::mGBP3
mCh::mGBP5
mCh::mGBP6
mCh::mGBP7
mCh::mGBP8
mCh::mGBP9
GFP::mGBP10

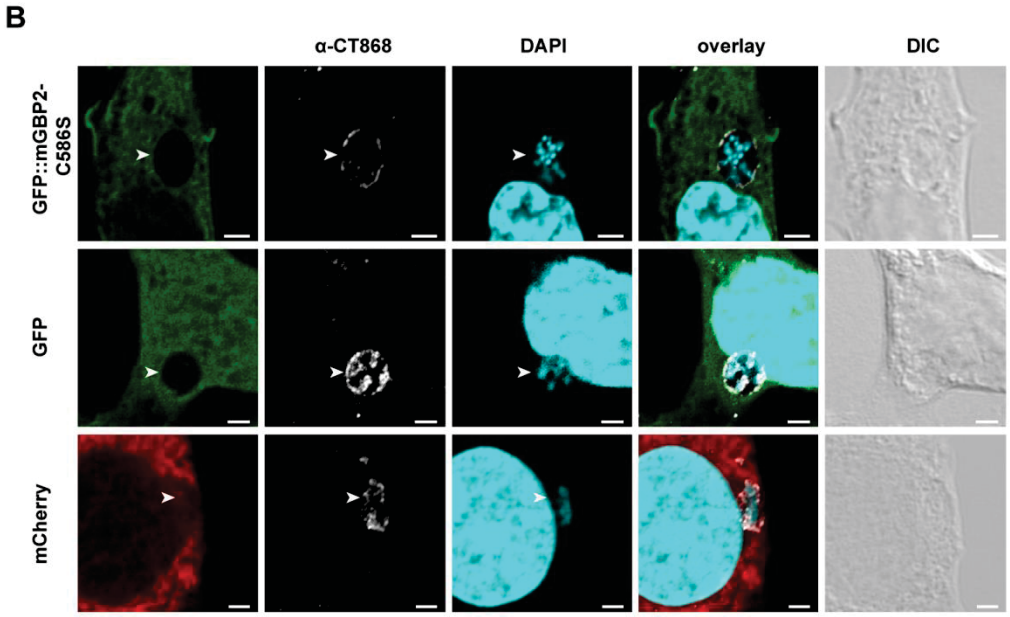

Figure 29: Colocalization with *C. trachomatis* inclusions by A) individual constitutively expressed mGBPs B) control vectors 14 hpi in NIH/3T3 fibroblasts stimulated with IFNγ 3 hpi, α-CT868 :: chlamydial inclusion membrane marker, DIC : differential interference contrast, bar : 2 µm.

Control constructs expressing only the fluorescent proteins or isoprenylation mutant mGBP2-C586S displayed a cytoplasmic distribution, were excluded from the chlamydial inclusion and no morphology compatible with accumulation onto the inclusion could be observed in any experiment.

4.3.2 Quantitative analysis of mGBP colocalization with pathogen containing compartments

To assess the relative contribution of each mGBP the observed recruitment events were subsequently quantified (Figure 30A). For *C. trachomatis,* colocalization with mGBP1 and mGBP2, 13 % and 17% respectively, closely resembled rates described previously (Finethy et al., 2015; Haldar et al., 2015; Haldar et al., 2014; Haldar et al., 2013). The mGBP2 C586S mutant showed virtually no colocalization, showing that isoprenylation is essential for localization towards chlamydial inclusions, as it is for recruitment to toxoplasma PVs (Degrandi et al., 2013; Kravets et al., 2016). Therefore, colocalization percentages with mGBP2 C586S were defined as background and by means of p-value other mGBPs are shown to localize to inclusions in Figure 30 into different groups based on frequency.

Comparable to mGBP1 and mGBP2, also mGBP3 and mGBP6 colocalize significantly with inclusions. Due to higher variance, mGBP7, mGBP9 and mGBP10 show a trend to localize considerably often towards inclusions. Remarkably, in a few experiments mGBP9 colocalized with chlamydia more frequently than mGBP2 (on average 13%). The third group consists of mGBP5 and mGBP8, which hardly localize towards chlamydia.

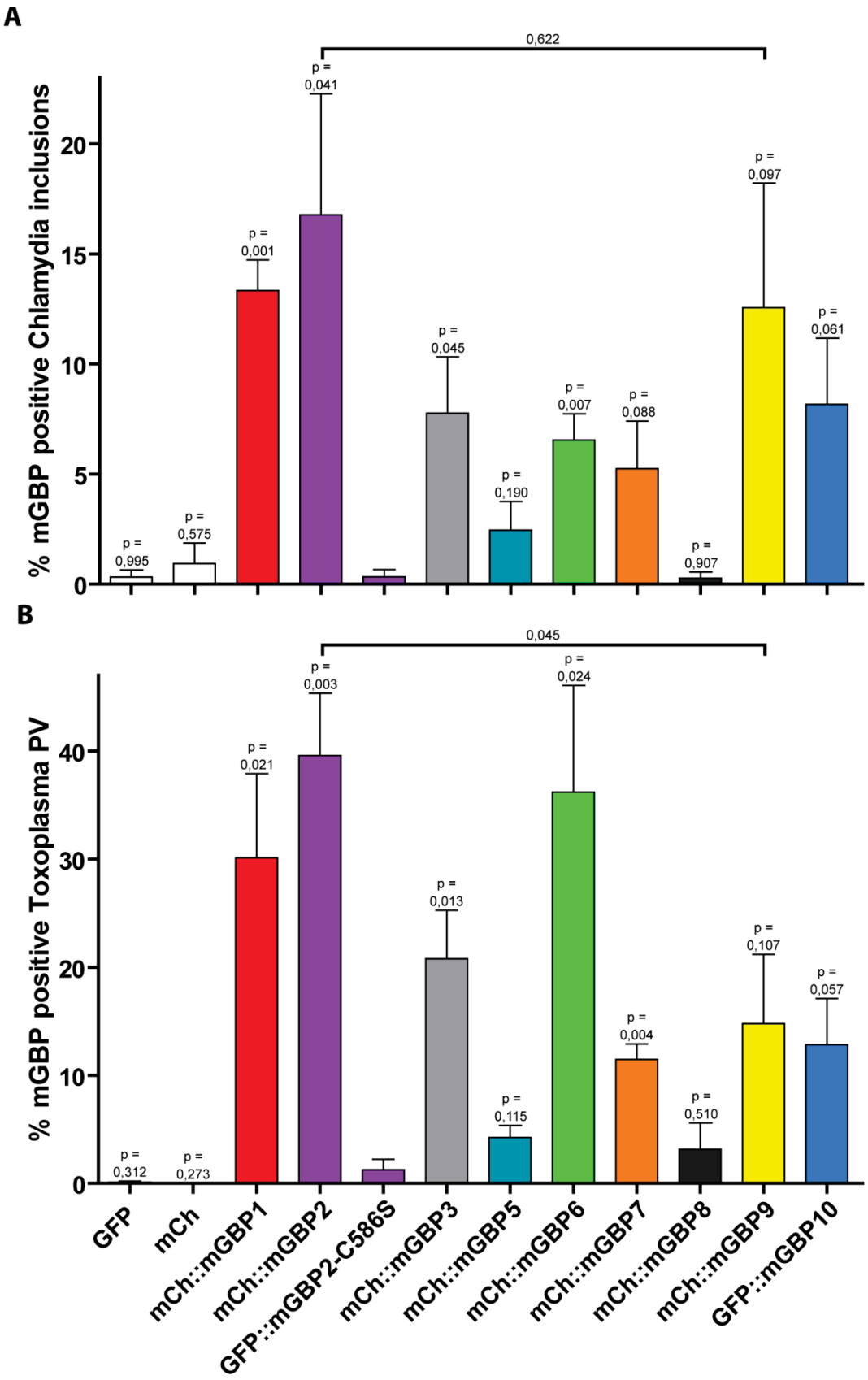

Figure 30: Qualitative analysis of mGBP colocalization with A) Chlamydial Inclusions 14 hpi B) Toxoplasma parasitophorous vacuoles 2 hpi. Approximately 200 cells were assessed for the presence of intracellular pathogens and subsequently for colocalization with individual mGBPs. Data of three independent experiments are depicted as mean percentages +SEM.

To compare between bacterial and apicomplexan pathogens, previously described recruitment frequencies towards *T. gondii* (Paragraph 4.2) were depicted as absolute instead of relative percentage of mGBP recruitment to intracellular pathogen containing compartments (Figure 30B). Previous observations that mGBP1, mGBP2, mGBP3, mGBP5, mGBP6, mGBP7 and mGBP9 recruit towards *T. gondii* PVs in mEFs and RAW 264.7 macrophages (Beuter-Gunia, 2008; Degrandi et al., 2007; Kravets et al., 2016) could be confirmed in NIH/3T3 fibroblasts. This study showed that mGBP1, mGBP2, mGBP3, mGBP6 and mGBP7 colocalize significantly with *T. gondii* PVs. Interestingly, in this infection the mGBP recruiting with the highest frequency to *T. gondii* PVs aside from mGBP2, is mGBP6. Considerably often mGBP5, mGBP9 and mGBP10 recruit to PVs, whereas mGBP8 and the mGBP2 isoprenylation mutant C586S hardly recruit towards *T. gondii*. The morphology of mGBP5 accumulation is distinct from other mGBPs and characterized by localization around the PV with a dispersed morphology, comparable to its morphology when localizing around chlamydial inclusions. Overall PV recruitment percentages compare to previous publications (Haldar et al., 2015; Kravets et al., 2012). Remarkable is mGBP9, since it displays a comparable frequency of colocalization as mGBP2 in chlamydial infection, whereas in toxoplasma infection it recruits significantly less often than mGBP2. This quantification implies that in different infection models not all mGBPs contribute equally towards cell autonomous immunity.

Previously (Figure 20 and Figure 26), it was observed that differences in the MFI among cell lines which constitutively express one of the fluorescent protein-tagged mGBPs are correlated with the frequency of colocalization which is counted using confocal microscopy. Therefore, fluorescence intensities of all cell lines constitutively expressing mCherry (Figure 31A) or GFP (Figure 31B) fused mGBPs and control cells were analysed and compared by flow cytometry.

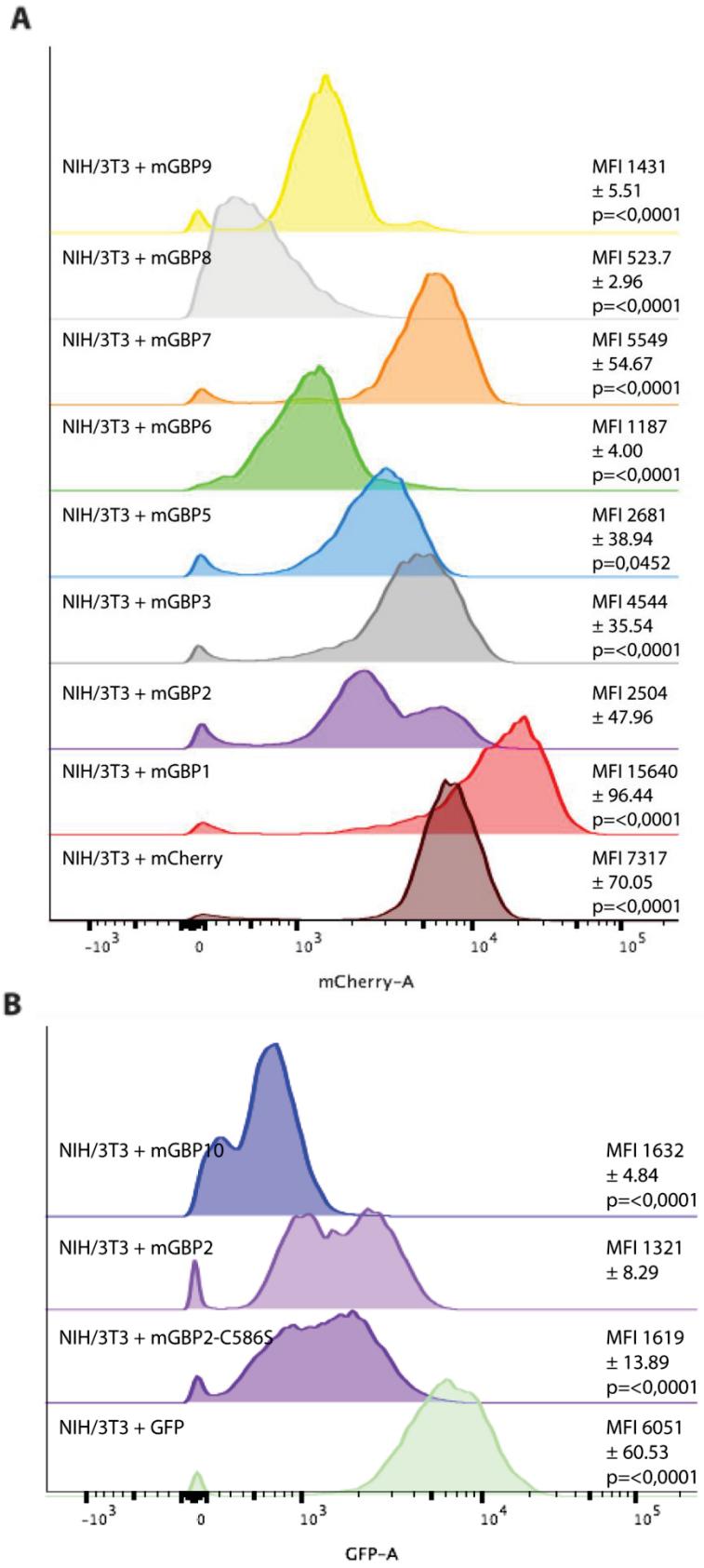

Figure 31: Representative histograms of fluorescence intensities of NIH/3T3 cell lines expressing mCherry (A) or GFP (B) as such or N-terminally fused to mGBPs, measured in triplicate on FACS Aria III.

The lowest MFI measured for mCherry was for mCh::mGBP8: 523,7 ±2,96, compared to the highest for mCh::mGBP1: 15640 ±96,44 (Figure 31A second and eighth histogram from the top). The lowest median fluorescence measured for GFP was for GFP::mGBP10: 1632 ±4,84, compared to the GFP control: 6051 ±60,53 (Figure 24B first and last histogram from the top). In general, all fluorescence intensities are significantly different from mGBP2, as exemplified by the histograms in Figure 31.

An interesting observation that arises from fluorescence analysis is that all mGBP2 and GFP::mGBP10 expressing cell lines show two populations, a dim and a brighter population.

4.3.3 Live cell imaging of mGBP recruitment to chlamydial inclusions

In the chlamydial research field new insights arose which questioned the authenticity of accumulation of proteins onto chlamydial inclusions after fixation (Kokes and Valdivia, 2015). To validate the previous observations, the most frequently colocalizing proteins, mGBP2 and mGBP9, were selected for further analysis without fixation by live cell microscopy. In order to visualise chlamydia in unfixed cells a non-toxic marker was sought. A pilot study was conducted with non-toxic DNA marker HOECHST, which showed that at the optimal concentration the fluorescence intensity was too low to allow credible identification of chlamydial inclusions in living cells. Therefore a *C. trachomatis* strain was obtained from a laboratory which made considerable advances in transforming this bacterium. *C. trachomatis*, containing a plasmid allowing GFP-expression under the SW2 promoter (Wang et al., 2011) was utilized to infect cells constitutively expressing mCherry-tagged mGBP2 and mGBP9 at an MOI of 10. Cells were seeded on imaging dishes in phenol-free or FluoroBrite cell culture media and incubated at 37°C with 8% CO_2 and humidity saturated air for 3 hours while images were taken every 10 minutes. After 3 hours IFNγ was added to reach a final concentration of 100 Units/ml and time lapse recordings were started once more. Recordings were continued until an accumulation event occurred and was completed, cells moved out of the field view, or for a maximum of 20 h. During these experiments it was often observed that chlamydial inclusions move through the cell cytoplasm with and without colocalized mGBPs for the entire duration of the recording. In very few cases however, the beginning or a decline of an mGBP2 accumulation were witnessed.

4.3.3.1 mGBP2

In the case of mGBP2, colocalization with chlamydial inclusions was quantified to be around 20% of inclusions in cells fixed 14 hpi (Figure 30A). Therefore, many time lapse videos, each of which contained several cells, were made to increase the chance to observe a colocalization event. Among these videos, one cell was observed which displayed 2 accumulation events (Figure 32). These cells were infected with GFP-expressing *C. trachomatis* and observed starting 30 minutes post infection.

9

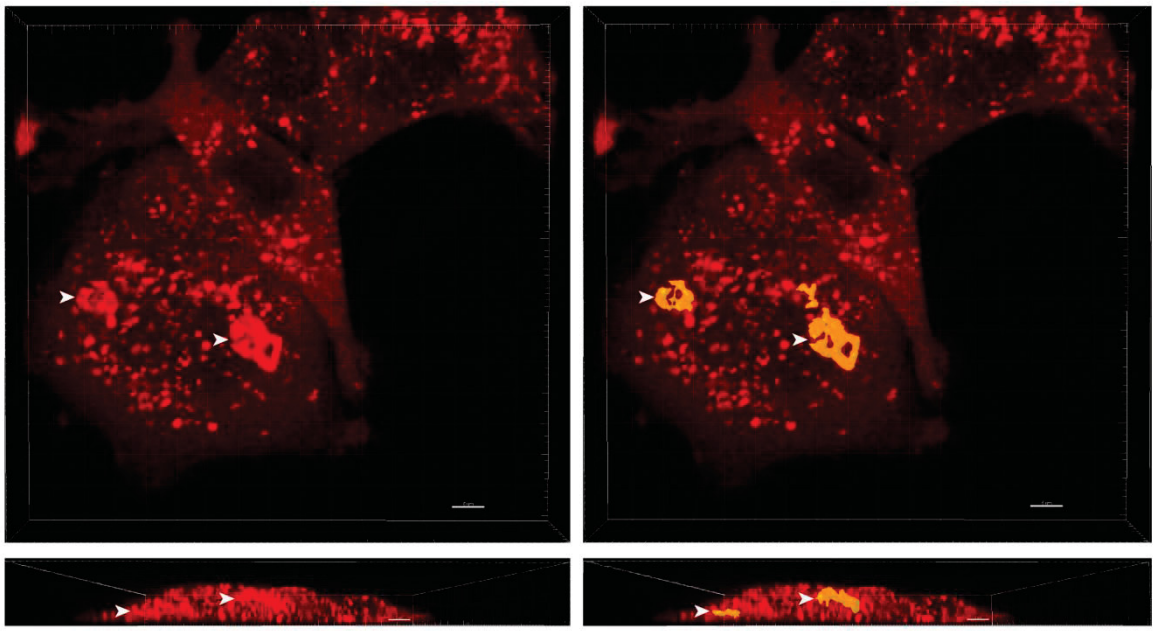

Figure 32: Orientation for two recruitments of mCh::mGBP2 in NIH/3T3 fibroblasts infected with *C. trachomatis* SW2::GFP (MOI 10, no GFP signal measured) in a time lapse recording at 1h40m. TOP: XY view. BOTTOM: ZX view, Right: same images with highlighted larger accumulations of mCherry.

Already within the first minutes a first accumulation of mGBP2 forms which develops a circular morphology beside, and slightly above the nucleus (displayed and highlighted in Figure 32 - right panel, right-hand side). A few minutes later a second accumulation arises within the same cell on the other side of the nucleus, in closer proximity to the coverslip (shown and highlighted in Figure 32 – right panel, left-hand side).

When isolating the Z-stack slides containing the second accumulation and following them in time (Figure 33) it can be seen that the accumulation starts between 40 and 50 minutes post infection. Surprisingly, this occurred prior to IFNγ stimulation thus showing that external stimulation is not required for accumulations to occur. The accumulation morphology resembles a ‘ball’ or a ‘ring’ 2-3 µm across and occurs transiently for a period of about 60 minutes. Afterwards, the structure dissolves and only the characteristic cytosolic distribution in VLS of mGBP2 can be seen.

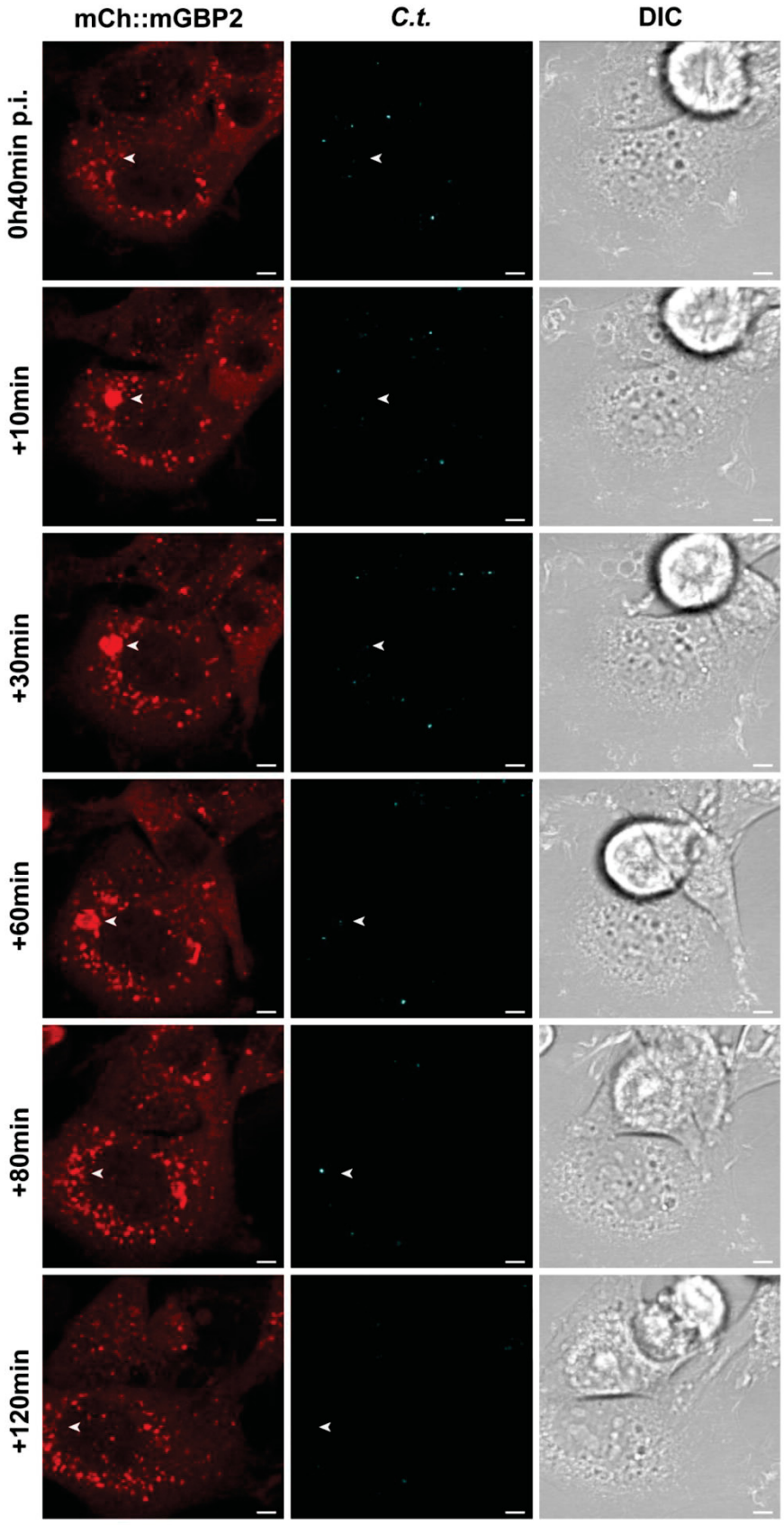

Figure 33: Accumulation of constitutively expressed mCh::mGBP2 in a living *C. trachomatis* pGFP::SW2 *(C.t.)* infected NIH/3T3 fibroblast, left-hand side (Figure 25), DIC : differential interference contrast, bar : 2 µm.

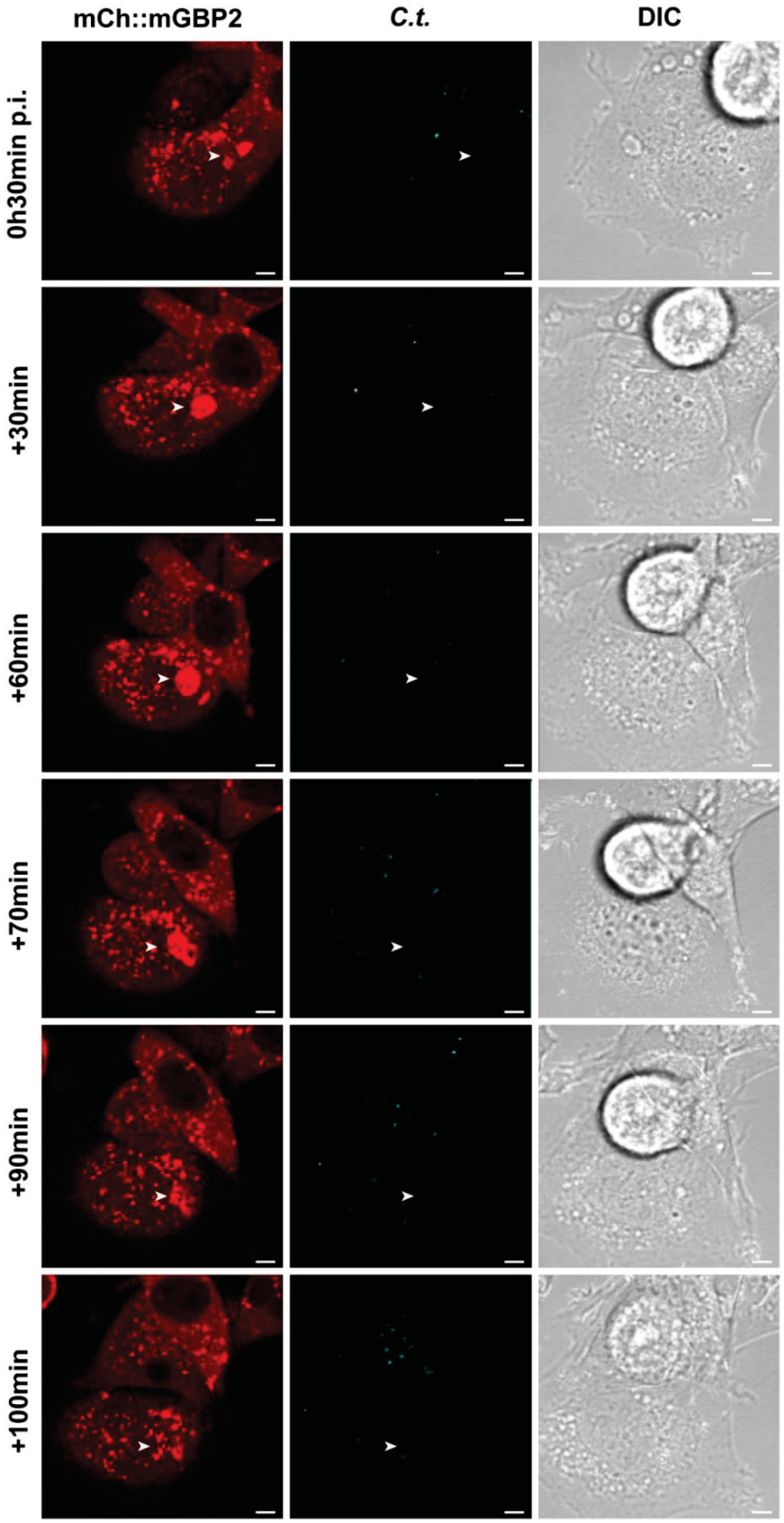

Figure 34: Accumulation of constitutively expressed mCh::mGBP2 in a living *C. trachomatis* pGFP::SW2 *(C.t.)* infected NIH/3T3 fibroblast, right-hand side (Figure 25), DIC : differential interference contrast, bar : 2 µm.

Figure 34 displays the Z-stack slides containing the main body of the accumulation occurring in the upper region of the cell. This accumulation occurs a few minutes earlier, potentially already before the start of the recording and develops during approximately 80 minutes. In the 3rd and 4th row it can be seen that the accumulation originally developed as a ball-like shape but develops into a peculiar morphology shaped like two connected rings with a structure blabbing outward (best seen in Figure 32, highlighted side view). This structure resembles the morphology of a disrupted *T. gondii* PV after mGBP2 recruitment (Kravets et al., 2016). At 2 hpi the accumulation at the *C. trachomatis* inclusion disappeared and only VLS could be observed.

Unfortunately, no chlamydial GFP signal could be detected. This can be caused either by suboptimal performance of the promoter driving GFP expression or the GFP expressed in the EBs with a size close to the diffraction limit of light does not allow recognition of chlamydial signal at a time point as early as several hours.

4.3.3.2 mGBP9

In the following, mGBP9 localization during *C. trachomatis* infection was further analysed since it frequently colocalizes with *C. trachomatis* (Figure 30). To improve detection sensitivity, further experiments were performed in a very low auto fluorescent medium (FluoroBrite). Among the different recordings, in one instance a larger sized inclusion allowed witnessing mGBP9 accumulation in a cage-like structure around it (Figure 28). The accumulation arose 9h20min pi and formed a ring around a dim but detectable GFP signal, signifying an inclusion. After approximately 2 h the mGBP9 accumulation reduced in intensity and size until it ultimately disappeared. This analysis displays the exceptional morphology of mGBP9 colocalization with chlamydia in live cell samples thus proving that mGBP accumulation onto chlamydial inclusions are no fixation artefact (Kokes and Valdivia, 2015).

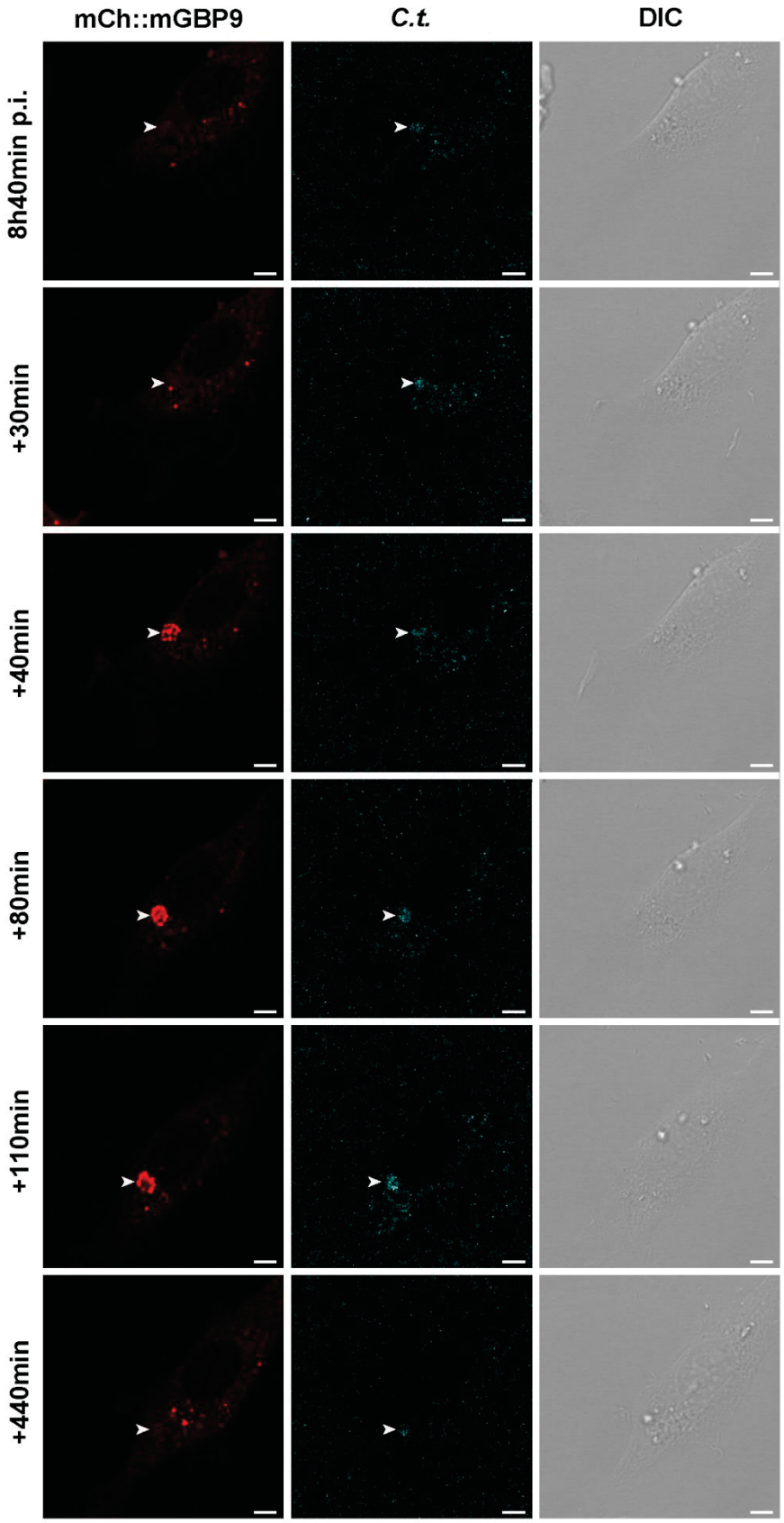

Figure 35: Accumulation of constitutively expressed mCh::mGBP9 onto chlamydial inclusion in a living *C. trachomatis* pGFP::SW2 *(C.t.)* infected NIH/3T3 fibroblast, DIC : differential interference contrast, bar : 2 µm.

4.3.4 Inhibition with 4-BPB does not affect inclusion formation

Accumulation of several mGBPs onto chlamydial inclusions has been unequivocally shown in this study. Nevertheless approximately 80% of inclusions do not attract mGBPs. The transient colocalization displayed in time-lapse recording allows the postulation that the actual colocalization rate throughout infection could be higher. Nonetheless, a majority of inclusions escaped this fate.

Based on fusion of different chlamydial inclusions within one host cell, in a co-infection model of *C. trachomatis* with *C. muridarum*, a working model has been proposed in which *C. trachomatis* expresses at least one factor actively interfering with cell autonomous immunity (Haldar, 2016). What this factor is, or via what mechanism chlamydia prevents mGBP accumulation is unknown. In this study an attempt to address this mechanism was made. Building on the similarities between *T. gondii* and *C. trachomatis* in respect to interferon induced GTPase mediated immunity, it was hypothesized that strategies which interfere with toxoplasma virulence might also affect chlamydia. It was shown that a small chemical inhibitor, 4-Bromophenacyl bromide (4-BPB), can inhibit toxoplasma's secretion of ROP kinases into the host cytoplasm and therefore parasite invasion and intracellular growth (Ravindran et al., 2009). In addition, it was confirmed that parasite invasion into fibroblasts is reduced but recruitment of mGBP2 towards those toxoplasma which do invade remains (Klümpers, 2013)-Figure 32. Using the same experimental strategy, cells were pre-incubated with freshly dissolved 4-BPB, thus chemically active, and subjected to *C. trachomatis* infection and fixed at 14 hours post infection as described previously. It was observed that chlamydial inclusions formed as customary and mGBP2 accumulated onto a percentage of those inclusions (Figure 36 - exemplary image). Therefore it can be concluded that chlamydia exert an alternative strategy compared to toxoplasma, in order to evade cell autonomous immunity.

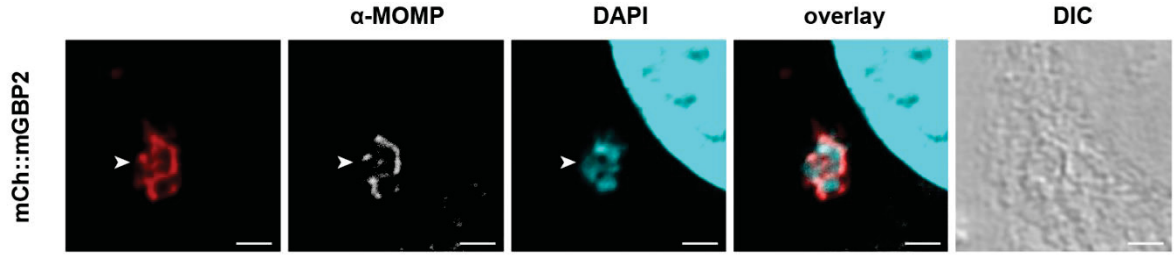

Figure 36: Inhibitor 4-BPB does not influence formation of chlamydial inclusions nor mCh::mGBP2 accumulation in NIH/3T3 fibroblasts, α-MOMP : chlamydial major outer membrane protein, DIC : differential interference contrast, bar : 2 µm.

4.3.5 Exploring mGBPs biological effect against Chlamydia

To analyse the efficacy of the chlamydial life cycle, primary mouse embryonic fibroblasts of mGBP2, mGBP5 and mGBP7 knockout mice (Degrandi et al., 2013) (Beuter-Gunia, C., Degrandi, D. personal communication September 30, 2016) and wild type (WT) controls were infected with *C. trachomatis* LGV (MOI=3) for 42 hours. Progeny was harvested via cell lysis with water and immediately used to infect confluent hEp-2 cells for 24 hours. hEp-2 cells were fixed and stained with PathfinderTM Chlamydia Culture Confirmation System to count inclusion forming units (Figure 37B). In parallel, total DNA was isolated by phenol-chloroform extraction. Subsequently, qRT-PCR analysis using Omp1 and IFNβ-specific primers and probes were conducted as described (Schaeffer A. & Henrich B. 2008) to quantify chlamydial genome equivalents (Figure 37A&C).

In each experiment the IFNγ treatment significantly reduced the amount of chlamydial replication as described previously (Nelson et al., 2005; Tietzel et al., 2009). No consistent differences in chlamydial replication between mGBP2$^{-/-}$, mGBP5$^{-/-}$ or mGBP7$^{-/-}$ cells compared to wild type cells were observed. The percentage of murine genomes was comparable between samples, thus no additional normalization was required. Different replicates display variation as supported by the comparability between genome equivalents and IFU from the same experiment. These experiments show that mGBP2, mGBP5 or mGBP7 cannot impede the chlamydial replication cycle, at least in this in vitro analysis system.

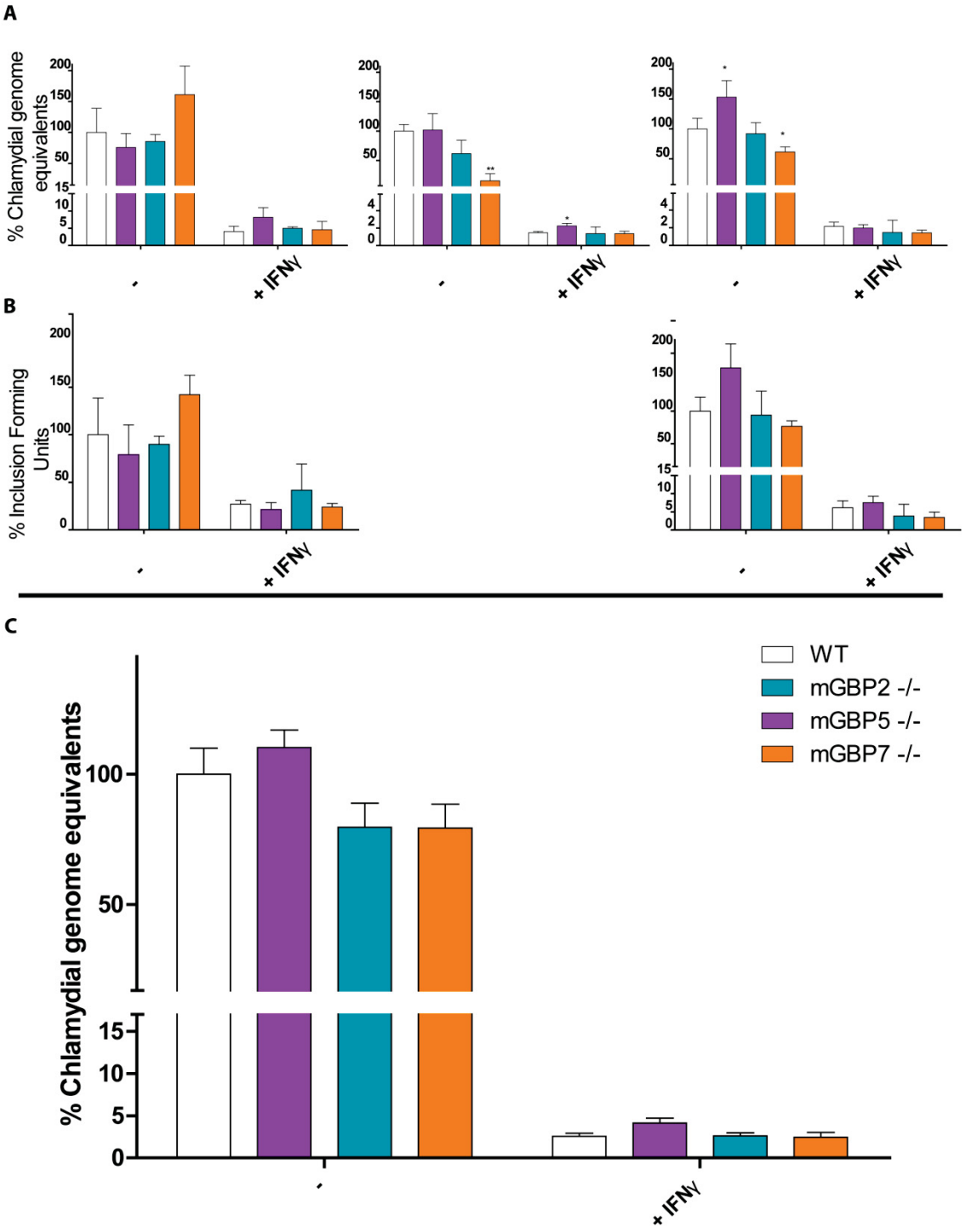

Figure 37: Analysis of chlamydial replication in primary mEFs from wild type, mGBP2$^{-/-}$, mGBP5$^{-/-}$ or mGBP7$^{-/-}$ mice. A) In three independent experiments genome equivalents were assessed via Omp-1 gene- copy numbers and B) two matching analyses of inclusion forming units. Normalised percentages are shown, WT is set at a 100%. Error bars indicate variation of triplicates +SD. C) Summary of A, error bars depict +SEM.

4.4 Characterization the mGBP5 deficient mouse line

To examine the roles of individual mGBPs knockout mice for mGBP2, mGBP5, and mGBP7 were established previously (Degrandi et al., 2013), (Beuter-Gunia, C., Degrandi, D. personal communication September 30, 2016). These mouse strains were subjected to toxoplasma infection in previous studies. Mice lacking mGBP2 or mGBP7 suffered more severe consequences of the infection compared to wild type mice (Beuter-Gunia, 2008; Degrandi et al., 2007), (Beuter-Gunia, C., Degrandi, D. personal communication September 30, 2016). However, the mGBP5$^{-/-}$ mouse did not display a phenotype after *T. gondii* infection (unpublished data). Therefore this study investigated the mGBP5$^{-/-}$ mouse in greater depth.

4.4.1 Phagocytosis capacity of macrophages

The diffuse morphology of mGBP5 accumulations onto chlamydial inclusions (Figure 29A) resembles previous observations in the laboratory which showed mGBP5 to localize around phagocytosed beads and *Mycobacterium bovis* BCG in fibroblasts (unpublished data). Because of these combined observations it was hypothesized that mGBP5 might be part of the phagosomal machinery. To test this hypothesis, it was investigated if the ability to phagocytose particles was affected in the absence of mGBPs. From wild type and mGBP5 knockout mice bone marrow cells were isolated and differentiated into macrophages (bone marrow derived macrophages, BMDMs). These BMDMs were left untreated or stimulated overnight with 100 Units/ml IFNγ and subsequently incubated for 30 or 120 min with fluorescent beads which are 2 µm in diameter. After incubation BMDMs were washed and subjected to FACS analysis. Of all cells the fluorescence histogram depicts the amount of cells with no bead, 1 bead, 2 beads, etc. which were gated accordingly (Figure 38B second graph first gate, highest peak and to right hand side second highest peak, etc. respectively). In Figure 38C the quantification displays that most phagocytosis events occur in the first minutes, and only a small percentage from 30 min onwards. BMDMs which did not phagocytose any beads made up around 40% of the population. In extreme cases, microscopy revealed that macrophages were completely filled with beads, but these population could not be further resolved via FACS analysis. Thus the last gate included cells with more than 4 phagocytosed beads.

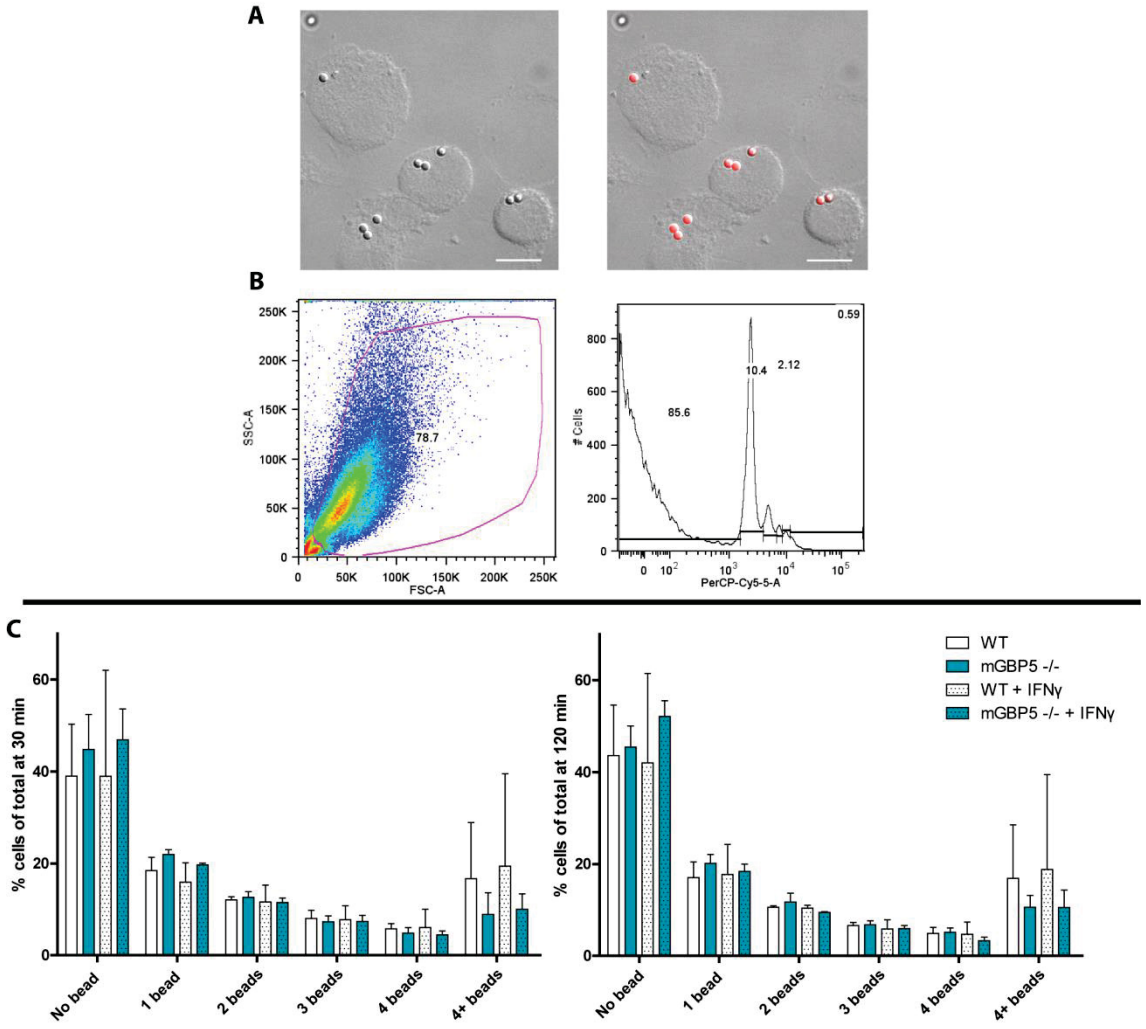

Figure 38: BMDMs ability to phagocytose beads A) exemplary image of cells phagocytosing beads in differential interference contrast and overlapping fluorescence of 4 cells which phagocytosed 1,2 and 3 beads, bar : 5µM B) gating strategy C) quantifications of phagocytosed 1µm beads. Representative data of 2 repeated experiments shown, error bars represent SD.

Comparing wild type and mGBP5$^{-/-}$ macrophages with more than 4 beads phagocytosed it appears the variation in this group is too large to allow drawing of conclusions. BMDMs which phagocytosed 1 bead amounted to around 20%, 2 beads around 15%, 3 beads slightly above 10% and 4 beads slightly below 10%, without an effect of IFNγ stimulation or contribution of mGBP5. Therefore it was concluded that mGBP5 does not play a role in phagocytosis by macrophages.

4.4.2 Immune cell populations in organs of mGBP5$^{-/-}$ mice

To explore whether naive mGBP5$^{-/-}$ mice have a defect in haematopoiesis the immune cell repertoire was analysed. Therefore spleens, livers and lymph nodes were isolated form wild type and mGBP5 deficient mice and prepared into single cell suspensions. On these cells surface molecules which define specific immune effector cell populations were stained with antibodies labelled with a fluorescent marker in order to estimate the

expression level of the marker by fluorescence intensity. The staining panels were optimised in order to measure multiple parameters on a FACS Canto device. All cells that were in the live gate (DAPI-negative) were taken into account (Figure 39A – top).

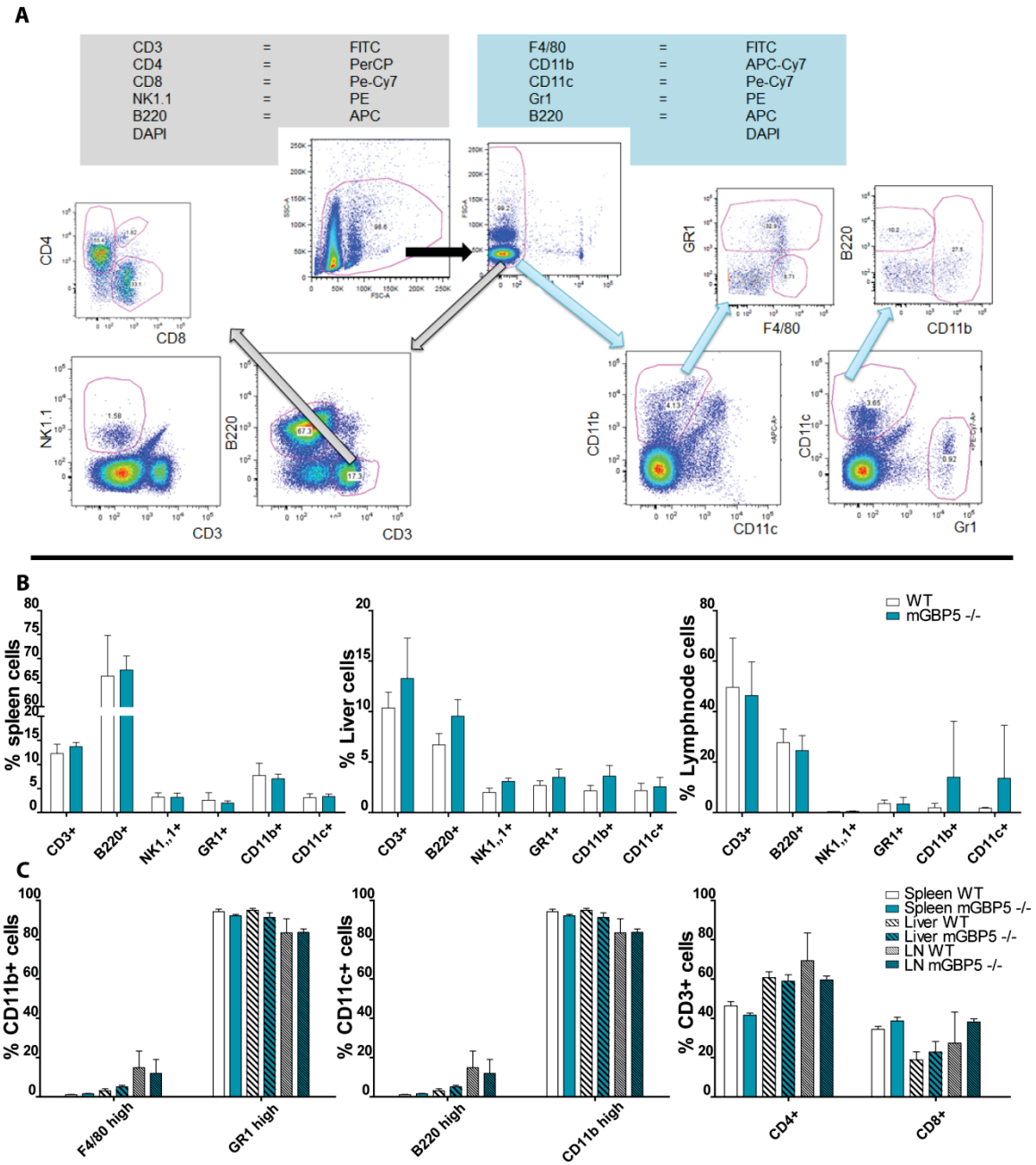

Figure 39: A) FACS staining strategy and B) quantification of cells positive for the indicated marker as a percentage of total cells in the organ C) quantification of cell-subsets as a percentage of total CD11b+, CD11c+ or CD3+ cells in the indicated organ. WT : wild type mice, LN : pooled lymph nodes, bars are depicted + SD Representative data of 2 repeated experiments shown.

Investigated were B cells (B220+) and natural killer (NK) cell (NK1.1) populations, for which no differences were observed in the spleen, liver or lymph nodes of wild type versus mGBP5$^{-/-}$ mice (Figure 39, A for gating and B for quantification). Granulocytes were compared both using single (Gr1+) and double staining (CD11b+, Gr1+) but no differences were observed (Figure 39A & B). Further cell populations investigated were

macrophages (CD11b+, F4/80+), cDCs (CD11c+, CD11b+) and pDCs (CD11c+, B220+) for which no differences were observed, although cells in the lymph nodes of mGBP5$^{-/-}$ mice appeared to have more variable numbers of CD11 populations in the lymph node compared to wild type mice. In order to analyse T cells, CD3-positive cells were compared and no differences were found. Subsequently, CD3+ cells, CD4 helper and CD8 cytotoxic T cell percentage was compared and no differences were observed in any of the investigated organs (Figure 39, B every first set of bars and C last graph).

4.4.3 mGBP5 deficient macrophage killing of mycobacteria

Previously, mGBP5 has been implied to play a role *in Mycobacterium bovis* Bacille Calmette Guerin (BCG) infection by others (Gengenbacher et al., 2016; Kim et al., 2011; Lun et al., 2009; Saban et al., 2007; Saiga et al., 2015). To investigate the anti-bacterial potential of mGBP5, the killing ability of wild type versus mGBP5$^{-/-}$ macrophages was compared. BMDMs were stimulated overnight with IFNγ or left untreated and subsequently infected with washed and sonicated mycobacteria (BCG or H37Rv) at MOI : 3 for 3 h. During this time, an amount of bacteria were taken up into the cells. After 3 hpi the antibiotic gentamycin was added, which kills all extracellular mycobacteria but does not enter the cell. After 4 days the cells are lysed, lysates were sonicated and resuspended in order to plate surviving mycobacteria. Colonies were counted when they became visible, approximately 10-12 days after plating (Figure 40A).

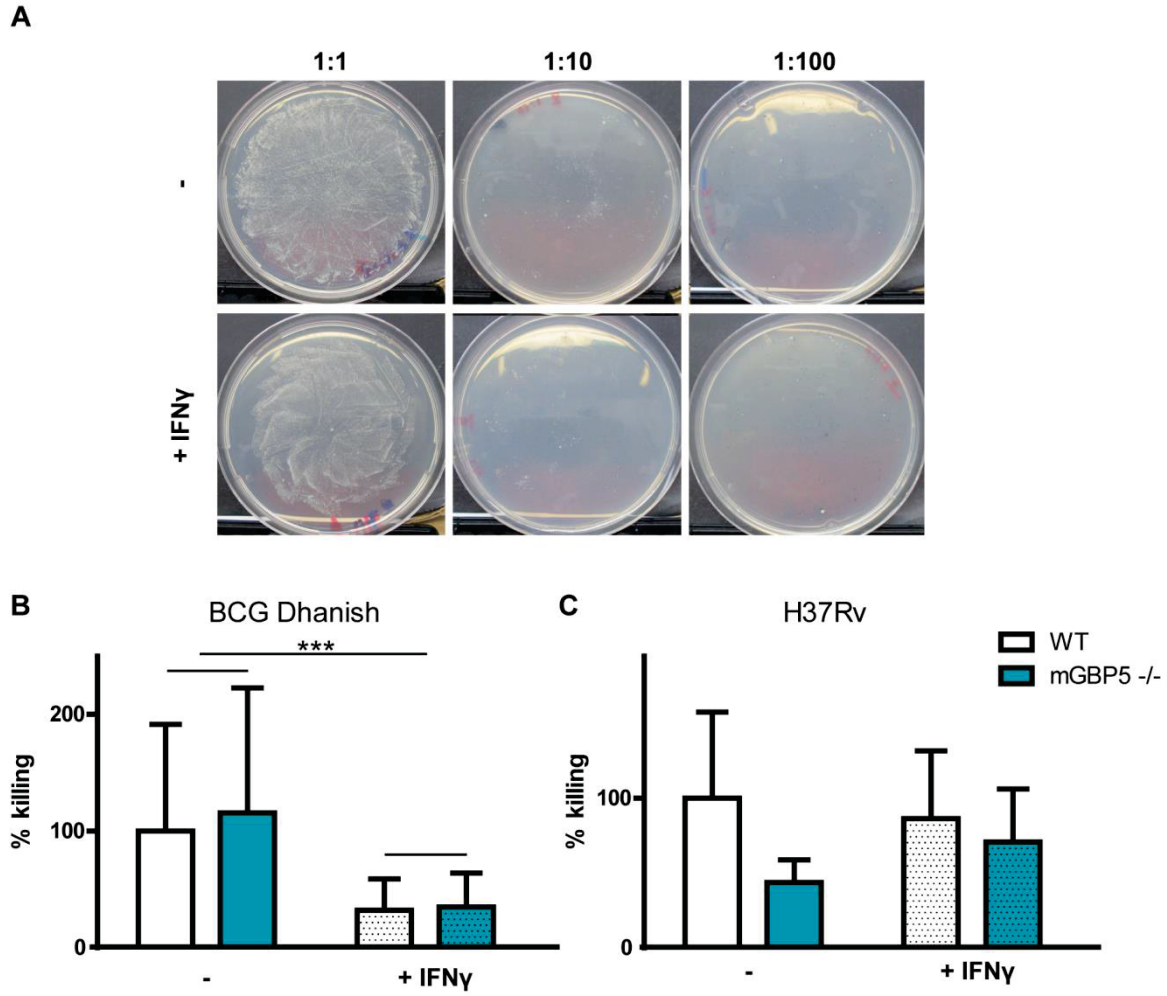

Figure 40: BMDMs derived from wild type or mGBP5$^{-/-}$ mice were stimulated with IFNγ or left untreated overnight. Then BMDMs were infected in vitro with *M. bovis* BCG or *M. tuberculosis* H37Rv at an MOI of 3. At 3 hpi gentamycin was added and macrophages were allowed to kill bacteria during a 4 day incubation period. Subsequently cell lysis with SDS containing buffer released surviving mycobacteria which were then plated in dilutions on Middlebrook-7H10 agar enriched with ADC and glycerine and incubated for 10-20 days until colonies were visible. A) Example of H37Rv dilution series B) quantification of colonies of BCG strain Dhanish and C) H37Rv in 3 independent experiments, percentage normalised to wild type, +SEM.

The amount of BCG which survived was comparable between wild type and mGBP5$^{-/-}$ in BMDMs. After stimulation with IFNγ, a significant increase in mycobacterial killing by macrophages was observed (Figure 40B). Thus concluding that mGBP5 does not have an anti-bacterial function in BMDMs.

However, BCG is an attenuated strain, compared to virulent mycobacteria it lacks genes encoding, amongst others, the ESX-1 secretion system (loss of 'region of difference 1', ΔRD1) (Pai et al., 2016). This locus is implicated in caspase-1-dependent production of IL1β and IL18 (Kurenuma et al., 2009) towards which, in chlamydial infection, the mGBPs on chromosome 3 also play a role (Finethy et al., 2015). Since secreted factors are implicated in hampering the GBP response in both *T. gondii* (Clough and Frickel,

2017) and *C. trachomatis* (Haldar et al., 2016) it is conceivable that virulent mycobacteria would do the same. Therefore testing macrophage killing with more virulent mycobacteria was considered. In addition, hGBP5 has been described as a marker for *Mycobacterium tuberculosis* in human infection (Laux da Costa et al., 2015; Satproedprai et al., 2015). Therefore, the same experiment as described above was repeated under BSL-3 conditions with the laboratory strain *Mycobacterium tuberculosis* H37Rv. However, no significant differences between wild type and mGBP5$^{-/-}$ BMDMs, nor of the IFNγ stimulation were observed on bacterial killing (Figure 40C).

These results show that mGBP5 plays no role in the ability of mycobacterial killing in BMDMs.

Taken together, no differences in immune cell populations, macrophage function, phagocytosis of beads or killing of mycobacteria could be observed in the mGBP5$^{-/-}$ derived cells. Thus the role of mGBP5 in infection remains enigmatic.

5 Discussion

Cell autonomous immune responses are the most essential resistance against pathogens which reside within our cells in order to evade systemic immunity. All pathogens described in this study, e.g. *T. gondii, C. trachomatis* and *M. bovis* and *M. tuberculosis,* manipulate the host cell in various ways to create an optimized intracellular vacuolar niche in which they hide and replicate (Clough and Frickel, 2017; Di Russo Case and Samuel, 2016). While suffering such on-going manipulation of transcription, signalling and membrane dynamics, the host cell retaliates by marking the pathogen containing vacuole (PCV) for destruction through rupture, autophagy or even host cell death (Pilla et al., 2014). In these processes the IFN inducible GTPases, such as the GBPs studied in this work, play a central role (Meunier and Broz, 2016). This study was performed to further the understanding of the mGBPs structure, kinetics and effector mechanisms which result in protection from intracellular pathogens.

5.1 Homology analysis of IFN-Inducible GTPases

Within this study a phylogenetic analysis of complete protein sequences of IFN-inducible GTPases in human and mouse was performed (Figure 14), in addition to solely GTPase domain-sequences published elsewhere (Kim et al., 2012a). This analysis resulted in clusters of GTPases similar to observations in previous publications (Bekpen et al., 2005; Kim et al., 2011; Kresse et al., 2008). Intriguing however, is the amount of splice variants in humans (11 genes, 8 splice variants = 21%) compared to mice (35 genes, 5 splice variants = 12,5 %). More splice variants might partly compensate for the reduced number of immunity related GTPase (IRG) and GBP genes encountered in in humans. Particularly human IRGM, gives rise to several spliced isoforms. Previously, human IRGM was considered a pseudogene due to several truncations and genetic alterations during evolution (Bekpen et al., 2010). Nevertheless, functional studies have found diverse roles for human IRGM splice variants in Crohn's disease (Li et al., 2014) and *M. tuberculosis* infection (Intemann et al., 2009). It was shown that human IRGM splice variants eliminate mycobacterial PCVs through induction of autophagy (Singh et al., 2006). In addition, IRGM was found to modulate mitochondrial membrane polarization, production of ROS and cell death (Singh et al., 2010). In detail, IRGM isoforms interact with pattern recognition receptor NOD2, and subsequently assemble the core autophagy machinery, e.g. ATG16L1, ULK1 and Beclin, to facilitate ubiquitination (Chauhan et al., 2015). These studies show that human IRGM is functional, falsifying its initial characterization as pseudogene. Consequently, potential roles for pseudogenes like mGBP4/mGBP4.1 and the Very Large inducible GTPases (VLIGs) cannot be excluded.

5.2 Exploring functional motifs required for the antimicrobial action of mGBPs

Previously, it was described that the anti-microbial activity of mGBP2 requires GTP binding-dependent multimerization, ability of GTP hydrolysis as well as C-terminal isoprenylation (Degrandi et al., 2013; Kravets et al., 2012) (Figure 17). This study found that colocalization of mGBP2 with another pathogen, *C. trachomatis*, is also dependent on its isoprenylation site, implying that membrane interactions are required to position mGBP2 at the inclusion membrane (See Figure 29B & 30). However, whether nucleotide-binding and GTPase activity are required for localization of mGBP2 to chlamydia, as shown for toxoplasma, is currently unknown. By utilizing a set of point- and truncation mutants of mGBP2 described previously (Degrandi et al., 2013; Kravets et al., 2012), these questions can be addressed in the future. It was also shown that mGBP2 multimerizes with mGBP1, and to a lesser extend with mGBP3, to form preassembled reservoirs in vesicle like structures (VLS). Upon infection these pre-assembled mGBPs relocate to the pathogen containing vacuole (PCV) (Kravets et al., 2016). However, it was found that mGBP6 and mGBP7 reside in distinct VLS, whereas dimerized mGBP5 homomers reside in the cytosol. Also, mGBPs from these independent reservoirs relocate to the PCV upon infection (Kravets et al., 2016; Reich, A., Kravets, E., personal communication, March 15, 2015). The necessity of isoprenylation for mGBP2 to translocate to toxoplasma and chlamydia PCVs indicates that membrane anchoring is required. However, only hGBP1, hGBP2, hGBP5, mGBP1, mGBP2, and mGBP5 contain a C-terminal CaaX-box, which allows isoprenylation and membrane anchoring (Nantais et al., 1996; Stickney and Buss, 2000; Tripal et al., 2007). This raises the question, how mGBP6 and mGBP7 translocate from VLS to the PCV without aid from an isoprenylation site or multimerization with isoprenylation site-containing mGBPs.

Previous work within the laboratory showed that mGBP6 localizes to the *T. gondii* PCV more often than mGBP10. This depends on a single, negatively charged, aspartic acid (D542) in the C-terminal region (Klümpers, 2013). When D542 was mutated to a neutrally charged residue, PCV targeting was reduced by approximately 50% in mEFs (Klümpers, 2013). In this study, NIH/3T3 fibroblasts which constitutively overexpress wild type or mutated mGBP6 were generated. After infection with type II *T. gondii* the amount of mGBP6 associated with PCVs was significantly reduced, around 40%, when mutating D542 to neutral asparagine (N), or, when mutating to a positively charged lysine (K) a non-significant reduction was observed (See Figure 20). This study supports the

previous observation, that the single aa D542 is important for mGBP6 localization to the *T. gondii* PCV. However, this feature is unique to mGBP6. Other mGBP family members with corresponding mutations generated in this study localized at the PV membrane, in similar rates as their wild type counterparts (Paragraphs 4.2.).

MGBP proteins contain several predicted sequence motifs. Aside from the GKS containing GTPase, and C-terminal domain, the other domains described (Table 1) were not conserved amongst all family members. Notably though, both mGBP6 and mGBP7 proteins are predicted to contain a HAUS augmin-like complex subunit 4 (HAUS4) super family and Fes/CIP4 homology Bin-Amphiphysin-Rvs167 (F-BAR) motif. Additionally, mGBP10 is also predicted to contain an F-BAR, but no HAUS4 motif.

The HAUS4 motif was described in the augmin-like complex, which interacts with microtubules to organize mitotic spindle assembly and maintenance of chromosome integrity (Sanchez-Huertas and Luders, 2015). Live-cell time lapse recordings (Videos in the appendix; Paragraph 4.3.3; Kravets et al., 2016) show movement of mGBP VLS, which more easily reconciled with Brownian, than microtubule-directed motion. Although hGBP1 has been found to remodel the cytoskeleton in T cells to regulate surface receptors, this solely relied on actin and not on microtubules (Forster et al., 2014; Ostler et al., 2014). Therefore, the predicted HAUS4 motif in mGBPs is deemed unlikely to play a functional role in mGBPs recruitment to PCVs.

F-BAR motifs contain scaffolding and amphipathic helices, which can bind membrane phospholipids to shape dynamic membrane processes, e.g. endocytosis, phagocytosis, filopodium, lamellipodium, cytokinesis, adhesion, and podosome formation (Frost et al., 2009; Roberts-Galbraith and Gould, 2010; Suetsugu, 2016). Also, disruption of the F-BAR motifs results in various diseases and in developmental disorders (Liu et al., 2015a). In general, F-BAR containing proteins act as dimers, sensing membrane curvature by inserting their amphipathic helix motifs into the lipid bilayer (Nguyen et al., 2017) and subsequently exert mechanic forces, leading to membrane curvature (Simunovic et al., 2015). Furthermore, proteins containing other BAR-motifs, have been found to recruit small Rho GTPases and influence their activation (Aspenstrom, 2014). It is tempting to speculate that PCV membrane localization of mGBP6, mGBP7 and potentially mGBP10 could be evoked by a F-BAR motif within the C-terminal domain of these mGBPs. If that is the case, it is conceivable that mGBP6, mGBP7 and/or mGBP10 is/are capable of preassembling heteromers with mGBP9 in VLS and direct mGBP9 to PCVs. In that case, the VLS reservoirs in uninfected cells are comprised of two groups,

one of the mGBPs described above and the other one by mGBP2 heteromerized with mGBP1 and/or mGBP3. However, further experimentation is required to confirm whether the predicted F-BAR motif in mGBPs is indeed present. An approach to address this hypothesis could be the introduction of several mutations, in order to disrupt the amphipathic helix structure, combined with multiparameter fluorescence image spectroscopy (MFIS) and co-immunoprecipitation pull down assays to investigate if these specific mGBPs can interact.

Next, a computer model of mGBPs was generated in cooperation with the research group of Prof. Dr. Schmitt (Figure 27). Aiming to analyse whether the mutation introduced in mGBP6, which reduces PCV colocalization, could influence the position of the C terminal α-helices. The orientation of the residue at position 542 in the α-chain 12 in mGBP6, is similar in mGBP2, mGBP7 and mGBP10 (Figure 41).

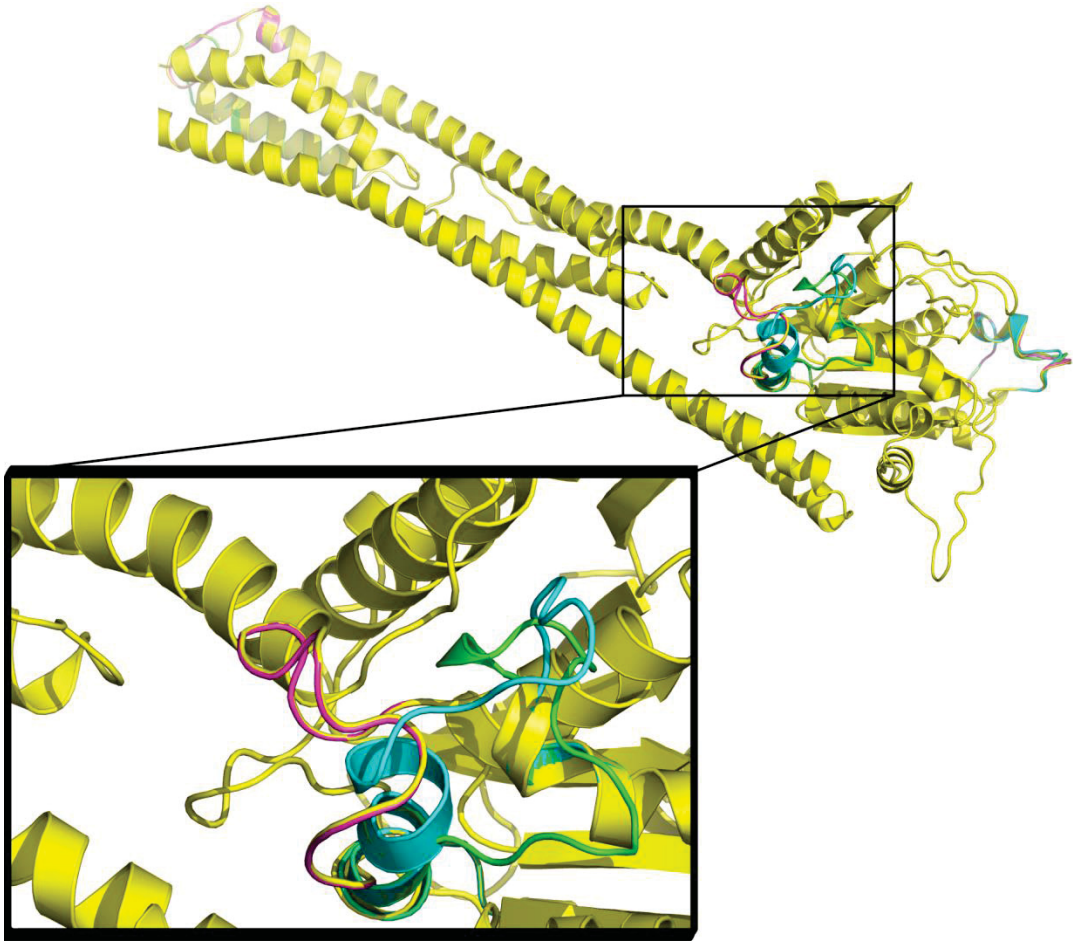

Figure 41: Structural model comparing mGBP2, mGBP6, mGBP7 and mGBP10 shows largely conserved structures except for a variable region (in mGBP6 amino acids 148-170) within the G-domain switch region between conserved G3 and G4 motifs. Quadrant is enlarged view, Blue : mGBP2, Pink : mGBP6, Yellow : mGBP7, Green : mGBP10.

The α-chain 13 is proposed to play a role in multimerization of hGBP1 (Syguda et al., 2012a; Vopel et al., 2014). This residue is directed outward of the protein, and away from

the α-chain 13. Therefore, it is unlikely that this aa plays a role in multimerization of mGBPs. Thus we can conclude that the C-terminal region of mGBP6 contains an interesting motif around aa 542, but further experimentation mutating multiple aa's must confirm the nature of this region and if it is essential for recruitment towards pathogens.

Intriguingly, the structural model comparing mGBP2, mGBP6, mGBP7 and mGBP10 revealed a variable region in the N-terminal G-domain (Figure 41). The conserved G3 and G4 motifs are connected through a flexible loop, which shape is shared among mGBP6 and mGBP7, but which arches differently in mGBP2 and inwardly in mGBP10. Due to the proximity to the G-domain, these distinct loops might influence the speed of GTP binding and hydrolysis, because the alteration of "budding" loops is considered to be a mechanism of structural innovation (Blouin et al., 2004). The different behaviours of mGBPs in infection might be dependent on structural differences in their GTPase domain loops which bar or improve GTPase activity. This hypothesis could be studied in the future using crystallography of mGBPs to ascertain if the loop between G3 and G4 is indeed positioned differently between these proteins.

5.3 Function of mGBPs in antimicrobial defence

5.3.1 Several mGBPs localize at chlamydia inclusions

C. trachomatis serovar L2 is a sexually transmittable intracellular bacterium to which cell autonomous immune responses are understood only in part. In this study, it is shown that not only mGBP1 and mGBP2 (Finethy et al., 2015; Haldar et al., 2013), but the majority of mGBPs colocalize with chlamydia inclusions. Colocalization at the chlamydial inclusion membrane was observed for mGBP1, mGBP2, mGBP3, mGBP6, and mGBP9, as well as for mGBP7 and mGBP10, albeit in lower percentages (Figure 29 and 30). A pilot experiment identified the optimal time point for encountering inclusions colocalizing with mGBPs at 14 hpi, as opposed to the previously published 20 hpi or later (Finethy and Coers, 2016). In addition, rare but distinct accumulations of mGBP5 around inclusions were observed with a more scattered morphology compared to other mGBPs, whereas mGBP8 virtually never recruited towards the chlamydial inclusions nor towards toxoplasma PVs. This implies that despite high sequence similarities among the mGBPs, individual family members respond differently in *C. trachomatis* infection. When comparing *C. trachomatis* and *T. gondii* infection, a specific pattern in recruitment of mGBPs appears. One example is mGBP6, which recruits more frequently to *T. gondii* PVs than to chlamydial inclusions (Figure 30). Contrarily, mGBP9 accumulates as often as mGBP1 and mGBP2 (13%, 13% and 17% respectively) onto intracellular chlamydial, but not onto *T. gondii* PVs (Figure 30). This quantification suggests that not all mGBPs contribute equally towards cell autonomous immunity, and that the players in chlamydial infection, aside from mGBP1 and mGBP2, can be extended to mGBP3, mGBP6, mGBP7, mGBP10 with a major role for mGBP9. Therefore, the functional role of mGBPs should be addressed in mGBP deficient mouse lines, particularly an mGBP9 deficient mouse line in the future

5.3.2 mGBPs enclose chlamydia inclusions in living cells

Results of Kokes & Valdivia in 2015 showed that fixation of chlamydia infected cells can cause accumulation and translocation of nearby aggregates, organelles, etc. over the chlamydia inclusion membrane (Kokes and Valdivia, 2015). Therefore, in this study, it was investigated whether mGBPs accumulate onto chlamydia inclusions in unfixed, living cells using cLSM and time lapse recordings. Due to the moderate percentage of colocalization in fixed cells and the associated imaging effort, only a selection of mGBPs from the characterized panel could be studied using this time consuming imaging technology. Previous studies showed that mGBP2 is recruited at the highest frequency,

compared to other mGBPs, towards *T. gondii* PVs, can destruct the pathogen containing vacuole and impede pathogen survival (Degrandi et al., 2007; Finethy et al., 2015; Haldar et al., 2013; Kravets et al., 2016; Kravets et al., 2012). In addition this study found that mGBP9 colocalizes with chlamydial inclusions in comparable amounts as mGBP2, implying that mGBP9 might be an important factor in the clearance of chlamydia. Therefore both mGBP2 and mGBP9 were selected to examine the time dependent colocalization with inclusions in unfixed cells.

Due to chlamydia's biphasic lifecycle, both the ~200 nm elementary bodies (EB) and the ~1 µM large reticulate bodies (RB) can be found inside an inclusion, depending on the time post infection (Elwell et al., 2016). Therefore the 'inclusions' in this study contain the larger metabolically active RBs due to observation limitations and the early time point in the infection cycle. Consequently, antecedent phases of infection in which the infectious EBs decondense and start shaping their vacuole, are small-scale. Prior to discussing the observations in this study, it has to be considered that these initial infection phases are often analysed by electron, rather than confocal microscopy. Similar resolution limitations in assessing early inclusions were observed when analysing live cells infected with *C. trachomatis* transformed with pGFP::SW2 (Wang et al., 2011). In this study, during the first few hours after infection, the GFP signal cannot be seen at all or is seen 'blinking on/off', in time lapse videos, indicative of little fluorescence yields at the border of the detectors sensing ability. More recently, an additional GFP-transformed chlamydial strain, p2TK2-SW2 IncDProm-RSGFP-IncDterm was generated (Agaisse and Derre, 2013) which has a three-fold stronger fluorescence signal and can be detected earlier than pGFP::SW2 (Vromman et al., 2014). In this publication, it was suggested that the *Neisseria*-derived promoter used in the pGFP::SW2 expression system might induce delayed expression, leaving chlamydia undetectable in early phases of infection. Either through size limitations or lack of GFP-expression in early inclusions (0-12 hpi, until RBs maturated) the study of events immediately after infection borders on the resolution of the confocal microscope and should be addressed by imaging technologies with higher resolution or sensitivity.

In time lapse recordings, it was observed that GFP-expressing chlamydial inclusions move through the cell cytoplasm with colocalized mGBP2 or mGBP9 for the entire duration of the recording (Paragraph 4.3.3), similar to observations made for mGBP2 recruited at the *T. gondii* PV membrane for more than 16 h without any noticeable change in vacuole or parasite morphology (Kravets et al., 2016). This confirms previous observations with fixed cells that colocalization of mGBPs with chlamydial inclusions is

bona fide and can occur over prolonged periods of time. Surprisingly, mGBP2 was localized towards inclusions during time lapse recording taken prior to IFNγ stimulation at 3 hpi (Figure 32-34). As early as 40 and 50 min pi, at two different sites within the cell, mGBP2 accumulated in balloon-like structures with an approximate size of an early inclusion, an event which was never seen in uninfected cells. Unfortunately, no GFP-signal from chlamydia could be measured in this early phase of infection; ergo this observation could not unequivocally be scored as a colocalization. Remarkable, is the morphology in Figure 34, where from +60 to +40 min pi the balloon-like shape is distorted into two connecting rings, reminiscent of membrane morphology after disruption of the inclusion depicted at 20 hpi (See Haldar et al., 2015 –Figure 7). In this study, after approximately 70 min the mGBP2 accumulations were observed to disappear and only vesicle like structures remained.

Similar transience was observed in the dynamics of mGBP9 accumulation during live cell imaging. Relocation of mGBP9 is a rapid process, initiated simultaneously at different sites of the inclusion (Figure 35). The mGBP9 accumulation occurred several hours after infection, suggesting that mGBP2 acts earlier than mGBP9. This hypothesis is corroborated by results from a study of toxoplasma infected cells co-expressing mGBP2 and mGBP9. This study shows *T. gondii* containing PCVs that are heavily decorated with mGBP2, and occasionally at the same time colocalized mGBP9 to a lesser abundance (See Kravets et al., 2016 - Supplementary Figure 9). In addition, time lapse recording in the cited study showed mGBP9 accumulation to be transient, occurring for a few hours only and dissolving afterwards, as early as 9 hpi. Thus showing similarities between mGBP9 accumulation dynamics in infection with *T. gondii* and chlamydial, the latter which was performed in this work. In summary, this study shows the occurrence, exceptional morphology and dynamics of mGBP9 colocalization with chlamydia inclusions in living cells.

Live cell imaging of mGBP2 or mGBP9 overexpressing cells, proves that mGBP colocalization with intracellular chlamydia is authentic. It also provides information on dynamics of recruitment, which was not available before. Since chlamydia infections occur asynchronously, the colocalization frequency depicted in this study at 14 hpi and those elsewhere at 20 hpi (Finethy et al., 2015; Haldar et al., 2015; Haldar et al., 2016; Haldar et al., 2014; Haldar et al., 2013), might be vastly underestimated due to quantification at one individual time point. Nevertheless, a large percentage of inclusions is not ‘recognized’ by mGBPs. A feature which will be discussed below (Paragraph 5.3.4).

In summary, this study discovered a potential chlamydia-specific role for mGBP9, which must be further explored in the future. Moreover, this study suggests a potential of mGBPs encoded on murine chromosome 5, which have up till now not been assigned a role in pathogen defence.

5.3.3 Measures to optimize quantification of mGBP colocalization at PCVs

The amount of colocalization of a single mGBP with PCVs was recognized in this study to potentially correlate with the mean fluorescence intensity (MFI) of cells constitutively expressing the mGBP in question, as observed in Figure 20, where wild type mGBP6 colocalizes most often, mutant D542K less often and mutant D542N least often, a pattern reflected in their MFIs depicted in Figure 26. Due to light sensitivity limitations of the microscope detectors (charge coupled devices, CCD) and the experimenters vision, quantification of fluorescent proteins in cell lines with lower fluorescence intensities might cause an under appreciation of events. Reassuringly, these differences do not directly correlate to other observed colocalization percentages. For example, the observations that mGBP9 colocalizes comparably often to chlamydial inclusions as mGBP2, whereas mGBP6 recruits very often to toxoplasma PVs. These results are accentuated, since the investigated cell lines expressing mGBP6 and mGBP9 had a lower mCherry MFI value, compared to the other mGBP fusion proteins transduced cells. If the fluorescence intensity of a cell line influences quantification of colocalization frequencies at all, these high colocalization frequencies would be underestimated. A further comparison of quantifications in Figure 30 with MFIs in Figure 31 argues against a correlation. It is observed in these figures, that cell lines with an MFI significantly higher than that of the mGBP2 expressing cell line, e.g. mGBP1, mGBP3, mGBP5 and mGBP7 expressing cells, display less colocalization of individual mGBPs to toxoplasma and chlamydia containing PCVs. This topic could be further addressed by cell sorting of one cell line, for example mGBP6 expressing fibroblasts, into sub-clones exhibiting low, intermediate or high MFI. Subsequently infecting these clones with *T. gondii* ME49 allows to quantify, in a blinded study, whether the frequencies of observed mGBP localization of at the PV correlates with the MFI.

For antimicrobial action of mGBPs, the stimulation with IFNγ is paramount in toxoplasma infection (Takacs et al., 2012; Yamamoto et al., 2011). The methods for quantifying toxoplasma growth used in these publications vary. A ratio between vacuoles containing rosettes and single parasites, was found to be markedly different in mGBP2 –deficient

mEFs (Degrandi et al., 2013). The chlamydial infection cycle is impeded by IFNγ stimulation. IFNγ stimulation results in differentiation into chlamydial aberrant bodies in human cells, or smaller inclusions containing fewer reticulate bodies (RBs) with normal, non-aberrant morphology in murine cells (Schoborg, 2011). In murine cells, the chlamydial production of infectious progeny is consequently reduced by IFNγ in a dose-dependent manner (Tietzel et al., 2009). Also the time point of IFNγ administration is crucial, since it was shown that IFNγ addition prior to, or together with, infectious particles abrogates chlamydial growth. Therefore, stimulation with IFNγ in this thesis was performed at a concentration of 100 Units/ml and 3 hpi, similar to other publications (Finethy et al., 2015; Haldar et al., 2015; Haldar et al., 2016; Haldar et al., 2014; Pilla et al., 2014) to increase comparability. Regarding IFNγ stimulation, the delicate balance between activating mGBPs, and impeding chlamydial replication, must be recognized. Possibly, a titration of IFNγ units reveals a more favourable window, to quantify mGBP colocalization with inclusions. Not depicted in this work is an effort made of an IFNγ titration. IFNγ stimulated and untreated murine fibroblasts were infected with *C. trachomatis* expressing pGFP::SW2 and fixated at 24 hpi. Fixation was performed with 4% PFA at 4°C overnight, prior to FACS analysis. Unfortunately, no results were obtained because the intracellular chlamydia lost their fluorescence. Interestingly, correspondence with other research groups confirmed this observed loss of fluorescence. Nevertheless, still other research groups published measurements where chlamydial fluorescence is unaffected by fixation (Vromman et al., 2014). When this issue has to be pursued further, different fixation protocols could be taken into account. It could be considered to use FA instead of PFA, since improved fluorescence preservation was observed when staining transcription factors in this way (Heinen et al., 2014). However, different fixation strategies should take the biosafety level 2 classification of chlamydia into account. Since aerosol formation during flow cytometry is possible (Holmes et al., 2014) and the ‘spore’-like EBs are not easily killed (Cosse et al., 2016).

5.3.4 Elucidating the mGBP anti-microbial action at the pathogen containing compartment

This study shows that, comparable to *T. gondii* infection, a discrete set of mGBPs colocalize at the chlamydial inclusion membrane immediately after infection for one to several hours (See Figures 33-35). Due to resolution limitations of cLSM, observation of mGBPs on the surface of EBs or RBs could not be assessed. Membrane disruption of chlamydial inclusions was described by others to occur as lysis in 20% of inclusions, evidenced by a breach of the chlamydial membrane marker CT813 in mGBP2, P62 or

TRAF6 positive inclusions (Haldar et al., 2015). Biochemically it is conceivable that the mGBPs, as membrane-interacting multimers, are capable of functioning as mechanoenzymes thus rupturing membranes. Alternatively, mGBP supramolecular complexes could function as assembly platforms, for additional interactions with other effector proteins (Kim et al., 2012a; Kravets et al., 2016). Current research efforts are directed at identifying GBP-interacting proteins. Some binding partners have been described, e.g. mGBP7 interacting with ATG4B and NADPH oxidase complexes, mGBP1 interacting with p62 (Kim et al., 2011) or GBP2 interacting with IRGM (Traver et al., 2011). Recently, an overlap of mGBPs with an additional assembly platform for immune signalling was found, namely inflammasomes (Man and Kanneganti, 2015).

Observations particularly suggestive of PCV rupture were not made in this study. A single exception occurred during live cell imaging of mGBP2 in *C. trachomatis* infected un-stimulated cells. In Figure 34, +70 min the morphology of the mGBP2 accumulation could be considered reminiscent of the GBP2 morphology depicted at a lysed inclusion by others (See Haldar et al., 2015 - Figure 7). Additional different morphological observations were made in this study. In the infection cycle of *C. trachomatis,* at 14 hpi several RBs should be loosely distributed throughout an inclusion. When examining the DAPI stain of the exemplary inclusion in cells overexpressing mGBP8, the expected spacious distribution of DNA within the inclusion is observed (See Figure 29). Compared to the DAPI stain in cells overexpressing mGBPs that do recruit to inclusions, e.g. mGBP1, mGBP2, mGBP3, mGBP6 and mGBP9, the chlamydial DNA appears to be packed closer. This compact particle composition is suggestive of a role for mGBPs in confining inclusion expansion. A confining mGBP function was also observed in *T. gondii* infections, where the mGBP2-associated PV membrane acquired a rounded shape consequently followed by disruption of the PV (Kravets et al., 2016). A different phenomenon was observed in inclusions colocalizing with mGBP7 and mGBP10, where the DAPI stain displayed expanded nuclei comparable to the morphology of aberrant chlamydial bodies, which persist under conditions stressful to the bacterium.

Additionally, during this study it was observed that inclusions on which mGBPs accumulate loose their GFP-expression or CT868 antibody-signal, in contrast to inclusions where no mGBPs colocalize. An example encountered 3.5 hpi in living cells constitutively expressing mGBP2 can be recognized (Figure 28) and in fixed cells where mGBP7 accumulates onto one of two inclusions in the depicted field, where no chlamydial CT868 signal is detectable, but bacterial DNA is still visible (Figure 29 - row 6). This suggests that the epitope recognized by the antibody or the GFP expressed

within chlamydial particles is masked or destroyed. These observations in colocalized inclusions, as opposed to inclusions without mGBP accumulation, hint at a localization-dependant anti-microbial function of mGBPs.

To address the antimicrobial mGBP function, a chlamydial progeny assay was set up to analyse chlamydial genome equivalents and infectious particles yielded 42 hpi of primary mEFs deficient for mGBP2, mGBP5 or mGBP7 as compared to wild type mEFs. The effect of IFNγ stimulation was highly significant, as described previously (Coers et al., 2008; Haldar et al., 2014). However, lack of mGBP2, mGBP5 or mGBP7 did not alter the amount of genome equivalents nor the amount of infectious particles. Therefore the conclusion must be drawn that these mGBPs do not impede the chlamydial replication cycle (Figure 37). This is surprising since the IFNγ effect on chlamydial growth was described to be mediated by the mGBPs on chromosome 3 (See Haldar et al., 2014 – Figure 5). Taken together, that implies solely mGBP1, solely mGBP3 or a combination of the GBPs on chromosome 3 is required to mediate the effect of IFNγ in reducing chlamydial genome replication. However, in the study referred to, mEFs were treated with 200 Units/ml IFNγ overnight, after which chlamydial infection was performed and growth was assessed 24 h later. These results contradict a study in murine oviduct epithelial cells (MECs), which observed essentially no growth when stimulating 4 h prior to infection with IFNγ (Nelson et al., 2005).

In human epithelial cells, infected with different chlamydial species, it was found that a relevant cell autonomous defence mechanism is IDO induction (Haldar et al., 2016; MacKenzie et al., 2007). Up regulation of IDO depletes tryptophan, and during chlamydia infection is bacteriostatic in nature. However, tryptophan-repletion uncovered an additional bactericidal mechanism, dependent on p62- and ubiquitination. This additional human effector mechanism reduces chlamydial genome copies, infectious particle formation and the number of inclusions per microscope field of *C. muridarum*, but not *C. trachomatis* (Haldar et al., 2016). When analysing co-infected human cells, fused inclusions containing both chlamydial species showed less ubiquitination than inclusions containing solely *C. muridarum*. Since *C. trachomatis* inclusions resist ubiquitination, these observations favour the hypothesis that *C. trachomatis* expresses a virulence factor capable of limiting inclusion ubiquitination in human cells (Haldar et al., 2016). However, in murine cells *C. trachomatis* cannot prevent ubiquitination of its inclusion (Haldar et al., 2015).

C. trachomatis evolved a virulence factor impeding the autophagy machinery specifically in human cells. *C. muridarum* is not recruited by IFNγ-inducible GTPases in murine cells (Coers et al., 2008). Allowing to hypothesize that *C. muridarum* might have evolved an orthologous virulence factor to impede specifically the murine autophagy machinery. Alternatively, *C. trachomatis* might encode additional factors targeting the mGBP-defence system. The differential colocalization percentages of mGBP9 on intracellular compartments between chlamydia and apicomplexan infection, might be interpreted as a chlamydia-specific adaptation of mGBP9. Such specificity implies a co-evolutionary arms race in which it is conceivable that mGBP9 circumvents the proposed chlamydia interference factor(s) to recruit to inclusions more effectively. Of course, such a claim requires in depth microbiological research to identify this factor. However, it is an interesting hypothesis which explains why not all chlamydial inclusions colocalize with mGBPs over time, why mGBP colocalization is transient and particularly why no large inclusions (the size customary at 24-30 hpi) were ever observed to colocalize with mGBPs. When approaching this issue hypothetically, lack of recruitment could be explained by an acquired virulence factor with similar function as *T. gondii* ROP54 which prevents mGBP2 loading onto the PV (Kim et al., 2016b) or ROP5/ROP18 which cooperate to inactivate mouse IRG proteins (Hermanns et al., 2016), while transience of GBP recruitment compares to *Shigella* infections, where virulence factor Ipha9.8 was found to ubiquitinate GBPs at the PCV causing their degradation and suppressing cell autonomous defences (Li, P., personal communication, March 22, 2017). In chlamydia, bacterial effectors with deubiquitination activity have been identified, e.g. ChlaDUB1 and ChlaDUB2. These may interfere with host-ubiquitination (Bastidas et al., 2013; Claessen et al., 2013), thus manipulating cellular processes like apoptosis (Fischer et al., 2017). In the future, further examination of the chlamydial genome will likely yield additional effectors that frustrate host-directed ubiquitination (Zhou and Zhu, 2015). Inactivation of the mGBP machinery, by an unknown virulence factor of *C. trachomatis*, would explain why no altered growth could be observed in cells lacking mGBPs (Figure 37). In order to accurately assess chlamydial growth, the genome equivalents, infectious progeny, inclusions per frame, average inclusion volume and chlamydial nuclei size should all be taken into account simultaneously to discriminate bacteriostatic from bactericidal and persistence inducing effects.

It remains intriguing, why at a given time point, approximately 50-85% of chlamydial inclusions, and around 35-60% of toxoplasma PVs do not acquire mGBPs (Figure 30) (Klümpers, 2013). In addition, after mGBP accumulation chlamydia inclusions do not completely loose GFP expression (Figure 35) implicating that the chlamydia are not

promptly destroyed. Similarly, 61.1% of mGBP2 recruited toxoplasma PVs do not show any apparent PV permeabilization or disruption (Kravets et al., 2016). What is happening with recruited mGBPs at these seemingly unaffected PCVs remains an open research questions to be addressed in the future.

Further insight in the role of mGBPs, could be gained from an alternative approach: *in vivo* infections of mice lacking single or multiple mGBPs and/or other proteins in the autophagy pathway. The chlamydial species and route of infection performed to investigate this infection in mice is essential. During infection *in vivo*, *C. muridarum* represses IFNγ induction, thus making it unlikely that mGBP-mediated immune responses are induced and/or activated when infecting with this chlamydial species. When using human pathogen *C. trachomatis* in mice, the infection is readily cleared. Nevertheless, *C. trachomatis* can establish a lasting infection in mice when extremely high doses or non-genital infection routes are used. However, such deviations from the physiological route of chlamydial infection have been found to alter immune responses (Abdelsamed et al., 2013; Borges et al., 2015; Jiang et al., 2010; Lyons et al., 2005; Miyairi et al., 2010; Murthy et al., 2007; Ziklo et al., 2016). Nevertheless, studying chlamydia infections in mice might yield interesting results that clarify the role of mGBPs in host immunity.

5.3.5 The role of mGBP5 in host immunity

Taken together, no alterations in immune cell populations (Figure 38), nor alterations in bone marrow derived macrophage (BMDM) phagocytosis of beads (Figure 39), or killing of attenuated BCG or virulent *M. tuberculosis* (H37Rv, Figure 40) could be observed *ex vivo* in cells of mGBP5$^{-/-}$ mice compared to control mice.

Nevertheless, a role has been assigned to mGBP5 in tuberculosis since its mRNA is up regulated *in vivo* after mycobacterium infection (Gengenbacher et al., 2016; Lun et al., 2009; Saban et al., 2007). Furthermore, specifically in mycobacterial control, it was shown that colony forming units increased after small interfering RNA knockdown of mGBP5 in murine derived macrophages after IFNγ stimulation (Kim et al., 2011). In addition, *Salmonella* and *Listeria* cell wall component-specific induction of mGBP5 was shown to induce mGBP5 tetramerization and binding of the G-domain to the pyrin domain of NLRP3. Subsequently, leading to NLRP3 oligomerization and ASC recruitment ultimately cleaving of caspase-1 and thus causing IL1β and IL18 secretion (Caffrey and Fitzgerald, 2012). Via this pathway, mGBP5 is linked to activation of the NLRP3-ASC inflammasome, previously observed in *Salmonella* infected cells (Rupper and Cardelli, 2008). Thus, alluding to the possibility that mGBP5 induced inflammasome activation and subsequent cell death might play a similar role in mycobacterial infection.

Nevertheless, kill assays using BMDMs derived from mGBP5 deficient and wild type mice, did not show a function of mGBP5 in killing BCG or virulent *M. tuberculosis* strains (Figure 40). When interpreting assays using BMDMs it should be taken into account that BMDM maturation and activation methods strongly polarize the immune functions exerted by the macrophage (Vogel et al., 2014). The use of L-cell supernatants favours polarization of macrophages in the alternatively activated M2 phenotype (Chamberlain et al., 2015) in which mGBP5 might play a diminished role, compared to M1-activated macrophages (Fujiwara et al., 2016). Potentially, differential macrophage activation prevents induction of mGBP5 in the kill assays performed in this study. A potential solution for this issue might be to explore the use of self-renewing macrophages in the future (Fejer et al., 2015; Fejer et al., 2013). After establishment of these macrophage cell lines, there is no additional need to supplement growth factors. Instead, when using BMDMs, growth factors are required for maturation, but also skew macrophage activation prior to experiment. Therefore, self-renewing macrophages allow a better assessment of macrophage heterogeneity in infection assays. How the morphology and polarization of macrophages and related cells, plays a central role in tuberculosis is being described in increasing detail (Feng et al., 2014), however, the full particulars are

currently lively debated (Crawford, 2015; Dorhoi et al., 2015). Moreover, the versatile nature of myeloid populations and subpopulations involved in mycobacterial infection (Dorhoi and Kaufmann, 2015) might not be sufficiently represented by a culture of BMDMs. Therefore the role of mGBP5 and other mGBPs in mycobacterial clearance is suggested to be evaluated *in vivo* by comparing wild type and mGBP deficient animals. When comparing mycobacterial infections *in vivo,* the genetic background of inbred mice must be considered. In this study, mice of the C57BL/6 background were used. These mice are less susceptible to *M. tuberculosis*, and thus display lower mycobacterial counts, than other mouse inbred strains might display (Lee et al., 2016).

Additionally, mGBP5 has been found to colocalize at the *T. gondii* PCV (Figure 19, Lindenberg et al., submitted; Kravets et al., 2016; Virreira Winter et al., 2011) and *C. trachomatis* inclusions (Figure 29, Lindenberg et al., submitted). Using a sensitive cLSM set up, it's morphology was observed to be more diffuse and slightly spatially distanced from the PCV membrane. Also the morphology of mGBP5 was always distinct from other recruited 'tightly accumulated' mGBPs. MGBP5 could be characterized as having a 'rough' shape as defined by Martens et al. who also correlated this morphology of mGBPs with closely apposed LC3, indicative of autophagy (Martens et al., 2005). The precise role of mGBP5 in these infection models should be investigated in more detail in the future.

Different infection models using *Francisella* spp. or *Salmonella* spp.as pathogens to probe cell autonomous immune responses found a role for mGBPs in bacterial rupture. The mGBPs targeted IRGB10 to cytoplasmic bacteria, compromising bacterial structural integrity and causing cytosolic release of pathogen ligands which activated the DNA-sensing AIM2 inflammasome leading to subsequent caspase-11 cleavage (Man et al., 2016a; Man et al., 2015; Man et al., 2016c; Meunier and Broz, 2016; Meunier et al., 2014; Meunier et al., 2015; Rupper and Cardelli, 2008). It was shown that occasionally mycobacteria are released into the cytosol (van der Wel et al., 2007). These examples suggest that, in principle, a potential role for mGBP-mediated bacterium lysis and inflammasome activation could exist in mycobacterium infection. Whether mGBP5 is an effector involved in this process remains to be explored.

The human ortholog of mGBP5 appears to be hGBP5. HGBP5 was observed to be induced in a cohort of tuberculosis patients (Berry et al., 2010; Satproedprai et al., 2015), which resulted in hGBP5 being defined as a biomarker for tuberculosis (Laux da Costa et al., 2015). This also suggests that an immune function in mycobacterial disease could

exist for hGBP5. Furthermore, hGBP5 was shown to be regulated by IFNγ in uterine microvascular endothelial cells (Kitaya et al., 2007), classically interferon-γ-activated macrophages (Fujiwara et al., 2016; Haudek-Prinz et al., 2012) and in specific tumor tissues (Britzen-Laurent et al., 2016; Cui et al., 2014; Fellenberg et al., 2004; Friedman et al., 2016; Wehner and Herrmann, 2010). Such regulation implies that in humans, hGBP5 might play an immune-modulatory role. Surprisingly, hGBP5 also mediates antiviral responses during influenza A virus infection (Feng et al., 2017), and can target HIV-1 envelope glycoproteins (Hotter et al., 2017; Krapp et al., 2016; McLaren et al., 2015). HGBP5 is also induced in patients with chronic active Epstein-Barr virus infection (Ito et al., 2008). Additionally, in porcines a role of GBP5 was found in viral immunity against Porcine Respiratory and Reproductive Syndrome virus (PRRSV) infection was described, which revealed three differentially spliced transcripts for porcine GBP5 (Koltes et al., 2015). These observations could indicate that hGBP5 has distinct roles in the defence against viral infections, which were not addressed in this study.

5.4 Future perspectives

This study compared mGBP recruitment to *C. trachomatis* and *T. gondii* PCVs extensively and thereby revealed a specific pattern in recruitment of mGBPs to distinct pathogens. This diverse action is remarkable, since these proteins are highly homologous. These differences might, in part, be contributed to kinetics of GTPase hydrolysis which is influenced by loops proximal to the G-domain, or by selected pre-assembly in cytosolic VLS. Furthermore it was shown that colocalization at the chlamydial inclusion is authentic, fast and transient for mGBP2 and mGBP9. Thus, this study displays the potential of mGBPs encoded on murine chromosome 5 (particularly mGBP9), which have up till now, not been assigned a role in pathogen defence. In the future, several projects could be proposed to develop our understanding of the action of mGBPs during infections.

5.4.1 Defining the function and prerequisites of mGBP9 recruitment during chlamydia infection

Although a profound phenotype of mGBP9 in chlamydial infection could be shown, the mechanism and biological relevance of this observation could not be uncovered in this study. Therefore elucidating these questions remains a major opportunity for further experimentation.

Future efforts could focus on prerequisites for mGBP9 to translocate to the chlamydia inclusion membrane. For example, evaluation of the necessity of nucleotide binding and hydrolysis for mGBP9 colocalization at chlamydial inclusions by generating point mutants of the G-domain could reveal how mGBP9 relocates to the chlamydia inclusion; mirroring the approach performed previously on mGBP2 in *T. gondii* infection (Kravets et al., 2012). Also, mGBP9 lacks an isoprenylation motif. It is feasible that mGBP9, like mGBP3, interacts with one or several other mGBPs which do contain an isoprenylation motif. It would be interesting to see if mGBP9 is pre-assembled in VLS, similar to mGBP3, which is pre-assembled with mGBP2. The hypothesis, whether mGBP9 can interact with other mGBPs, and potentially IRGs, can be addressed by using multiparameter fluorescence image spectroscopy, and/or co-immunoprecipitation pull down assays combined with mass spectroscopy. If such interactions are found, these can be further illustrated by live cell imaging of infected cells that express two distinctly labelled mGBPs. If no interaction partners are found, mGBP9 could relocate independently and subsequently localize solely at the PCV membrane with other mGBPs. In that case, in depth analysis of the mGBP9 C-terminus might yield membrane-

interacting moieties, e.g. mGBP9 has been predicted to carry a Nop25 super family motif (See Table 1), which subsequently could be mutated to proof its necessity.

To address the biological function of mGBP9 in chlamydia infection further experimentation should assess chlamydial growth by measuring in parallel: the genome equivalents, infectious progeny, inclusions per frame, average inclusion volume and chlamydial nuclei size, in order to discriminate bacteriostatic from bactericidal and chlamydial persistence inducing effects in mGBP deficient cell lines. Additionally, inclusion rupture could be visualised by transfecting of transducing a cytoplasmic marker tagged with a fluorescent protein, which does not limit resolution of mCherry- or GFP-tagged mGBPs. Fluorescent tags that could be considered are blue mTagBFP (Subach et al., 2011) or far-red mPlum (Yoon et al., 2016). If PCV membrane permeabilization or rupture occurs, these cytosolic markers can diffuse into the inclusion lumen (according to Klümpers, 2013; Kravets et al., 2016). Mild effects on chlamydial growth could be quantified by analysing large numbers of cells, using FACS analysis (Haridas et al., 2017).

A systematic approach to evaluate biological relevance is *in vivo* infection of mice deficient for a single, or for multiple mGBPs. Towards this purpose, an mGBP9-deficient mouse could be developed using challenging conventional or novel CRISPR/Cas9 technologies (Joung et al., 2017; Peng et al., 2016; Singh et al., 2017).

If proceeding research, focusses on mGBP action early after chlamydial invasion, it could be considered to visualize potential interactions with a recently developed *C. trachomatis* strain p2TK2-SW2 IncDProm-RSGFP-IncDterm (Agaisse and Derre, 2013), rather than *C. trachomatis* pGFP::SW2. In addition, imaging technologies with higher resolution or sensitivity should be considered.

Overall, further investigation of mGBP9 function will provide an opportunity for the research group to firmly establish the relevance of mGBPs on murine chromosome 5. Thus making an argument for the diverse action among mGBPs, and positioning this protein family as a central modulator of cell autonomous immune responses.

5.4.2 A potential role for mGBP5 in mycobacterial infection

Amongst the mGBPs, the member showing the most distinct morphological distribution is mGBP5. MGBP5 displays a cytosolic distribution and upon infection accumulates at PCVs with a ‘rough’ morphology; compared to pre-assembly in VLS and tight

recruitment. For this reason, it is interesting to further examine mGBP5 to explore differences in action compared to other mGBPs. This study did not find a phenotype *ex vivo* in mGBP5-deficient BMDMs stimulated with IFNγ. Future studies can consider generation of self-renewing macrophage cell lines, to better represent the macrophage heterogeneity during infection assays. Since, other publications have proposed a role for mGBP5 in mycobacterial infection, a collaboration was forged with the research group of Prof. Dr. Stefan Kaufmann at the Max Planck Institute for Infection Biology in Berlin. This collaboration partner repeated mycobacterial kill assays using BMDMs. They confirmed that no differences could be observed in mycobacterial growth in mGBP-deficient macrophages. However, this laboratory has the ability to perform *in vivo* assays under biosafety level 3 conditions. Therefore, mice deficient for mGBP2, mGBP5 and wild type controls were transported to Berlin. To date, a single round of attenuated BCG, and a single round of virulent *M. tuberculosis* H37Rv infections have been performed. These studies yielded interesting preliminary results, but need to be repeated in the near future.

5.4.3 Roles for mGBPs in other infections

This study found a specific pattern in recruitment of mGBPs to distinct pathogens. Different cytosolic or vacuolar pathogens, for which mGBP action is conceivable, could be similarly analysed for mGBP colocalization and subsequently pathogen fitness. An example from a distinct kingdom, is the poxvirus *Vaccinia* and the attenuated modified-vaccinia-ankara-virus strain (MVA). *Vaccinia* replicates in lipid-lined viral factories, within the host cell cytoplasm and might therefore be potential target of mGBP's. Using the previously created NIH/3T3 fibroblast cell lines, evaluation of mGBPs colocalization with a pathogen like *Vaccinia*, could be speedily evaluated. Subsequently, growth assays like colony or plaque forming units can be performed in the same fibroblasts, to compare mGBP-overexpressing cells with wild type and mGBP-deficient fibroblasts. MGBP deficient fibroblasts could be obtained through CRISPR/Cas9-mediated deletion. Currently, an mGBP9-deficient fibroblasts cell line is being generated within our research group. Using this approach, utilizing the panel of mGBP-overexpressing and prospective mGBP-deficient fibroblasts, an *in vitro* workflow could be established in which any pathogen that readily grows in fibroblasts can be tested. Those pathogens that are affected by mGBPs will be selected for further investigation to elucidate the mechanism of mGBP action. By studying different infection models, additional insights will be gained into mGBP mediated host immunity.

Literature

Abdelrahman, Y.M., and Belland, R.J. (2005). The chlamydial developmental cycle. FEMS microbiology reviews *29*, 949-959.

Abdelsamed, H., Peters, J., and Byrne, G.I. (2013). Genetic variation in Chlamydia trachomatis and their hosts: impact on disease severity and tissue tropism. Future microbiology *8*, 1129-1146.

Abdul-Sater, A.A., Koo, E., Hacker, G., and Ojcius, D.M. (2009). Inflammasome-dependent caspase-1 activation in cervical epithelial cells stimulates growth of the intracellular pathogen Chlamydia trachomatis. The Journal of biological chemistry *284*, 26789-26796.

Abdul-Sater, A.A., Said-Sadier, N., Lam, V.M., Singh, B., Pettengill, M.A., Soares, F., Tattoli, I., Lipinski, S., Girardin, S.E., Rosenstiel, P.*, et al.* (2010a). Enhancement of reactive oxygen species production and chlamydial infection by the mitochondrial Nod-like family member NLRX1. The Journal of biological chemistry *285*, 41637-41645.

Abdul-Sater, A.A., Said-Sadier, N., Padilla, E.V., and Ojcius, D.M. (2010b). Chlamydial infection of monocytes stimulates IL-1beta secretion through activation of the NLRP3 inflammasome. Microbes and infection *12*, 652-661.

Abdullah, N., Balakumari, M., and Sau, A.K. (2010). Dimerization and its role in GMP formation by human guanylate binding proteins. Biophysical journal *99*, 2235-2244.

Abi Abdallah, D.S., and Denkers, E.Y. (2012). Neutrophils cast extracellular traps in response to protozoan parasites. Frontiers in immunology *3*, 382.

Aeberhard, L., Banhart, S., Fischer, M., Jehmlich, N., Rose, L., Koch, S., Laue, M., Renard, B.Y., Schmidt, F., and Heuer, D. (2015). The Proteome of the Isolated Chlamydia trachomatis Containing Vacuole Reveals a Complex Trafficking Platform Enriched for Retromer Components. PLoS pathogens *11*, e1004883.

Agaisse, H., and Derre, I. (2013). A C. trachomatis cloning vector and the generation of C. trachomatis strains expressing fluorescent proteins under the control of a C. trachomatis promoter. PloS one *8*, e57090.

Al-Zeer, M.A., Al-Younes, H.M., Braun, P.R., Zerrahn, J., and Meyer, T.F. (2009). IFN-gamma-inducible Irga6 mediates host resistance against Chlamydia trachomatis via autophagy. PloS one *4*, e4588.

Al-Zeer, M.A., Al-Younes, H.M., Lauster, D., Abu Lubad, M., and Meyer, T.F. (2013). Autophagy restricts Chlamydia trachomatis growth in human macrophages via IFNG-inducible guanylate binding proteins. Autophagy *9*, 50-62.

Alaganan, A., Fentress, S.J., Tang, K., Wang, Q., and Sibley, L.D. (2014). Toxoplasma GRA7 effector increases turnover of immunity-related GTPases and contributes to acute virulence in the mouse. Proceedings of the National Academy of Sciences of the United States of America *111*, 1126-1131.

Alberts, B., Johnson, A., Lewis, J., Morgan, D., Raff, M., Roberts, K., and Walter, P. (2014). Molecular Biology of the Cell (6th edition) (711 T hird Avenue, 8th floor, New York, NY 1 0017, USA: Garland Science (Taylor & Francis Group, LLC)).

Alonso, S., Pethe, K., Russell, D.G., and Purdy, G.E. (2007). Lysosomal killing of Mycobacterium mediated by ubiquitin-derived peptides is enhanced by autophagy. Proceedings of the National Academy of Sciences of the United States of America *104*, 6031-6036.

Amaral, E.P., Lasunskaia, E.B., and D'Imperio-Lima, M.R. (2016). Innate immunity in tuberculosis: how the sensing of mycobacteria and tissue damage modulates macrophage death. Microbes and infection *18*, 11-20.

Andrade, W.A., Souza Mdo, C., Ramos-Martinez, E., Nagpal, K., Dutra, M.S., Melo, M.B., Bartholomeu, D.C., Ghosh, S., Golenbock, D.T., and Gazzinelli, R.T. (2013). Combined action of nucleic acid-sensing Toll-like receptors and TLR11/TLR12 heterodimers imparts resistance to Toxoplasma gondii in mice. Cell host & microbe *13*, 42-53.

Antczak, M., Dzitko, K., and Dlugonska, H. (2016). Human toxoplasmosis-Searching for novel chemotherapeutics. Biomedicine & pharmacotherapy = Biomedecine & pharmacotherapie *82*, 677-684.

Aspenstrom, P. (2014). BAR domain proteins regulate Rho GTPase signaling. Small GTPases *5*, 7.

Asundi, V.K., Stahl, R.C., Showalter, L., Conner, K.J., and Carey, D.J. (1994). Molecular cloning and characterization of an isoprenylated 67 kDa protein. Biochimica et biophysica acta *1217*, 257-265.

Awuh, J.A., and Flo, T.H. (2017). Molecular basis of mycobacterial survival in macrophages. Cellular and molecular life sciences : CMLS *74*, 1625-1648.

Balasubramanian, S., Messmer-Blust, A.F., Jeyaratnam, J.A., and Vestal, D.J. (2011). Role of GTP binding, isoprenylation, and the C-terminal alpha-helices in the inhibition of cell spreading by the interferon-induced GTPase, mouse guanylate-binding protein-2. Journal of interferon & cytokine research : the official journal of the International Society for Interferon and Cytokine Research *31*, 291-298.

Bastidas, R.J., Elwell, C.A., Engel, J.N., and Valdivia, R.H. (2013). Chlamydial intracellular survival strategies. Cold Spring Harbor perspectives in medicine *3*, a010256.

Bastidas, R.J., and Valdivia, R.H. (2016). Emancipating Chlamydia: Advances in the Genetic Manipulation of a Recalcitrant Intracellular Pathogen. Microbiology and molecular biology reviews : MMBR *80*, 411-427.

Behar, S.M., Divangahi, M., and Remold, H.G. (2010). Evasion of innate immunity by Mycobacterium tuberculosis: is death an exit strategy? Nature reviews Microbiology *8*, 668-674.

Behnke, M.S., Dubey, J.P., and Sibley, L.D. (2016). Genetic Mapping of Pathogenesis Determinants in Toxoplasma gondii. Annual review of microbiology *70*, 63-81.

Bekpen, C., Hunn, J.P., Rohde, C., Parvanova, I., Guethlein, L., Dunn, D.M., Glowalla, E., Leptin, M., and Howard, J.C. (2005). The interferon-inducible p47 (IRG) GTPases in vertebrates: loss of the cell autonomous resistance mechanism in the human lineage. Genome biology *6*, R92.

Bekpen, C., Marques-Bonet, T., Alkan, C., Antonacci, F., Leogrande, M.B., Ventura, M., Kidd, J.M., Siswara, P., Howard, J.C., and Eichler, E.E. (2009). Death and resurrection of the human IRGM gene. PLoS genetics *5*, e1000403.

Bekpen, C., Xavier, R.J., and Eichler, E.E. (2010). Human IRGM gene "to be or not to be". Seminars in immunopathology *32*, 437-444.

Belland, R.J., Zhong, G., Crane, D.D., Hogan, D., Sturdevant, D., Sharma, J., Beatty, W.L., and Caldwell, H.D. (2003). Genomic transcriptional profiling of the developmental cycle of Chlamydia trachomatis. Proceedings of the National Academy of Sciences of the United States of America *100*, 8478-8483.

Bernstein-Hanley, I., Coers, J., Balsara, Z.R., Taylor, G.A., Starnbach, M.N., and Dietrich, W.F. (2006). The p47 GTPases Igtp and Irgb10 map to the Chlamydia trachomatis susceptibility locus Ctrq-3 and mediate cellular resistance in mice. Proceedings of the National Academy of Sciences of the United States of America *103*, 14092-14097.

Berry, M.P., Graham, C.M., McNab, F.W., Xu, Z., Bloch, S.A., Oni, T., Wilkinson, K.A., Banchereau, R., Skinner, J., Wilkinson, R.J., *et al.* (2010). An interferon-inducible neutrophil-driven blood transcriptional signature in human tuberculosis. Nature *466*, 973-977.

Bestebroer, J., V'Kovski, P., Mauthe, M., and Reggiori, F. (2013). Hidden behind autophagy: the unconventional roles of ATG proteins. Traffic *14*, 1029-1041.

Betts, H.J., Wolf, K., and Fields, K.A. (2009). Effector protein modulation of host cells: examples in the Chlamydia spp. arsenal. Current opinion in microbiology *12*, 81-87.

Beuter-Gunia, C. (2008). Identifizierung und Charakterisierung von IFN regulierten Effektormolekülen (mGBP7, SSPII) in der antimikrobiellen Immunantwort. In Mathematisch-Naturwissenschaftlichen Fakultät (Heinrich-Heine-Universität Düsseldorf).

Beutler, B., Jiang, Z., Georgel, P., Crozat, K., Croker, B., Rutschmann, S., Du, X., and Hoebe, K. (2006). Genetic analysis of host resistance: Toll-like receptor signaling and immunity at large. Annual review of immunology *24*, 353-389.

Birnboim, H.C., and Doly, J. (1979). A rapid alkaline extraction procedure for screening recombinant plasmid DNA. Nucleic acids research *7*, 1513-1523.

Blader, I.J., and Koshy, A.A. (2014). Toxoplasma gondii development of its replicative niche: in its host cell and beyond. Eukaryotic cell *13*, 965-976.

Blanco, P., Palucka, A.K., Pascual, V., and Banchereau, J. (2008). Dendritic cells and cytokines in human inflammatory and autoimmune diseases. Cytokine & growth factor reviews *19*, 41-52.

Bliss, S.K., Butcher, B.A., and Denkers, E.Y. (2000). Rapid recruitment of neutrophils containing prestored IL-12 during microbial infection. Journal of immunology *165*, 4515-4521.

Bloom, B.R., and Modlin, R.L. (2016). Mechanisms of Defense against Intracellular Pathogens Mediated by Human Macrophages. Microbiology spectrum *4*.

Blouin, C., Butt, D., and Roger, A.J. (2004). Rapid evolution in conformational space: a study of loop regions in a ubiquitous GTP binding domain. Protein science : a publication of the Protein Society *13*, 608-616.

Boehm, U., Guethlein, L., Klamp, T., Ozbek, K., Schaub, A., Futterer, A., Pfeffer, K., and Howard, J.C. (1998). Two families of GTPases dominate the complex cellular response to IFN-gamma. Journal of immunology *161*, 6715-6723.

Boehm, U., Klamp, T., Groot, M., and Howard, J.C. (1997). Cellular responses to interferon-gamma. Annual review of immunology *15*, 749-795.

Bogdan, C. (2015). Nitric oxide synthase in innate and adaptive immunity: an update. Trends in immunology *36*, 161-178.

Bogunovic, D., Boisson-Dupuis, S., and Casanova, J.L. (2013). ISG15: leading a double life as a secreted molecule. Experimental & molecular medicine *45*, e18.

Bohme, L., and Rudel, T. (2009). Host cell death machinery as a target for bacterial pathogens. Microbes and infection *11*, 1063-1070.

Bonelli, M., Shih, H.Y., Hirahara, K., Singelton, K., Laurence, A., Poholek, A., Hand, T., Mikami, Y., Vahedi, G., Kanno, Y., *et al.* (2014). Helper T cell plasticity: impact of extrinsic and intrinsic signals on transcriptomes and epigenomes. Current topics in microbiology and immunology *381*, 279-326.

Borges, V., and Gomes, J.P. (2015). Deep comparative genomics among Chlamydia trachomatis lymphogranuloma venereum isolates highlights genes potentially involved in pathoadaptation. Infection, genetics and evolution : journal of molecular epidemiology and evolutionary genetics in infectious diseases *32*, 74-88.

Borges, V., Pinheiro, M., Antelo, M., Sampaio, D.A., Vieira, L., Ferreira, R., Nunes, A., Almeida, F., Mota, L.J., Borrego, M.J., *et al.* (2015). Chlamydia trachomatis In Vivo to In Vitro Transition Reveals Mechanisms of Phase Variation and Down-Regulation of Virulence Factors. PloS one *10*, e0133420.

Bougdour, A., Durandau, E., Brenier-Pinchart, M.P., Ortet, P., Barakat, M., Kieffer, S., Curt-Varesano, A., Curt-Bertini, R.L., Bastien, O., Coute, Y., *et al.* (2013). Host cell subversion by Toxoplasma GRA16, an exported dense granule protein that targets the host cell nucleus and alters gene expression. Cell host & microbe *13*, 489-500.

Bougdour, A., Tardieux, I., and Hakimi, M.A. (2014). Toxoplasma exports dense granule proteins beyond the vacuole to the host cell nucleus and rewires the host genome expression. Cellular microbiology *16*, 334-343.

Bourne, H.R. (1995). GTPases: a family of molecular switches and clocks. Philosophical transactions of the Royal Society of London Series B, Biological sciences *349*, 283-289.

Bourne, H.R., Sanders, D.A., and McCormick, F. (1990). The GTPase superfamily: a conserved switch for diverse cell functions. Nature *348*, 125-132.

Bourne, H.R., Sanders, D.A., and McCormick, F. (1991). The GTPase superfamily: conserved structure and molecular mechanism. Nature *349*, 117-127.

Boyle, K.B., and Randow, F. (2013). The role of 'eat-me' signals and autophagy cargo receptors in innate immunity. Current opinion in microbiology *16*, 339-348.

Bradley, P.J., and Sibley, L.D. (2007). Rhoptries: an arsenal of secreted virulence factors. Current opinion in microbiology *10*, 582-587.

Braun, L., Brenier-Pinchart, M.P., Yogavel, M., Curt-Varesano, A., Curt-Bertini, R.L., Hussain, T., Kieffer-Jaquinod, S., Coute, Y., Pelloux, H., Tardieux, I., *et al.* (2013). A Toxoplasma dense granule protein, GRA24, modulates the early immune response to infection by promoting a direct and sustained host p38 MAPK activation. The Journal of experimental medicine *210*, 2071-2086.

Briken, V. (2013). Mycobacterium tuberculosis genes involved in regulation of host cell death. Advances in experimental medicine and biology *783*, 93-102.

Briken, V., Ahlbrand, S.E., and Shah, S. (2013). Mycobacterium tuberculosis and the host cell inflammasome: a complex relationship. Frontiers in cellular and infection microbiology *3*, 62.

Britzen-Laurent, N., Bauer, M., Berton, V., Fischer, N., Syguda, A., Reipschlager, S., Naschberger, E., Herrmann, C., and Sturzl, M. (2010). Intracellular trafficking of guanylate-binding proteins is regulated by heterodimerization in a hierarchical manner. PloS one *5*, e14246.

Britzen-Laurent, N., Herrmann, C., Naschberger, E., Croner, R.S., and Sturzl, M. (2016). Pathophysiological role of guanylate-binding proteins in gastrointestinal diseases. World journal of gastroenterology *22*, 6434-6443.

Broz, P. (2016). Immune Response: Intracellular pathogens under attack. eLife *5*.

Broz, P., and Dixit, V.M. (2016). Inflammasomes: mechanism of assembly, regulation and signalling. Nature reviews Immunology *16*, 407-420.

Cadwell, K. (2016). Crosstalk between autophagy and inflammatory signalling pathways: balancing defence and homeostasis. Nature reviews Immunology *16*, 661-675.

Caffrey, D.R., and Fitzgerald, K.A. (2012). Immunology. Select inflammasome assembly. Science *336*, 420-421.

Caldwell, H.D., Wood, H., Crane, D., Bailey, R., Jones, R.B., Mabey, D., Maclean, I., Mohammed, Z., Peeling, R., Roshick, C., *et al.* (2003). Polymorphisms in Chlamydia trachomatis tryptophan synthase genes differentiate between genital and ocular isolates. The Journal of clinical investigation *111*, 1757-1769.

Cannella, D., Brenier-Pinchart, M.P., Braun, L., van Rooyen, J.M., Bougdour, A., Bastien, O., Behnke, M.S., Curt, R.L., Curt, A., Saeij, J.P., *et al.* (2014). miR-146a and miR-155 delineate a MicroRNA fingerprint associated with Toxoplasma persistence in the host brain. Cell reports *6*, 928-937.

Cardoso, C.M., Jordao, L., and Vieira, O.V. (2010). Rab10 regulates phagosome maturation and its overexpression rescues Mycobacterium-containing phagosomes maturation. Traffic *11*, 221-235.

Carruthers, V.B., and Tomley, F.M. (2008). Microneme proteins in apicomplexans. Sub-cellular biochemistry *47*, 33-45.

Carter, C.C., Gorbacheva, V.Y., and Vestal, D.J. (2005). Inhibition of VSV and EMCV replication by the interferon-induced GTPase, mGBP-2: differential requirement for wild-type GTP binding domain. Archives of virology *150*, 1213-1220.

Chamberlain, L.M., Holt-Casper, D., Gonzalez-Juarrero, M., and Grainger, D.W. (2015). Extended culture of macrophages from different sources and maturation results in a common M2 phenotype. Journal of biomedical materials research Part A *103*, 2864-2874.

Chauhan, S., Mandell, M.A., and Deretic, V. (2015). IRGM governs the core autophagy machinery to conduct antimicrobial defense. Molecular cell *58*, 507-521.

Chen, K.W., and Schroder, K. (2013). Antimicrobial functions of inflammasomes. Current opinion in microbiology *16*, 311-318.

Cheng, Y.S., Colonno, R.J., and Yin, F.H. (1983). Interferon induction of fibroblast proteins with guanylate binding activity. The Journal of biological chemistry *258*, 7746-7750.

Cheng, Y.S., Patterson, C.E., and Staeheli, P. (1991). Interferon-induced guanylate-binding proteins lack an N(T)KXD consensus motif and bind GMP in addition to GDP and GTP. Molecular and cellular biology *11*, 4717-4725.

Choi, J., Biering, S.B., and Hwang, S. (2016). Quo vadis? Interferon-inducible GTPases go to their target membranes via the LC3-conjugation system of autophagy. Small GTPases, 1-9.

Choi, J., Park, S., Biering, S.B., Selleck, E., Liu, C.Y., Zhang, X., Fujita, N., Saitoh, T., Akira, S., Yoshimori, T., *et al.* (2014). The parasitophorous vacuole membrane of Toxoplasma gondii is targeted for disruption by ubiquitin-like conjugation systems of autophagy. Immunity *40*, 924-935.

Christian, D.A., Koshy, A.A., Reuter, M.A., Betts, M.R., Boothroyd, J.C., and Hunter, C.A. (2014). Use of transgenic parasites and host reporters to dissect events that promote interleukin-12 production during toxoplasmosis. Infection and immunity *82*, 4056-4067.

Cianciotto, N.P., and White, R.C. (2017). Expanding Role of Type II Secretion in Bacterial Pathogenesis and Beyond. Infection and immunity *85*.

Claessen, J.H., Witte, M.D., Yoder, N.C., Zhu, A.Y., Spooner, E., and Ploegh, H.L. (2013). Catch-and-release probes applied to semi-intact cells reveal ubiquitin-specific protease expression in Chlamydia trachomatis infection. Chembiochem : a European journal of chemical biology *14*, 343-352.

Clarke, I.N. (2011). Evolution of Chlamydia trachomatis. Annals of the New York Academy of Sciences *1230*, E11-18.

Clough, B., and Frickel, E.M. (2017). The Toxoplasma Parasitophorous Vacuole: An Evolving Host-Parasite Frontier. Trends in parasitology.

Cocchiaro, J.L., Kumar, Y., Fischer, E.R., Hackstadt, T., and Valdivia, R.H. (2008). Cytoplasmic lipid droplets are translocated into the lumen of the Chlamydia trachomatis parasitophorous vacuole. Proceedings of the National Academy of Sciences of the United States of America *105*, 9379-9384.

Cocchiaro, J.L., and Valdivia, R.H. (2009). New insights into Chlamydia intracellular survival mechanisms. Cellular microbiology *11*, 1571-1578.

Coers, J. (2013). Self and non-self discrimination of intracellular membranes by the innate immune system. PLoS pathogens *9*, e1003538.

Coers, J., Bernstein-Hanley, I., Grotsky, D., Parvanova, I., Howard, J.C., Taylor, G.A., Dietrich, W.F., and Starnbach, M.N. (2008). Chlamydia muridarum evades growth restriction by the IFN-gamma-inducible host resistance factor Irgb10. Journal of immunology *180*, 6237-6245.

Coers, J., Gondek, D.C., Olive, A.J., Rohlfing, A., Taylor, G.A., and Starnbach, M.N. (2011). Compensatory T cell responses in IRG-deficient mice prevent sustained Chlamydia trachomatis infections. PLoS pathogens *7*, e1001346.

Coers, J., and Haldar, A.K. (2015). Ubiquitination of pathogen-containing vacuoles promotes host defense to Chlamydia trachomatis and Toxoplasma gondii. Communicative & integrative biology *8*, e1115163.

Coll, R.C., O'Neill, L., and Schroder, K. (2016). Questions and controversies in innate immune research: what is the physiological role of NLRP3? Cell death discovery *2*, 16019.

Collingro, A., Tischler, P., Weinmaier, T., Penz, T., Heinz, E., Brunham, R.C., Read, T.D., Bavoil, P.M., Sachse, K., Kahane, S., *et al.* (2011). Unity in variety--the pan-genome of the Chlamydiae. Molecular biology and evolution *28*, 3253-3270.

Colonne, P.M., Winchell, C.G., and Voth, D.E. (2016). Hijacking Host Cell Highways: Manipulation of the Host Actin Cytoskeleton by Obligate Intracellular Bacterial Pathogens. Frontiers in cellular and infection microbiology *6*, 107.

Conrad, A.T., Yang, Z., Ojcius, D., and Zhong, G. (2013). A path forward for the chlamydial virulence factor CPAF. Microbes and infection *15*, 1026-1032.

Cosse, M.M., Hayward, R.D., and Subtil, A. (2016). One Face of Chlamydia trachomatis: The Infectious Elementary Body. Current topics in microbiology and immunology.

Crawford, C.L. (2015). The Epithelioid Cell in Tuberculosis is Secretory and Not a Macrophage. The Journal of infectious diseases *212*, 1172-1173.

Cui, J., Chen, Y., Wang, H.Y., and Wang, R.F. (2014). Mechanisms and pathways of innate immune activation and regulation in health and cancer. Human vaccines & immunotherapeutics *10*, 3270-3285.

Da Costa, C.U., Wantia, N., Kirschning, C.J., Busch, D.H., Rodriguez, N., Wagner, H., and Miethke, T. (2004). Heat shock protein 60 from Chlamydia pneumoniae elicits an unusual set of inflammatory responses via Toll-like receptor 2 and 4 in vivo. European journal of immunology *34*, 2874-2884.

Damiani, M.T., Gambarte Tudela, J., and Capmany, A. (2014). Targeting eukaryotic Rab proteins: a smart strategy for chlamydial survival and replication. Cellular microbiology *16*, 1329-1338.

Darnell, J.E., Jr. (1997). STATs and gene regulation. Science *277*, 1630-1635.

Daugherty, M.D., and Malik, H.S. (2012). Rules of engagement: molecular insights from host-virus arms races. Annual review of genetics *46*, 677-700.

Daumke, O., and Praefcke, G.J. (2016). Invited review: Mechanisms of GTP hydrolysis and conformational transitions in the dynamin superfamily. Biopolymers *105*, 580-593.

de Vasconcelos, N.M., Van Opdenbosch, N., and Lamkanfi, M. (2016). Inflammasomes as polyvalent cell death platforms. Cellular and molecular life sciences : CMLS *73*, 2335-2347.

Deckert-Schluter, M., Rang, A., Weiner, D., Huang, S., Wiestler, O.D., Hof, H., and Schluter, D. (1996). Interferon-gamma receptor-deficiency renders mice highly susceptible to toxoplasmosis by decreased macrophage activation. Laboratory investigation; a journal of technical methods and pathology *75*, 827-841.

Degrandi, D., Konermann, C., Beuter-Gunia, C., Kresse, A., Wurthner, J., Kurig, S., Beer, S., and Pfeffer, K. (2007). Extensive characterization of IFN-induced GTPases mGBP1 to mGBP10 involved in host defense. Journal of immunology *179*, 7729-7740.

Degrandi, D., Kravets, E., Konermann, C., Beuter-Gunia, C., Klumpers, V., Lahme, S., Wischmann, E., Mausberg, A.K., Beer-Hammer, S., and Pfeffer, K. (2013). Murine guanylate binding protein 2 (mGBP2) controls Toxoplasma gondii replication. Proceedings of the National Academy of Sciences of the United States of America *110*, 294-299.

Delevoye, C., Nilges, M., Dehoux, P., Paumet, F., Perrinet, S., Dautry-Varsat, A., and Subtil, A. (2008). SNARE protein mimicry by an intracellular bacterium. PLoS pathogens *4*, e1000022.

Denkers, E.Y., Bzik, D.J., Fox, B.A., and Butcher, B.A. (2012). An inside job: hacking into Janus kinase/signal transducer and activator of transcription signaling cascades by the intracellular protozoan Toxoplasma gondii. Infection and immunity *80*, 476-482.

Derbigny, W.A., Shobe, L.R., Kamran, J.C., Toomey, K.S., and Ofner, S. (2012). Identifying a role for Toll-like receptor 3 in the innate immune response to Chlamydia muridarum infection in murine oviduct epithelial cells. Infection and immunity *80*, 254-265.

Deretic, V. (2012). Autophagy as an innate immunity paradigm: expanding the scope and repertoire of pattern recognition receptors. Current opinion in immunology *24*, 21-31.

Deretic, V. (2016). Autophagy in leukocytes and other cells: mechanisms, subsystem organization, selectivity, and links to innate immunity. Journal of leukocyte biology *100*, 969-978.

Deretic, V., Delgado, M., Vergne, I., Master, S., De Haro, S., Ponpuak, M., and Singh, S. (2009). Autophagy in immunity against mycobacterium tuberculosis: a model system to dissect immunological roles of autophagy. Current topics in microbiology and immunology *335*, 169-188.

Deretic, V., Saitoh, T., and Akira, S. (2013). Autophagy in infection, inflammation and immunity. Nature reviews Immunology *13*, 722-737.

Derouin, F., Pelloux, H., and Parasitology, E.S.G.o.C. (2008). Prevention of toxoplasmosis in transplant patients. Clinical microbiology and infection : the official publication of the European Society of Clinical Microbiology and Infectious Diseases *14*, 1089-1101.

Desai, M., Fang, R., and Sun, J. (2015). The role of autophagy in microbial infection and immunity. ImmunoTargets and therapy *4*, 13-26.

Detels, R., Green, A.M., Klausner, J.D., Katzenstein, D., Gaydos, C., Handsfield, H., Pequegnat, W., Mayer, K., Hartwell, T.D., and Quinn, T.C. (2011). The incidence and correlates of symptomatic and asymptomatic Chlamydia trachomatis and Neisseria gonorrhoeae infections in selected populations in five countries. Sexually transmitted diseases *38*, 503-509.

Di Francesco, A., Favaroni, A., and Donati, M. (2013). Host defense peptides: general overview and an update on their activity against Chlamydia spp. Expert review of anti-infective therapy *11*, 1215-1224.

Di Russo Case, E., and Samuel, J.E. (2016). Contrasting Lifestyles Within the Host Cell. Microbiology spectrum *4*.

Diamond, M.S., and Farzan, M. (2013). The broad-spectrum antiviral functions of IFIT and IFITM proteins. Nature reviews Immunology *13*, 46-57.

Diebel, N.D., Jr., and Williams, J.K. (1995). Chlamydia trachomatis. A trojan horse. The Journal of the Florida Medical Association *82*, 411-414.

Doherty, M., Wallis, R.S., Zumla, A., and group, W.H.-T.D.R.E.C.j.e.c. (2009). Biomarkers for tuberculosis disease status and diagnosis. Current opinion in pulmonary medicine *15*, 181-187.

Dorhoi, A., Feng, Y., and Kaufmann, S.H. (2015). Reply to Crawford. The Journal of infectious diseases *212*, 1173-1174.

Dorhoi, A., and Kaufmann, S.H. (2015). Versatile myeloid cell subsets contribute to tuberculosis-associated inflammation. European journal of immunology *45*, 2191-2202.

Dortet, L., Mostowy, S., Samba-Louaka, A., Gouin, E., Nahori, M.A., Wiemer, E.A., Dussurget, O., and Cossart, P. (2011). Recruitment of the major vault protein by InlK: a Listeria monocytogenes strategy to avoid autophagy. PLoS pathogens *7*, e1002168.

Dostert, C., Meylan, E., and Tschopp, J. (2008). Intracellular pattern-recognition receptors. Advanced drug delivery reviews *60*, 830-840.

Drewry, L.L., and Sibley, L.D. (2015). Toxoplasma Actin Is Required for Efficient Host Cell Invasion. mBio *6*, e00557.

Dubey, J.P. (2009). History of the discovery of the life cycle of Toxoplasma gondii. International journal for parasitology *39*, 877-882.

Dubey, J.P., Lindsay, D.S., and Speer, C.A. (1998). Structures of Toxoplasma gondii tachyzoites, bradyzoites, and sporozoites and biology and development of tissue cysts. Clinical microbiology reviews *11*, 267-299.

Dubey, J.P., Miller, N.L., and Frenkel, J.K. (1970). Toxoplasma gondii life cycle in cats. Journal of the American Veterinary Medical Association *157*, 1767-1770.

Dumoux, M., and Hayward, R.D. (2016). Membrane contact sites between pathogen-containing compartments and host organelles. Biochimica et biophysica acta *1861*, 895-899.

Dumoux, M., Nans, A., Saibil, H.R., and Hayward, R.D. (2015). Making connections: snapshots of chlamydial type III secretion systems in contact with host membranes. Current opinion in microbiology *23*, 1-7.

Dunay, I.R., Damatta, R.A., Fux, B., Presti, R., Greco, S., Colonna, M., and Sibley, L.D. (2008). Gr1(+) inflammatory monocytes are required for mucosal resistance to the pathogen Toxoplasma gondii. Immunity *29*, 306-317.

Dunn, J.D., and Valdivia, R.H. (2010). Uncivil engineers: Chlamydia, Salmonella and Shigella alter cytoskeleton architecture to invade epithelial cells. Future microbiology *5*, 1219-1232.

Dupont, C.D., Christian, D.A., and Hunter, C.A. (2012). Immune response and immunopathology during toxoplasmosis. Seminars in immunopathology *34*, 793-813.

Ealick, S.E., Cook, W.J., Vijay-Kumar, S., Carson, M., Nagabhushan, T.L., Trotta, P.P., and Bugg, C.E. (1991). Three-dimensional structure of recombinant human interferon-gamma. Science *252*, 698-702.

Egami, Y., Fukuda, M., and Araki, N. (2011). Rab35 regulates phagosome formation through recruitment of ACAP2 in macrophages during FcgammaR-mediated phagocytosis. Journal of cell science *124*, 3557-3567.

Egan, C.E., Sukhumavasi, W., Butcher, B.A., and Denkers, E.Y. (2009). Functional aspects of Toll-like receptor/MyD88 signalling during protozoan infection: focus on Toxoplasma gondii. Clinical and experimental immunology *156*, 17-24.

Egarter, S., Andenmatten, N., Jackson, A.J., Whitelaw, J.A., Pall, G., Black, J.A., Ferguson, D.J., Tardieux, I., Mogilner, A., and Meissner, M. (2014). The toxoplasma Acto-MyoA motor complex is important but not essential for gliding motility and host cell invasion. PloS one *9*, e91819.

Ehrt, S., Schnappinger, D., Bekiranov, S., Drenkow, J., Shi, S., Gingeras, T.R., Gaasterland, T., Schoolnik, G., and Nathan, C. (2001). Reprogramming of the macrophage transcriptome in response to interferon-gamma and Mycobacterium tuberculosis: signaling roles of nitric oxide synthase-2 and phagocyte oxidase. The Journal of experimental medicine *194*, 1123-1140.

Elmore, S.A., Jones, J.L., Conrad, P.A., Patton, S., Lindsay, D.S., and Dubey, J.P. (2010). Toxoplasma gondii: epidemiology, feline clinical aspects, and prevention. Trends in parasitology *26*, 190-196.

Elwell, C., Mirrashidi, K., and Engel, J. (2016). Chlamydia cell biology and pathogenesis. Nature reviews Microbiology *14*, 385-400.

Elwell, C.A., and Engel, J.N. (2012). Lipid acquisition by intracellular Chlamydiae. Cellular microbiology *14*, 1010-1018.

Engstrom, P., Bergstrom, M., Alfaro, A.C., Syam Krishnan, K., Bahnan, W., Almqvist, F., and Bergstrom, S. (2015). Expansion of the Chlamydia trachomatis inclusion does not require bacterial replication. International journal of medical microbiology : IJMM *305*, 378-382.

Etheridge, R.D., Alaganan, A., Tang, K., Lou, H.J., Turk, B.E., and Sibley, L.D. (2014). The Toxoplasma pseudokinase ROP5 forms complexes with ROP18 and ROP17 kinases that synergize to control acute virulence in mice. Cell host & microbe *15*, 537-550.

Ewald, S.E., Chavarria-Smith, J., and Boothroyd, J.C. (2014). NLRP1 is an inflammasome sensor for Toxoplasma gondii. Infection and immunity *82*, 460-468.

Fairn, G.D., and Grinstein, S. (2012). How nascent phagosomes mature to become phagolysosomes. Trends in immunology *33*, 397-405.

Farrar, M.A., and Schreiber, R.D. (1993). The molecular cell biology of interferon-gamma and its receptor. Annual review of immunology *11*, 571-611.

Fejer, G., Sharma, S., and Gyory, I. (2015). Self-renewing macrophages--a new line of enquiries in mononuclear phagocytes. Immunobiology *220*, 169-174.

Fejer, G., Wegner, M.D., Gyory, I., Cohen, I., Engelhard, P., Voronov, E., Manke, T., Ruzsics, Z., Dolken, L., Prazeres da Costa, O., *et al.* (2013). Nontransformed, GM-CSF-dependent macrophage lines are a unique model to study tissue macrophage functions. Proceedings of the National Academy of Sciences of the United States of America *110*, E2191-2198.

Fellenberg, F., Hartmann, T.B., Dummer, R., Usener, D., Schadendorf, D., and Eichmuller, S. (2004). GBP-5 splicing variants: New guanylate-binding proteins with tumor-associated expression and antigenicity. The Journal of investigative dermatology *122*, 1510-1517.

Feng, J., Cao, Z., Wang, L., Wan, Y., Peng, N., Wang, Q., Chen, X., Zhou, Y., and Zhu, Y. (2017). Inducible GBP5 Mediates the Antiviral Response via Interferon-Related Pathways during Influenza A Virus Infection. Journal of innate immunity.

Feng, Y., Dorhoi, A., Mollenkopf, H.J., Yin, H., Dong, Z., Mao, L., Zhou, J., Bi, A., Weber, S., Maertzdorf, J., *et al.* (2014). Platelets direct monocyte differentiation into epithelioid-like multinucleated giant foam cells with suppressive capacity upon mycobacterial stimulation. The Journal of infectious diseases *210*, 1700-1710.

Ferrell, J.C., and Fields, K.A. (2016). A working model for the type III secretion mechanism in Chlamydia. Microbes and infection *18*, 84-92.

Fessler, M.B. (2016). The Intracellular Cholesterol Landscape: Dynamic Integrator of the Immune Response. Trends in immunology *37*, 819-830.

Finethy, R., and Coers, J. (2016). Sensing the enemy, containing the threat: cell-autonomous immunity to Chlamydia trachomatis. FEMS microbiology reviews.

Finethy, R., Jorgensen, I., Haldar, A.K., de Zoete, M.R., Strowig, T., Flavell, R.A., Yamamoto, M., Nagarajan, U.M., Miao, E.A., and Coers, J. (2015). Guanylate binding proteins enable rapid activation of canonical and noncanonical inflammasomes in Chlamydia-infected macrophages. Infection and immunity *83*, 4740-4749.

Fink, S.L., and Cookson, B.T. (2005). Apoptosis, pyroptosis, and necrosis: mechanistic description of dead and dying eukaryotic cells. Infection and immunity *73*, 1907-1916.

Finlay, B.B., and McFadden, G. (2006). Anti-immunology: evasion of the host immune system by bacterial and viral pathogens. Cell *124*, 767-782.

Fischer, A., Harrison, K.S., Ramirez, Y., Auer, D., Chowdhury, S.R., Prusty, B.K., Sauer, F., Dimond, Z., Kisker, C., Scott Hefty, P., *et al.* (2017). Chlamydia trachomatis-containing vacuole serves as deubiquitination platform to stabilize Mcl-1 and to interfere with host defense. eLife *6*.

Fleckenstein, M.C., Reese, M.L., Konen-Waisman, S., Boothroyd, J.C., Howard, J.C., and Steinfeldt, T. (2012). A Toxoplasma gondii pseudokinase inhibits host IRG resistance proteins. PLoS biology *10*, e1001358.

Flegr, J., and Markos, A. (2014). Masterpiece of epigenetic engineering - how Toxoplasma gondii reprogrammes host brains to change fear to sexual attraction. Molecular ecology *23*, 5934-5936.

Forster, F., Paster, W., Supper, V., Schatzlmaier, P., Sunzenauer, S., Ostler, N., Saliba, A., Eckerstorfer, P., Britzen-Laurent, N., Schutz, G., *et al.* (2014). Guanylate binding protein 1-mediated interaction of T cell antigen receptor signaling with the cytoskeleton. Journal of immunology *192*, 771-781.

Fountoulakis, M., Zulauf, M., Lustig, A., and Garotta, G. (1992). Stoichiometry of interaction between interferon gamma and its receptor. European journal of biochemistry *208*, 781-787.

Franco, M., Panas, M.W., Marino, N.D., Lee, M.C., Buchholz, K.R., Kelly, F.D., Bednarski, J.J., Sleckman, B.P., Pourmand, N., and Boothroyd, J.C. (2016). A Novel Secreted Protein, MYR1, Is Central to Toxoplasma's Manipulation of Host Cells. mBio *7*, e02231-02215.

Friedman, K., Brodsky, A.S., Lu, S., Wood, S., Gill, A.J., Lombardo, K., Yang, D., and Resnick, M.B. (2016). Medullary carcinoma of the colon: a distinct morphology reveals a distinctive immunoregulatory microenvironment. Modern pathology : an official journal of the United States and Canadian Academy of Pathology, Inc *29*, 528-541.

Frost, A., Unger, V.M., and De Camilli, P. (2009). The BAR domain superfamily: membrane-molding macromolecules. Cell *137*, 191-196.

Fuchs, A. (2016). ILC1s in Tissue Inflammation and Infection. Frontiers in immunology *7*, 104.

Fujiwara, Y., Hizukuri, Y., Yamashiro, K., Makita, N., Ohnishi, K., Takeya, M., Komohara, Y., and Hayashi, Y. (2016). Guanylate-binding protein 5 is a marker of interferon-gamma-induced classically activated macrophages. Clinical & translational immunology *5*, e111.

Garib, F.Y., Rizopulu, A.P., Kuchmiy, A.A., and Garib, V.F. (2016). Inactivation of Inflammasomes by Pathogens Regulates Inflammation. Biochemistry Biokhimiia *81*, 1326-1339.

Gasper, R., Meyer, S., Gotthardt, K., Sirajuddin, M., and Wittinghofer, A. (2009). It takes two to tango: regulation of G proteins by dimerization. Nature reviews Molecular cell biology *10*, 423-429.

Gay, G., Braun, L., Brenier-Pinchart, M.P., Vollaire, J., Josserand, V., Bertini, R.L., Varesano, A., Touquet, B., De Bock, P.J., Coute, Y.*, et al.* (2016). Toxoplasma gondii TgIST co-opts host chromatin repressors dampening STAT1-dependent gene regulation and IFN-gamma-mediated host defenses. The Journal of experimental medicine *213*, 1779-1798.

Gazzinelli, R.T., and Denkers, E.Y. (2006). Protozoan encounters with Toll-like receptor signalling pathways: implications for host parasitism. Nature reviews Immunology *6*, 895-906.

Gazzinelli, R.T., Mendonca-Neto, R., Lilue, J., Howard, J., and Sher, A. (2014). Innate resistance against Toxoplasma gondii: an evolutionary tale of mice, cats, and men. Cell host & microbe *15*, 132-138.

Gehre, L., Gorgette, O., Perrinet, S., Prevost, M.C., Ducatez, M., Giebel, A.M., Nelson, D.E., Ball, S.G., and Subtil, A. (2016). Sequestration of host metabolism by an intracellular pathogen. eLife *5*, e12552.

Gengenbacher, M., Nieuwenhuizen, N., Vogelzang, A., Liu, H., Kaiser, P., Schuerer, S., Lazar, D., Wagner, I., Mollenkopf, H.J., and Kaufmann, S.H. (2016). Deletion of nuoG from the Vaccine Candidate Mycobacterium bovis BCG DeltaureC::hly Improves Protection against Tuberculosis. mBio *7*.

Ghosh, A., Praefcke, G.J., Renault, L., Wittinghofer, A., and Herrmann, C. (2006). How guanylate-binding proteins achieve assembly-stimulated processive cleavage of GTP to GMP. Nature *440*, 101-104.

Gold, D.A., Kaplan, A.D., Lis, A., Bett, G.C., Rosowski, E.E., Cirelli, K.M., Bougdour, A., Sidik, S.M., Beck, J.R., Lourido, S.*, et al.* (2015). The Toxoplasma Dense Granule Proteins GRA17 and GRA23 Mediate the Movement of Small Molecules between the Host and the Parasitophorous Vacuole. Cell host & microbe *17*, 642-652.

Goldberg, M.F., Saini, N.K., and Porcelli, S.A. (2014). Evasion of Innate and Adaptive Immunity by Mycobacterium tuberculosis. Microbiology spectrum *2*.

Goodnow, C.C., Vinuesa, C.G., Randall, K.L., Mackay, F., and Brink, R. (2010). Control systems and decision making for antibody production. Nature immunology *11*, 681-688.

Gorbacheva, V.Y., Lindner, D., Sen, G.C., and Vestal, D.J. (2002). The interferon (IFN)-induced GTPase, mGBP-2. Role in IFN-gamma-induced murine fibroblast proliferation. The Journal of biological chemistry *277*, 6080-6087.

Gorfu, G., Cirelli, K.M., Melo, M.B., Mayer-Barber, K., Crown, D., Koller, B.H., Masters, S., Sher, A., Leppla, S.H., Moayeri, M.*, et al.* (2014). Dual role for inflammasome sensors NLRP1 and NLRP3 in murine resistance to Toxoplasma gondii. mBio *5*.

Greenlund, A.C., Schreiber, R.D., Goeddel, D.V., and Pennica, D. (1993). Interferon-gamma induces receptor dimerization in solution and on cells. The Journal of biological chemistry *268*, 18103-18110.

Gregory, C.D., and Pound, J.D. (2011). Cell death in the neighbourhood: direct microenvironmental effects of apoptosis in normal and neoplastic tissues. The Journal of pathology *223*, 177-194.

Grieshaber, N.A., Fischer, E.R., Mead, D.J., Dooley, C.A., and Hackstadt, T. (2004). Chlamydial histone-DNA interactions are disrupted by a metabolite in the methylerythritol phosphate pathway of isoprenoid biosynthesis. Proceedings of the National Academy of Sciences of the United States of America *101*, 7451-7456.

Grieshaber, S.S., Grieshaber, N.A., and Hackstadt, T. (2003). Chlamydia trachomatis uses host cell dynein to traffic to the microtubule-organizing center in a p50 dynamitin-independent process. Journal of cell science *116*, 3793-3802.

Grode, L., Seiler, P., Baumann, S., Hess, J., Brinkmann, V., Nasser Eddine, A., Mann, P., Goosmann, C., Bandermann, S., Smith, D.*, et al.* (2005). Increased vaccine efficacy against tuberculosis of recombinant Mycobacterium bovis bacille Calmette-Guerin mutants that secrete listeriolysin. The Journal of clinical investigation *115*, 2472-2479.

Grover, H.S., Chu, H.H., Kelly, F.D., Yang, S.J., Reese, M.L., Blanchard, N., Gonzalez, F., Chan, S.W., Boothroyd, J.C., Shastri, N., *et al.* (2014). Impact of regulated secretion on antiparasitic CD8 T cell responses. Cell reports *7*, 1716-1728.

Guenzi, E., Topolt, K., Cornali, E., Lubeseder-Martellato, C., Jorg, A., Matzen, K., Zietz, C., Kremmer, E., Nappi, F., Schwemmle, M., *et al.* (2001). The helical domain of GBP-1 mediates the inhibition of endothelial cell proliferation by inflammatory cytokines. The EMBO journal *20*, 5568-5577.

Guenzi, E., Topolt, K., Lubeseder-Martellato, C., Jorg, A., Naschberger, E., Benelli, R., Albini, A., and Sturzl, M. (2003). The guanylate binding protein-1 GTPase controls the invasive and angiogenic capability of endothelial cells through inhibition of MMP-1 expression. The EMBO journal *22*, 3772-3782.

Gupta, S.L., Rubin, B.Y., and Holmes, S.L. (1979). Interferon action: induction of specific proteins in mouse and human cells by homologous interferons. Proceedings of the National Academy of Sciences of the United States of America *76*, 4817-4821.

Gutierrez, M.G., Master, S.S., Singh, S.B., Taylor, G.A., Colombo, M.I., and Deretic, V. (2004). Autophagy is a defense mechanism inhibiting BCG and Mycobacterium tuberculosis survival in infected macrophages. Cell *119*, 753-766.

Hakansson, S., Charron, A.J., and Sibley, L.D. (2001). Toxoplasma evacuoles: a two-step process of secretion and fusion forms the parasitophorous vacuole. The EMBO journal *20*, 3132-3144.

Hakimi, M.A., Olias, P., and Sibley, L.D. (2017). Toxoplasma Effectors Targeting Host Signaling and Transcription. Clinical microbiology reviews *30*, 615-645.

Haldar, A.K., Foltz, C., Finethy, R., Piro, A.S., Feeley, E.M., Pilla-Moffett, D.M., Komatsu, M., Frickel, E.M., and Coers, J. (2015). Ubiquitin systems mark pathogen-containing vacuoles as targets for host defense by guanylate binding proteins. Proceedings of the National Academy of Sciences of the United States of America *112*, E5628-5637.

Haldar, A.K., Piro, A.S., Finethy, R., Espenschied, S.T., Brown, H.E., Giebel, A.M., Frickel, E.M., Nelson, D.E., and Coers, J. (2016). Chlamydia trachomatis Is Resistant to Inclusion Ubiquitination and Associated Host Defense in Gamma Interferon-Primed Human Epithelial Cells. mBio *7*.

Haldar, A.K., Piro, A.S., Pilla, D.M., Yamamoto, M., and Coers, J. (2014). The E2-like conjugation enzyme Atg3 promotes binding of IRG and Gbp proteins to Chlamydia- and Toxoplasma-containing vacuoles and host resistance. PloS one *9*, e86684.

Haldar, A.K., Saka, H.A., Piro, A.S., Dunn, J.D., Henry, S.C., Taylor, G.A., Frickel, E.M., Valdivia, R.H., and Coers, J. (2013). IRG and GBP host resistance factors target aberrant, "non-self" vacuoles characterized by the missing of "self" IRGM proteins. PLoS pathogens *9*, e1003414.

Haldar, K. (2016). Protein trafficking in apicomplexan parasites: crossing the vacuolar Rubicon. Current opinion in microbiology *32*, 38-45.

Haller, O., Staeheli, P., Schwemmle, M., and Kochs, G. (2015). Mx GTPases: dynamin-like antiviral machines of innate immunity. Trends in microbiology *23*, 154-163.

Hammerschlag, M.R. (2002). The intracellular life of chlamydiae. Seminars in pediatric infectious diseases *13*, 239-248.

Han, B.H., Park, D.J., Lim, R.W., Im, J.H., and Kim, H.D. (1998). Cloning, expression, and characterization of a novel guanylate-binding protein, GBP_3 in murine erythroid progenitor cells. Biochimica et biophysica acta *1384*, 373-386.

Haridas, V., Ranjbar, S., Vorobjev, I.A., Goldfeld, A.E., and Barteneva, N.S. (2017). Imaging flow cytometry analysis of intracellular pathogens. Methods *112*, 91-104.

Harris, S.R., Clarke, I.N., Seth-Smith, H.M., Solomon, A.W., Cutcliffe, L.T., Marsh, P., Skilton, R.J., Holland, M.J., Mabey, D., Peeling, R.W., *et al.* (2012). Whole-genome analysis of diverse Chlamydia trachomatis strains identifies phylogenetic relationships masked by current clinical typing. Nature genetics *44*, 413-419, S411.

Haudek-Prinz, V.J., Klepeisz, P., Slany, A., Griss, J., Meshcheryakova, A., Paulitschke, V., Mitulovic, G., Stockl, J., and Gerner, C. (2012). Proteome signatures of inflammatory activated primary human peripheral blood mononuclear cells. Journal of proteomics *76 Spec No.*, 150-162.

Heinen, A.P., Wanke, F., Moos, S., Attig, S., Luche, H., Pal, P.P., Budisa, N., Fehling, H.J., Waisman, A., and Kurschus, F.C. (2014). Improved method to retain cytosolic reporter protein fluorescence while staining for nuclear proteins. Cytometry Part A : the journal of the International Society for Analytical Cytology *85*, 621-627.

Heintzelman, M.B. (2015). Gliding motility in apicomplexan parasites. Seminars in cell & developmental biology *46*, 135-142.

Henry, S.C., Daniell, X.G., Burroughs, A.R., Indaram, M., Howell, D.N., Coers, J., Starnbach, M.N., Hunn, J.P., Howard, J.C., Feng, C.G., *et al.* (2009). Balance of Irgm protein activities determines IFN-gamma-induced host defense. Journal of leukocyte biology *85*, 877-885.

Hermanns, T., Muller, U.B., Konen-Waisman, S., Howard, J.C., and Steinfeldt, T. (2016). The Toxoplasma gondii rhoptry protein ROP18 is an Irga6-specific kinase and regulated by the dense granule protein GRA7. Cellular microbiology *18*, 244-259.

Hertzog, P., Forster, S., and Samarajiwa, S. (2011). Systems biology of interferon responses. Journal of interferon & cytokine research : the official journal of the International Society for Interferon and Cytokine Research *31*, 5-11.

Hertzog, P.J., O'Neill, L.A., and Hamilton, J.A. (2003). The interferon in TLR signaling: more than just antiviral. Trends in immunology *24*, 534-539.

Herweg, J.A., and Rudel, T. (2016). Interaction of Chlamydiae with human macrophages. The FEBS journal *283*, 608-618.

Heuer, D., Rejman Lipinski, A., Machuy, N., Karlas, A., Wehrens, A., Siedler, F., Brinkmann, V., and Meyer, T.F. (2009). Chlamydia causes fragmentation of the Golgi compartment to ensure reproduction. Nature *457*, 731-735.

Holmes, K.L., Fontes, B., Hogarth, P., Konz, R., Monard, S., Pletcher, C.H., Jr., Wadley, R.B., Schmid, I., and Perfetto, S.P. (2014). International Society for the Advancement of Cytometry cell sorter biosafety standards. Cytometry Part A : the journal of the International Society for Analytical Cytology *85*, 434-453.

Hotter, D., Sauter, D., and Kirchhoff, F. (2017). Guanylate binding protein 5: Impairing virion infectivity by targeting retroviral envelope glycoproteins. Small GTPases *8*, 31-37.

Howard, J.C. (2007). Introduction: cell-autonomous immunity. Microbes and infection *9*, 1633-1635.

Howard, J.C., Hunn, J.P., and Steinfeldt, T. (2011). The IRG protein-based resistance mechanism in mice and its relation to virulence in Toxoplasma gondii. Current opinion in microbiology *14*, 414-421.

Howe, D.K., and Sibley, L.D. (1995). Toxoplasma gondii comprises three clonal lineages: correlation of parasite genotype with human disease. The Journal of infectious diseases *172*, 1561-1566.

Hu, X., Chakravarty, S.D., and Ivashkiv, L.B. (2008). Regulation of interferon and Toll-like receptor signaling during macrophage activation by opposing feedforward and feedback inhibition mechanisms. Immunological reviews *226*, 41-56.

Hu, X., and Ivashkiv, L.B. (2009). Cross-regulation of signaling pathways by interferon-gamma: implications for immune responses and autoimmune diseases. Immunity *31*, 539-550.

Hume, D.A. (2008). Macrophages as APC and the dendritic cell myth. Journal of immunology *181*, 5829-5835.

Hunn, J.P., Feng, C.G., Sher, A., and Howard, J.C. (2011). The immunity-related GTPases in mammals: a fast-evolving cell-autonomous resistance system against intracellular pathogens. Mammalian genome : official journal of the International Mammalian Genome Society *22*, 43-54.

Hunn, J.P., and Howard, J.C. (2010). The mouse resistance protein Irgm1 (LRG-47): a regulator or an effector of pathogen defense? PLoS pathogens *6*, e1001008.

Hunn, J.P., Koenen-Waisman, S., Papic, N., Schroeder, N., Pawlowski, N., Lange, R., Kaiser, F., Zerrahn, J., Martens, S., and Howard, J.C. (2008). Regulatory interactions between IRG resistance GTPases in the cellular response to Toxoplasma gondii. The EMBO journal *27*, 2495-2509.

Hunter, C.A., and Sibley, L.D. (2012). Modulation of innate immunity by Toxoplasma gondii virulence effectors. Nature reviews Microbiology *10*, 766-778.

Hybiske, K., and Stephens, R. (2015). Cellular Exit Strategies of Intracellular Bacteria. Microbiology spectrum *3*.

Hybiske, K., and Stephens, R.S. (2007a). Mechanisms of Chlamydia trachomatis entry into nonphagocytic cells. Infection and immunity *75*, 3925-3934.

Hybiske, K., and Stephens, R.S. (2007b). Mechanisms of host cell exit by the intracellular bacterium Chlamydia. Proceedings of the National Academy of Sciences of the United States of America *104*, 11430-11435.

Indraccolo, S., Pfeffer, U., Minuzzo, S., Esposito, G., Roni, V., Mandruzzato, S., Ferrari, N., Anfosso, L., Dell'Eva, R., Noonan, D.M., *et al.* (2007). Identification of genes selectively regulated by IFNs in endothelial cells. Journal of immunology *178*, 1122-1135.

Intemann, C.D., Thye, T., Niemann, S., Browne, E.N., Amanua Chinbuah, M., Enimil, A., Gyapong, J., Osei, I., Owusu-Dabo, E., Helm, S., *et al.* (2009). Autophagy gene variant IRGM -261T contributes to protection from tuberculosis caused by Mycobacterium tuberculosis but not by M. africanum strains. PLoS pathogens *5*, e1000577.

Isaacs, A., and Lindenmann, J. (1957). Virus interference. I. The interferon. Proceedings of the Royal Society of London Series B, Biological sciences *147*, 258-267.

Ito, Y., Shibata-Watanabe, Y., Ushijima, Y., Kawada, J., Nishiyama, Y., Kojima, S., and Kimura, H. (2008). Oligonucleotide microarray analysis of gene expression profiles followed by real-time reverse-transcriptase polymerase chain reaction assay in chronic active Epstein-Barr virus infection. The Journal of infectious diseases *197*, 663-666.

Jankute, M., Nataraj, V., Lee, O.Y., Wu, H.H.T., Ridell, M., Garton, N.J., Barer, M.R., Minnikin, D.E., Bhatt, A., and Besra, G.S. (2017). The role of hydrophobicity in tuberculosis evolution and pathogenicity. Scientific reports *7*, 1315.

Jewett, T.J., Dooley, C.A., Mead, D.J., and Hackstadt, T. (2008). Chlamydia trachomatis tarp is phosphorylated by src family tyrosine kinases. Biochemical and biophysical research communications *371*, 339-344.

Jiang, X., Shen, C., Yu, H., Karunakaran, K.P., and Brunham, R.C. (2010). Differences in innate immune responses correlate with differences in murine susceptibility to Chlamydia muridarum pulmonary infection. Immunology *129*, 556-566.

Johnson, H.M., and Ahmed, C.M. (2006). Gamma interferon signaling: insights to development of interferon mimetics. Cellular and molecular biology *52*, 71-76.

Johnson, L.L., and Sayles, P.C. (2002). Deficient humoral responses underlie susceptibility to Toxoplasma gondii in CD4-deficient mice. Infection and immunity *70*, 185-191.

Johnson, R.M., and Brunham, R.C. (2016). Tissue-Resident T Cells as the Central Paradigm of Chlamydia Immunity. Infection and immunity *84*, 868-873.

Johnston, A.C., Piro, A., Clough, B., Siew, M., Virreira Winter, S., Coers, J., and Frickel, E.M. (2016). Human GBP1 does not localize to pathogen vacuoles but restricts Toxoplasma gondii. Cellular microbiology *18*, 1056-1064.

Jones, J.L., and Dubey, J.P. (2012). Foodborne toxoplasmosis. Clinical infectious diseases : an official publication of the Infectious Diseases Society of America *55*, 845-851.

Joung, J., Konermann, S., Gootenberg, J.S., Abudayyeh, O.O., Platt, R.J., Brigham, M.D., Sanjana, N.E., and Zhang, F. (2017). Genome-scale CRISPR-Cas9 knockout and transcriptional activation screening. Nature protocols *12*, 828-863.

Juarez, E., Carranza, C., Hernandez-Sanchez, F., Leon-Contreras, J.C., Hernandez-Pando, R., Escobedo, D., Torres, M., and Sada, E. (2012). NOD2 enhances the innate response of alveolar macrophages to Mycobacterium tuberculosis in humans. European journal of immunology *42*, 880-889.

Juarez, E., Carranza, C., Hernandez-Sanchez, F., Loyola, E., Escobedo, D., Leon-Contreras, J.C., Hernandez-Pando, R., Torres, M., and Sada, E. (2014). Nucleotide-oligomerizing domain-1 (NOD1) receptor activation induces pro-inflammatory responses and autophagy in human alveolar macrophages. BMC pulmonary medicine *14*, 152.

Jutras, I., Abrami, L., and Dautry-Varsat, A. (2003). Entry of the lymphogranuloma venereum strain of Chlamydia trachomatis into host cells involves cholesterol-rich membrane domains. Infection and immunity *71*, 260-266.

Kagan, J.C., and Iwasaki, A. (2012). Phagosome as the organelle linking innate and adaptive immunity. Traffic *13*, 1053-1061.

Kaiser, F., Kaufmann, S.H., and Zerrahn, J. (2004). IIGP, a member of the IFN inducible and microbial defense mediating 47 kDa GTPase family, interacts with the microtubule binding protein hook3. Journal of cell science *117*, 1747-1756.

Kakutani, R., Adachi, Y., Takata, H., Kuriki, T., and Ohno, N. (2012). Essential role of Toll-like receptor 2 in macrophage activation by glycogen. Glycobiology *22*, 146-159.

Kanatani, S., Uhlen, P., and Barragan, A. (2015). Infection by Toxoplasma gondii Induces Amoeboid-Like Migration of Dendritic Cells in a Three-Dimensional Collagen Matrix. PloS one *10*, e0139104.

Karki, R., Man, S.M., Malireddi, R.K., Gurung, P., Vogel, P., Lamkanfi, M., and Kanneganti, T.D. (2015). Concerted activation of the AIM2 and NLRP3 inflammasomes orchestrates host protection against Aspergillus infection. Cell host & microbe *17*, 357-368.

Kaspers, B. (1996). Chicken Guanylate-binding Protein. Journal of Biological Chemistry *271*, 10304-10308.

Kaufmann, S.H. (2013). Tuberculosis vaccines: time to think about the next generation. Seminars in immunology *25*, 172-181.

Kawai, T., and Akira, S. (2010). The role of pattern-recognition receptors in innate immunity: update on Toll-like receptors. Nature immunology *11*, 373-384.

Kawamoto, Y., Nakajima, Y.I., and Kuranaga, E. (2016). Apoptosis in Cellular Society: Communication between Apoptotic Cells and Their Neighbors. International journal of molecular sciences *17*.

Kearney, C.J., and Martin, S.J. (2017). An Inflammatory Perspective on Necroptosis. Molecular cell *65*, 965-973.

Kim, B.H., Chee, J.D., Bradfield, C.J., Park, E.S., Kumar, P., and MacMicking, J.D. (2016a). Interferon-induced guanylate-binding proteins in inflammasome activation and host defense. Nature immunology *17*, 481-489.

Kim, B.H., Shenoy, A.R., Kumar, P., Bradfield, C.J., and MacMicking, J.D. (2012a). IFN-inducible GTPases in host cell defense. Cell host & microbe *12*, 432-444.

Kim, B.H., Shenoy, A.R., Kumar, P., Das, R., Tiwari, S., and MacMicking, J.D. (2011). A family of IFN-gamma-inducible 65-kD GTPases protects against bacterial infection. Science *332*, 717-721.

Kim, E.W., Nadipuram, S.M., Tetlow, A.L., Barshop, W.D., Liu, P.T., Wohlschlegel, J.A., and Bradley, P.J. (2016b). The Rhoptry Pseudokinase ROP54 Modulates Toxoplasma gondii Virulence and Host GBP2 Loading. mSphere *1*.

Kim, H.J., Zhong, Q., Sheng, Z.H., Yoshimori, T., Liang, C., and Jung, J.U. (2012b). Beclin-1-interacting autophagy protein Atg14L targets the SNARE-associated protein Snapin to coordinate endocytic trafficking. Journal of cell science *125*, 4740-4750.

Kitaya, K., Yasuo, T., Yamaguchi, T., Fushiki, S., and Honjo, H. (2007). Genes regulated by interferon-gamma in human uterine microvascular endothelial cells. International journal of molecular medicine *20*, 689-697.

Klamp, T., Boehm, U., Schenk, D., Pfeffer, K., and Howard, J.C. (2003). A giant GTPase, very large inducible GTPase-1, is inducible by IFNs. Journal of immunology *171*, 1255-1265.

Klümpers, V. (2013). Funktionelle Charakterisierung der Kolokalisation von Guanylat-bindenden Proteinen (GBPs) mit intrazellulären Erregern. In Mathematisch-Naturwissenschaftlichen Fakultät (Heinrich-Heine-Universität Düsseldorf).

Knight, E., Jr., and Korant, B.D. (1979). Fibroblast interferon induces synthesis of four proteins in human fibroblast cells. Proceedings of the National Academy of Sciences of the United States of America *76*, 1824-1827.

Kobayashi, A., and Suzuki, Y. (1987). Suppression of antibody responses by Toxoplasma infection in mice. Zentralblatt fur Bakteriologie, Mikrobiologie, und Hygiene Series A, Medical microbiology, infectious diseases, virology, parasitology *264*, 312-318.

Koblansky, A.A., Jankovic, D., Oh, H., Hieny, S., Sungnak, W., Mathur, R., Hayden, M.S., Akira, S., Sher, A., and Ghosh, S. (2013). Recognition of profilin by Toll-like receptor 12 is critical for host resistance to Toxoplasma gondii. Immunity *38*, 119-130.

Kokes, M., and Valdivia, R.H. (2015). Differential Translocation of Host Cellular Materials into the Chlamydia trachomatis Inclusion Lumen during Chemical Fixation. PloS one *10*, e0139153.

Koltes, J.E., Fritz-Waters, E., Eisley, C.J., Choi, I., Bao, H., Kommadath, A., Serao, N.V., Boddicker, N.J., Abrams, S.M., Schroyen, M.*, et al.* (2015). Identification of a putative quantitative trait nucleotide in guanylate binding protein 5 for host response to PRRS virus infection. BMC genomics *16*, 412.

Konermann, C., Kresse, A., Beuter-Gunia, C., Wurthner, J., Degrandi, D., Pfeffer, K., and Beer, S. (2007). In silico and in vitro characterization of mGBP4 splice variants. DNA and cell biology *26*, 847-851.

Kozak, R.A., Alexander, D.C., Liao, R., Sherman, D.R., and Behr, M.A. (2011). Region of difference 2 contributes to virulence of Mycobacterium tuberculosis. Infection and immunity *79*, 59-66.

Krapp, C., Hotter, D., Gawanbacht, A., McLaren, P.J., Kluge, S.F., Sturzel, C.M., Mack, K., Reith, E., Engelhart, S., Ciuffi, A.*, et al.* (2016). Guanylate Binding Protein (GBP) 5 Is an Interferon-Inducible Inhibitor of HIV-1 Infectivity. Cell host & microbe *19*, 504-514.

Krause, C.D., and Pestka, S. (2007). Historical developments in the research of interferon receptors. Cytokine & growth factor reviews *18*, 473-482.

Kravets, E., Degrandi, D., Ma, Q., Peulen, T.O., Klumpers, V., Felekyan, S., Kuhnemuth, R., Weidtkamp-Peters, S., Seidel, C.A., and Pfeffer, K. (2016). Guanylate binding proteins directly attack Toxoplasma gondii via supramolecular complexes. eLife *5*.

Kravets, E., Degrandi, D., Weidtkamp-Peters, S., Ries, B., Konermann, C., Felekyan, S., Dargazanli, J.M., Praefcke, G.J., Seidel, C.A., Schmitt, L.*, et al.* (2012). The GTPase activity of murine guanylate-binding protein 2 (mGBP2) controls the intracellular localization and recruitment to the parasitophorous vacuole of Toxoplasma gondii. The Journal of biological chemistry *287*, 27452-27466.

Kresse, A., Konermann, C., Degrandi, D., Beuter-Gunia, C., Wuerthner, J., Pfeffer, K., and Beer, S. (2008). Analyses of murine GBP homology clusters based on in silico, in vitro and in vivo studies. BMC genomics *9*, 158.

Krishnamurthy, S., Konstantinou, E.K., Young, L.H., Gold, D.A., and Saeij, J.P. (2017). The human immune response to Toxoplasma: Autophagy versus cell death. PLoS pathogens *13*, e1006176.

Kumar, D., and Rao, K.V. (2011). Regulation between survival, persistence, and elimination of intracellular mycobacteria: a nested equilibrium of delicate balances. Microbes and infection *13*, 121-133.

Kumar, Y., and Valdivia, R.H. (2009). Leading a sheltered life: intracellular pathogens and maintenance of vacuolar compartments. Cell host & microbe *5*, 593-601.

Kunzelmann, S., Praefcke, G.J., and Herrmann, C. (2006). Transient kinetic investigation of GTP hydrolysis catalyzed by interferon-gamma-induced hGBP1 (human guanylate binding protein 1). The Journal of biological chemistry *281*, 28627-28635.

Kurenuma, T., Kawamura, I., Hara, H., Uchiyama, R., Daim, S., Dewamitta, S.R., Sakai, S., Tsuchiya, K., Nomura, T., and Mitsuyama, M. (2009). The RD1 locus in the Mycobacterium tuberculosis genome contributes to activation of caspase-1 via induction of potassium ion efflux in infected macrophages. Infection and immunity *77*, 3992-4001.

Laliberte, J., and Carruthers, V.B. (2008). Host cell manipulation by the human pathogen Toxoplasma gondii. Cellular and molecular life sciences : CMLS *65*, 1900-1915.

Lambert, H., Hitziger, N., Dellacasa, I., Svensson, M., and Barragan, A. (2006). Induction of dendritic cell migration upon Toxoplasma gondii infection potentiates parasite dissemination. Cellular microbiology *8*, 1611-1623.

Lane, B.J., Mutchler, C., Al Khodor, S., Grieshaber, S.S., and Carabeo, R.A. (2008). Chlamydial entry involves TARP binding of guanine nucleotide exchange factors. PLoS pathogens *4*, e1000014.

Larsen, M.H., Biermann, K., Tandberg, S., Hsu, T., and Jacobs, W.R., Jr. (2007). Genetic Manipulation of Mycobacterium tuberculosis. Current protocols in microbiology *Chapter 10*, Unit 10A 12.

Larsson, A. (2014). AliView: a fast and lightweight alignment viewer and editor for large datasets. Bioinformatics *30*, 3276-3278.

Late de Late, P., Pineda, M., Harnett, M., Harnett, W., Besteiro, S., and Langsley, G. (2017). Apicomplexan autophagy and modulation of autophagy in parasite-infected host cells. Biomedical journal *40*, 23-30.

Laux da Costa, L., Delcroix, M., Dalla Costa, E.R., Prestes, I.V., Milano, M., Francis, S.S., Unis, G., Silva, D.R., Riley, L.W., and Rossetti, M.L. (2015). A real-time PCR signature to discriminate between tuberculosis and other pulmonary diseases. Tuberculosis *95*, 421-425.

Le Negrate, G., Krieg, A., Faustin, B., Loeffler, M., Godzik, A., Krajewski, S., and Reed, J.C. (2008). ChlaDub1 of Chlamydia trachomatis suppresses NF-kappaB activation and inhibits IkappaBalpha ubiquitination and degradation. Cellular microbiology *10*, 1879-1892.

Lee, H.J., Ko, H.J., and Jung, Y.J. (2016). Insufficient Generation of Mycobactericidal Mediators and Inadequate Level of Phagosomal Maturation Are Related with Susceptibility to Virulent Mycobacterium tuberculosis Infection in Mouse Macrophages. Frontiers in microbiology *7*, 541.

Lee, Y., Sasai, M., Ma, J.S., Sakaguchi, N., Ohshima, J., Bando, H., Saitoh, T., Akira, S., and Yamamoto, M. (2015). p62 Plays a Specific Role in Interferon-gamma-Induced Presentation of a Toxoplasma Vacuolar Antigen. Cell reports *13*, 223-233.

Levine, B. (2005). Eating oneself and uninvited guests: autophagy-related pathways in cellular defense. Cell *120*, 159-162.

Li, G., Zhang, J., Sun, Y., Wang, H., and Wang, Y. (2009). The evolutionarily dynamic IFN-inducible GTPase proteins play conserved immune functions in vertebrates and cephalochordates. Molecular biology and evolution *26*, 1619-1630.

Li, L.X., and McSorley, S.J. (2015). A re-evaluation of the role of B cells in protective immunity to Chlamydia infection. Immunology letters *164*, 88-93.

Li, Y., Feng, S.T., Yao, Y., Yang, L., Xing, Y., Wang, Y., and You, J.H. (2014). Correlation between IRGM genetic polymorphisms and Crohn's disease risk: a meta-analysis of case-control studies. Genetics and molecular research : GMR *13*, 10741-10753.

Liang, M., Habib, Z., Sakamoto, K., Chen, X., and Cao, G. (2017). Mycobacteria and Autophagy: Many Questions and Few Answers. Current issues in molecular biology *21*, 63-72.

Lilue, J., Muller, U.B., Steinfeldt, T., and Howard, J.C. (2013). Reciprocal virulence and resistance polymorphism in the relationship between Toxoplasma gondii and the house mouse. eLife *2*, e01298.

Lim, A.I., Verrier, T., Vosshenrich, C.A., and Di Santo, J.P. (2017). Developmental options and functional plasticity of innate lymphoid cells. Current opinion in immunology *44*, 61-68.

Lim, D.C., Cooke, B.M., Doerig, C., and Saeij, J.P. (2012). Toxoplasma and Plasmodium protein kinases: roles in invasion and host cell remodelling. International journal for parasitology *42*, 21-32.

Lindenberg, V., Mölleken, K., Kravets, E., Stallmann, S., Hegemann, J., Degrandi, D., and Pfeffer, K. (2017). Broad recruitment of mGBP family members to Chlamydia trachomatis inclusions PloS one.

Ling, Y.M., Shaw, M.H., Ayala, C., Coppens, I., Taylor, G.A., Ferguson, D.J., and Yap, G.S. (2006). Vacuolar and plasma membrane stripping and autophagic elimination of Toxoplasma gondii in primed effector macrophages. The Journal of experimental medicine *203*, 2063-2071.

Liu, S., Xiong, X., Zhao, X., Yang, X., and Wang, H. (2015a). F-BAR family proteins, emerging regulators for cell membrane dynamic changes-from structure to human diseases. Journal of hematology & oncology *8*, 47.

Liu, Z., Gerner, M.Y., Van Panhuys, N., Levine, A.G., Rudensky, A.Y., and Germain, R.N. (2015b). Immune homeostasis enforced by co-localized effector and regulatory T cells. Nature *528*, 225-230.

Long, S., Brown, K.M., Drewry, L.L., Anthony, B., Phan, I.Q.H., and Sibley, L.D. (2017). Calmodulin-like proteins localized to the conoid regulate motility and cell invasion by Toxoplasma gondii. PLoS pathogens *13*, e1006379.

Lu, H., Shen, C., and Brunham, R.C. (2000). Chlamydia trachomatis infection of epithelial cells induces the activation of caspase-1 and release of mature IL-18. Journal of immunology *165*, 1463-1469.

Lubeseder-Martellato, C., Guenzi, E., Jörg, A., Töpolt, K., Naschberger, E., Kremmer, E., Zietz, C., Tschachler, E., Hutzler, P., Schwemmle, M.*, et al.* (2002). Guanylate-Binding Protein-1 Expression Is Selectively Induced by Inflammatory Cytokines and Is an Activation Marker of Endothelial Cells during Inflammatory Diseases. The American Journal of Pathology *161*, 1749-1759.

Luder, C.G., Walter, W., Beuerle, B., Maeurer, M.J., and Gross, U. (2001). Toxoplasma gondii down-regulates MHC class II gene expression and antigen presentation by murine macrophages via interference with nuclear translocation of STAT1alpha. European journal of immunology *31*, 1475-1484.

Lun, Y., Zhang, L., Sun, S., Yan, D., Du, B., and Zhu, X. (2009). Detection of Membranous Protein Alterations on BCG-activated Macrophages Involved in Contact-dependent Tumoricidal Processes. Journal of Proteomics & Bioinformatics *1*, 175-184.

Lyadova, I.V., and Panteleev, A.V. (2015). Th1 and Th17 Cells in Tuberculosis: Protection, Pathology, and Biomarkers. Mediators of inflammation *2015*, 854507.

Lyons, J.M., Morre, S.A., Airo-Brown, L.P., Pena, A.S., and Ito, J.I. (2005). Comparison of multiple genital tract infections with Chlamydia trachomatis in different strains of female mice. Journal of microbiology, immunology, and infection = Wei mian yu gan ran za zhi *38*, 383-393.

Lyons, R.E., McLeod, R., and Roberts, C.W. (2002). Toxoplasma gondii tachyzoite-bradyzoite interconversion. Trends in parasitology *18*, 198-201.

Ma, J.S., Sasai, M., Ohshima, J., Lee, Y., Bando, H., Takeda, K., and Yamamoto, M. (2014). Selective and strain-specific NFAT4 activation by the Toxoplasma gondii polymorphic dense granule protein GRA6. The Journal of experimental medicine *211*, 2013-2032.

Macallan, D.C., Borghans, J.A., and Asquith, B. (2017). Human T Cell Memory: A Dynamic View. Vaccines *5*.

MacKenzie, C.R., Heseler, K., Muller, A., and Daubener, W. (2007). Role of indoleamine 2,3-dioxygenase in antimicrobial defence and immuno-regulation: tryptophan depletion versus production of toxic kynurenines. Current drug metabolism *8*, 237-244.

MacMicking, J.D. (2004). IFN-inducible GTPases and immunity to intracellular pathogens. Trends in immunology *25*, 601-609.

MacMicking, J.D. (2005). Immune control of phagosomal bacteria by p47 GTPases. Current opinion in microbiology *8*, 74-82.

MacMicking, J.D. (2012). Interferon-inducible effector mechanisms in cell-autonomous immunity. Nature reviews Immunology *12*, 367-382.

MacMicking, J.D. (2014). Cell-autonomous effector mechanisms against mycobacterium tuberculosis. Cold Spring Harbor perspectives in medicine *4*.

MacMicking, J.D., Taylor, G.A., and McKinney, J.D. (2003). Immune control of tuberculosis by IFN-gamma-inducible LRG-47. Science *302*, 654-659.

Madigan, T.M., Martinko, J.M., Stahl, D.A., and Clark, D.P. (2012). Brock biology of microorganisms - 13th edition (1301 Sansome Street, San Francisco, CA 94111: Benjamin Cummings (Pearson Education, Inc)).

Mahauad-Fernandez, W.D., and Okeoma, C.M. (2016). The role of BST-2/Tetherin in host protection and disease manifestation. Immunity, inflammation and disease *4*, 4-23.

Majoros, A., Platanitis, E., Kernbauer-Holzl, E., Rosebrock, F., Muller, M., and Decker, T. (2017). Canonical and Non-Canonical Aspects of JAK-STAT Signaling: Lessons from Interferons for Cytokine Responses. Frontiers in immunology *8*, 29.

Man, S.M., and Kanneganti, T.D. (2015). Regulation of inflammasome activation. Immunological reviews *265*, 6-21.

Man, S.M., and Kanneganti, T.D. (2016). Converging roles of caspases in inflammasome activation, cell death and innate immunity. Nature reviews Immunology *16*, 7-21.

Man, S.M., Karki, R., and Kanneganti, T.D. (2016a). AIM2 inflammasome in infection, cancer, and autoimmunity: Role in DNA sensing, inflammation, and innate immunity. European journal of immunology *46*, 269-280.

Man, S.M., Karki, R., and Kanneganti, T.D. (2016b). DNA-sensing inflammasomes: regulation of bacterial host defense and the gut microbiota. Pathogens and disease *74*, ftw028.

Man, S.M., Karki, R., Malireddi, R.K., Neale, G., Vogel, P., Yamamoto, M., Lamkanfi, M., and Kanneganti, T.D. (2015). The transcription factor IRF1 and guanylate-binding proteins target activation of the AIM2 inflammasome by Francisella infection. Nature immunology *16*, 467-475.

Man, S.M., Karki, R., Sasai, M., Place, D.E., Kesavardhana, S., Temirov, J., Frase, S., Zhu, Q., Malireddi, R.K., Kuriakose, T., *et al.* (2016c). IRGB10 Liberates Bacterial Ligands for Sensing by the AIM2 and Caspase-11-NLRP3 Inflammasomes. Cell *167*, 382-396 e317.

Man, S.M., Place, D.E., Kuriakose, T., and Kanneganti, T.D. (2017). Interferon-inducible guanylate-binding proteins at the interface of cell-autonomous immunity and inflammasome activation. Journal of leukocyte biology *101*, 143-150.

Mantegazza, A.R., Magalhaes, J.G., Amigorena, S., and Marks, M.S. (2013). Presentation of phagocytosed antigens by MHC class I and II. Traffic *14*, 135-152.

Maric-Biresev, J., Hunn, J.P., Krut, O., Helms, J.B., Martens, S., and Howard, J.C. (2016). Loss of the interferon-gamma-inducible regulatory immunity-related GTPase (IRG), Irgm1, causes activation of effector IRG proteins on lysosomes, damaging lysosomal function and predicting the dramatic susceptibility of Irgm1-deficient mice to infection. BMC biology *14*, 33.

Martens, S., and Howard, J. (2006). The interferon-inducible GTPases. Annual review of cell and developmental biology *22*, 559-589.

Martens, S., Parvanova, I., Zerrahn, J., Griffiths, G., Schell, G., Reichmann, G., and Howard, J.C. (2005). Disruption of Toxoplasma gondii parasitophorous vacuoles by the mouse p47-resistance GTPases. PLoS pathogens *1*, e24.

Martens, S., Sabel, K., Lange, R., Uthaiah, R., Wolf, E., and Howard, J.C. (2004). Mechanisms regulating the positioning of mouse p47 resistance GTPases LRG-47 and IIGP1 on cellular membranes: retargeting to plasma membrane induced by phagocytosis. Journal of immunology *173*, 2594-2606.

Martin, C.J., Booty, M.G., Rosebrock, T.R., Nunes-Alves, C., Desjardins, D.M., Keren, I., Fortune, S.M., Remold, H.G., and Behar, S.M. (2012). Efferocytosis is an innate antibacterial mechanism. Cell host & microbe *12*, 289-300.

Martinon, F., Burns, K., and Tschopp, J. (2002). The inflammasome: a molecular platform triggering activation of inflammatory caspases and processing of proIL-beta. Molecular cell *10*, 417-426.

Matsumoto, K., Kusaka, J., Nishibori, A., and Hara, H. (2006). Lipid domains in bacterial membranes. Molecular microbiology *61*, 1110-1117.

McFadden, G.I., and Yeh, E. (2017). The apicoplast: now you see it, now you don't. International journal for parasitology *47*, 137-144.

McLaren, P.J., Gawanbacht, A., Pyndiah, N., Krapp, C., Hotter, D., Kluge, S.F., Gotz, N., Heilmann, J., Mack, K., Sauter, D., *et al.* (2015). Identification of potential HIV restriction factors by combining evolutionary genomic signatures with functional analyses. Retrovirology *12*, 41.

McLeod, R., Boyer, K.M., Lee, D., Mui, E., Wroblewski, K., Karrison, T., Noble, A.G., Withers, S., Swisher, C.N., Heydemann, P.T., *et al.* (2012). Prematurity and severity are associated with Toxoplasma gondii alleles (NCCCTS, 1981-2009). Clinical infectious diseases : an official publication of the Infectious Diseases Society of America *54*, 1595-1605.

Mehlitz, A., Banhart, S., Hess, S., Selbach, M., and Meyer, T.F. (2008). Complex kinase requirements for Chlamydia trachomatis Tarp phosphorylation. FEMS microbiology letters *289*, 233-240.

Mehlitz, A., and Rudel, T. (2013). Modulation of host signaling and cellular responses by Chlamydia. Cell communication and signaling : CCS *11*, 90.

Meireles, L.R., Ekman, C.C., Andrade j, R.H., and Luna, E.J. (2015). Human Toxoplasmosis Outbreaks and the Agent Infecting Form. Findings from a Systematic Review. Revista do Instituto de Medicina Tropical de Sao Paulo *57*, 369-376.

Mercier, C., and Cesbron-Delauw, M.F. (2015). Toxoplasma secretory granules: one population or more? Trends in parasitology *31*, 60-71.

Messmer-Blust, A.F., Balasubramanian, S., Gorbacheva, V.Y., Jeyaratnam, J.A., and Vestal, D.J. (2010). The interferon-gamma-induced murine guanylate-binding protein-2 inhibits rac activation during cell spreading on fibronectin and after platelet-derived growth factor treatment: role for phosphatidylinositol 3-kinase. Molecular biology of the cell *21*, 2514-2528.

Meunier, E., and Broz, P. (2016). Interferon-inducible GTPases in cell autonomous and innate immunity. Cellular microbiology *18*, 168-180.

Meunier, E., Dick, M.S., Dreier, R.F., Schurmann, N., Kenzelmann Broz, D., Warming, S., Roose-Girma, M., Bumann, D., Kayagaki, N., Takeda, K., *et al.* (2014). Caspase-11 activation requires lysis of pathogen-containing vacuoles by IFN-induced GTPases. Nature *509*, 366-370.

Meunier, E., Wallet, P., Dreier, R.F., Costanzo, S., Anton, L., Ruhl, S., Dussurgey, S., Dick, M.S., Kistner, A., Rigard, M., *et al.* (2015). Guanylate-binding proteins promote activation of the AIM2 inflammasome during infection with Francisella novicida. Nature immunology *16*, 476-484.

Meylan, E., Tschopp, J., and Karin, M. (2006). Intracellular pattern recognition receptors in the host response. Nature *442*, 39-44.

Mills, E.L., Kelly, B., and O'Neill, L.A.J. (2017). Mitochondria are the powerhouses of immunity. Nature immunology *18*, 488-498.

Mirrashidi, K.M., Elwell, C.A., Verschueren, E., Johnson, J.R., Frando, A., Von Dollen, J., Rosenberg, O., Gulbahce, N., Jang, G., Johnson, T., *et al.* (2015). Global Mapping of the Inc-Human Interactome Reveals that Retromer Restricts Chlamydia Infection. Cell host & microbe *18*, 109-121.

Misaghi, S., Balsara, Z.R., Catic, A., Spooner, E., Ploegh, H.L., and Starnbach, M.N. (2006). Chlamydia trachomatis-derived deubiquitinating enzymes in mammalian cells during infection. Molecular microbiology *61*, 142-150.

Miyairi, I., Mahdi, O.S., Ouellette, S.P., Belland, R.J., and Byrne, G.I. (2006). Different growth rates of Chlamydia trachomatis biovars reflect pathotype. The Journal of infectious diseases *194*, 350-357.

Miyairi, I., Ramsey, K.H., and Patton, D.L. (2010). Duration of untreated chlamydial genital infection and factors associated with clearance: review of animal studies. The Journal of infectious diseases *201 Suppl 2*, S96-103.

Miyairi, I., Tatireddigari, V.R., Mahdi, O.S., Rose, L.A., Belland, R.J., Lu, L., Williams, R.W., and Byrne, G.I. (2007). The p47 GTPases Iigp2 and Irgb10 regulate innate immunity and inflammation to murine Chlamydia psittaci infection. Journal of immunology *179*, 1814-1824.

Modiano, N., Lu, Y.E., and Cresswell, P. (2005). Golgi targeting of human guanylate-binding protein-1 requires nucleotide binding, isoprenylation, and an IFN-gamma-inducible cofactor. Proceedings of the National Academy of Sciences of the United States of America *102*, 8680-8685.

Modlin, R.L., and Bloom, B.R. (2013). TB or not TB: that is no longer the question. Science translational medicine *5*, 213sr216.

Mohammadpour, M., Abrishami, M., Masoumi, A., and Hashemi, H. (2016). Trachoma: Past, present and future. Journal of current ophthalmology *28*, 165-169.

Moliva, J.I., Turner, J., and Torrelles, J.B. (2017). Immune Responses to Bacillus Calmette-Guerin Vaccination: Why Do They Fail to Protect against Mycobacterium tuberculosis? Frontiers in immunology *8*, 407.

Molleken, K., Becker, E., and Hegemann, J.H. (2013). The Chlamydia pneumoniae invasin protein Pmp21 recruits the EGF receptor for host cell entry. PLoS pathogens *9*, e1003325.

Molleken, K., Schmidt, E., and Hegemann, J.H. (2010). Members of the Pmp protein family of Chlamydia pneumoniae mediate adhesion to human cells via short repetitive peptide motifs. Molecular microbiology *78*, 1004-1017.

Montoya, J.G., and Liesenfeld, O. (2004). Toxoplasmosis. Lancet *363*, 1965-1976.

Mordue, D.G., Hakansson, S., Niesman, I., and Sibley, L.D. (1999). Toxoplasma gondii resides in a vacuole that avoids fusion with host cell endocytic and exocytic vesicular trafficking pathways. Experimental parasitology *92*, 87-99.

Moretti, J., and Blander, J.M. (2017). Cell-autonomous stress responses in innate immunity. Journal of leukocyte biology *101*, 77-86.

Mortaz, E., Adcock, I.M., Tabarsi, P., Masjedi, M.R., Mansouri, D., Velayati, A.A., Casanova, J.L., and Barnes, P.J. (2015). Interaction of Pattern Recognition Receptors with Mycobacterium Tuberculosis. Journal of clinical immunology *35*, 1-10.

Moulder, J.W. (1966). The relation of the psittacosis group (Chlamydiae) to bacteria and viruses. Annual review of microbiology *20*, 107-130.

Mourik, B.C., Lubberts, E., de Steenwinkel, J.E.M., Ottenhoff, T.H.M., and Leenen, P.J.M. (2017). Interactions between Type 1 Interferons and the Th17 Response in Tuberculosis: Lessons Learned from Autoimmune Diseases. Frontiers in immunology *8*, 294.

Mpiga, P., and Ravaoarinoro, M. (2006). Chlamydia trachomatis persistence: an update. Microbiological research *161*, 9-19.

Muller, M., Briscoe, J., Laxton, C., Guschin, D., Ziemiecki, A., Silvennoinen, O., Harpur, A.G., Barbieri, G., Witthuhn, B.A., Schindler, C., *et al.* (1993). The protein tyrosine kinase JAK1 complements defects in interferon-alpha/beta and -gamma signal transduction. Nature *366*, 129-135.

Muller, U.B., and Howard, J.C. (2016). The impact of Toxoplasma gondii on the mammalian genome. Current opinion in microbiology *32*, 19-25.

Muniz-Feliciano, L., Van Grol, J., Portillo, J.A., Liew, L., Liu, B., Carlin, C.R., Carruthers, V.B., Matthews, S., and Subauste, C.S. (2013). Toxoplasma gondii-induced activation of EGFR prevents autophagy protein-mediated killing of the parasite. PLoS pathogens *9*, e1003809.

Murphy, K.P., Travers, P., and Walport, M. (2012). Janeway's Immunobiology (8th edition) (711 T hird Avenue, 8th floor, New York, NY 1 0017, USA: Garland Science (Taylor & Francis Group, LLC)).

Murthy, A.K., Chambers, J.P., Meier, P.A., Zhong, G., and Arulanandam, B.P. (2007). Intranasal vaccination with a secreted chlamydial protein enhances resolution of genital Chlamydia muridarum infection, protects against oviduct pathology, and is highly dependent upon endogenous gamma interferon production. Infection and immunity *75*, 666-676.

Nam, H.W. (2009). GRA proteins of Toxoplasma gondii: maintenance of host-parasite interactions across the parasitophorous vacuolar membrane. The Korean journal of parasitology *47 Suppl*, S29-37.

Nans, A., Ford, C., and Hayward, R.D. (2015). Host-pathogen reorganisation during host cell entry by Chlamydia trachomatis. Microbes and infection *17*, 727-731.

Nantais, D.E., Schwemmle, M., Stickney, J.T., Vestal, D.J., and Buss, J.E. (1996). Prenylation of an interferon-gamma-induced GTP-binding protein: the human guanylate binding protein, huGBP1. Journal of leukocyte biology *60*, 423-431.

Nash, P.B., Purner, M.B., Leon, R.P., Clarke, P., Duke, R.C., and Curiel, T.J. (1998). Toxoplasma gondii-infected cells are resistant to multiple inducers of apoptosis. Journal of immunology *160*, 1824-1830.

Nelson, D.E., Virok, D.P., Wood, H., Roshick, C., Johnson, R.M., Whitmire, W.M., Crane, D.D., Steele-Mortimer, O., Kari, L., McClarty, G., *et al.* (2005). Chlamydial IFN-gamma immune evasion is linked to host infection tropism. Proceedings of the National Academy of Sciences of the United States of America *102*, 10658-10663.

Neubauer, H., Cumano, A., Muller, M., Wu, H., Huffstadt, U., and Pfeffer, K. (1998). Jak2 deficiency defines an essential developmental checkpoint in definitive hematopoiesis. Cell *93*, 397-409.

Neun, R., Richter, M.F., Staeheli, P., and Schwemmle, M. (1996). GTPase properties of the interferon-induced human guanylate-binding protein 2. FEBS letters *390*, 69-72.

Nguyen, B.D., Cunningham, D., Liang, X., Chen, X., Toone, E.J., Raetz, C.R., Zhou, P., and Valdivia, R.H. (2011). Lipooligosaccharide is required for the generation of infectious elementary bodies in Chlamydia trachomatis. Proceedings of the National Academy of Sciences of the United States of America *108*, 10284-10289.

Nguyen, B.D., and Valdivia, R.H. (2012). Virulence determinants in the obligate intracellular pathogen Chlamydia trachomatis revealed by forward genetic approaches. Proceedings of the National Academy of Sciences of the United States of America *109*, 1263-1268.

Nguyen, N., Shteyn, V., and Melia, T.J. (2017). Sensing Membrane Curvature in Macroautophagy. Journal of molecular biology *429*, 457-472.

Nguyen, T.T., Hu, Y., Widney, D.P., Mar, R.A., and Smith, J.B. (2002). Murine GBP-5, a new member of the murine guanylate-binding protein family, is coordinately regulated with other GBPs in vivo and in vitro. Journal of interferon & cytokine research : the official journal of the International Society for Interferon and Cytokine Research *22*, 899-909.

Nordmann, A., Wixler, L., Boergeling, Y., Wixler, V., and Ludwig, S. (2012). A new splice variant of the human guanylate-binding protein 3 mediates anti-influenza activity through inhibition of viral transcription and replication. FASEB journal : official publication of the Federation of American Societies for Experimental Biology *26*, 1290-1300.

Nunes-Hasler, P., and Demaurex, N. (2017). The ER phagosome connection in the era of membrane contact sites. Biochimica et biophysica acta.

Nunes, A., Borrego, M.J., and Gomes, J.P. (2013). Genomic features beyond Chlamydia trachomatis phenotypes: what do we think we know? Infection, genetics and evolution : journal of molecular epidemiology and evolutionary genetics in infectious diseases *16*, 392-400.

O'Connell, C.M., AbdelRahman, Y.M., Green, E., Darville, H.K., Saira, K., Smith, B., Darville, T., Scurlock, A.M., Meyer, C.R., and Belland, R.J. (2011). Toll-like receptor 2 activation by Chlamydia trachomatis is plasmid dependent, and plasmid-responsive chromosomal loci are coordinately regulated in response to glucose limitation by C. trachomatis but not by C. muridarum. Infection and immunity *79*, 1044-1056.

O'Connell, C.M., and Ferone, M.E. (2016). Chlamydia trachomatis Genital Infections. Microbial cell *3*, 390-403.

O'Connell, C.M., Ingalls, R.R., Andrews, C.W., Jr., Scurlock, A.M., and Darville, T. (2007). Plasmid-deficient Chlamydia muridarum fail to induce immune pathology and protect against oviduct disease. Journal of immunology *179*, 4027-4034.

O'Connell, C.M., Ionova, I.A., Quayle, A.J., Visintin, A., and Ingalls, R.R. (2006). Localization of TLR2 and MyD88 to Chlamydia trachomatis inclusions. Evidence for signaling by intracellular TLR2 during infection with an obligate intracellular pathogen. The Journal of biological chemistry *281*, 1652-1659.

O'Garra, A., Redford, P.S., McNab, F.W., Bloom, C.I., Wilkinson, R.J., and Berry, M.P. (2013). The immune response in tuberculosis. Annual review of immunology *31*, 475-527.

Ohshima, J., Lee, Y., Sasai, M., Saitoh, T., Su Ma, J., Kamiyama, N., Matsuura, Y., Pann-Ghill, S., Hayashi, M., Ebisu, S., *et al.* (2014). Role of mouse and human autophagy proteins in IFN-gamma-induced cell-autonomous responses against Toxoplasma gondii. Journal of immunology *192*, 3328-3335.

Ohshima, J., Sasai, M., Liu, J., Yamashita, K., Ma, J.S., Lee, Y., Bando, H., Howard, J.C., Ebisu, S., Hayashi, M., *et al.* (2015). RabGDIalpha is a negative regulator of interferon-gamma-inducible GTPase-dependent cell-autonomous immunity to Toxoplasma gondii. Proceedings of the National Academy of Sciences of the United States of America *112*, E4581-4590.

Olekhnovitch, R., and Bousso, P. (2015). Induction, Propagation, and Activity of Host Nitric Oxide: Lessons from Leishmania Infection. Trends in parasitology *31*, 653-664.

Olias, P., Etheridge, R.D., Zhang, Y., Holtzman, M.J., and Sibley, L.D. (2016). Toxoplasma Effector Recruits the Mi-2/NuRD Complex to Repress STAT1 Transcription and Block IFN-gamma-Dependent Gene Expression. Cell host & microbe *20*, 72-82.

Olszewski, M.A., Gray, J., and Vestal, D.J. (2006). In silico genomic analysis of the human and murine guanylate-binding protein (GBP) gene clusters. Journal of interferon & cytokine research : the official journal of the International Society for Interferon and Cytokine Research *26*, 328-352.

Opsteegh, M., Kortbeek, T.M., Havelaar, A.H., and van der Giessen, J.W. (2015). Intervention strategies to reduce human Toxoplasma gondii disease burden. Clinical infectious diseases : an official publication of the Infectious Diseases Society of America *60*, 101-107.

Orme, I.M., and Ordway, D.J. (2016). Mouse and Guinea Pig Models of Tuberculosis. Microbiology spectrum *4*.

Ostler, N., Britzen-Laurent, N., Liebl, A., Naschberger, E., Lochnit, G., Ostler, M., Forster, F., Kunzelmann, P., Ince, S., Supper, V., *et al.* (2014). Gamma interferon-induced guanylate binding protein 1 is a novel actin cytoskeleton remodeling factor. Molecular and cellular biology *34*, 196-209.

Ozato, K., Shin, D.M., Chang, T.H., and Morse, H.C., 3rd (2008). TRIM family proteins and their emerging roles in innate immunity. Nature reviews Immunology *8*, 849-860.

Pai, M., Behr, M.A., Dowdy, D., Dheda, K., Divangahi, M., Boehme, C.C., Ginsberg, A., Swaminathan, S., Spigelman, M., Getahun, H., *et al.* (2016). Tuberculosis. Nature reviews Disease primers *2*, 16076.

Papic, N., Hunn, J.P., Pawlowski, N., Zerrahn, J., and Howard, J.C. (2008). Inactive and active states of the interferon-inducible resistance GTPase, Irga6, in vivo. The Journal of biological chemistry *283*, 32143-32151.

Pappas, G., Roussos, N., and Falagas, M.E. (2009). Toxoplasmosis snapshots: global status of Toxoplasma gondii seroprevalence and implications for pregnancy and congenital toxoplasmosis. International journal for parasitology *39*, 1385-1394.

Pareja, M.E., and Colombo, M.I. (2013). Autophagic clearance of bacterial pathogens: molecular recognition of intracellular microorganisms. Frontiers in cellular and infection microbiology *3*, 54.

Parmley, S.F., Yang, S., Harth, G., Sibley, L.D., Sucharczuk, A., and Remington, J.S. (1994). Molecular characterization of a 65-kilodalton Toxoplasma gondii antigen expressed abundantly in the matrix of tissue cysts. Molecular and biochemical parasitology *66*, 283-296.

Paulus, G.L., and Xavier, R.J. (2015). Autophagy and checkpoints for intracellular pathogen defense. Current opinion in gastroenterology *31*, 14-23.

Pauwels, A.M., Trost, M., Beyaert, R., and Hoffmann, E. (2017). Patterns, Receptors, and Signals: Regulation of Phagosome Maturation. Trends in immunology.

Pawlowski, N., Khaminets, A., Hunn, J.P., Papic, N., Schmidt, A., Uthaiah, R.C., Lange, R., Vopper, G., Martens, S., Wolf, E., *et al.* (2011). The activation mechanism of Irga6, an interferon-inducible GTPase contributing to mouse resistance against Toxoplasma gondii. BMC biology *9*, 7.

Peddireddy, V., Doddam, S.N., and Ahmed, N. (2017). Mycobacterial Dormancy Systems and Host Responses in Tuberculosis. Frontiers in immunology *8*, 84.

Peng, R., Lin, G., and Li, J. (2016). Potential pitfalls of CRISPR/Cas9-mediated genome editing. The FEBS journal *283*, 1218-1231.

Pepper, M., Dzierszinski, F., Wilson, E., Tait, E., Fang, Q., Yarovinsky, F., Laufer, T.M., Roos, D., and Hunter, C.A. (2008). Plasmacytoid dendritic cells are activated by Toxoplasma gondii to present antigen and produce cytokines. Journal of immunology *180*, 6229-6236.

Persico, M., Petrella, L., Orteca, N., Di Dato, A., Mariani, M., Andreoli, M., De Donato, M., Scambia, G., Novellino, E., Ferlini, C., *et al.* (2015). GTP is an allosteric modulator of the interaction between the guanylate-binding protein 1 and the prosurvival kinase PIM1. European journal of medicinal chemistry *91*, 132-144.

Personnic, N., Barlocher, K., Finsel, I., and Hilbi, H. (2016). Subversion of Retrograde Trafficking by Translocated Pathogen Effectors. Trends in microbiology *24*, 450-462.

Pestka, S. (2007). The interferons: 50 years after their discovery, there is much more to learn. The Journal of biological chemistry *282*, 20047-20051.

Pestka, S., Langer, J.A., Zoon, K.C., and Samuel, C.E. (1987). Interferons and their actions. Annual review of biochemistry *56*, 727-777.

Pifer, R., Benson, A., Sturge, C.R., and Yarovinsky, F. (2011). UNC93B1 is essential for TLR11 activation and IL-12-dependent host resistance to Toxoplasma gondii. The Journal of biological chemistry *286*, 3307-3314.

Pilla-Moffett, D., Barber, M.F., Taylor, G.A., and Coers, J. (2016). Interferon-Inducible GTPases in Host Resistance, Inflammation and Disease. Journal of molecular biology *428*, 3495-3513.

Pilla, D.M., Hagar, J.A., Haldar, A.K., Mason, A.K., Degrandi, D., Pfeffer, K., Ernst, R.K., Yamamoto, M., Miao, E.A., and Coers, J. (2014). Guanylate binding proteins promote caspase-11-dependent pyroptosis in response to cytoplasmic LPS. Proceedings of the National Academy of Sciences of the United States of America *111*, 6046-6051.

Pindel, A., and Sadler, A. (2011). The role of protein kinase R in the interferon response. Journal of interferon & cytokine research : the official journal of the International Society for Interferon and Cytokine Research *31*, 59-70.

Plattner, F., and Soldati-Favre, D. (2008). Hijacking of host cellular functions by the Apicomplexa. Annual review of microbiology *62*, 471-487.

Plattner, F., Yarovinsky, F., Romero, S., Didry, D., Carlier, M.F., Sher, A., and Soldati-Favre, D. (2008). Toxoplasma profilin is essential for host cell invasion and TLR11-dependent induction of an interleukin-12 response. Cell host & microbe *3*, 77-87.

Ponpuak, M., Davis, A.S., Roberts, E.A., Delgado, M.A., Dinkins, C., Zhao, Z., Virgin, H.W.t., Kyei, G.B., Johansen, T., Vergne, I., *et al.* (2010). Delivery of cytosolic components by autophagic adaptor protein p62 endows autophagosomes with unique antimicrobial properties. Immunity *32*, 329-341.

Praefcke, G.J., Kloep, S., Benscheid, U., Lilie, H., Prakash, B., and Herrmann, C. (2004). Identification of residues in the human guanylate-binding protein 1 critical for nucleotide binding and cooperative GTP hydrolysis. Journal of molecular biology *344*, 257-269.

Praefcke, G.J., and McMahon, H.T. (2004). The dynamin superfamily: universal membrane tubulation and fission molecules? Nature reviews Molecular cell biology *5*, 133-147.

Prakash, B., Renault, L., Praefcke, G.J., Herrmann, C., and Wittinghofer, A. (2000). Triphosphate structure of guanylate-binding protein 1 and implications for nucleotide binding and GTPase mechanism. The EMBO journal *19*, 4555-4564.

Pupovac, A., and Good-Jacobson, K.L. (2017). An antigen to remember: regulation of B cell memory in health and disease. Current opinion in immunology *45*, 89-96.

Rajaram, K., and Nelson, D.E. (2015). Chlamydia muridarum infection of macrophages elicits bactericidal nitric oxide production via reactive oxygen species and cathepsin B. Infection and immunity *83*, 3164-3175.

Randow, F., MacMicking, J.D., and James, L.C. (2013). Cellular self-defense: how cell-autonomous immunity protects against pathogens. Science *340*, 701-706.

Rani, A., Pandita, E., Rahman, S., Deep, S., and Sau, A.K. (2012). Insight into temperature dependence of GTPase activity in human guanylate binding protein-1. PloS one *7*, e40487.

Ravindran, S., and Boothroyd, J.C. (2008). Secretion of proteins into host cells by Apicomplexan parasites. Traffic *9*, 647-656.

Ravindran, S., Lodoen, M.B., Verhelst, S.H., Bogyo, M., and Boothroyd, J.C. (2009). 4-Bromophenacyl bromide specifically inhibits rhoptry secretion during Toxoplasma invasion. PloS one *4*, e8143.

Rawre, J., Juyal, D., and Dhawan, B. (2017). Molecular typing of Chlamydia trachomatis: An overview. Indian journal of medical microbiology *35*, 17-26.

Redgrove, K.A., and McLaughlin, E.A. (2014). The Role of the Immune Response in Chlamydia trachomatis Infection of the Male Genital Tract: A Double-Edged Sword. Frontiers in immunology *5*, 534.

Reese, M.L. (2013). Immune to defeat. eLife *2*, e01599.

Reese, M.L., Shah, N., and Boothroyd, J.C. (2014). The Toxoplasma pseudokinase ROP5 is an allosteric inhibitor of the immunity-related GTPases. The Journal of biological chemistry *289*, 27849-27858.

Reid, A.J., Vermont, S.J., Cotton, J.A., Harris, D., Hill-Cawthorne, G.A., Konen-Waisman, S., Latham, S.M., Mourier, T., Norton, R., Quail, M.A., *et al.* (2012). Comparative genomics of the apicomplexan parasites Toxoplasma gondii and Neospora caninum: Coccidia differing in host range and transmission strategy. PLoS pathogens *8*, e1002567.

Rivera, A., Siracusa, M.C., Yap, G.S., and Gause, W.C. (2016). Innate cell communication kick-starts pathogen-specific immunity. Nature immunology *17*, 356-363.

Roberts-Galbraith, R.H., and Gould, K.L. (2010). Setting the F-BAR: functions and regulation of the F-BAR protein family. Cell cycle *9*, 4091-4097.

Robertsen, B., Zou, J., Secombes, C., and Leong, J.A. (2006). Molecular and expression analysis of an interferon-gamma-inducible guanylate-binding protein from rainbow trout (Oncorhynchus mykiss). Developmental and comparative immunology *30*, 1023-1033.

Robertson, D.K., Gu, L., Rowe, R.K., and Beatty, W.L. (2009). Inclusion biogenesis and reactivation of persistent Chlamydia trachomatis requires host cell sphingolipid biosynthesis. PLoS pathogens *5*, e1000664.

Rockey, D.D., Scidmore, M.A., Bannantine, J.P., and Brown, W.J. (2002). Proteins in the chlamydial inclusion membrane. Microbes and infection *4*, 333-340.

Rodig, S.J., Meraz, M.A., White, J.M., Lampe, P.A., Riley, J.K., Arthur, C.D., King, K.L., Sheehan, K.C., Yin, L., Pennica, D., *et al.* (1998). Disruption of the Jak1 gene demonstrates obligatory and nonredundant roles of the Jaks in cytokine-induced biologic responses. Cell *93*, 373-383.

Rohde, G., Straube, E., Essig, A., Reinhold, P., and Sachse, K. (2010). Chlamydial zoonoses. Deutsches Arzteblatt international *107*, 174-180.

Rohde, K., Yates, R.M., Purdy, G.E., and Russell, D.G. (2007). Mycobacterium tuberculosis and the environment within the phagosome. Immunological reviews *219*, 37-54.

Roshick, C., Wood, H., Caldwell, H.D., and McClarty, G. (2006). Comparison of gamma interferon-mediated antichlamydial defense mechanisms in human and mouse cells. Infection and immunity *74*, 225-238.

Rosowski, E.E., Lu, D., Julien, L., Rodda, L., Gaiser, R.A., Jensen, K.D., and Saeij, J.P. (2011). Strain-specific activation of the NF-kappaB pathway by GRA15, a novel Toxoplasma gondii dense granule protein. The Journal of experimental medicine *208*, 195-212.

Rupper, A.C., and Cardelli, J.A. (2008). Induction of guanylate binding protein 5 by gamma interferon increases susceptibility to Salmonella enterica serovar Typhimurium-induced pyroptosis in RAW 264.7 cells. Infection and immunity *76*, 2304-2315.

Rusinova, I., Forster, S., Yu, S., Kannan, A., Masse, M., Cumming, H., Chapman, R., and Hertzog, P.J. (2013). Interferome v2.0: an updated database of annotated interferon-regulated genes. Nucleic acids research *41*, D1040-1046.

Russell, D.G., Barry, C.E., 3rd, and Flynn, J.L. (2010). Tuberculosis: what we don't know can, and does, hurt us. Science *328*, 852-856.

Rybicka, J.M., Balce, D.R., Chaudhuri, S., Allan, E.R., and Yates, R.M. (2012). Phagosomal proteolysis in dendritic cells is modulated by NADPH oxidase in a pH-independent manner. The EMBO journal *31*, 932-944.

Saadatnia, G., and Golkar, M. (2012). A review on human toxoplasmosis. Scandinavian journal of infectious diseases *44*, 805-814.

Saban, M.R., Hellmich, H.L., Simpson, C., Davis, C.A., Lang, M.L., Ihnat, M.A., O'Donnell, M.A., Wu, X.R., and Saban, R. (2007). Repeated BCG treatment of mouse bladder selectively stimulates small GTPases and HLA antigens and inhibits single-spanning uroplakins. BMC cancer *7*, 204.

Saeij, J.P., Boyle, J.P., Coller, S., Taylor, S., Sibley, L.D., Brooke-Powell, E.T., Ajioka, J.W., and Boothroyd, J.C. (2006). Polymorphic secreted kinases are key virulence factors in toxoplasmosis. Science *314*, 1780-1783.

Saeij, J.P., Coller, S., Boyle, J.P., Jerome, M.E., White, M.W., and Boothroyd, J.C. (2007). Toxoplasma co-opts host gene expression by injection of a polymorphic kinase homologue. Nature *445*, 324-327.

Saiga, H., Nieuwenhuizen, N., Gengenbacher, M., Koehler, A.B., Schuerer, S., Moura-Alves, P., Wagner, I., Mollenkopf, H.J., Dorhoi, A., and Kaufmann, S.H. (2015). The Recombinant BCG DeltaureC::hly Vaccine Targets the AIM2 Inflammasome to Induce Autophagy and Inflammation. The Journal of infectious diseases *211*, 1831-1841.

Saka, H.A., and Valdivia, R.H. (2010). Acquisition of nutrients by Chlamydiae: unique challenges of living in an intracellular compartment. Current opinion in microbiology *13*, 4-10.

Samarajiwa, S.A., Forster, S., Auchettl, K., and Hertzog, P.J. (2009). INTERFEROME: the database of interferon regulated genes. Nucleic acids research *37*, D852-857.

Sanchez-Huertas, C., and Luders, J. (2015). The augmin connection in the geometry of microtubule networks. Current biology : CB *25*, R294-299.

Saraf, P., Shwab, E.K., Dubey, J.P., and Su, C. (2017). On the determination of Toxoplasma gondii virulence in mice. Experimental parasitology *174*, 25-30.

Satproedprai, N., Wichukchinda, N., Suphankong, S., Inunchot, W., Kuntima, T., Kumpeerasart, S., Wattanapokayakit, S., Nedsuwan, S., Yanai, H., Higuchi, K., *et al.* (2015). Diagnostic value of blood gene expression signatures in active tuberculosis in Thais: a pilot study. Genes and immunity *16*, 253-260.

Scanga, C.A., Aliberti, J., Jankovic, D., Tilloy, F., Bennouna, S., Denkers, E.Y., Medzhitov, R., and Sher, A. (2002). Cutting edge: MyD88 is required for resistance to Toxoplasma gondii infection and regulates parasite-induced IL-12 production by dendritic cells. Journal of immunology *168*, 5997-6001.

Scanga, C.A., and Flynn, J.L. (2014). Modeling tuberculosis in nonhuman primates. Cold Spring Harbor perspectives in medicine *4*, a018564.

Schaeffer, A., and Henrich, B. (2008). Rapid detection of Chlamydia trachomatis and typing of the Lymphogranuloma venereum associated L-Serovars by TaqMan PCR. BMC infectious diseases *8*, 56.

Schneider, W.M., Chevillotte, M.D., and Rice, C.M. (2014). Interferon-stimulated genes: a complex web of host defenses. Annual review of immunology *32*, 513-545.

Schoborg, R.V. (2011). Chlamydia persistence -- a tool to dissect chlamydia--host interactions. Microbes and infection *13*, 649-662.

Schoenborn, J.R., and Wilson, C.B. (2007). Regulation of interferon-gamma during innate and adaptive immune responses. Advances in immunology *96*, 41-101.

Schroder, K., Hertzog, P.J., Ravasi, T., and Hume, D.A. (2004). Interferon-gamma: an overview of signals, mechanisms and functions. Journal of leukocyte biology *75*, 163-189.

Schroder, K., Sweet, M.J., and Hume, D.A. (2006). Signal integration between IFNgamma and TLR signalling pathways in macrophages. Immunobiology *211*, 511-524.

Schwemmle, M., Kaspers, B., Irion, A., Staeheli, P., and Schultz, U. (1996). Chicken guanylate-binding protein. Conservation of GTPase activity and induction by cytokines. The Journal of biological chemistry *271*, 10304-10308.

Schwemmle, M., and Staeheli, P. (1994). The interferon-induced 67-kDa guanylate-binding protein (hGBP1) is a GTPase that converts GTP to GMP. The Journal of biological chemistry *269*, 11299-11305.

Seeber, F., and Steinfelder, S. (2016). Recent advances in understanding apicomplexan parasites. F1000Research *5*.

Selleck, E.M., Fentress, S.J., Beatty, W.L., Degrandi, D., Pfeffer, K., Virgin, H.W.t., Macmicking, J.D., and Sibley, L.D. (2013). Guanylate-binding protein 1 (Gbp1) contributes to cell-autonomous immunity against Toxoplasma gondii. PLoS pathogens *9*, e1003320.

Selleck, E.M., Orchard, R.C., Lassen, K.G., Beatty, W.L., Xavier, R.J., Levine, B., Virgin, H.W., and Sibley, L.D. (2015). A Noncanonical Autophagy Pathway Restricts Toxoplasma gondii Growth in a Strain-Specific Manner in IFN-gamma-Activated Human Cells. mBio *6*, e01157-01115.

Sharma, M., and Rudel, T. (2009). Apoptosis resistance in Chlamydia-infected cells: a fate worse than death? FEMS immunology and medical microbiology *55*, 154-161.

Shen, B., and Sibley, L.D. (2012). The moving junction, a key portal to host cell invasion by apicomplexan parasites. Current opinion in microbiology *15*, 449-455.

Shenoy, A.R., Kim, B.H., Choi, H.P., Matsuzawa, T., Tiwari, S., and MacMicking, J.D. (2007). Emerging themes in IFN-gamma-induced macrophage immunity by the p47 and p65 GTPase families. Immunobiology *212*, 771-784.

Shenoy, A.R., Wellington, D.A., Kumar, P., Kassa, H., Booth, C.J., Cresswell, P., and MacMicking, J.D. (2012). GBP5 promotes NLRP3 inflammasome assembly and immunity in mammals. Science *336*, 481-485.

Sher, A., Tosh, K., and Jankovic, D. (2017). Innate recognition of Toxoplasma gondii in humans involves a mechanism distinct from that utilized by rodents. Cellular & molecular immunology *14*, 36-42.

Sherrid, A.M., and Hybiske, K. (2017). Chlamydia trachomatis Cellular Exit Alters Interactions with Host Dendritic Cells. Infection and immunity *85*.

Shi, L., Eugenin, E.A., and Subbian, S. (2016). Immunometabolism in Tuberculosis. Frontiers in immunology *7*, 150.

Shin, S., and Brodsky, I.E. (2015). The inflammasome: Learning from bacterial evasion strategies. Seminars in immunology *27*, 102-110.

Shintani, T., and Klionsky, D.J. (2004). Autophagy in health and disease: a double-edged sword. Science *306*, 990-995.

Shotland, Y., Kramer, H., and Groisman, E.A. (2003). The Salmonella SpiC protein targets the mammalian Hook3 protein function to alter cellular trafficking. Molecular microbiology *49*, 1565-1576.

Shtrichman, R., and Samuel, C.E. (2001). The role of gamma interferon in antimicrobial immunity. Current opinion in microbiology *4*, 251-259.

Sibley, L.D., Khan, A., Ajioka, J.W., and Rosenthal, B.M. (2009). Genetic diversity of Toxoplasma gondii in animals and humans. Philosophical transactions of the Royal Society of London Series B, Biological sciences *364*, 2749-2761.

Simunovic, M., Voth, G.A., Callan-Jones, A., and Bassereau, P. (2015). When Physics Takes Over: BAR Proteins and Membrane Curvature. Trends in cell biology *25*, 780-792.

Singh, S.B., Davis, A.S., Taylor, G.A., and Deretic, V. (2006). Human IRGM induces autophagy to eliminate intracellular mycobacteria. Science *313*, 1438-1441.

Singh, S.B., Ornatowski, W., Vergne, I., Naylor, J., Delgado, M., Roberts, E., Ponpuak, M., Master, S., Pilli, M., White, E., *et al.* (2010). Human IRGM regulates autophagy and cell-autonomous immunity functions through mitochondria. Nature cell biology *12*, 1154-1165.

Singh, V., Braddick, D., and Dhar, P.K. (2017). Exploring the potential of genome editing CRISPR-Cas9 technology. Gene *599*, 1-18.

Slany, A., Bileck, A., Kreutz, D., Mayer, R.L., Muqaku, B., and Gerner, C. (2016). Contribution of Human Fibroblasts and Endothelial Cells to the Hallmarks of Inflammation as Determined by Proteome Profiling. Molecular & cellular proteomics : MCP *15*, 1982-1997.

Spekker, K., Leineweber, M., Degrandi, D., Ince, V., Brunder, S., Schmidt, S.K., Stuhlsatz, S., Howard, J.C., Schares, G., Degistirici, O., *et al.* (2013). Antimicrobial effects of murine mesenchymal stromal cells directed against Toxoplasma gondii and Neospora caninum: role of immunity-related GTPases (IRGs) and guanylate-binding proteins (GBPs). Medical microbiology and immunology *202*, 197-206.

Springer, H.M., Schramm, M., Taylor, G.A., and Howard, J.C. (2013). Irgm1 (LRG-47), a regulator of cell-autonomous immunity, does not localize to mycobacterial or listerial phagosomes in IFN-gamma-induced mouse cells. Journal of immunology *191*, 1765-1774.

Staeheli, P., Colonno, R.J., and Cheng, Y.S. (1983). Different mRNAs induced by interferon in cells from inbred mouse strains A/J and A2G. Journal of virology *47*, 563-567.

Stallmann, S. (2015). Identifizierung und Charakterisierung neuer Adhäsine bei Chlamydia trachomatis. In Mathematisch-Naturwissenschaftlichen Fakultät (Heinrich-Heine-Universität Düsseldorf).

Stallmann, S., and Hegemann, J.H. (2016). The Chlamydia trachomatis Ctad1 invasin exploits the human integrin beta1 receptor for host cell entry. Cellular microbiology *18*, 761-775.

Steinfeldt, T., Konen-Waisman, S., Tong, L., Pawlowski, N., Lamkemeyer, T., Sibley, L.D., Hunn, J.P., and Howard, J.C. (2010). Phosphorylation of mouse immunity-related GTPase (IRG) resistance proteins is an evasion strategy for virulent Toxoplasma gondii. PLoS biology *8*, e1000576.

Stephen-Victor, E., Bosschem, I., Haesebrouck, F., and Bayry, J. (2017). The Yin and Yang of regulatory T cells in infectious diseases and avenues to target them. Cellular microbiology.

Stephens, R.S., Myers, G., Eppinger, M., and Bavoil, P.M. (2009). Divergence without difference: phylogenetics and taxonomy of Chlamydia resolved. FEMS immunology and medical microbiology *55*, 115-119.

Stickney, J.T., and Buss, J.E. (2000). Murine guanylate-binding protein: incomplete geranylgeranyl isoprenoid modification of an interferon-gamma-inducible guanosine triphosphate-binding protein. Molecular biology of the cell *11*, 2191-2200.

Subach, O.M., Cranfill, P.J., Davidson, M.W., and Verkhusha, V.V. (2011). An enhanced monomeric blue fluorescent protein with the high chemical stability of the chromophore. PloS one *6*, e28674.

Subauste, C.S. (2009). Autophagy as an antimicrobial strategy. Expert review of anti-infective therapy *7*, 743-752.

Suetsugu, S. (2016). Higher-order assemblies of BAR domain proteins for shaping membranes. Microscopy *65*, 201-210.

Sumpter, R., Jr., and Levine, B. (2010). Autophagy and innate immunity: triggering, targeting and tuning. Seminars in cell & developmental biology *21*, 699-711.

Suzuki, Y., Orellana, M.A., Schreiber, R.D., and Remington, J.S. (1988). Interferon-gamma: the major mediator of resistance against Toxoplasma gondii. Science *240*, 516-518.

Syguda, A., Bauer, M., Benscheid, U., Ostler, N., Naschberger, E., Ince, S., Sturzl, M., and Herrmann, C. (2012a). Tetramerization of human guanylate-binding protein 1 is mediated by coiled-coil formation of the C-terminal alpha-helices. The FEBS journal *279*, 2544-2554.

Syguda, A., Kerstan, A., Ladnorg, T., Stuben, F., Woll, C., and Herrmann, C. (2012b). Immobilization of biotinylated hGBP1 in a defined orientation on surfaces is crucial for uniform interaction with analyte proteins and catalytic activity. Langmuir : the ACS journal of surfaces and colloids *28*, 6411-6418.

Szabo, E.K., and Finney, C.A. (2017). Toxoplasma gondii: One Organism, Multiple Models. Trends in parasitology *33*, 113-127.

Takacs, A.C., Swierzy, I.J., and Luder, C.G. (2012). Interferon-gamma restricts Toxoplasma gondii development in murine skeletal muscle cells via nitric oxide production and immunity-related GTPases. PloS one *7*, e45440.

Tardieux, I., and Baum, J. (2016). Reassessing the mechanics of parasite motility and host-cell invasion. The Journal of cell biology *214*, 507-515.

Taylor, G.A., Collazo, C.M., Yap, G.S., Nguyen, K., Gregorio, T.A., Taylor, L.S., Eagleson, B., Secrest, L., Southon, E.A., Reid, S.W., *et al.* (2000). Pathogen-specific loss of host resistance in mice lacking the IFN-gamma-inducible gene IGTP. Proceedings of the National Academy of Sciences of the United States of America *97*, 751-755.

Taylor, G.A., Feng, C.G., and Sher, A. (2007). Control of IFN-gamma-mediated host resistance to intracellular pathogens by immunity-related GTPases (p47 GTPases). Microbes and infection *9*, 1644-1651.

Taylor, G.A., Jeffers, M., Largaespada, D.A., Jenkins, N.A., Copeland, N.G., and Vande Woude, G.F. (1996). Identification of a novel GTPase, the inducibly expressed GTPase, that accumulates in response to interferon gamma. The Journal of biological chemistry *271*, 20399-20405.

Taylor, G.A., Stauber, R., Rulong, S., Hudson, E., Pei, V., Pavlakis, G.N., Resau, J.H., and Vande Woude, G.F. (1997). The inducibly expressed GTPase localizes to the endoplasmic reticulum, independently of GTP binding. The Journal of biological chemistry *272*, 10639-10645.

Tenter, A.M., Heckeroth, A.R., and Weiss, L.M. (2000). Toxoplasma gondii: from animals to humans. International journal for parasitology *30*, 1217-1258.

Tietzel, I., El-Haibi, C., and Carabeo, R.A. (2009). Human guanylate binding proteins potentiate the anti-chlamydia effects of interferon-gamma. PloS one *4*, e6499.

Tipton, A.R., Nyabuto, G.O., Trendel, J.A., Mazur, T.M., Wilson, J.P., Wadi, S., Justinger, J.S., Moore, G.L., Nguyen, P.T., and Vestal, D.J. (2016). Guanylate-Binding Protein-1 protects ovarian cancer cell lines but not breast cancer cell lines from killing by paclitaxel. Biochemical and biophysical research communications *478*, 1617-1623.

Tiwari, S., Choi, H.P., Matsuzawa, T., Pypaert, M., and MacMicking, J.D. (2009). Targeting of the GTPase Irgm1 to the phagosomal membrane via PtdIns(3,4)P(2) and PtdIns(3,4,5)P(3) promotes immunity to mycobacteria. Nature immunology *10*, 907-917.

Travar, M., Petkovic, M., and Verhaz, A. (2016). Type I, II, and III Interferons: Regulating Immunity to Mycobacterium tuberculosis Infection. Archivum immunologiae et therapiae experimentalis *64*, 19-31.

Traver, M.K., Henry, S.C., Cantillana, V., Oliver, T., Hunn, J.P., Howard, J.C., Beer, S., Pfeffer, K., Coers, J., and Taylor, G.A. (2011). Immunity-related GTPase M (IRGM) proteins influence the localization of guanylate-binding protein 2 (GBP2) by modulating macroautophagy. The Journal of biological chemistry *286*, 30471-30480.

Tripal, P., Bauer, M., Naschberger, E., Mortinger, T., Hohenadl, C., Cornali, E., Thurau, M., and Sturzl, M. (2007). Unique features of different members of the human guanylate-binding protein family. Journal of interferon & cytokine research : the official journal of the International Society for Interferon and Cytokine Research *27*, 44-52.

Valdivia, R.H. (2008). Chlamydia effector proteins and new insights into chlamydial cellular microbiology. Current opinion in microbiology *11*, 53-59.

Van den Bossche, J., O'Neill, L.A., and Menon, D. (2017). Macrophage Immunometabolism: Where Are We (Going)? Trends in immunology.

van der Wel, N., Hava, D., Houben, D., Fluitsma, D., van Zon, M., Pierson, J., Brenner, M., and Peters, P.J. (2007). M. tuberculosis and M. leprae translocate from the phagolysosome to the cytosol in myeloid cells. Cell *129*, 1287-1298.

Verma, V., Dhanda, R.S., Moller, N.F., and Yadav, M. (2016). Inflammasomes and Their Role in Innate Immunity of Sexually Transmitted Infections. Frontiers in immunology *7*, 540.

Vestal, D.J. (2005). The guanylate-binding proteins (GBPs): proinflammatory cytokine-induced members of the dynamin superfamily with unique GTPase activity. Journal of interferon & cytokine research : the official journal of the International Society for Interferon and Cytokine Research *25*, 435-443.

Vestal, D.J., Buss, J.E., Kelner, G.S., Maciejewski, D., Asundi, V.K., and Maki, R.A. (1996). Rat p67 GBP is induced by interferon-gamma and isoprenoid-modified in macrophages. Biochemical and biophysical research communications *224*, 528-534.

Vestal, D.J., Buss, J.E., McKercher, S.R., Jenkins, N.A., Copeland, N.G., Kelner, G.S., Asundi, V.K., and Maki, R.A. (1998). Murine GBP-2: a new IFN-gamma-induced member of the GBP family of GTPases isolated from macrophages. Journal of interferon & cytokine research : the official journal of the International Society for Interferon and Cytokine Research *18*, 977-985.

Vestal, D.J., Gorbacheva, V.Y., and Sen, G.C. (2000). Different subcellular localizations for the related interferon-induced GTPases, MuGBP-1 and MuGBP-2: implications for different functions? Journal of interferon & cytokine research : the official journal of the International Society for Interferon and Cytokine Research *20*, 991-1000.

Villasenor, T., Madrid-Paulino, E., Maldonado-Bravo, R., Urban-Aragon, A., Perez-Martinez, L., and Pedraza-Alva, G. (2017). Activation of the Wnt Pathway by Mycobacterium tuberculosis: A Wnt-Wnt Situation. Frontiers in immunology *8*, 50.

Virreira Winter, S., Niedelman, W., Jensen, K.D., Rosowski, E.E., Julien, L., Spooner, E., Caradonna, K., Burleigh, B.A., Saeij, J.P., Ploegh, H.L., *et al.* (2011). Determinants of GBP recruitment to Toxoplasma gondii vacuoles and the parasitic factors that control it. PloS one *6*, e24434.

Vogel, D.Y., Glim, J.E., Stavenuiter, A.W., Breur, M., Heijnen, P., Amor, S., Dijkstra, C.D., and Beelen, R.H. (2014). Human macrophage polarization in vitro: maturation and activation methods compared. Immunobiology *219*, 695-703.

Vopel, T., Hengstenberg, C.S., Peulen, T.O., Ajaj, Y., Seidel, C.A., Herrmann, C., and Klare, J.P. (2014). Triphosphate induced dimerization of human guanylate binding protein 1 involves association of the C-terminal helices: a joint double electron-electron resonance and FRET study. Biochemistry *53*, 4590-4600.

Vopel, T., Kunzelmann, S., and Herrmann, C. (2009). Nucleotide dependent cysteine reactivity of hGBP1 uncovers a domain movement during GTP hydrolysis. FEBS letters *583*, 1923-1927.

Vopel, T., Syguda, A., Britzen-Laurent, N., Kunzelmann, S., Ludemann, M.B., Dovengerds, C., Sturzl, M., and Herrmann, C. (2010). Mechanism of GTPase-activity-induced self-assembly of human guanylate binding protein 1. Journal of molecular biology *400*, 63-70.

Vorobjeva, N.V., and Pinegin, B.V. (2014). Neutrophil extracellular traps: mechanisms of formation and role in health and disease. Biochemistry Biokhimiia *79*, 1286-1296.

Vromman, F., Laverriere, M., Perrinet, S., Dufour, A., and Subtil, A. (2014). Quantitative monitoring of the Chlamydia trachomatis developmental cycle using GFP-expressing bacteria, microscopy and flow cytometry. PloS one *9*, e99197.

Wang, Y., Kahane, S., Cutcliffe, L.T., Skilton, R.J., Lambden, P.R., and Clarke, I.N. (2011). Development of a transformation system for Chlamydia trachomatis: restoration of glycogen biosynthesis by acquisition of a plasmid shuttle vector. PLoS pathogens *7*, e1002258.

Wang, Y., Liu, Q., Chen, D., Guan, J., Ma, L., Zhong, G., Shu, H., and Wu, X. (2017). Chlamydial Lipoproteins Stimulate Toll-Like Receptors 1/2 Mediated Inflammatory Responses through MyD88-Dependent Pathway. Frontiers in microbiology *8*, 78.

Warren, E., Teskey, G., and Venketaraman, V. (2017). Effector Mechanisms of Neutrophils within the Innate Immune System in Response to Mycobacterium tuberculosis Infection. Journal of clinical medicine *6*.

Watling, D., Guschin, D., Muller, M., Silvennoinen, O., Witthuhn, B.A., Quelle, F.W., Rogers, N.C., Schindler, C., Stark, G.R., Ihle, J.N., *et al.* (1993). Complementation by the protein tyrosine kinase JAK2 of a mutant cell line defective in the interferon-gamma signal transduction pathway. Nature *366*, 166-170.

Watts, E., Zhao, Y., Dhara, A., Eller, B., Patwardhan, A., and Sinai, A.P. (2015). Novel Approaches Reveal that Toxoplasma gondii Bradyzoites within Tissue Cysts Are Dynamic and Replicating Entities In Vivo. mBio *6*, e01155-01115.

Wehner, M., and Herrmann, C. (2010). Biochemical properties of the human guanylate binding protein 5 and a tumor-specific truncated splice variant. The FEBS journal *277*, 1597-1605.

Wehner, M., Kunzelmann, S., and Herrmann, C. (2012). The guanine cap of human guanylate-binding protein 1 is responsible for dimerization and self-activation of GTP hydrolysis. The FEBS journal *279*, 203-210.

Weiss, L.M., and Kim, K. (2000). The development and biology of bradyzoites of Toxoplasma gondii. Frontiers in bioscience : a journal and virtual library *5*, D391-405.

Wheelhouse, N., and Longbottom, D. (2012). Endemic and emerging chlamydial infections of animals and their zoonotic implications. Transboundary and emerging diseases *59*, 283-291.

White, M.W., Radke, J.R., and Radke, J.B. (2014). Toxoplasma development - turn the switch on or off? Cellular microbiology *16*, 466-472.

Whitelaw, J.A., Latorre-Barragan, F., Gras, S., Pall, G.S., Leung, J.M., Heaslip, A., Egarter, S., Andenmatten, N., Nelson, S.R., Warshaw, D.M., *et al.* (2017). Surface attachment, promoted by the actomyosin system of Toxoplasma gondii is important for efficient gliding motility and invasion. BMC biology *15*, 1.

Wilson, D.P., Whittum-Hudson, J.A., Timms, P., and Bavoil, P.M. (2009). Kinematics of intracellular chlamydiae provide evidence for contact-dependent development. Journal of bacteriology *191*, 5734-5742.

Wynn, T.A., Nicolet, C.M., and Paulnock, D.M. (1991). Identification and characterization of a new gene family induced during macrophage activation. Journal of immunology *147*, 4384-4392.

Wyrick, P.B. (2000). Intracellular survival by Chlamydia. Cellular microbiology *2*, 275-282.

Wyrick, P.B. (2010). Chlamydia trachomatis persistence in vitro: an overview. The Journal of infectious diseases *201 Suppl 2*, S88-95.

Yamamoto, M., Ma, J.S., Mueller, C., Kamiyama, N., Saiga, H., Kubo, E., Kimura, T., Okamoto, T., Okuyama, M., Kayama, H.*, et al.* (2011). ATF6beta is a host cellular target of the Toxoplasma gondii virulence factor ROP18. The Journal of experimental medicine *208*, 1533-1546.

Yamamoto, M., Okuyama, M., Ma, J.S., Kimura, T., Kamiyama, N., Saiga, H., Ohshima, J., Sasai, M., Kayama, H., Okamoto, T.*, et al.* (2012). A cluster of interferon-gamma-inducible p65 GTPases plays a critical role in host defense against Toxoplasma gondii. Immunity *37*, 302-313.

Yang, L.L., Li, R.M., Pan, X.H., Qian, M., and Du, B. (2012). [Construction of P2Y6 constitutive knock down breast cancer cell line and evaluation of its proliferation]. Xi bao yu fen zi mian yi xue za zhi = Chinese journal of cellular and molecular immunology *28*, 510-513.

Yarovinsky, F. (2014). Innate immunity to Toxoplasma gondii infection. Nature reviews Immunology *14*, 109-121.

Yarovinsky, F., Zhang, D., Andersen, J.F., Bannenberg, G.L., Serhan, C.N., Hayden, M.S., Hieny, S., Sutterwala, F.S., Flavell, R.A., Ghosh, S.*, et al.* (2005). TLR11 activation of dendritic cells by a protozoan profilin-like protein. Science *308*, 1626-1629.

Yasukawa, H., Sasaki, A., and Yoshimura, A. (2000). Negative regulation of cytokine signaling pathways. Annual review of immunology *18*, 143-164.

Yates, R.M., Hermetter, A., and Russell, D.G. (2005). The kinetics of phagosome maturation as a function of phagosome/lysosome fusion and acquisition of hydrolytic activity. Traffic *6*, 413-420.

Yin, Z., Pascual, C., and Klionsky, D.J. (2016). Autophagy: machinery and regulation. Microbial cell *3*, 588-596.

Yoon, E., Konold, P.E., Lee, J., Joo, T., and Jimenez, R. (2016). Far-Red Emission of mPlum Fluorescent Protein Results from Excited-State Interconversion between Chromophore Hydrogen-Bonding States. The journal of physical chemistry letters *7*, 2170-2174.

Zamboni, D.S., and Lima-Junior, D.S. (2015). Inflammasomes in host response to protozoan parasites. Immunological reviews *265*, 156-171.

Zeiner, G.M., Norman, K.L., Thomson, J.M., Hammond, S.M., and Boothroyd, J.C. (2010). Toxoplasma gondii infection specifically increases the levels of key host microRNAs. PloS one *5*, e8742.

Zeng, J., Parvanova, I.A., and Howard, J.C. (2009). A dedicated promoter drives constitutive expression of the cell-autonomous immune resistance GTPase, Irga6 (IIGP1) in mouse liver. PloS one *4*, e6787.

Zhang, Y., Yeruva, L., Marinov, A., Prantner, D., Wyrick, P.B., Lupashin, V., and Nagarajan, U.M. (2014). The DNA sensor, cyclic GMP-AMP synthase, is essential for induction of IFN-beta during Chlamydia trachomatis infection. Journal of immunology *193*, 2394-2404.

Zhao, C., Collins, M.N., Hsiang, T.Y., and Krug, R.M. (2013). Interferon-induced ISG15 pathway: an ongoing virus-host battle. Trends in microbiology *21*, 181-186.

Zhao, Y., Ferguson, D.J., Wilson, D.C., Howard, J.C., Sibley, L.D., and Yap, G.S. (2009a). Virulent Toxoplasma gondii evade immunity-related GTPase-mediated parasite vacuole disruption within primed macrophages. Journal of immunology *182*, 3775-3781.

Zhao, Y.O., Khaminets, A., Hunn, J.P., and Howard, J.C. (2009b). Disruption of the Toxoplasma gondii parasitophorous vacuole by IFNgamma-inducible immunity-related GTPases (IRG proteins) triggers necrotic cell death. PLoS pathogens *5*, e1000288.

Zhao, Y.O., Konen-Waisman, S., Taylor, G.A., Martens, S., and Howard, J.C. (2010). Localisation and mislocalisation of the interferon-inducible immunity-related GTPase, Irgm1 (LRG-47) in mouse cells. PloS one *5*, e8648.

Zhou, J., Lu, G., and He, S. (2016). Analysis of structures and epitopes of a novel secreted protein MYR1 in Toxoplasma gondii. Folia parasitologica *63*.

Zhou, Y., and Zhu, Y. (2015). Diversity of bacterial manipulation of the host ubiquitin pathways. Cellular microbiology *17*, 26-34.

Ziklo, N., Huston, W.M., Hocking, J.S., and Timms, P. (2016). Chlamydia trachomatis Genital Tract Infections: When Host Immune Response and the Microbiome Collide. Trends in microbiology *24*, 750-765.

Zuck, M., Feng, C., and Hybiske, K. (2015). Using Fluorescent Proteins to Visualize and Quantitate Chlamydia Vacuole Growth Dynamics in Living Cells. Journal of visualized experiments : JoVE.

Publications

The results of the work presented here, were in part presented at international conferences and submitted for publication in a peer reviewed scientific journal with the title:

'**Broad recruitment of mGBP family members to Chlamydia trachomatis inclusions**' by Valesca Lindenberg, Katja Mölleken, Elisabeth Kravets, Sonja Stallmann, Johannes Hegemann, Daniel Degrandi, Klaus Pfeffer.

Appendices

Appendix 1:
Supplementary video 1: mGBP2 encloses chlamydia inclusions in living cells
Live cell microscopy showing accumulation of constitutively expressed mCh::mGBP9 in a *C. trachomatis* pGFP::SW2 (C.t.) infected NIH/3T3 fibroblast, left-hand side (Figure 25), DIC : differential interference contrast, bar : 5 µm. Video (.mov) corresponding to snapshots in figure 32-34. Please see attached USB-flash drive

Appendix 2:
Supplementary video 2: mGBP9 accumulations in chlamydia infected living cells
Live cell microscopy showing accumulation of constitutively expressed mCh::mGBP2 in a *C. trachomatis* pGFP::SW2 (C.t.) infected NIH/3T3 fibroblast, left-hand side (Figure 25), DIC : differential interference contrast, bar : 5 µm. Video (.mov) corresponding to snapshots in figure 35. Please see attached USB-flash drive

Appendix 3:
Protein sequences of murine IFNγ-inducible GTPases used in the alignment (Figure 14A). See below for sequences and attached USB-flash drive for alignment.

Appendix 4:
Protein sequences of human IFNγ-inducible GTPases used in the alignment (Figure 14B). See below for sequences and attached USB-flash drive for alignment.

Appendix 5: Eidesstattliche Erklärung

Appendix 3:

Protein sequences of murine IFNγ-inducible GTPases used for alignment
(Incorporated in Figure 14A).

Name	Source	ORF
Gbp1(Gbp2b)	NP_034389.2	MASEIHMKGPVCLIKNSGEQLEVYQEALDILSAIQNPVVVVAIVGFYHTGKSYLMNKLAGKQKGFSLGSTVQSHTKGIWMWCMPHPEK PEHTLVLLDTEGLKDMQKGDNQNDCWIFALAVLLSSTFIYNSIGTINQQAMDQLHYVTELTDLIKSKSSPDQSDVDNSANFVGFFPIFVW TLRDFSLDLEFDGESITPDEYLETSLALRKGTDENTKKFNMPRLCIRKFFPKRKCFIFDRPGDRKQLSKLEWIQEDQLNKEFVEQVAEFTSYI FSYSGVKTLSGGITVNGPRLKSLVQTYVSAICSGELPCMENAVLTLAQIENSAAVQKAITYYEEQMNQKIHMPTETLQELLDLHRTCEREAI EVFMKNSFKDVDQKFQEELGAQLEAKRDAFVKKNMDMSSAHCSDLLEGLFAHLEEEVKQGTFYKPGGYYLFLQRKQELEKKYIQTPGK GLQAEVMLRKYFESKEDLADTLLKMDQSLTEKEKQIEMERIKAEAAEAANRALAEMQKKHEMLMEQKEQSYQEHMKQLTEKMEQER KELMAEQQRIISLKLQEQERLLKQGFQNESLQLRQEIEKIKNMPPPRSCTIL
Gbp2	NP_034390.1	MASEIHMSEPMCLIENTEAQLVINQEALRILSAITQPVVVVAIVGLYRTGKSYLMNKLAGKRTGFSLGSTVQSHTKGIWMWCVPHPKKA GQTLVLLDTEGLEDVEKGDNQNDCWIFALAVLLSSTFIYNSIGTINQQAMDQLHYVTELTDLIKSKSSPDQSGVDDSANFVGFFPTFVWT LRDFSLELEVNGKPVTSDEYLEHSLTLKKGADKKTKSFNEPRLCIRKFFPKRKCFIFDRPAQRKQLSKLETLREEELCGEFVEQVAEFTSYILSY SSVKTLCGGIIVNGPRLKSLVQTYVGAISNGSLPCMESAVLTLAQIENSAAVQKAITHYEEQMNQKIQMPTETLQELLDLHRPIESEAIEVF LKNSFKDVDQKFQTELGNLLVAKRDAFIKKNMDVSSARCSDLLEDIFGPLEEEVKLGTFSKPGGYYLFLQMRQELEKKYNQAPGKGLQAE AMLKNYFDSKADVVETLLQTDQSLTEAAKEVEEERTKAEAAEAANRELEKKQKEFELMMQQKEKSYQEHVKKLTEKMKDEQKQLLAEQ ENIIAAKLREQEKFLKEGFENESKKLIREIDTLKQNKSSGKCTIL
Gbp3	NP_001276421.1	MEAPICLVENWKNQLTVNLEAIRILEQIAQPLVVVAIVGLYRTGKSYLMNRLAGRNHGFSLGSTVQSETKGIWMWCVPHPTKPTHTLVL LDTEGLGDVEKGDPKNDSWIFALAVLLSSTFVYNSMSTINQQALEQLHFVTELTQLIRAKSSPREDKVKDSSEFVGFFPDFIWAVRDFALE LKLNGRPITEDEYLENALKLIQGDNLKVQQSNMTRECIRYFFPVRKCFVFDRPTSDKRLLLQIENVPENQLERNFQVESEKFCSYIFTNGKT KTLRGGVIVTGNRLGTLVQTYVNAINSGTVPCLENAVTTLAQRENSIAVQKAADHYSEQMAQRMRLPTDTLQELLTVHAACEKEAIAVF MEHSFKDDEQEFQKKLVVTIEERKEEFIRQNEAASIRHCQAELERLSESLRKSISCGAFSVPGGHSLYLEARKKIELGYQQVLRKGVKAKEVL KSFLQSQAIMEDSILQSDKALTDGERAIAAERTKKEVAEKELELLRQRQKEQEQVMEAQERSFRENIAKLQEKMESEKEMLLREQEKMLE HKLKVQEELLIEGFREKSDMLKNEISHLREEMERTRRKPSLFGQILDTIGNAFIMILPGAGKLFGVGLKFLGSLSS
Gbp4 iso1	NP_001242934.1	MTQPQMAPICLVENHNEQLSVNQEAIEILDKISQPVVVVAIVGWSHTGKSYLMNCLAGQNHVSGTLPTSQRFPSGLHRAVSDQGHLD VVHAPPHQARALVLLDTEGLGDVEKGDPKNDLWIFALSVLLSSTFVYNSMNTINHQALEQLHYVTELTELIRAKSSPNPHGIKNSTEFVSF FPDFVWTVRDFMLELKLNGEDITSDEYLENALKLIPGNNPRIQASNSARECIRRFFPNRKCFVFEWPTHDIELIKQLETISEDQLDPTFKESA MAFASYIFTYAKIKTLREGIKVTGNGLGTLVTTYVDAINSGAVPCLDDAVTTLAQRENSVAVQKAASHYSEQMAQRLSLPTDTIQELLDVH AACEKEAMAVFMEHSFKDENQQFLKKLVELLREKNGLFLLKNEEASDKYCQEELDRLSKDLMDNISTFSVPGGHRLYMDMREKIEHDY WQVPRKGVKASEVFQNFLQSQAIIESSILQADTALTAGQKAIAEKHTKKEAAEKEQDLLRQKQKEHQEYMEAQEKRNKENLEQLRRKLE QEREQLIKDHNMMLEKLTKEQKTFREEGYKTQAEELRREIHQLGHNIKEMKQNGDSLVESILRSWFSFISPPSESEKAISSVLSLLRKKDRL
Gbp4 iso2	NP_032646.2	MNTINHQALEQLHYVTELTELIRAKSSPNPHGIKNSTEFVSFFPDFVWTVRDFMLELKLNGEDITSDEYLENALKLIPGNNPRIQASNSARE CIRRFFPNRKCFVFEWPTHDIELIKQLETISEDQLDPTFKESAMAFASYIFTYAKIKTLREGIKVTGNGLGTLVTTYVDAINSGAVPCLDDAVT TLAQRENSVAVQKAASHYSEQMAQRLSLPTDTIQELLDVHAACEKEAMAVFMEHSFKDENQQFLKKLVELLREKNGLFLLKNEEASDKY CQEELDRLSKDLMDNISTFSVPGGHRLYMDMREKIEHDYWQVPRKGVKASEVFQNFLQSQAIIESSILQADTALTAGQKAIAEKHTKKEA AEKEQDLLRQKQKEHQEYMEAQEKRNKENLEQLRRKLEQEREQLIKDHNMMLEKLTKEQKTFREEGYKTQAEELRREIHQLGHNIKEM KQNGDSLVESILRSWFSFISPPSESEKAISSVLSLLRKKDRL
Gbp5	NP_705792.2	MAPEIHMPEPLCLIGSTEGHLVTNQEALKILSAITQPVVVVAIVGLYRTGKSYLMNKLAGKEKGFSVGSTVQSHTKGIWMWCVPHPQKP DHTLVLLDTEGLGDVEKDDKKNDTQIFALAILLSSTFVYNTMNKIDQGAIDLLHNVTELTDLLRTRNSSDSNQTEGEGPADMSFFPDLVW TLRDFFLDLQANGHAITSDEYLENSLKLKQGSDERTQTFNLPRLCIQKFFPVKKCFVFDAPALGSKLSQLPTLSNEELNSDFVQDLSEFCSHI FTQSKTKTLPGGIQVNGPRLESLVLTYVDAINSGALPSIENTVVTLARRENSAAVQKAIGHYDQLMSEKVQLPTETLQELLDLHRTCEREAI EIFRKHSFKDEGEFFQKELESLLSAKQDEICKKNADASAALCSTLLGSIFKPLEQEVAQEFYHKPGGHKLFLQRMEQLKANYRQQPGKGTQ AEEVLQTYLNAKETVSRTILQTDQVLTDKEIQSKAEQERAEAARLEAQRLEAIRIQEEQRKAEMERQHQEQLRQIALEKARVAQEQQWIL KQRAQEEADRIKAEQEAQLRALQQQLQHMREMNHHRRHHHDCVIS

Gbp5a	AAN52282.1	MAPEIHMPEPLCLIGSTEGHLVTNQEALKILSAITQPVVVVAIVGLYRTGKSYLMNKLAGKEKDLVWTLRDFFLDLQANGHAITSDEYLEN SLKLKQGSDERTQTFNLPRLCIQKFFPVKKCFVFDAPALGSKLSQLPTLSNEELNSDFVQDLSEFCSHIFTQSKTKTLPGGIQVNGPRLESLV LTYVDAINSGALPSIENTVVTLARRENSAAVQKAIGHYDQLMSEKVQLPTETLQELLDLHRTCEREAIEIFRKHSFKDEGEFFQKELESLLSA KQDEICKKNADASAALCSTLLGSIFKPLEQEVAQEFYHKPGGHKLFLQRMEQLKANYRQQPGKGTQAEEVLQTYLNAKETVSRTILQTDQ VLTDKEIQKKAEQERAEAARLKAQRLEAIRIQEEQRKAEMERQHQEQLRQIALEKARVAQEQQWILKQRAQGRCPVIWCLDLLLAEDEG PKQDLSQKLCCFGQEGGRLSGAEDGAASEALWISPFPETAGLCIPHCHPSNLPSVESRSQGGSRRGLRHKPLRPGGPLCTHQEGARLSG AEDGTASEALWLSPVLETVGLFIPHPHPCSLPSTDSRSEGGSRRGLRQKPLGLVDPCALTRKVAGCL
Gbp6	NP_919317.2	MTQPQMAPICLVENHNEQLSVNQEAIEILDKISQPVVVVAIVGLYRTGKSYLMNCLAGQNHGFPLGSTVQSQTKGIWMWCMPHPTKP EHTLVLLDTEGLGDVEKGDPKNDLWIFALSVLLSSTFIYNSMITINHQALEQLHYVTELTELIRAKSSPNPAGIKNSTEFVSFFPDFVWTVRD FMLELKLNGEDITSDDYLENALKLIPGDKPRMQASNSCRECIRLFFPNRKCFVFDRPTHDKELLQKLDSITEDQLDPKFQEVTKAFVSYIFTY AKIKTLKEGIKVTGNRLGILVTTYVNAINSGAVPCLDDAVTTLAQRENSVAVQKAADHYSEQMAQRLRLPTETLQELLDVHAACEKEAMA VFMEHSFKDENQQFLKKLVELIGENKELFLSKNEEASNKYCQEELDRLSKDFMENISTFFVPCGHKLYMDKREKIEHDYWQVPRKGVKAS EVFQSFLQSQAFIESSILQADTALTAGEKAIAEERAQKVAAEKEQELLRQKQKEQQEYMEAQEKSHKENLEQLRRKLEQEREQDIKDHD MMLKKLMKDQKAFLEEGFKKKAEEMNKEIQQLRDVIKDKKRNTDRIKEALLNGFSTVLFHYLVRYLKHL
Gbp7	NP_663520.2	MASGPNMEAPVCLVENENEELRVNSKAINILERITQPVVVVAIVGLYRTGKSYLMNRLAGQNHGFNLGTTVRSETKGIWMWCVPHPSK PKFTLVLLDTEGLGDVEKGDPKNDSWIFALAVLLSSTFVYNSMSTINHQALEQLHYVTELTERIRAKSTSRSEEVDDSDEFVSFFPDFIWTV RDFVLELKLEGRVITADEYLENALKLIPGMSIKAQKANLPRECIRHFFPRRKCFVFDRPTKDKELLVHVEEMPEDQLDHSFQVQSKEFCSYIF SNSKAKTLKEGIVVNGNRLATLVTTYVDAINSGDVPCLENAVTTLAQRENSIAVQKAADHYSEQMAQRMRLPTDTLQELLTVHTACEKE AIAVFMEHSFKDENQQFQKNLVVTIEEKKEDFLRQNEAASLSHCQAELDKLSESLRESISRGVFSVPGGHRLYLEARKKVEQDYERVPRKG VKANHVLQSFLQSQISIEDSIMQSDKALTDGQKAMEAERAQKEAAEKEQELLRQKQKELQQVMEAQERSYKENVAQLHEKMETERKNI LREQEVKLEHKLKIQKDMLNEGFKRKCEAMDLEISQLQKEIQLNKEKNSSLGAKILDGFGDVLISVVPGSGKYFGLGLKILSSQMNQTQNS DKVRKL
Gbp8	NP_083785.3	MTQPQMAPICLVENHNEHLSVNHEAIEILEKISQPVVVVAIVGLYRTGKSYLMNRLAGQNHGFPLGSTVQSQTKGIWMWCMPHPTKP EHTLVLLDTEGLGDVEKGDPKNDLWIFALSVLLSSTFIYNSMNTISHDSLEKLHYVTELTELIRAKSSPNPDGIKNSTEFVSFFPDFVWTVRD FMLELKLNGEDITSDEYLENALKLIPGLGILVTTYVDAINSGAVPCVDDAVTTLAQRENSVAVQRAADHYSEQMVQRLSLPTDTLQELLDV HAACEKEAMAVFMEHSFKDENQQFLKKLVELIGEAKVLFLLKNEEASDKYCQEELDRLSKDLMDNISTFSVPGGHRLYMDMREKIEHDY WQVPRKGVKAREVFQSFLQSQAIIESSILQADTALTAGQKAIAEERTKKEAAEKEQDLLRQKQKEQQEYMEAQEKRNKENIEQLRRKLEQ EREQLIKDHNMMVEKKLKEQKALLEEGFKKKAEEMDGEIQQLKHNIEDMKKKQWFHFRYYYKRSCFIYFFSHFND
Gbp9	NP_766365.1	MTQPQMAPICLVENHNEQLLVNQEAIEILEKISQPVVVVAIVGLYRTGKSYLMNCLAGQNHGFPLGSTVQSQTKGIWMWCMPHPTKP EHTLVLLDTEGLGDVEKSNPKNDSWIFALSVLLSSTFVYNSMSTINHQALEQLHYVTELTELIRSKSSRNPHGIKNSTEFVSFFPDFVWTVR DFMLELKLNGEDITSDEYLENALKLIPGYNPRVQASNSARECIRCFFPNRKCFVFDRPTHDRELLQKLETISEDQLDLKFREGTKAFVSYVFT YAKIKTLREGIKVTGNRLGTLVTTYVDAINSGAVPCLDDAMTSVARRENSVAVQKAADHYSEQMAQRLRLPTDTLQELLDVHAACEKEA MAVFMEHSFKDENQQFLKKLVEIISEKIAFFWLKNEEASNKYCQEELDRLSKDFMDNISTFSVPGGHRIYTDMRKKIERDYWQVPRKGV KACEVFQNFLQSQYIIESSILQADRALTAGEKAIAEERAQKEVAEKEQELLRQKQKEQQEYMEAQEKRNKENLEQLRRKLMQEREQDIKD HDMMLEKQLKDQKAFLEEGFTNKAEEINAEIERLEHNIKDKKENIGPILELIEKAFCAGVFSSLIMVALLTHNPSLLRK
Gbp10	NP_001034735.2	MTQPQMAPICLVENHNEQLSVNQEAIEILDKISQPVVVVAIVGWSRTGKSYLMNCLAGQNHGFPLGSTVQSQTKGIWMWCMPHPTK PEHTLVLLDTEGLGDVEKGDPKNDLWIFALSVLLSSTFIYNSMITINHQALEQLHYVTELTELIRAKSSPNPAGIKNSTEFVSFFPDFVWIVR DFMLELKLNGEDITSDDYLENALKLIPGDKPRMQASNSCRECIRLFFPNRKCFVFDRPTHDKELLQKLDSITEDQLDPKFQEVTKAFVSYIFT YAKIKTLKEGIKVTGNKLGILVTTYVDAINSGAVPCLDDAVTTLAQRENSVAVQKAADHYSEQMAQRLRLPTETLQELLDVHAACEKEAM AVFMEHSFKDENQQFLKKLVELIGENKELFLSKNEEASNKYCQEELDRLSKDFMENISTFFVPCGHKLYMDKREKIEHDYWQVPRKGVKA SEVFQSFLQSQAFIESSILQADTALTAGKKAIAEERAQKVAAEKEQDLLRQKQKEQQEYMEAQEKSHKENIEQLRRKLMQEREQLIKDHN MMLKKQLKDQKAFLEEGFKKKAEEMNKEIQQLRDVIKDKKRNTDRIKDALLNGFSTVLFHYLVRYLKHL
Gbp11	NP_001034736.3	MTQPQMAPICLVENHNEQLLVNQEAIEILDKISQPVVVVAIVGLYRTGKSYLMNRLAGQNHGFPLGSTVQSQTKGIWMWCVPHPTKP EHTLVLLDTEGLGDVEKGDPKNDLWIFALSVLLSSNFIYNSMNTISHDSLEKLHYVTELTELIRAKSSPNPHGIKNSTEFVSFFPDFVWTVRD FTLKLKLNGEDITSDGYLENALKLIPDNNPRMQASNLARECIRRFFPNRKCFVFDRPTYDIELLQKLETISEDQLDPMFQKRTKAFVSYIFNY AKIKTLKEGIKVTGNGLGILVTTYVDAINSGAVPCLHDAVTTLAQRENSVAVQKAADHYSEQMAQRLRLPTETLQELLDVHAACEKEAM AVFMEHSFKDENQQFLKKLVELISEKNGLFLLKNEEASDKYCQEELDRLSKDLMDNISTFSVPGGHRLYMDMREKIEHDYWQVPRKGVK AIEVFQSFLQSQAIIESSILQADTALIAGQKAIAEKCTNKEAAEKEQDLLRQKQKEQQKYMEAQEKRNKENLEQLRRKLMQEREQLIKDH NMMLEKLMKEQKALLEEGYKKKAEEMRREIYRLRHNIKDMKQNSDFFVDSAVRDLALFLSSLLIEKAIKGLISFFRSK
Irga1	Bekpen 2005	MGQLFSLLKNKCQFLVSSVAEYFKKFKKIVIIILQEVTTSIELDMKKENFQEANSAICDALKEIDSSLVNVAVTGETGSGKSSFINTLRGIGHE EEGAAKTGVVEATMERHPYKHPNMPNVVFWDLPGIGSTKFPPKTYLEKMKFYEYDFFIIISATCFKKNDIDLAKAISMMKKEFYFVRTKV DTDLRNEEDFKPQTFDKEKVLQDIRLNCVNTFKENGIAEPPIFLISNENVCHYDFPVLMDKLISDLPDYKRHNFMLSLPNITDSVIETKRQSL KQRHWLQGFAGVLLSYLH

Irga2	Bekpen 2005	MGQLFSSRRSEDQDLSSSFIEYLKECEKGINIIPHEIITSIEINMKKGNIQEVNSTVRDMLREIDNTPLNVALTGETGSGKSSFINTLRGIGHEE GGAAHTGVTDKTKERHPYEHPKMPNVVFWDLPGTGSEDFQPKTYLEKMKFYEYDFFIIISATRFKKNDIDLAKAIGIMKKEFYFVRTQVD SDLRNEEDFKPQTFDREKVLQDIRLNCVNTFRENGIAEPPIFLISNKNVCHYDFPVLMDKLISDLPVFKRQNFMFSLPNITDSVIEKKRNFLR WKTWLEGFADGLLSFFLESDLETLEKSMKFYRTVFGVDDASLQRLARAWEIDQVDQVRAMIKSPAVFTPTDEETIQERLSRYNQEFCLA NGYLLPKNHCREILYLKLYFLDMVTEDAKTLLKEICLRN
Irga3	Bekpen 2005	MGQLFSHIPKDEDKGNLESSFTEYFRNYKQETKIISEETTRSIELCLKRGDFQRANSVISDALKNIDNTPINIAVTGESGAGKSSLINALREVK AEEESAAEVGVTETTMKVSSYKHPKVKNLTLWDLPGIGTMKFQPKDYLEKVEFKKYDFFIIVSSSRFTKLELDLAKATRIMKKNYYFVRSKV DCDLDNEKKSKPRNFNRENTLNQVRNSYLDTFRESKIDEPQVFLISNHDLSDYDFPVLMDTLLKDLPAEKRQNFLLSLPNITEAAIQKKYNS TKQIIWLQATKDGLLATVPVVGILKDLDKERLKKRLDYYRDLFGVDDESLMFMAKDAQVPVELLIKNLKSPNLLKCKEETLEELLLNCVEKF ASANGGLLAAGLYFRKTYYLQFHFLDTVAEDAKVLLKAAQTHFAHSF
Irga4	Bekpen 2005	MGQLLSDTSKTEDNEDLVSSFNEYFKNIKTEKIISQETIDLIKLYLNKGNIHGANSLISDALRNIDNAPINIAVTGESGAGKSSLINALIGIGPEE EGAAEVGVIETTMKRTSYKHPKIETLTLWDLPGIGTQKFPPKTYLEEVKFKEYDFFIIVSATRFTKLELDLAKAITNMKKNYYFVRTKVDIDVE NERKSKPRTFEREKALKQIQSYSVKIFNDNNMAVPPIFLISNYDLSDYDFPFLVDTLIKELHVQKRHNFMLSLPNFTDQAIDRKYKATQQFI WLEAFKIGVVAIFPVLGNLRNKDMKKIKNTLNYYQKIFGVDDESLELVAKDFQVPVEQVKKTMKTPHLLKKYREETFRNDFKKLVSTFGRL LAVGLYFPAIYYLQLHILDTVTEDAKVLLRWKYSKPRSNSTYP
Irga5	Bekpen 2005	MGQLFSGTSKSEALCSSFTEYFQKFKVENKIISQEISTLIELYLTLGDVQQANNAITYALRXLARTPQNVALIGESGRGKYSFINVFRGLDMK RKMATVGVVETTMNRTPYRNPNIPNVIIWDLPGIGTTNFPPKHYLKKMQFYVMYDFFIIVSATCFRKNDIDLSKAVVMIKKKDFLLRTKE DIDIENEN
Irga6	NP_001139747.1	MGQLFSSPKSDENNDLPSSFTGYFKKFNTGRKIISQEILNLIELRMRKGNIQLTNSAISDALKEIDSSVLNVAVTGETGSGKSSFINTLRGIGN EEEGAAKTGVVEVTMERHPYKHPNIPNVVFWDLPGIGSTNFPPNTYLEKMKFYEYDFFIIISATRFKKNDIDIAKAISMMKKEFYFVRTKV DSDITNEADGKPQTFDKEKVLQDIRLNCVNTFRENGIAEPPIFLLSNKNVCHYDFPVLMDKLISDLPIYKRHNFMVSLPNITDSVIEKKRQFL KQRIWLEGFAADLVNIIPSLTFLLDSDLETLKKSMKFYRTVFGVDETSLQRLARDWEIEVDQVEAMIKSPAVFKPTDEETIQERLSRYIQEFC LANGYLLPKNSFLKEIFYLKYYFLDMVTEDAKTLLKEICLRNKLLSN
Irga6homo	NP_001013850.1	MGQLFSSPQSEHQDLASSFTEYFKKFKMGNKIISQDIISLVELSMAKGNIQGANSAIKNALKEIDSTPLNVAVTGESGSGKSSFINTLRGIG HEEKGAAKTGVMEETMERHPYKHPNMPNVVFWDLPGIGTTKFPPKTYLEKMKFYEYDFFIIISATRFKKNDIDLAKAISMMKKEFYFVRT KVDSDLNNEEDFKPQNFDREKVLQNIRLNCVNNFKENGIAEPPIFLVSNKNVCHYDFPVLMDKLISDLPVYKRHNFMLSLPNITESAIEKK RQFLKQRIWLEGFAADLMSIIPTLTFLLDSDLETLKKSMKFYRTVFGVDEASLKSLATAWKIPVDQVEAMMKSPAVFKPTDEETIQERLSR YVREFCLANGFLVTKNHYLREIFYLKYYFLDMVTEDAKTLLKEICLRNKLLSN
Irga7	Bekpen 2005	MDQLLSDTSKNEDNDDLVSSFNAYFKNIKTENKIISQETIDLIELHLNKGNIHGANSLIREALKNIDNAPINIAVTGESGVGKSSFINALIGTG PEEEGAAEVGVIETTMKRNFYKHPKIETLTLWDLPGIGTQKFPPKTYLEEVKFKEYDFFIIVSSTRFTKHELDLAKAIGIMKKNYYFVRTKVDI DLENERKSKPRTFDREKTLKQIQSYAMNTFSDNNMAIPPIFMVSNYDLSKYDFPVMMDTLIKDLHAEKRHNFMLSLPGITEAAIDRKHKA TQQIVWLEAFNVGLLANFPVTGILGDNDVKKLEKSLNYYRKIFGVDDESLELVAKDFQVPVEQVKEIMKSPHLLKTNGKETLGEKLLKYLE KFETATGGLLAVGLYFRKTYYLQLHFLDTVTEDAKVLLRWKYSKPRSNSTYP
Irga8	Bekpen 2005	MGQLFSNMPKDEDKGNLESSFTEYFRNYKQETKIISEETTRSIELCLKKGDIQRANSIISDALKNIDNAPINIAVTGESGAGKSSLINALREIK AEEESAAEVGVTETTMKVYSYKHPKVKNLTLWDLPGIGTKKFPPKTYLETVEFKKYDFFIIVSAIRFTNHEIELAKAIRIMKKNYYFVRSKVDF DLYNEEKSKPRNFNRENTLNQVRNYYLDTFRESKIDEPQVFLISNHDLSDYDFPVLMDTLLKDLPAEKRHNFLLSLPNITEAAIQKKYNSPK QYIWLQAMEDGLLATVPAVGILKDLDKERLKRSLDYYRDLFGVDDESLMFMAKDAQVPFELLKIKLKSPYLLELEEETLGGLILNCVEKFAS ANGGLLATGLYFRKTYYLQFHFLDTVAEDAKVLLKEAY
Irgb1	Bekpen 2005	QHPPLNTATCQTSTGRTSQITAQLLEFNFKNFFKNFKKESKILSEETITLIESHLENKNLKEALTVISHALRNIDKAPLNIAVTGETGTGKSSFI NALRGISSEEKDAAPTGVIETTMKRTPYPHPKLPNVTIWDLPGIGSTNFPPQNYLTEMKFGEYDFFIIISATRFKEIDAHLAKAIAKMNIKFY FVRTKIDQDISNEQRSKPKSFNRDSVLKKIKDECLGLLQKVLSSQPPIFLVSNFDVSDFDFPKLETTLLKELPAHKRHLFMMSLHSVTETTIAR KRDFLRQKIWLEALKAGLWATIPLGGLVRDKMQKLEETLTLYRSYFGLDEASLENIAKDFNVSVNEIKAHLRSLQLLTKNNDMSFKEKLLKY IEYISCVTGGPLASGLYFSKTYYWQSLFIDTVASDAKSLLNKEEFLSEKPGSCLSDLPEYWETGMEL
Irgb2b1	NP_001039005.1	MGQTSSSTSPPKEDPPLTFQVKTKVLSQELIASIESSLEDGNLQETVSAISSALGDIEKVPLNIAVMGETGAGKSSLINALQGVGDDEEGAA ASTGVVHTTTERTPYTYTKFPSVTLWDLPSIGSTAFQPHDYLKKIEFEEYDFFIIVSAIRIKQSDIELAKAIVQMNRGLYFVRTKTDSDLENEKL CNPMRFNRENILKSIRICLSSNLKERFQQEPPVFLVSNFDVSDFDFPKLESTLLSQLPAYKHQIFMSTLQVVINAIVDRKRDMLKQKIWKESI MPRAWATIPSRGLTQKDMEMLQQTLNDYRSSFGLNEASLENIAEDLNVTLEELKANIKSPHLFSDEPDTSLTEKLLKYIGNPYFSKVFHLQ NYFIDTVASDAKIILSKEELFTEQHPPLNTATCQTSTGRTSQITAQLLEFNFKNFFKNFKKESKILSEETITLIESHLENKNLKEALTVISHALRNI DKAPLNIAVTGETGTGKSSFINALRGISSEEKDAAPTGVIETTMKRTPYPHPKLPNVTIWDLPGIGSTNFPPQNYLTEMKFGEYDFFIIISAT RFKEIDAHLAKAIAKMNIKFYFVRTKIDQDISNEQRSKPKSFNRDSVLKKIKDECLGLLQKVLSSQPPIFLVSNFDVSDFDFPKLETTLLKELPA HKRHLFMMSLHSVTETTIARKRDFLRQKIWLEALKAGLWATIPLGGLVRDKMQKLEETLTLYRSYFGLDEASLENIAKDFNVSVNEIKAHL RSLQLLTKNNDMSFKEKLLKYIEYISCVTGGPLASGLYFSKTYYWQSLFIDTVASDAKSLLNKEEFLSEKPGSCLSDLPEYWETGMEL

Irgb3	Bekpen 2005	MAQLLVFSFENFFKNFKKESKILSEETITLIESHLEDKNLQGALSEISHALSNIDKAPLNIAVTGETGTGKSSFINALRGVRDEEEGAAPTGVV ETTMKRTPYPHPKLPNVTIWDLPGIGSTTFPPQNYLTEMKFGEYDFFIIISATRFKEIDAHLAKTIEKMNTKFYFVRTKIDQDVSNEQRSKPR SFNRDSVLKKIRDDCSGHLQKALSSQPPVFLVSNFDVSDFDFPKLETTLLRELPSHKRHLFMMSLHSVTETAIARKRDFLRQKIWLEALKAG LWATIPLGGLVRNKMQKLEETLTLYRSYFGLDEASLENIAKDFNVSVNEIKAHLRFLQLFTKNNDMSFKEKLLKYIEYISCVTGGPLASGLYF RKTYYWQSLFIDTVASDAKSLLNKEEFLSEKPGSCLSDLPEYWETGMEL
Irgb4	Bekpen 2005	QHPPLHTATCQPSSSRPSRLTLQLLVFSFENFFKNFKKESKILSEETITLIESHLEDKNLQGALTEISHALSNIDKAPLNIAVTGETGTGKSSFIN ALRGVRDEEEGAAPTGVVETTMKRTPYPHPKLPNVTIWDLPGIGSTTFPPQNYLTEMKFGEYDFFIIISATRFKEIDAHLAKTIEKMNTKFY FVRTKIDQDVSNEQRSKPRSFNRDSVLKKIRDDCSGHLQKALSSQPPVFLVSNFDVSDFDFPKLETTLLRELPSHKRHLFMMSLHSVTETAI ARKRDFLRQKIWLEALKAGLWATIPLGGLVRNKMQKLEETLTLYRSYFGLDEASLENIAKDFNVSVNEIKAHLRSLQLFTKNNDMSFKEKL LKYIEYISCVTGGPLASGLYFRKTYYWQSLFIDTVASDAKSLLNKEEFLSEKPGSCLSDLPEYWETGMEL
Irgb6	NP_035709.3	MAWASSFDAFFKNFKRESKIISEYDITLIMTYIEENKLQKAVSVIEKVLRDIESAPLHIAVTGETGAGKSTFINTLRGVGHEEKGAAPTGAIET TMKRTPYPHPKLPNVTIWDLPGIGTTNFTPQNYLTEMKFGEYDFFIIISATRFKENDAQLAKAIAQMGMNFYFVRTKIDSDLDNEQKFKP KSFNKEEVLKNIKDYCSNHLQESLDSEPPVFLVSNVDISKYDFPKLETKLLQDLPAHKRHVFSLSLQSLTEATINYKRDSLKQKVFLEAMKAG ALATIPLGGMISDILENLDETFNLYRSYFGLDDASLENIAQDLNMSVDDFKVHLRFPHLFAEHNDESLEDKLFKYIKHISSVTGGPVAAVTY YRMAYYLQNLFLDTAANDAIALLNSKALFEKKVGPYISEPPEYWEA
Irgb6homolog	NP_001138636.1	MAWASSFDAFFKNFKRESKIISEYDITLIMTYIEENKLQKAVSVIEKVLRDIESAPLHIAVTGETGAGKSTFINTLRGVGHEEKGAAPTGAIET TMKRTPYPHPKLPNVTIWDLPGIGTTNFTPQNYLTEMKFGEYDFFIIISATRFKENDAQLAKAIAQMGMNFYFVRTKIDSDLDNEQKFKP KSFNKEEVLKNIKDYCSNHLQESLDSEPPVFLVSNVDISKYDFPKLETKLLQDLPAHKRHVFSLSLQSLTEATINYKRDSLKQKVFLEAMKAG ALATIPLGGMISDILENLDETFNLYRSYFGLDDASLENIAQDLNMSVDDFKVHLRFPHLFAEHNDESLEDKLFKYIKHISSVTGGPVAAVTY YRMAYYLQNLFLDTAANDAIALLNSKALFEKKVGPYISEPPEYWEA
Irgb7	Bekpen 2005	PFWFVPPLGTIDICQDWVKLPLLHPLQRRILLLTFQMKTKILSQELITFIELYLEDGNLXETVSAISSALGDIEKVPLNIAVMGETGAGKSSLIN ALQGTGADEDGVTAPVGVVYTTIEKKSYPYAKFPSAILWELPAIGFHHFQPHDYLKKIKFEEYDFIIVSAGRIKHSDVELAKAIVQMNRGLY FNRTKTDIDLKNEKLYNPMRFNRENTLKSLQICISSNLKECFHQEPPVFLVSNFDVSDFDFPKLESTLLSQLPAYKHQIFMRTLQVVINAIVD WKRDMLKQKVWKESTTPRAWATIPSLGLTQKDMEMLQQTLNDYRSSFGLDEASLKNIAEDLNVTLEELKANIKSPHLLSDEPDTSLTEKL LKYIGNPYFSKVFHLQNYFIDTVASDVKIILSKEELFTEQVSSFNSKASPYREESVGEVFPVGPGSTFLFHFFEMFQSDSDKLCHVHVLLLLTS WGLSGETVT
Irgb8	Bekpen 2005	MAQLLVISFENFFKNFKKESKILSEETITLIESHLEDKNLQGALSEISHALSNIDKAPLNIAVTGETGTGKSSFINALRGVRGEEEGAAPTGVV ETTMKRTPYPHPKLPNVTIWDLPGIGSTNFQPQNYLTEMKFGEYDFFIIISATRFKEIDAHLAKAIAKMNTKFYFVRTKIDQDVSNEQRSKP KSFNRDSVLKKIRDDCSGHLQKVLSSQPPVFLVSNFDVSDFDFPKLENTLLRELPAHKRHLFMMSLHSVTETAIDRKRDFLRQRIWLEALK AGVWTTIPLGGLVRDKMQKLEETLTLYRSYFGLDEASLENIAKDFNVSVNEIKAHLRSLQLLTKNNDMSFKEKLLKYIEYISCVTGGPLASGL YFRKTYYWQSLFIDTVASDAKSLLNKEEFLSEKPGSCLSDLPEYWETGMEL
Irgb9	Bekpen 2005	MGQTSSSTLPPKDDPDFIASFGTNLQNFKMKTKILSQELIAFIESSLEDGNLRETVSAISSALGGIEKAPLNIAVMGETGAGKSSLINALQGV GDDEEGAAASTGVVHTTTERTPYTYTKFPSVTLWDLPGIGSTAFQPHDYLKKIEFEEYDFFIIVSSGRFKHNDAELAKAIVQMNRSFYFVRT HTDLDLMVVKLSDPRKFNKENILEQIRNSISNILKEVTHQEPPVFLVSNFDVSDFDFPNLESTLLSQLPAYKHHMFMLTLPIVTDSTIDRKR DMLKQKIWKESIMPRAWATIPSRGLTQKDMEMLQQTLNDYRSSFGLDEASLENIAEDLNVTLEELKANIKSPHLLSDEPDTSLTEKLLKYI GNPYFSKVFHLQNYFIDTVASDVKIILSKEELFTEQVSSFNSKASPYWEESVGKVFPVGPGSTFLFHFFEMFQSDSDKLCHVHVLLLLTSWG LSGETVT
Irgb10	NP_001128587.1	MGQSSSKPDAKAHNMASSLTEFFKNFKMESKIISKETIDSIQSCIQEGDIQKVISIINAALTDIEKAPLNIAVTGETGAGKSTFINALRGIGHE ESESAESGAVETTKDRKKYTHPKFPNVTIWDLPGVGTTNFKPEEYLKKMKFQEYDFFLIISSARFRDNEAQLAEAIKKMKKKFYFVRTKIDS DLWNEKKAKPSSYNREKILEVIRSDCVKNLQNANAASTRVFLVSSFEVAQFDFPSLESTLLEELPAHKRHIFVQCLPTITEPAIDRRRDVLKQ TIWLEALKAGASATIPMMSFFNDDIEEFEKILSHYRACFGLDDESLENMAKEWSMSVEELESTIKSPHLLSSEPNESVADKLVKTMEKIFAV TGGFVATGLYFRKSYYMQNYFLDTVTEDAKVLLKKKVFLQDSVDSE
Irgc	NP_950178.2	MATSRLPAVPEETTILMAKEELEALRTAFESGDIPQAASRLRELLANSETTRLEVGVTGESGAGKSSLINALRGLGAEDPGAALTGVVETT MQPSPYPHPQFPDVTLWDLPGAGSPGCSADKYLKQVDFGRYDFFLLVSPRRCGAVESRLASEILRQGKKFYFVRTKVDEDLAATRSQRP SGFSEAAVLQEIRDHCTERLRVAGVNDPRIFLVSNLSPTRYDFPMLVTTWEHDLPAHRRHAGLLSLPDISLEALQKKKDMLQEQVLKTAL VSGVIQALPVPGLAAAYDDALLIRSLRGYHRSFGLDDDSLAKLAEQVGKQAGDLRSVIRSPLANEVSPETVLRLYSQSSDGAMRVARAFE RGIPVFGTLVAGGISFGTVYTMLQGCLNEMAEDAQRVRIKALEEDEPQGGEVSLEAAGDNLVEKRSTGEGTSEEAPLSTRRKLGLLLKYIL DSWKRRDLSEDK
Irgd	NP_001258605.1	MDQFISAFLKGASENSFQQLAKEFLPQYSALISKAGGMLSPETLTGIHKALQEGNLSDVMIQIQKAISAAENAILEVAVIGQSGTGKSSFIN ALRGLGHEADESADVGTVETTMCKTPYQHPKYPKVIFWDLPGTGTPNFHADAYLDQVGFANYDFFIIISSSRFSLNDALLAQKIKDAGKK FYFVRTKVDSDLYNEQKAKPIAFKKEKVLQQIRDYCVTNLIKTGVTEPCIFLISNLDLGAFDFPKLEETLLKELPGHKRHMFALLLPNISDASIE LKKHFLREKIWLEALKSAAVSFIPFMTFFKGFDLPEQEQCLKDYRSYFGLDDQSIKEIAEKLGAPLADIKGELKCLDFWSLVKDNSIIAQATS AAEAFCAVKGGPESSAFQALKVYYRRTQFLNIVVDDAKHLLRKIETVNVA

Irgm1	NP_032352.1	MKPSHSSCEAAPLLPNMAETHYAPLSSAFPFVTSYQTGSSRLPEVSRSTERALREGKLLELVYGIKETVATLSQIPVSIFVTGDSGNGMSSFI NALRVIGHDEDASAPTGVVRTTKTRTEYSSSHFPNVVLWDLPGLGATAQTVEDYVEEMKFSTCDLFIIIASEQFSSNHVKLSKIIQSMGKR FYIVWTKLDRDLSTSVLSEVRLLQNIQENIRENLQKEKVKYPPVFLVSSLDPLLYDFPKLRDTLHKDLSNIRCCEPLKTLYGTYEKIVGDKVAV WKQRIANESLKNSLGVRDDDNMGECLKVYRLIFGVDDESVQQVAQSMGTVVMEYKDNMKSQNFYTLRREDWKLRLMTCAIVNAFFR LLRFLPCVCCCLRRLRHKRMLFLVAQDTKNILEKILRDSIFPPQI
Irgm2	NP_062313.3	MEEAVESPEVKEFEYFSDAVFIPKDGNTLSVGVIKRIETAVKEGEVVKVVSIVKEIIQNVSRNKIKIAVTGDSGNGMSSFINALRLIGHEEKD SAPTGVVRTTQKPTCYFSSHFPYVELWDLPGLGATAQSVESYLEEMQISIYDLIIIVASEQFSLNHVKLAITMQRMRKRFYVVWTKLDRDL STSTFPEPQLLQSIQRNIRDSLQKEKVKEHPMFLVSVFKPESHDFPKLRETLQKDLPVIKYHGLVETLYQVCEKTVNERVESIKKSIDEDNLH TEFGISDPGNAIEIRKAFQKTFGLDDISLHLVALEMKNKHFNTSMESQETQRYQQDDWVLARLYRTGTRVGSIGFDYMKCCFTSHHSRC KQQKDILDETAAKAKEVLLKILRLSIPHP
Irgm3	NP_061208.3	MDLVTKLPQNIWKTFTLFINMANYLKRLISPWSKSMTAGESLYSSQNSSSPEVIEDIGKAVTEGNLQKVIGIVKDEIQSKSRYRVKIAVTGD SGNGMSSFINALRFIGHEEEDSAPTGVVRTTKKPACYSSDSHFPYVELWDLPGLGATAQSVESYLEEMQISTFDLIIIVASEQFSSNHVKLAI TMQRMRKRFYVVWTKLDRDLSTSTFPEPQLLQSIQRNIRENLQQAQVRDPPLFLISCFSPSFHDFPELRNTLQKDIFSIRYRDPLEIISQVC DKCISNKAFSLKEDQMLMKDLEAAVSSEDDTANLERGLQTYQKLFGVDDGSLQQVARSTGRLEMGSRALQFQDLIKMDRRLELMMCF AVNKFLRLLESSWWYGLWNVVTRYFRHQRHKLVIEIVAENTKTSLRKALKDSVLPPEIH
Irgq	Bekpen 2005	RLLPPAQDGFEVLGAAELEAVREAFETGGLEAALSWVRAGLERLGSARLDLAVAGTTNVGLVLDMLLGLDPGDPGAAPASAPTGPTPYP APERPNVVLWTVPLGPTATSPAVTPHPTHYDALILVTPGAPTEENWAQVRSLVSPDAPLVGVRTDGQGEDPPEVLEEEKAQNASDGNS GDARSEGKKAGIGDSGCTAARSPEDELWEVLEEAPPPVFPMRPGGLPGLGTWLQHALPTAQAGALLLALPPASPRAARRKAAALRAGA WRPALLASLAAAAAAPVPGLGWACDVALLRGQLAEWRRALGLEPAAVARRERALGLAPGVLATRTRFPGPVTRAEVEARLGSWAGEGT AGGAALSALSFLWPTGGAAATGGLGYRAAHGVLLQALDEMLADAEAVLGPPEPNQ
Mx1	NP_034976.1	MDSVNNLCRHYEEKVRPCIDLIDTLRALGVEQDLALPAIAVIGDQSSGKSSVLEALSGVALPRGSGIVTRCPLVLKLRKLKEGEEWRGKVSY DDIEVELSDPSEVEEAINKGQNFIAGVGLGISDKLISLDVSSPNVPDLTLIDLPGITRVAVGNQPADIGRQIKRLIKTYIQKQETINLVVVPSN VDIATTEALSMAQEVDPEGDRTIGVLTKPDLVDRGAEGKVLDVMRNLVYPLKKGYMIVKCRGQQDIQEQLSLTEAFQKEQVFFKDHSYF SILLEDGKATVPCLAERLTEELTSHICKSLPLLEDQINSSHQSASEELQKYGADIPEDDRTRMSFLVNKISAFNRNIMNLIQAQETVSEGDSR LFTKLRNEFLAWDDHIEEYFKKDSPEVQSKMKEFENQYRGRELPGFVDYKAFESIIKKRVKALEESAVNMLRRVTKMVQTAFVKILSNDF GDFLNLCCTAKSKIKEIRLNQEKEAENLIRLHFQMEQIVYCQDQVYKETLKTIREKEAEKEKTKALINPATFQNNSQFPQKGLTTTEMTQHL KAYYQECRRNIGRQIPLIIQYFILKTFGEEIEKMMLQLLQDTSKCSWFLEEQSDTREKKKFLKRRLLRLDEARQKLAKFSD
Mx2	NP_038634.1	MVLSTEENTGVDSVNLPSGETGLGEKDQESVNNLCSQYEEKVRPCIDLIDSLRALGVEQDLALPAIAVIGDQSSGKSSVLEALSGVALPRG SGIVTRCPLVLKLRKLNEGEEWRGKVSYDDIEVELSDPSEVEEAINKGQNFIAGVGLGISDKLISLDVSSPNVPDLTLIDLPGITRVAVGNQP ADIGRQIKRLIKTYIQKQETINLVVVPSNVDIATTEALSMAQEVDPEGDRTIGILTKPDLVDRGTEDKVVDVVRNLVYHLKKGYMIVKCRG QQDIQEQLSLTEALQNEQIFFKEHPHFRVLLEDGKATVPCLAERLTAELILHICKSLPLLENQIKESHQSASEELQKYGMDIPEDDSEKTFFLI EKINAFNQDITALVQGEENVAEGECRLFTRLRKEFLSWSKEIEKNFAKGYAVLYNEVWAFEKQYRGRELPGFVNYKTFENIIRRQIKTLEEP AIEMLHTVTEIVRAAFTSVSEKNFSEFYNLHRTTKSKLEDIRLEQEKEAEMSIRLHFKMEQIIYCQDQIYRGALQKVREEEAEEEKKTKHGTS SSSQSQDLQTSSMAEIFQHLNAYRQEAHNRISSHVPLIIQYFILKMFAERLQKGMLQLLQDKDSCSWLLKEQSDTSEKRKFLKERLARLAQ ARRRLAKFPG
Rac1	AAH51053.1	MQAIKCVVVGDGAVGKTCLLISYTTNAFPGEYIPTVFDNYSANVMVDGKPVNLGLWDTAGQEDYDRLRPLSYPQTDVFLICFSLVSPASF ENVRAKWYPEVRHHCPNTPIILVGTKLDLRDDKDTIEKLKEKKLTPITYPQGLAMAKEIGAVKYLECSALTQRGLKTVFDEAIRAVLCPPPV KKRKRKCLLL

Alignment (see USB-flash drive)

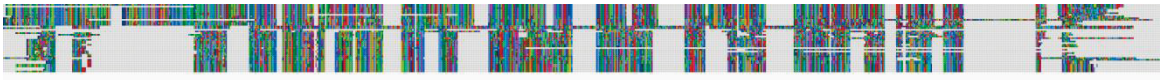

Appendix 4:

Protein sequences of human IFNγ-inducible GTPases used for alignment
(Incorporated in Figure 14B).

Name	Source	ORF
GBP1	NP_002044.2	MASEIHMTGPMCLIENTNGRLMANPEALKILSAITQPMVVVAIVGLYRTGKSYLMNKLAGKKKGFSLGSTVQSHTKGIWMWCVPHPK KPGHILVLLDTEGLGDVEKGDNQNDSWIFALAVLLSSTFVYNSIGTINQQAMDQLYYVTELTHRIRSKSSPDENENEVEDSADFVSFFPDF VWTLRDFSLDLEADGQPLTPDEYLTYSLKLKKGTSQKDETFNLPRLCIRKFFPKKKCFVFDRPVHRRKLAQLEKLQDEELDPEFVQQVADF CSYIFSNSKTKTLSGGIQVNGPRLESLVLTYVNAISSGDLPCMENAVLALAQIENSAAVQKAIAHYEQQMGQKVQLPTETLQELLDLHRDS EREAIEVFIRSSFKDVDHLFQKELAAQLEKKRDDFCKQNQEASSDRCSALLQVIFSPLEEEVKAGIYSKPGGYRLFVQKLQDLKKKYYEEPRK GIQAEEILQTYLKSKESMTDAILQTDQTLTEKEKEIEVERVKAESAQASAKMLQEMQRKNEQMMEQKERSYQEHLKQLTEKMENDRVQ LLKEQERTLALKLQEQEQLLKEGFQKESRIMKNEIQDLQTKMRRRKACTIS
GBP2	NP_004111.2	MAPEINLPGPMSLIDNTKGQLVVNPEALKILSAITQPVVVVAIVGLYRTGKSYLMNKLAGKKNGFSLGSTVKSHTKGIWMWCVPHPKKP EHTLVLLDTEGLGDIEKGDNENDSWIFALAILLSSTFVYNSMGTINQQAMDQLHYVTELTDRIKANSSPGNNSVDDSADFVSFFPAFVWT LRDFTLELEVDGEPITADDYLELSLKLRKGTDKKSKSFNDPRLCIRKFFPKRKCFVFDWPAPKKYLAHLEQLKEEELNPDFIEQVAEFCSYILS HSNVKTLSGGIPVNGPRLESLVLTYVNAISSGDLPCMENAVLALAQIENSAAVEKAIAHYEQQMGQKVQLPTETLQELLDLHRDSEREAIE VFMKNSFKDVDQMFQRKLGAQLEARRDDFCKQNSKASSDCCMALLQDIFGPLEEDVKQGTFSKPGGYRLFTQKLQELKNKYYQVPRK GIQAKEVLKKYLESKEDVADALLQTDQSLSEKEKAIEVERIKAESAEAAKKMLEEIQKKNEEMMEQKEKSYQEHVKQLTEKMERDRAQL MAEQEKTLALKLQEQERLLKEGFENESKRLQKDIWDIQMRSKSLEPICNIL
GBP3 iso1	NP_060754.2	MAPEIHMTGPMCLIENTNGELVANPEALKILSAITQPVVVVAIVGLYRTGKSYLMNKLAGKNKGFSLGSTVKSHTKGIWMWCVPHPKK PEHTLVLLDTEGLGDVKKGDNQNDSWIFTLAVLLSSTLVYNSMGTINQQAMDQLYYVTELTHRIRSKSSPDENENEDSADFVSFFPDFV WTLRDFSLDLEADGQPLTPDEYLEYSLKLTQGTSQKDKNFNLPRLCIRKFFPKKKCFVFDLPIHRRKLAQLEKLQDEELDPEFVQQVADFCS YIFSNSKTKTLSGGIKVNGPRLESLVLTYINAISRGDLPCMENAVLALAQIENSAAVQKAIAHYDQQMGQKVQLPAETLQELLDLHRVSER EATEVYMKNSFKDVDHLFQKKLAAQLDKKRDDFCKQNQEASSDRCSALLQVIFSPLEEEVKAGIYSKPGGYCLFIQKLQDLEKKYYEEPRK GIQAEEILQTYLKSKESVTDAILQTDQILTEKEKEIEVECVKAESAQASAKMVEEMQIKYQQMMEEKEKSYQEHVKQLTEKMERERAQLL EEQEKTLTSKLQEQARVLKERCQGESTQLQNEIQKLQKTLKKKTKRYMSHKLKI
GBP3 iso2	NP_001306108.1	MWCVPHPKKPEHTLVLLDTEGLGDVKKGDNQNDSWIFTLAVLLSSTLVYNSMGTINQQAMDQLYYVTELTHRIRSKSSPDENENEDSA DFVSFFPDFVWTLRDFSLDLEADGQPLTPDEYLEYSLKLTQGTSQKDKNFNLPRLCIRKFFPKKKCFVFDLPIHRRKLAQLEKLQDEELDPEF VQQVADFCSYIFSNSKTKTLSGGIKVNGPRLESLVLTYINAISRGDLPCMENAVLALAQIENSAAVQKAIAHYDQQMGQKVQLPAETLQE LLDLHRVSEREATEVYMKNSFKDVDHLFQKKLAAQLDKKRDDFCKQNQEASSDRCSALLQVIFSPLEEEVKAGIYSKPGGYCLFIQKLQDL EKKYYEEPRKGIQAEEILQTYLKSKESVTDAILQTDQILTEKEKEIEVECVKAESAQASAKMVEEMQIKYQQMMEEKEKSYQEHVKQLTEK MERERAQLLEEQEKTLTSKLQEQARVLKERCQGESTQLQNEIQKLQKTLKKKTKRYMSHKLKI
GBP3 iso3	NP_001306109.1	MQVQRRDPIYVTELTHRIRSKSSPDENENEDSADFVSFFPDFVWTLRDFSLDLEADGQPLTPDEYLEYSLKLTQGTSQKDKNFNLPRLCIR KFFPKKKCFVFDLPIHRRKLAQLEKLQDEELDPEFVQQVADFCSYIFSNSKTKTLSGGIKVNGPRLESLVLTYINAISRGDLPCMENAVLALA QIENSAAVQKAIAHYDQQMGQKVQLPAETLQELLDLHRVSEREATEVYMKNSFKDVDHLFQKKLAAQLDKKRDDFCKQNQEASSDRC SALLQVIFSPLEEEVKAGIYSKPGGYCLFIQKLQDLEKKYYEEPRKGIQAEEILQTYLKSKESVTDAILQTDQILTEKEKEIEVECVKAESAQASA KMVEEMQIKYQQMMEEKEKSYQEHVKQLTEKMERERAQLLEEQEKTLTSKLQEQARVLKERCQGESTQLQNEIQKLQKTLKKKTKRYM SHKLKI
GBP3 iso4	NP_001306110.1	MAPEIHMTGPMCLIENTNGELVANPEALKILSAITQPVVVVAIVGLYRTGKSYLMNKLAGKNKGFSLGSTVKSHTKGIWMWCVPHPKK PEHTLVLLDTEGLGDVKKGDNQNDSWIFTLAVLLSSTLVYNSMGTINQQAMDQLYYVTELTHRIRSKSSPDENENEDSADFVSFFPDFV WTLRDFSLDLEADGQPLTPDEYLEYSLKLTQGTSQKDKNFNLPRLCIRKFFPKKKCFVFDLPIHRRKLAQLEKLQDEELDPEFVQQVADFCS YIFSNSKTKTLSGGIKVNGPRLESLVLTYINAISRGDLPCMENAVLALAQIENSAAVQKAIAHYDQQMGQKVQLPAETLQELLDLHRAQLD KKRDDFCKQNQEASSDRCSALLQVIFSPLEEEVKAGIYSKPGGYCLFIQKLQDLEKKYYEEPRKGIQAEEILQTYLKSKESVTDAILQTDQILT EKEKEIEVECVKAESAQASAKMVEEMQIKYQQMMEEKEKSYQEHVKQLTEKMERERAQLLEEQEKTLTSKLQVSKCITLWFVFLFSLCSS
GBP4	NP_443173.2	MGERTLHAAVPTPGYPESESIMMAPICLVENQEEQLTVNSKALEILDKISQPVVVVAIVGLYRTGKSYLMNRLAGKRNGFPLGSTVQSET KGIWMWCVPHLSKPNHTLVLLDTEGLGDVEKSNPKNDSWIFALAVLLSSSFVYNSVSTINHQALEQLHYVTELAELIRAKSCPRPDEAED SSEFASFFPDFIWTVRDFTLELKLDGNPITEDEYLENALKLIPGKNPKIQNSNMPRECIRHFFRKRKCFVFDRPTNDKQYLNHMDEVPEEN LERHFLMQSDNFCSYIFTHAKTKTLREGIIVTGKRLGTLVVTYVDAINSGAVPCLENAVTALAQLENPAAVQRAADHYSQQMAQQLRLPT DTLQELLDVHAACEREAIAVFMEHSFKDENHEFQKKLVDTIEKKKGDFVLQNEEASAKYCQAELKRLSEHLTESILRGIFSVPGGHNLYLEE

		KKQVEWDYKLVPRKGVKANEVLQNFLQSQVVVEESILQSDKALTAGEKAIAAERAMKEAAEKEQELLREKQKEQQQMMEAQERSFQE YMAQMEKKLEEERENLLREHERLLKHKLKVQEEMLKEEFQKKSEQLNKEINQLKEKIESTKNEQLRLLKILDMASNIMIVTLPGASKLLGV GTKYLGSRI
GBP5	NP_001127958.1	MALEIHMSDPMCLIENFNEQLKVNQEALEILSAITQPVVVVAIVGLYRTGKSYLMNKLAGKNKGFSVASTVQSHTKGIWIWCVPHPNW PNHTLVLLDTEGLGDVEKADNKNDIQIFALALLLSSTFVYNTVNKIDQGAIDLLHNVTELTDLLKARNSPDLDRVEDPADSASFFPDLVWT LRDFCLGLEIDGQLVTPDEYLENSLRPKQGSDQRVQNFNLPRLCIQKFFPKKKCFIFDLPAHQKKLAQLETLPDDELEPEFVQQVTEFCSYIF SHSMTKTLPGGIMVNGSRLKNLVLTYVNAISSGDLPCIENAVLALAQRENSAAVQKAIAHYDQQMGQKVQLPMETLQELLDLHRTSERE AIEVFMKNSFKDVDQSFQKELETLLDAKQNDICKRNLEASSDYCSALLKDIFGPLEEAVKQGIYSKPGGHNLFIQKTEELKAKYYREPRKGI QAEEVLQKYLKSKESVSHAILQTDQALTETEKKKKEAQVKAEAEKAEAQRLAAIQRQNEQMMQERERLHQEQVRQMEIAKQNWLAEQ QKMQEQQMQEQAAQLSTTFQQNRSLLSELQHAQRTVNNDDPCVLL
GBP6 iso1	NP_940862.2	MESGPKMLAPVCLVENNNEQLLVNQQAIQILEKISQPVVVVAIVGLYRTGKSYLMNHLAGQNHGFPLGSTVQSETKGIWMWCVPHPS KPNHTLVLLDTEGLGDVEKGDPKNDSWIFALAVLLCSTFVYNSMSTINHQALEQLHYVTELTELIKAKSSPRPDGVEDSTEFVSFFPDFLW TVRDFTLELKLNGHPITEDEYLENALKLIQGNNPRVQTSNFPRECIRRFFPKRKCFVFDRPTNDKDLLANIEKVSEKQLDPKFQEQTNIFCSY IFTHARTKTLREGITVTGNRLGTLAVTYVEAINSGAVPCLENAVITLAQRENSAAVQRAADYYSQQMAQRVKLPTDTLQELLDMHAACE REAIAIFMEHSFKDENQEFQKKFMETTMNKKGDFLLQNEESSVQYCQAKLNELSKGLMESISAGSFSVPGGHKLYMETKERIEQDYWQ VPRKGVKAKEVFQRFLESQMVIEESILQSDKALTDREKAVAVDRAKKEAAEKEQELLKQKLQEQQQQMEAQDKSRKENIAQLKEKLQM EREHLLREQIMMLEHTQKVQNDWLHEGFKKKYEEMNAEISQFKRMIDTTKNDDTPWIARTLDNLADELTAILSAPAKLIGHGVKGVSSL FKKHKLPF
GBP6 iso2	NP_001307186.1	MSTINHQALEQLHYVTELTELIKAKSSPRPDGVEDSTEFVSFFPDFLWTVRDFTLELKLNGHPITEDEYLENALKLIQGNNPRVQTSNFPRE CIRRFFPKRKCFVFDRPTNDKDLLANIEKVSEKQLDPKFQEQTNIFCSYIFTHARTKTLREGITVTGNRLGTLAVTYVEAINSGAVPCLENAVI TLAQRENSAAVQRAADYYSQQMAQRVKLPTDTLQELLDMHAACEREAIAIFMEHSFKDENQEFQKKFMETTMNKKGDFLLQNEESSV QYCQAKLNELSKGLMESISAGSFSVPGGHKLYMETKERIEQDYWQVPRKGVKAKEVFQRFLESQMVIEESILQSDKALTDREKAVAVDR AKKEAAEKEQELLKQKLQEQQQQMEAQDKSRKENIAQLKEKLQMEREHLLREQIMMLEHTQKVQNDWLHEGFKKKYEEMNAEISQF KRMIDTTKNDDTPWIARTLDNLADELTAILSAPAKLIGHGVKGVSSLFKKHKLPF
GBP7	NP_997281.2	MASEIHMPGPVCLTENTKGHLVVNSEALEILSAITQPVVVVAIVGLYRTGKSYLMNKLAGKNKGFPLGCTVKSETKGIWMWCVPHPSKP NHTLILLDTEGLGDMEKSDPKSDSWIFALAVLLSSSFVYNSMGTINHQALEQLHYVTELTELIRAKSCPRPDEVEDSSEFVSFFPDFIWTVR DFTLELKLDGHPITEDEYLENALKLISGKNPQIQNSNKPREWIRHFFPKQKCFVFDRPINDKKLLLHVEEVREDQLDSNFQMQSENFCSYIF THAKTKTLREGILVTGNRLGMLVETYLDAINSGATPCLENAMAVLAQCENSAAVQRAANHYSQQMAQQVRFPTDTLQELLDVHAVCE REAIAVFMEYSFKDKSQEFQKKLVDTMEKKKEDFVLQNEEASAKYCQAELKRLSELLTESISRGTFFVPGGHNIYLEAKKKIEQDYTLVPRK GVKADEVLQSFLQSQVVIEESILQSDKALTAGEKAIAAKQAKKEAAEKEQELLRQKQKEQQQMMEAQERSFQENIAQLKKKMERERENY MRELRKMLSHKMKVLEELLTEGFKEIFESLNEEINRLKEQIEAAENEEPSVFSQILDVAGSIFIAALPGAAKLVDLGMKILSSLCNRLRNPG KKIIS
IRGC	NP_062558.1	MATSKLPVVPGEEENTILMAKERLEALRTAFESGDLPQAASHLQELLASTESIRLEVGVTGESGAGKSSLINALRGLEAEDPGAALTGVME TTMQPSPYPHPQFPDVTLWDLPGAGSPGCPADKYLKQVDFSRYDFFLLVSPRRCGAVETRLAAEILCQGKKFYFVRTKVDEDLAATRTQ RPSGFREAAVLQEIRDHCAERLREAGVADPRIFLVSNLSPARYDFPTLVSTWEHDLPSHRRHAGLLSLPDISLEALQKKKAMLQEQVLKTA LVLGVIQALPVPGLAAAYDDALLIHSLRGYHRSFGLDDDSLAKLAEQVGKQAGDLRSVIRSPLANEVSPETVLRLYSQSSDGAMRVARAFE RGIPVFGTLVAGGISFGAVYTMLQGCLNEMAEDAQRVRIKALEDDEPQPEVSLEVASDNGVEKGGSGEGGGEEAPLSTCRKLGLLLKYIL DSWKKHDSEEK
IRGM	NP_001333486.1	MEAMNVEKASADGNLPEVISNIKETLKIVSRTPVNITMAGDSGNGMSTFISALRNTGHEGKASPPTELVKATQRCASYFSSHFSNVVLW DLPGTGSATTTLENYLMEMQFNRYDFIMVASAQFSMNHVMLAKTAEDMGKKFYIVWTKLDMDLSTGALPEVQLLQIRENVLENLQKE RLACHEKYLKSTPENSTRPRNIPSRRKLYVNLLRIFNS
IRGM	NP_001139277.1	MEAMNVEKASADGNLPEVISNIKETLKIVSRTPVNITMAGDSGNGMSTFISALRNTGHEGKASPPTELVKATQRCASYFSSHFSNVVLW DLPGTGSATTTLENYLMEMQFNRYDFIMVASAQFSMNHVMLAKTAEDMGKKFYIVWTKLDMDLSTGALPEVQLLQIRENVLENLQKE RVCEY
Mx1 isoA1=T0	NP_001138397.1	MVVSEVDIAKADPAAASHPLLLNGDATVAQKNPGSVAENNLCSQYEEKVRPCIDLIDSLRALGVEQDLALPAIAVIGDQSSGKSSVLEALS GVALPRGSGIVTRCPLVLKLKKLVNEDKWRGKVSYQDYEIEISDASEVEKEINKAQNAIAGEGMGISHELITLEISSRDVPDLTLIDLPGITRV AVGNQPADIGYKIKTLIKKYIQRQETISLVVVPSNVDIATTEALSMAQEVDPEGDRTIGILTKPDLVDKGTEDKVVDVVRNLVFHLKKGYMI VKCRGQQEIQDQLSLSEALQREKIFFENHPYFRDLLEEGKATVPCLAEKLTSELITHICKSLPLLENQIKETHQRITEELQKYGVDIPEDENEK MFFLIDKVNAFNQDITALMQGEETVGEEDIRLFTRLRHEFHKWSTIIENNFQEGHKILSRKIQKFENQYRGRELPGFVNYRTFETIVKQQIK ALEEPAVDMLHTVTDMVRLAFTDVSIKNFEEFFNLHRTAKSKIEDIRAEQEREGEKLIRLHFQMEQIVYCQDQVYRGALQKVREKELEEEK

		KKKSWDFGAFQSSSATDSSMEEIFQHLMAYHQEASKRISSHIPLIIQFFMLQTYGQQLQKAMLQLLQDKDTYSWLLKERSDTSDKRKFLK ERLARLTQARRRLAQFPG
MX1 isoA2	NP_001171517.1	MVVSEVDIAKADPAAASHPLLLNGDATVAQKNPGSVAENNLCSQYEEKVRPCIDLIDSLRALGVEQDLALPAIAVIGDQSSGKSSVLEALS GVALPRGSGIVTRCPLVLKLKKLVNEDKWRGKVSYQDYEIEISDASEVEKEINKAQNAIAGEGMGISHELITLEISSRDVPDLTLIDLPGITRV AVGNQPADIGYKIKTLIKKYIQRQETISLVVVPSNVDIATTEALSMAQEVDPEGDRTIGILTKPDLVDKGTEDKVVDVVRNLVFHLKKGYMI VKCRGQQEIQDQLSLSEALQREKIFFENHPYFRDLLEEGKATVPCLAEKLTSELITHICKSLPLLENQIKETHQRITEELQKYGVDIPEDENEK MFFLIDKVNAFNQDITALMQGEETVGEEDIRLFTRLRHEFHKWSTIIENNFQEGHKILSRKIQKFENQYRGRELPGFVNYRTFETIVKQQIK ALEEPAVDMLHTVTDMVRLAFTDVSIKNFEEFFNLHRTAKSKIEDIRAEQEREGEKLIRLHFQMEQIVYCQDQVYRGALQKVREKELEEEK KKKSWDFGAFQSSSATDSSMEEIFQHLMAYHQEASKRISSHIPLIIQFFMLQTYGQQLQKAMLQLLQDKDTYSWLLKERSDTSDKRKFLK ERLARLTQARRRLAQFPG
MX1 isoA3=T1	NP_002453.2	MVVSEVDIAKADPAAASHPLLLNGDATVAQKNPGSVAENNLCSQYEEKVRPCIDLIDSLRALGVEQDLALPAIAVIGDQSSGKSSVLEALS GVALPRGSGIVTRCPLVLKLKKLVNEDKWRGKVSYQDYEIEISDASEVEKEINKAQNAIAGEGMGISHELITLEISSRDVPDLTLIDLPGITRV AVGNQPADIGYKIKTLIKKYIQRQETISLVVVPSNVDIATTEALSMAQEVDPEGDRTIGILTKPDLVDKGTEDKVVDVVRNLVFHLKKGYMI VKCRGQQEIQDQLSLSEALQREKIFFENHPYFRDLLEEGKATVPCLAEKLTSELITHICKSLPLLENQIKETHQRITEELQKYGVDIPEDENEK MFFLIDKVNAFNQDITALMQGEETVGEEDIRLFTRLRHEFHKWSTIIENNFQEGHKILSRKIQKFENQYRGRELPGFVNYRTFETIVKQQIK ALEEPAVDMLHTVTDMVRLAFTDVSIKNFEEFFNLHRTAKSKIEDIRAEQEREGEKLIRLHFQMEQIVYCQDQVYRGALQKVREKELEEEK KKKSWDFGAFQSSSATDSSMEEIFQHLMAYHQEASKRISSHIPLIIQFFMLQTYGQQLQKAMLQLLQDKDTYSWLLKERSDTSDKRKFLK ERLARLTQARRRLAQFPG
MX1 isoB=varMxA	NP_001269849.1	MVVSEVDIAKADPAAASHPLLLNGDATVAQKNPGSVAENNLCSQYEEKVRPCIDLIDSLRALGVEQDLALPAIAVIGDQSSGKSSVLEALS GVALPRGSGIVTRCPLVLKLKKLVNEDKWRGKVSYQDYEIEISDASEVEKEINKAQNAIAGEGMGISHELITLEISSRDVPDLTLIDLPGITRV AVGNQPADIGYKIKTLIKKYIQRQETISLVVVPSNVDIATTEALSMAQEVDPEGDRTIGILTKPDLVDKGTEDKVVDVVRNLVFHLKKGYMI VKCRGQQEIQDQLSLSEALQREKIFFENHPYFRDLLEEGKATVPCLAEKLTSELITHICKSLPLLENQIKETHQRITEELQKYGVDIPEDENEK MFFLIDKVNAFNQDITALMQGEETVGEEDIRLFTRLRHEFHKWSTIIENNFQEGGQQAHLQPHPFDHPVLHAPDVRPAASEGHAAAPA GQGHLQLAPEGAERHQRQAEVPEGAACTADAGSAPACPVPRLTTLCPAP
MX2	NP_002454.1	MSKAHKPWPYRRRSQFSSRKYLKKEMNSFQQQPPPFGTVPPQMMFPPNWQGAEKDAAFLAKDFNFLTLNNQPPPGNRSQPRAMG PENNLYSQYEQKVRPCIDLIDSLRALGVEQDLALPAIAVIGDQSSGKSSVLEALSGVALPRGSGIVTRCPLVLKLKKQPCEAWAGRISYRNT ELELQDPGQVEKEIHKAQNVMAGNGRGISHELISLEITSPEVPDLTIIDLPGITRVAVDNQPRDIGLQIKALIKKYIQRQQTINLVVVPCNVD IATTEALSMAHEVDPEGDRTIGILTKPDLMDRGTEKSVMNVVRNLTYPLKKGYMIVKCRGQQEITNRLSLAEATKKEITFFQTHPYFRVLL EEGSATVPRLAERLTTELIMHIQKSLPLLEGQIRESHQKATEELRRCGADIPSQEADKMFFLIEKIKMFNQDIEKLVEGEEVVRENETRLYNK IREDFKNWVGILATNTQKVKNIIHEEVEKYEKQYRGKELLGFVNYKTFEIIVHQYIQQLVEPALSMLQKAMEIIQQAFINVAKKHFGEFFNL NQTVQSTIEDIKVKHTAKAENMIQLQFRMEQMVFCQDQIYSVVLKKVREEIFNPLGTPSQNMKLNSHFPSNESSVSSFTEIGIHLNAYFLE TSKRLANQIPFIIQYFMLRENGDSLQKAMMQILQEKNRYSWLLQEQSETATKRRILKERIYRLTQARHALCQFSSKEIH
Rac1	CAB53579.5	MQAIKCVVVGDGAVGKTCLLISYTTNAFPGEYIPTVFDNYSANVMVDGKPVNLGLWDTAGQEDYDRLRPLSYPQTDVFLICFSLVSPASF ENVRAKWYPEVRHHCPNTPIILVGTKLDLRDDKDTIEKLKEKKLTPITYPQGLAMAKEIGAVKYLECSALTQRGLKTVFDEAIRAVLCPPPV KKRKRKCLLL

Alignment (see USB-flash drive)

Thanks to

First and foremost, I would like to thank Prof. Dr. Klaus Pfeffer for giving me the opportunity to perform my promotional research in this interesting field and in this fascinating country. Additional thanks are in order, for his continuous support both scientifically as on a personal level, prior, during and after my promotion.

I would like to thank Prof. Dr. Lutz Schmitt for fulfilling the role of co-supervisor and the constructive brainstorming sessions.

Warm thanks go to Dr. Daniel Degrandi and Dr. Elisabeth Kravets for excellent supervision, fruitful discussions and around the clock help with laboratory affairs. For excellent continuous technical support, I want to thank Karin Buchholz, Nicole Küpper, and Julia Mock. I thank Tobias Lerchner for enthusiastic collaboration during his studies.

For research ideas, philosophical and pragmatic discussions I want to thank Prof. Dr. Mirko Trilling and Dr. Sander Smits. For friendly support and assistance during my first research efforts under biosafety level 3 conditions I want to thank Prof. Dr. Rainer Kalscheuer, Dr. Milena Hänisch, Nidja Rehberg and Prof. Dr. Heiner Schaal. Also indispensable, was the knowledge of chlamydial biology of Prof. Dr. Johannes Hegemann and Dr. Katja Mölleken, for which I am very grateful.

Thomas Rudel is thanked for providing the GFP-expressing *C. trachomatis* L2 strain (SW2::GFP) which was initially generated by Ian Clarke (Barnhart).

Within the university, I could effortlessly integrate, through help of Anja Wegener and Natalie Böddicker from the *Hochschuldidaktik* Programme, Ekaterina Masetkina from SelmaMeyerMentoring and the RTG 1949 headed by Prof. Dr. Jörg Timm, Astrid M. Westendorf and coordinated by Daniela Catrini, whom I all want to thank. I also want to thank the Research Training group 1949 ‘Immune Response in Infectious Diseases’ for financing this promotional research.

All colleagues at the institute supported my research efforts, but also social activities (including the recurring German necessity for a ‘*Grillparty*’), and yearly festivities (like the regional ‘*Karnaval*’). For these fantastic experiences I would like to give all a heartfelt thanks. Especially, for fun carpools I thank Gregor Ciupka, Tina Senff, Janine Brinkmann, Elisabeth Lang and Dennis Lapuente. For great traveling experiences at (and around) conferences I’d like to thank Dr. Elisabeth Kravets, Valentina Antoni, Patrick Oblinger and particularly Anja Schulze (‘*die Weinberg-Freundin*’). I have had a marvellous time in Germany and at the institute, a time in which I’ve grown professionally and met the love of my life. I am looking forward to a future career in Germany, and beyond.

Eidesstattliche Erklärung

Eidesstattliche Versicherung

Ich, Frau M.Sc. Valesca Lindenberg, versichere an Eides statt, dass die vorliegende Dissertation von mir selbstständig und ohne unzulässige fremde Hilfe unter Beachtung der „Grundsätze zur Sicherung guter wissenschaftlicher Praxis an der Heinrich-Heine-Universität Düsseldorf“ erstellt worden ist.

Düsseldorf, der 7. Juni 2017

Unterschrift